

**DEVELOPMENT OF SOLAR AIR HEATERS &
THERMAL ENERGY STORAGE SYSTEM FOR DRYING
APPLICATIONS IN FOOD PROCESSING INDUSTRIES**

*Thesis submitted to Cochin University of Science and Technology
for the award of the degree of*

Doctor of Philosophy

by

Sreekumar.A

**Department of Physics
Cochin University of Science and Technology
Kochi - 22
India**

November 2007

Dr.K.P.Vijayakumar
Professor


Department of Physics
**Cochin University of Science and
Technology**
COCHIN-682022
INDIA

Ph:(off):0484-2577404
(res):0484-2577103
Fax:0484-2577595
Email kpv@cusat.ac.in

Certificate

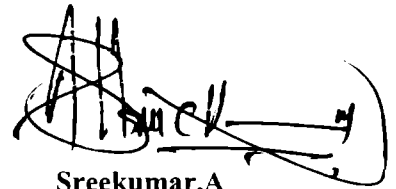
Certified that the work presented in the thesis entitled
*“Development of Solar Air Heaters & Thermal Energy Storage
System for Drying Applications in Food Processing Industries”* is
based on the bonafide research work done by Mr. Sreekumar.A, under
my guidance in the Department of Physics, Cochin University of Science
and Technology, Kochi-22 and has not been included in any other thesis
submitted previously for the award of any degree.

Kochi-22
29-11-2007


Prof. K. P. Vijayakumar
(Supervising Guide)

DECLARATION

Certified that the work presented in this thesis entitled "*Development of Solar Air Heaters & Thermal Energy Storage System for Drying Applications in Food Processing Industries*" is based on the original research work done by me under the guidance and supervision of **Prof. K. P. Vijayakumar**, Department of Physics, Cochin University of Science and Technology, Kochi-22 and has never been included in any other thesis submitted previously for the award of any degree.



Sreekumar.A

Kochi-22
29-11-2007

....to my beloved parents & brother

Acknowledgement

I take this opportunity to place on record my profound sense of indebtedness and deep appreciation to my supervising guide, Prof. K. P. Vijayakumar for his personnel encouragement, unending benevolence, patronly behaviour, stimulating discussions and able guidance right from the beginning to date as a consequence of which the present study reached fruition. My gratitude to him knows no bounds.

I am deeply indebted to Dr. C. Sudha Kartha, for all the assistance that she extended to me during my research work. She was always a source of encouragement and showed keen interest in my progress.

I am extremely thankful to Dr. Godfrey Louis, Professor & Head of the Department of Physics, CUSAT for all the facilities extended to me in the department. I also highly indebted to Dr. Ramesh Babu, the former Head, Department of Physics for his support and encouragement throughout out the work.

I am indebted to those who have directly or indirectly contributed to fulfill this work like Dr. T.M. Thomas Isaac, M.L.A., Mararikulam Constituency (presently the Hon'ble Finance Minister, Kerala), for healthy discussion and sanction of the Solar drying project at Cherthala and Mr. T.K. Jose, IAS., Fomer Executive Director, 'Kudumbasree' (Presently Higher Education Secretary and Vice Chancellor of Cochin University of Science and Technology), for his keen interest to install and depute us to the development of a solar air heating system in Marangattupilli, Pala, under Kudumbasree scheme.

I wish to express my sincere thanks to Mr.G.M.Pillai IAS., Director General, World Institute of Sustainable Energy, Pune for his constant advice and encouragement. I am also grateful to him for sanctioning the leave for a longer period from the Institute, for the submission of the thesis.

Mr. Mahindra, Cumins, Pune extended his help to materialize the numerical simulation analysis and his timely help is gratefully acknowledged.

I am grateful to Ministry of New and Renewable Energy (MNRE), Govt. of India, New Delhi for providing research fellowship through NRE scheme. Sincere thanks to MNRE, due to its NRE scheme is one of the examples of strong determination and dedication for fast deployment of renewable energy technology in India. The effective coordination of the Project coordinator, IIT, New Delhi for the timely distribution of the fund is also highly acknowledged.

I would like to express my sincere thanks to all the faculty members of Department of Physics, CUSAT and the members of the non-teaching staff for their timely help and co operation.

I would like to share deep appreciation to Mr. Vimal, who always assisted me during experimental studies. It is a pleasure to express my appreciation to all my lab mates, junior colleagues, and friends in the Department of Physics for their immense support and for having a cheerful life in the campus during my research period.

Mr. C.P. Bineesh shared a strong bond of friendship and cordiality with me. I am indeed thankful to him for his whole-hearted support.

Most of all it is time to recollect the motivation and fortification rendered by my beloved brother, Dr.A.Krishnakumar.

Whatever I write here will be insufficient to express my sense of indebtedness to my father and mother. My efforts bore fruit to a great extent owing to the solid support that the members of my family lent me.

*With extreme pleasure and God's grace, let me dedicate this work to my adored parents and bother, **The Guiding Light** on all my endeavors.*

Sreekumar A

CONTENTS

Preface	I
Publications	XI
Chapter 1 Introduction to Solar Energy and Thermal Applications	
1.1 Introduction	1
1.2 The Sun	3
1.2.1 Solar Spectrum	5
1.2.2 Availability of Solar Radiation	5
1.2.3 Direct and Diffuse Radiation	6
1.2.4 Air Mass Ratio	7
1.3 Solar Energy	8
1.3.1 Various Methods of Solar Energy Utilization	9
1.3.2 Various Applications of Solar Energy	10
1.3.2.1 Direct thermal utilization	11
1.3.2.2 Electrical utilization	15
1.4 Other Methods of Solar Energy Utilization	16
1.4.1 Wind Energy	16
1.4.2 Wave Energy	16
1.4.3 Ocean Thermal Energy Conversion (OTEC)	16
1.4.4 Energy from Biomass	17
1.5 Flat Plate Collector (FPC)	18
1.6 Solar Air Heaters	19
1.7 General Description on SAH	20
1.8 Components of Solar Air Heaters	21
1.8.1 Absorber Plate	21
1.8.2 Cover Plate	22
1.8.3 Insulation	23
1.9 Classification of Solar Air Heater	23
1.9.1 Nonporous Type Solar Air Heaters	23
1.9.2 Porous Type Solar Air Heaters	25
1.10 Parameters Associated with the Construction of an Air Heater	27
1.10.1 Heater Configuration	27
1.10.2 Airflow	27
1.10.3 Transmittance Properties of the Cover	27
1.10.4 Absorber Plate Material	28
1.10.5 Natural Convection Barriers	28

1.10.6 Plate-to-air Heat Transfer Coefficient	28
1.10.7 Insulation	28
1.10.8 Solar Radiation Data	28
1.11 Performance Analysis of a Conventional Solar Air Heater	28
1.12 Heat Transfer and Pressure Drop in a Parallel Plate Duct	30
1.13 Testing Procedures	31
1.14 Applications of Solar Air Heater	34
1.14.1 Space Heating and Cooling of Buildings	34
1.14.2 Drying and Curing of Agricultural Products	35
1.14.3 Industrial Applications	35
<i>Nomenclature</i>	36
<i>References</i>	38
Chapter 2 Review on Solar Air Heaters, Solar Dryers and Latent Heat Thermal Energy Storage	
2.1 Solar Air Heaters	45
2.2 Solar Dryers	55
2.3 Solar PCM Thermal Storage	65
<i>References</i>	67
Chapter 3 Design and Development of Various Types of Solar Air Heaters	
3.1 Introduction	89
3.2 Solar Air Heaters Developed	91
3.2.1 a) Underflow Copper Collector with Baffles	92
3.2.1 b) Underflow Copper Collector without Baffles	95
3.2.2 a) Overflow Galvanized Iron (GI) Collector with Baffles	95
3.2.2 b) Overflow Galvanized Iron (GI) Collector without Baffles	98
3.2.3 a) Overflow Aluminium Collector with Baffles	98
3.2.3 b) Overflow Aluminium Collector without Baffles	100
3.2.4 a) Double Passage Solar Air Heater with Baffles	100
3.2.4 b) Double Passage Solar Air Heater without Baffles	102
3.2.5 Matrix Collector	103
3.3 Other Materials/Components Used	105
3.3.1 Selective Coating	105

3.3.2 Cover Plate	106
3.3.3 Insulation	106
3.4 Performance Equation	107
3.5 Instrumentation and Measurement of Various Thermo-physical Parameters	109
3.6 Experimental Procedure	110
3.7 Performance Test, Results and Discussion	111
3.7.1 Underflow Copper Collector	111
3.7.2 Overflow Collector-Corrugated GI Sheet as Absorber Plate	117
3.7.3 Overflow Collector-Aluminium as Absorber Plate	122
3.7.4 Double Flow Collector-Aluminium as Absorber Plate	128
3.7.5 Matrix Collector-GI Mesh as Absorber Plate	133
3.8 Comparison of all Types of Solar Air Heaters Developed	138
3.9 Conclusion	141
<i>References</i>	143

Chapter 4 Design and Performance Study of a Solar Air Heating System for Food Processing Industries

4.1 Introduction	147
4.2 Classification and Selection of Dryers	150
4.3 Comparing Solar Drying with Other Options	150
4.4 Basic Principles	152
4.5 Design Consideration	153
4.5.1 Design Consideration for Solar Drying Chamber	155
4.5.1.1 Thermodynamical aspects	156
4.5.1.2 Mechanical Aspects	160
4.6 Description of the Solar Air Heater	161
4.7 Description of the Dryer	164
4.8 Working	168
4.9 Attractive Design Features	168
4. 10 Investigation of the Performance of the Dryer	169
4.10.1 Instruments	169
4.10.2 Materials and Methods	169
4.10.3 Economic Analysis	170
4.10.3.1 Annualized cost method	171
4.10.3.2 Life cycle savings	172
4.10.3.3 Payback period	174

4.11 Results and Discussion	174
4.11.1 Economic Analysis	176
4.11.1.1 Annualized cost method	177
4.11.1.2 Life cycle savings	178
4.11.1.3 Payback period	178
4.12 Conclusion	180
<i>Nomenclature</i>	181
<i>References</i>	184

Chapter 5 Performance of an Indirect Solar Cabinet Dryer with Thermal Energy Storage

5.1 Introduction	187
5.2 Energy Storage	188
5.2.1 Sensible Heat Storage	189
5.2.2 Latent Heat Storage	190
5.2.3 Thermochemical Heat Storage	191
5.3 PCM in Solar Drying	191
5.4 Experimental Set-up	193
5.4.1 Description of the Solar Dryer	193
5.4.2 PCM Container	195
5.4.3 Phase Change Material (PCM) Investigated	197
5.5 Working	199
5.6 Attractive Design Features	200
5.7 Investigation of the Performance of the System	201
5.7.1 Instruments	201
5.7.2 Materials	202
5.7.3 Methods	203
5.7.3.1 Design of PCM container	203
5.8 Experimental Procedure	206
5.8.1 Test without PCM	206
5.8.1.1 Test of the dryer without load and axial fans switched off (Condition -1)	206
5.8.1.2 Test without load and axial fans in operating condition (Condition -2)	206
5.8.1.3 Test with product loaded in the dryer (Condition -3)	206
5.8.1.4 Economic analysis	207
5.8.2 Test with PCM	207
5.8.2.1 Test on dryer with PCM (Condition-4)	207
5.8.2.2 Test on dryer with PCM, product loaded and axial fans in running condition (Condition-5)	207
5.9 Results and Discussion	208
5.9.1 Condition -1	208

5.9.2 Condition -2	209
5.9.3 Condition -3	211
5.9.4 Economic Analysis	213
5.9.4.1 Annualized cost method	214
5.9.4.2 Life cycle savings	214
5.9.4.3 Payback period	215
5.9.5 Condition -4	217
5.9.6 Condition -5	218
5.10 Conclusion	221
<i>References</i>	223
Chapter 6 Design and Development of a Solar Greenhouse for Industrial Drying	
6.1 Introduction	227
6.2 Description of the Greenhouse	229
6.3 Theoretical Analysis	231
6.3.1 The Substrate	231
6.3.2 The Floor	232
6.3.3 The Greenhouse Air	232
6.3.4 The Greenhouse Envelope	233
6.4 Instrumentation and Experimental Procedure	234
6.5 Results and Discussion	234
6.6 Conclusion	237
<i>Nomenclature</i>	238
<i>References</i>	240
Chapter 7 Numerical Simulation Study on Solar Air Heaters	
7.1 Introduction	243
7.2 Advantages of the Numerical Simulation on Solar Air Heaters	244
7.3 Geometry Model	244
7.4 CFD Model	245
7.4.1 Grid Generation	245
7.4.2 Physical Model	245
7.4.3 Boundary Conditions	246
7.4.4 Solver Settings	247
7.5 Results and Discussion	247
7.5.1 Flow Field	248
7.5.2 Temperature Output with and without Baffles	257
7.5.3 Pressure Drop with and without Baffles	258
7.5.4 Effect of Number Baffles for Temperature Output	259
7.5.5 Variation of Pressure Drop with Number of Baffles	260

7.6 Conclusion	261
<i>References</i>	263
Chapter 8 Summary and Conclusions	265
Suggestions and Recommendations	269

Preface

The world is hurtling towards two major crises: serious energy shortages and accelerating climate change. Together, they threaten to destroy the achievements of human civilization. Solutions to both the crises are interlinked; the diversification of the fuel base and adoption of emerging clean and green alternative for energy production. Fortunately, such clean and diverse alternatives have emerged on the technology horizon. But society-wide barriers to their adoption are legion, especially in the developing world.

Solar energy is one eternal source of energy, whose widespread adoption is shrouded in misgivings and doubts. Globally, it is the well accepted source of energy with an annual average growth of 35%, as seen during the past few years. While the world is racing ahead for getting energy directly from the sun, solar energy development in India has been tardy. The only one area where discernible achievements have been made is in 'solar water heating'. The vast potential of solar energy in food processing industries is not well exploited. Cumulative installation of solar photovoltaic in India remained stagnant at around 16 MW_p in 2005, whereas power from solar thermal concentrating technology was nil.

The food crisis which is bitterly felt in the third world can be effectively tackled by two methods, viz. (i) by increasing the available supply of food materials and (ii) by bringing the population growth rate at par with the rate of increase in food production. The total world population by the year 2005 is 6.47 billion and it has been estimated that the population will cross 9 billion by the year 2050. It is also estimated that 852 million people across the world do not have enough food to consume and this number is likely to increase with the increase in population. With the increasing demand for food, caused by post harvest losses has become an

urgent priority. In many developing countries, large amount of post harvest losses occur from spoilage, microbial contamination, insect infestation, birds and rodents and deterioration in storage. The amount of moisture present in the food product is the most important factor in determining the extent of deterioration in storage. Most agricultural products at the time of harvesting have high moisture content, which causes the deterioration, due to the growth of fungi and bacteria. For the preservation and long term storage of agricultural produce, maximum moisture contents have been determined (known as “safe moisture content”), below which the produce can be stored for definite duration, without the possibility of spoilage at ambient temperature. There are several ways of preserving food for later use. Drying is the traditional method for preserving food. It also helps in easy transport, since the food becomes lighter, because of moisture loss. Drying of crops prevents germination and growth of fungi and bacteria. There are recommended drying temperature and moisture content for different crops to be stored over a year or more. The principal objective of drying operation is the supply of required heat in an optimum manner to yield the best quality product, with a minimum overall expenditure of energy.

Drying is a complicated process involving simultaneous heat and mass transfer. Conventional drying techniques utilize air dryers that consume large quantity of fossil fuel. But the escalating prices and shortage of fossil fuels increased the emphasis on the usage of solar energy as an alternate energy source, especially in developing countries. Electrical heating of air for drying is preferred; but it is very expensive and not feasible in rural areas of developing countries. Thus the usage of renewable energy sources along with conventional sources to meet the demand of energy for ecologically sustainable development in urban and rural areas become inevitable. The techno-economic viability of a number of systems and devices, based on renewable energy sources, has been developed

successfully in the domestic, commercial and industrial sector. Among the other energy sources, solar energy may be the most promising answer to the demands of drying, particularly in developing countries, most of which receive a high degree of solar radiation throughout the year. India is blessed with abundant solar energy [on an average of the order of $5 \text{ kWh/m}^2\text{-day}$] for over 300 days/year. This amount of energy could be well utilized for thermal applications like agricultural crops drying. To achieve efficient drying process, design of the drying systems has paramount importance since it involves complex heat and mass transfer phenomena.

The intermittent and variable nature of solar energy generally results in a mismatch between the rate and time of collection of solar energy. As a result, it is often necessary to incorporate a storage system to meet the energy requirements during non solar hours. The storage system stores energy when the collected amount is in excess and discharges energy when the collected amount is inadequate. Among different solar thermal energy systems, latent heat thermal energy storage has the advantages of high energy density.

Several types of solar air heaters have been developed over the years. Among the solar air heaters, flat plate type is the most common. It is simple to construct, easy to operate, and less costly to maintain. Since air is the working fluid in air heaters, the problem of freezing or boiling of the fluid does not occur. One disadvantage is that it has low density, low thermal capacity and small heat conductivity of air, thus requiring larger ducts to transport the required energy. These are probably the important negative points of air panels; but probably their low cost and reliability make them attractive. A conventional solar air heater generally consists of an absorber plate with a parallel plate below, forming a passage of high aspect ratio, through which the air to be heated flows. A transparent cover system is provided above the absorber plate, while a sheet metal container filled with

insulation is provided on the bottom and sides. There are two possible alternatives for maximizing useful energy collection from air heaters. Obviously, the first one is to maximize the collector area by lengthening the absorber plate while keeping channel depth and mass flow rate constants. For system with design constraints on fan power and collector length, however, the only evident alternative is to employ higher air rates, by constructing the channel deeper.

In the present work, we have designed and developed all types of solar air heaters called porous and nonporous collectors. The developed solar air heaters were subjected to different air mass flow rates in order to standardize the flow per unit area of the collector. Much attention was given to investigate the performance of the solar air heaters fitted with baffles. The output obtained from the experiments on pilot models, helped the installation of solar air heating system for industrial drying applications also. Apart from these, various types of solar dryers, for small and medium scale drying applications, were also built up. The feasibility of 'latent heat thermal energy storage system' based on Phase Change Material was also undertaken. The application of solar greenhouse for drying industrial effluent was analyzed in the present study and a solar greenhouse was developed. The effectiveness of Computational Fluid Dynamics (CFD) in the field of solar air heaters was also analyzed. The thesis is divided into eight chapters and a brief description of the contents of each chapter is given below.

CHAPTER 1 is a general introduction to solar energy and its different thermal applications. It begins with the origin and use of solar energy and the need to proliferate the widespread deployment of solar energy in the current scenario of fast dwindling of conventional fuels. It describes the working principle of different solar thermal gadgets and gives an elaborated

scanning of various types of solar air heaters. The chapter is concluded with the enormous potentiality of solar air heaters in different sectors.

CHAPTER 2 presents an exhaustive review on solar air heaters, solar dryers and latent heat thermal energy storage systems, pertaining to the present work.

The design and standardization of solar air heaters of various models depending on the type of air flow and other design parameters, is described in **CHAPTER 3**. Five different types of solar air heaters were developed for the standardization study. Two collectors were ‘overflow’ type. The absorber plate of the one air heater was corrugated Galvanized Iron (GI) sheet while that of the other one was plane aluminium sheet. An ‘underflow’ collector with an absorber plate made up of thin black chrome copper was also designed and investigated. The fourth model was a ‘double flow’ collector having plane aluminium sheet as the absorber plate. Separate studies were undertaken in all these collectors, with and without the provision of baffles. A matrix collector was also developed in which double layered GI mesh was used as the absorber. Each collector was subjected to different air mass flow rates. The solar radiation flux at a horizontal surface was measured by using a Solarimeter. Air velocity was measured with the help of Digital thermo-anemometer. A 0.5 HP centrifugal fan was used to push air through the collector. Velocity of the centrifugal blower was adjusted using an externally controlled regulator. Temperatures of ambient, air from the outlet of the collector, top glass, absorber plate and the inlet air were monitored using LM 35 sensor. The sensor was connected to the computer using RS 232 interface through a 16-channel data logger. It recorded the temperature at the required points in every minute. The pressure drop across the collector was studied by using a U-tube manometer using water. The experiments were conducted for different mass flow rates for the two types of experimental set up, i.e., with and without baffles. The pressure drop measurements were also carried out

for each mass flow rate. The instantaneous and average efficiency for each mass flow rates were found out. The pressure drop and corresponding pumping power required for each mass flow rate in all the collectors with and without baffles were also evaluated.

CHAPTER 4 narrates the development and testing of a 46 m² roof integrated solar air heater with a batch type solar dryer, particularly meant for drying fruits and vegetables. The maximum temperature recorded at the output of the solar collector was 76.6°C. The dryer was loaded with 200 kg pineapple and the desired moisture content was achieved within 8 hours. A detailed economic analysis was done by 3 methods namely 'annualized cost method', 'present worth of annual savings' and 'present worth of cumulative savings'. The drying cost for 1 kg pineapple was calculated as Rs. 11 and it was Rs. 19.73, in the case of electric dryer. The life span of the solar dryer was assumed to be 20 years. The payback period was calculated as 0.54 years, which was very less considering the life of the system (20 years).

The development and testing of a new type of efficient solar dryer, particularly meant for drying vegetables and fruits, is described in **CHAPTER 5**. The dryer has two compartments: one for collecting solar radiation and producing thermal energy and other for spreading the product to be dried. This arrangement was made to absorb maximum solar radiation by the absorber plate and to protect the product from direct exposure to solar radiation. The dryer was loaded with 4 kg bitter melon having an initial moisture content of 95% and the final desired moisture content of 5% was achieved within 6 hours without losing the product colour, while it was 11 hours for open sun drying. A detailed performance analysis was done by 3 methods namely 'annualized cost method', 'present worth of annual savings' and 'present worth of cumulative savings'. The drying cost for 1 kg bitter melon was calculated as Rs. 17.52 and it was Rs. 41.35, in the case of electric dryer. The life span of the solar dryer was assumed to be 20 years.

The cumulative present worth of annual savings over the life of the solar dryer was calculated for drying bitter gourd which turned out to be Rs. 31660. This was much higher than the capital cost of the dryer (Rs. 6500). The payback period was calculated as 3.26 years, which was also very short considering the life of the system (20 years). The chapter also describes in detail about the design and investigation on latent heat thermal energy storage system based on Phase Change Material (PCM). Acetamide (CH_3CONH_2) was used as PCM and it was filled in a specially fabricated stainless steel container having adequate heat transfer facility. The PCM container was integrated with the solar cabinet dryer to study the feasibility of energy storage for drying applications. A detailed study was undertaken with the PCM integrated into the dryer to know the drying performance. This was compared with open sun drying. In this work the dryer was loaded with 4 kg ripe banana having an initial moisture content of 78%. Final (desired) moisture content of 15% was achieved within 12.5 hours, but the sample kept in the open sun drying could not reach its final desired moisture content in the same duration. It was found that the product loaded in the dryer, during night time, had a reduction in moisture content of 2.41% and the reduction in moisture during evening drying was 3.21%. The PCM integrated dryer, designed and fabricated in the present work, could reduce the drying duration and maintained a warm atmosphere inside the dryer during night hours. This prevented the deterioration of the product even if there was no sunlight.

A cost effective and simple 'solar greenhouse' was designed and fabricated for evaluating its suitability for industrial drying application and this is presented in **CHAPTER 6**. The greenhouse was loaded with copper cake, which was an effluent generated by a zinc manufacturing industry. Two courses of studies were mainly undertaken with the present experimental set up. Maximum temperature recorded in the greenhouse,

when it was loaded with 60kg and 550 kg of copper cake, were 46.8°C and 50.6°C respectively. The objective of the study was to reduce the drying duration of copper cake, which is a valuable effluent, generated by the industry. The initial moisture content at the time of loading was 40% and the final desired moisture content for the separation of copper was 10%. The normal drying duration of this effluent, without any arrangement, was more than one to two months, while it was only ten days when the system was loaded with 550kg sample. With the present experimental set up, the drying duration of the sample reduced considerably along with the reduction of storage space, required for the effluent material in the factory premises.

The **CHAPTER 7** gives the numerical simulation of solar air heaters to optimize the flow path and heat transfer performance. Main objective of this study was to analyze the prototype of a solar air heater in order to enhance flow path and heat transfer performance. Since the design and fabrication of all prototype solar air heaters for experimental study was a complicated process, optimization was carried using CFD analysis. CFD has distinct advantages like as cost, turn around time, detailed information and ability to simulate real condition to name few. The educational/commercial version of the software “Fluent” was used for the numerical simulations. Typical CFD analysis involves pre-processing (building 2D/3D model, grid generation, assigning boundary conditions), solving for given accuracy and post-processing of the results. 2D/3D models were generated in CAD packages like Catia, Pro/E etc and were incorporated in pre-processor of CFD as CAD data. In this work, 3D model of solar air heater was built and meshed using Gambit as preprocessor. Model was solved for the prediction of flow path and heat transfer, using solver of Fluent. Finally results from Fluent were post processed to visualize flow path, pressure drop, rise in temperature (heat transfer) with different baffle configuration and mass flow rates of air. Efforts were taken to compare the results from CFD with

available prototype experimental data. CFD may play instrumental role in order to decide the optimized configuration of solar air heater.

CHAPTER 8 is a summary of the entire work. All the important points are highlighted here.

Journals

1. Performance of a roof-integrated solar air heating system for drying fruit and vegetables

A.Sreekumar, T.V.Vimalkumar and K.P.Vijayakumar
Energy Conversion and Management (under review)

2. On the performance of an underflow copper solar air heater with baffles

A.Sreekumar, T.V.Vimalkumar and K.P.Vijayakumar
Energy Conversion and Management (under review)

3. Experimental studies on overflow corrugated solar air heater with baffles

A.Sreekumar, T.V.Vimalkumar and K.P.Vijayakumar
Renewable Energy (under review)

4. Performance of an indirect solar cabinet dryer

A.Sreekumar, P.E. Manikantan and K.P.Vijayakumar
Energy Conversion and Management (under review)

5. Performance of a PCM integrated forced circulation indirect solar cabinet dryer

A.Sreekumar, T.V.Vimalkumar, K.P.Vijayakumar
Energy Conversion and Management (under review)

6. Performance of a low cost solar green house to dry industrial waste

A.Sreekumar and K.P.Vijayakumar
Energy (under review)

7. Experimental studies on a high flow channel depth solar air heater with metal matrix absorber
A.Sreekumar, T.V Vimalkumar and K.P.Vijayakumar
Energy (under review)

8. Thermal performance of a double flow solar air heater with baffles
A.Sreekumar, T.V.Vimalkumar and K.P.Vijayakumar
Energy (under review)

9. Solar air heating system for energy efficient drying needs
A.Sreekumar and K.P.Vijayakumar
Energy & Fuel Users Journal LV (2), 74-78, 2005.

10. Potential for solar thermal applications in India
A.Sreekumar
Green Energy 3(4), 26-27, 2007.

11. Europe: Solar thermal strategy and action plan
A.Sreekumar
Green Energy 3(4), 43-46, 2007.

Conferences

1. Copper solar air heater for better thermal energy conversion to drying needs
A.Sreekumar, T.V Vimalkumar and K.P.Vijayakumar
Discussion Meeting on Materials for Future Energy Systems, Material Research Society of India (Mumbai Chapter), Mumbai, 2006

2. A 40 m² solar air heating system for vegetables drying

A.Sreekumar and K.P.Vijayakumar

Asia Pacific Drying Conference (ADC-2005), Central Mechanical Engineering Research Institute, Kolkata, 2005.

3. Solar air heating systems for energy efficient drying needs

A.Sreekumar and K.P.Vijayakumar

National Conference on Energy Management in Changing Business Scenario (EMCBS-2005), Centre for Renewable Energy and Environment Development, Birla Institute of Technology and Science, Pilani, Rajasthan, 2005.

4. Solar air heating system for drying fruits and vegetables: Design and fabrication

A.Sreekumar, C. Sudha Kartha and K.P.Vijayakumar

National Seminar on Recent Trends and Issues in the Evolution of Appropriate Technologies for Integrated Rural Development, Gandhigram Rural Institute, Gandhigram, Tamil Nadu, 2005.

5. Solar drying of chillies-a viable alternative to conventional drying

A.Sreekumar, C. Sudha Kartha and K.P.Vijayakumar

National Conference on Environment and Sustainable Development, CUSAT, Kochi, 2004.

6. Design and Performance of a solar air heating system for chilli drying -

A.Sreekumar, C. Sudha Kartha and K.P.Vijayakumar

National Conference on Solar Drying, Technology and their Applications in India, Society for Energy, Environment and Social Development, Hyderabad, 2003.

7. Design, fabrication and performance evaluation of a solar cooker cum dryer with latent heat storage

A.Sreekumar

Thirteenth Kerala Science Congress, State Committee on Science, Technology and Environment, KILA, Thrissur, 2001.

8. Construction and performance study of a salt gradient solar pond

A.Sreekumar

National Renewable Energy Convention (NREC'99), School of Energy and Environmental Studies, Devi Ahilya Vishwavidyalaya, Indore, 1999.

INTRODUCTION TO SOLAR ENERGY AND THERMAL APPLICATIONS

1.1 Introduction

Energy is the prime mover of economic growth and is vital to the sustenance of a modern economy. Future economic growth crucially depends on the long-term availability of energy from sources that are affordable, accessible and environmentally friendly technology. The known resources of fossil fuels in the world are depleting very fast and it is estimated that, by AD 2030, man will have to increasingly depend upon renewable sources of energy. The proven global coal, oil and gas reserves were estimated to be, respectively, 9,09,064 million tones, 1208.2 billion barrels and 181.46 trillion cubic metres by the end of 2006. World oil and gas reserves are estimated at just 45 years and 65 years respectively. Coal is likely to last a little over 200 years [1].

Apart from being freely available in nature, renewable energy resources can be used in a decentralized manner, reducing the cost of transmission and distribution of power. Renewed interest in solar energy has developed since 1970 as a result of increasing costs of energy from conventional resources and the problems of importing and extracting fuels that are acceptable from environmental standpoints. In the second half of the 18th century, coal came into use and helped the industrialization of the world. In the second half of the 19th century, only about 150 years ago, mineral oil started to be widely exploited, not only providing a lighting source, but also making possible the individual long distance transport of large numbers of people. Today several hundred million motor vehicles are in use worldwide, with a correspondingly huge market impact [2,3].

The renaissance of interest in solar energy began in the early 1970s, due to three predominant reasons. First, the oil crisis of that decade brought back to mind that the raw materials available in the Earth's crust for fossil and nuclear energy are finite. Moreover, this was concentrated in a limited number of countries as to predestine, by geographical happenstance, oligopolistic potentials. The second reason is that the liberal use of fossil fuels is causing irreversible ecological damage at an increasing rate to nature in general, to mankind, fauna and flora. In addition, irreplaceable cultural monuments of a shared human heritage are being destroyed. The complex relationship between the environment and the industrial and agricultural behaviour of modern man is not yet well understood. Much remains still hidden because of the long time scale, extending from decades to centuries, against which nature's reactions need to be measured [4-8]. The urgency of this situation becomes evident with the realization that 90% or more of the world's energy consumed today is carbon-containing fossil energy, be it coal, oil, or natural gas, and be it wood or agricultural and forestry waste products. Invariably their utilization involves combustion processes with air as oxidizer. The resulting oxidation reactants are being unavoidably released into the environment. This includes CO, CO₂, SO₂, NO_x, residual C_nH_m, toxicants and heavy metals, as well as dust, and occasionally soot and particulate. Again, if desulfurizing or denoxing equipment is used, gypsum or surplus NH₃ are also resulted. Only the CO₂ release from biomass combustion is environmentally neutral because of the CO₂ which is released will be taken from the environment when the biomass is formed [9-11]. The third and last reason for the renaissance of interest in solar energy is the fact that nuclear energy is only reluctantly tolerated in many countries and restricted by moratoria or quasi-moratoria in others. Failure to resolve the radioactive waste disposal problem may provide an even more serious limitation.

Solar energy usage has two fundamental facets [12]. The first one comprises a variety of local applications characterized by collection, conversion and consumption of the solar energy *on site*. To this group, belong passive solar energy usage in buildings, heat production by solar radiation collectors, photovoltaic arrays for electricity generation, ambient heat use in heat pumps, and the conversion of wind, hydropower, or biomass into electrical energy, heat and gaseous or liquid fuels. What these solar energy technologies have in common is that they are not restricted only to those regions of the world that offer ideal solar conditions.

The *off-site* facet comprises thermal solar power plants with their need for high direct irradiation, photovoltaic solar power plants, large hydropower complexes and ocean thermal energy conversion (OTEC) systems, etc. All belong to the category of solar energy converters whose common feature is the necessity to deliver secondary energy over distances up to several thousand kilometers as their primary users rarely reside in the vicinity of the plant.

1.2 The Sun

Sun is an enormous fusion reactor at a distance of 150×10^6 km from earth, which turns hydrogen into helium at the rate of 4 million tones per second. It radiates energy towards the earth by virtue of its high surface temperature, approximately 6000°C . The quantity of solar energy flowing to and from the earth and its atmosphere is very large. Amount of solar energy incident on the earth every year is

Equivalent to 160 times the energy stored in the world's proven reserves of fossil fuels.

Equivalent to more than 15000 times the world's annual use of fossil, nuclear fuels and hydropower [13].

Spectrum of solar radiation extends from 200 to 3000 nm in wavelength. It is almost identical with the 6000 K black body radiation spectrum. The radiation is distinguished as:

- (a) Ultra-violet radiation (200 to 380 nm) producing photochemical effects, bleaching, sunburn, etc.
- (b) Visible light [380 nm (violet) to 700 nm (red)].
- (c) Infra-red radiation (700 to 3000 nm) or radiant heat, with some photochemical effects.

As the solar radiation passes through the earth's atmosphere [Fig. 1.1], it is absorbed or scattered or reflected according to the following processes [12].

- (a) A portion of the solar radiation is scattered when striking on molecules of air, water vapor, and dust particles. The portion scattered downward through the atmosphere arrived at the earth surface in the form of diffuse radiation (30%).
- (b) Another portion of solar radiation is absorbed (19%), and
- (c) The remaining portion of the solar radiation traverses through the atmosphere and reaches the earth's surface in the form of direct radiation (51%).

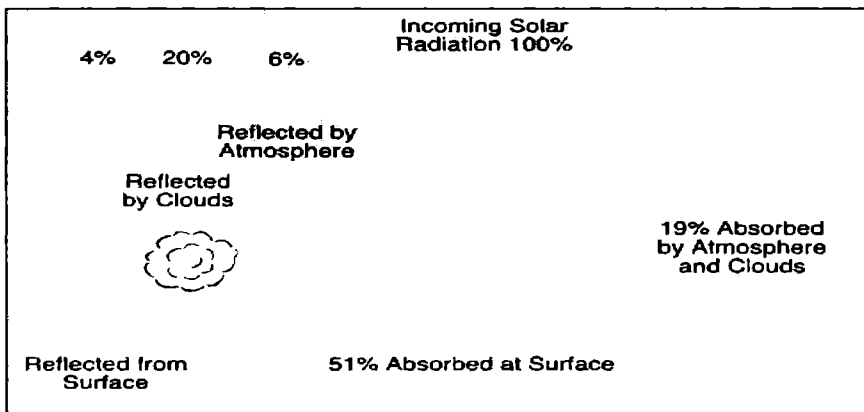


Fig. 1.1 Global modification of incoming solar radiation by atmospheric and surface processes

1.2.1 Solar Spectrum

We perceive solar radiation as white light. In fact, it spreads over a wider spectrum of wavelength, from infrared (longer than red light) to ultraviolet (shorter than violet). Pattern of wavelength distribution is critically determined by the temperature of the surface of the sun [14]. Spectral distribution of sunlight is given in Fig. 1.2.

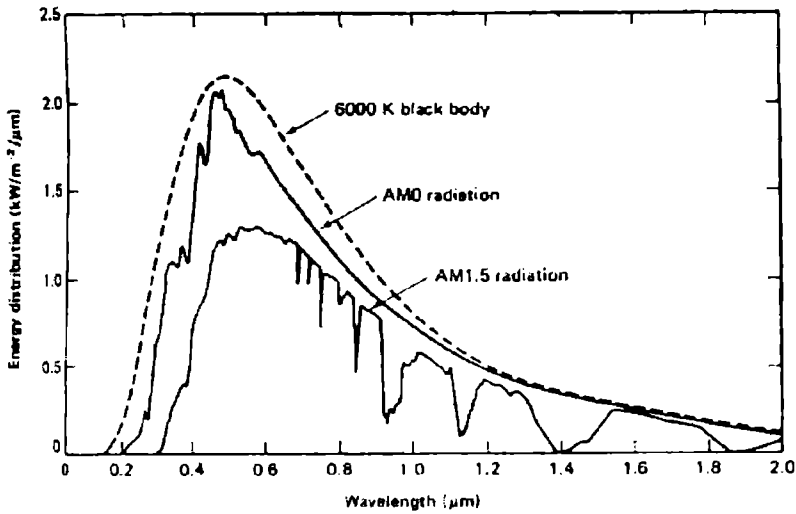


Fig. 1.2 Spectral distribution of sunlight. Shown are the cases of AM 0 and AM 1.5 radiation together with the radiation distribution expected from the sun if it were a black body at 6000 K

1.2.2 Availability of Solar Radiation

Despite the absorption and scattering of the solar radiation in the earth's atmosphere, amount of energy received on earth's surface in one hour would still be enough to cover the energy requirements of the whole world for one year. Hence the issue is not one of availability of solar energy, but of the feasibility of converting it into forms suitable for human use. As indicated earlier, 30% of solar radiation is reflected immediately back to the space. The remaining 70% is mainly used to warm the earth's surface,

atmosphere and oceans (47%) or is absorbed for the evaporation of water (23%). Relatively very small proportions are used to drive the winds, waves and for plants (in photosynthesis). Ultimately, all the energy used on earth is radiated back to space, in the form of infrared radiation.

1.2.3 Direct and Diffuse Radiation

The earth is surrounded by atmosphere, which contains various gaseous constituents, suspended dust and other minute solid and liquid particulate matter and clouds of various types. Therefore, solar radiation is depleted during its passage through the atmosphere before reaching the earth's surface. If the atmosphere is very clear then the depletion in the solar radiation occurs simultaneously by three distinct physical processes:

- (i) Selective absorption by water vapor, molecular oxygen, ozone and carbon dioxide in certain wavelengths
- (ii) Rayleigh scattering by molecules of different gases and dust particles that constitute the atmosphere and
- (iii) Mie scattering, which takes place where the size of the scattering particles is greater than the wavelength of radiation.

Hence depletion in the solar radiation occurs both by true scattering (involving a redistribution of incident energy) as well as by absorption by the particles, where part of the radiant energy is transformed into heat. The radiation received after its direction has been changed by scattering and reflection is known as "diffuse radiation" During clear days, magnitude of diffuse radiation is about 10 to 14% of the total solar radiation received at the earth's surface. Only diffuse radiation may reach the earth's surface during extremely cloudy days. Radiation received without any change in direction or scattering is known as "direct radiation" (beam radiation). On a clear day, direct radiation falling on earth's surface can have the maximum power density of 1 kW/m^2 and is known as '1 sun' for solar collector testing

purposes [12]. Direct and diffuse radiations are useful for most solar thermal applications. But only direct radiation can be focused to generate very high temperatures. On the other hand, it is the diffuse radiation that provides most of our “day light” Sum of these two is called “total radiation” or “global radiation”

1.2.4 Air Mass Ratio

Radiation available on the surface of earth is less than the radiation available outside the earth’s atmosphere and this reduction in intensity depends on atmospheric conditions (amount of dust particles, water vapor, ozone content, atmospheric pressure, cloudiness, etc.) and solar altitude. The later factor determines the length of atmosphere through which solar beam has to travel before reaching the earth’s surface. If the altitude of the sun is small, the length traversed by the beam is long. On the other hand if the sun is at the zenith (overhead), solar beam traverses a vertical path, which is the shortest path through the atmosphere. Path length of solar beam through atmosphere is accounted through the term ‘air mass’ which is a numerical comparison between the path length (which the solar beam actually traverses) and the vertical path through the atmosphere [15]. Thus at the sea level air mass (m), is unity when the sun is at the zenith. In general,

$$\text{Air mass} = \frac{\text{Path length traversed}}{\text{Vertical depth of atmosphere}} \quad (1.1)$$

In space, solar radiation is obviously unaffected by the earth’s atmosphere and has a power density of approximately 1365 W/m^2 . The characteristic spectral power distribution of solar radiation, as measured in space is described as *Air Mass 0 (AM0)* distribution. When the sun is at its zenith (i.e., directly overhead) the path length of solar beam is minimum, the characteristic spectral power distribution of solar radiation is known as the *Air Mass 1 (AM1)* distribution.

When the sun is at a given angle θ_z to the zenith (as perceived by an observer at sea level) the air mass is defined as the ratio of the path length of the sun's rays under these conditions to the path length when the sun is at its zenith. This leads to the second definition of Air Mass ratio as:

$$\text{Air Mass} \sim 1/\text{Cos} \theta_z \quad (1.2)$$

The zenith angle θ_z is the angle made by the sun's rays with the normal to a horizontal surface. It can be shown approximately that for locations at sea level and zenith angles from 0 to 70°, the air mass is equal to the secant of the zenith angle. Thus air mass zero (AM0) corresponds to extra-terrestrial radiation, air mass one (AM1) corresponds to the case of the sun at its zenith, and air mass two (AM2) corresponds to the case of a zenith angle of 60°

An air mass distribution of 1.5, as specified by the standard test conditions, therefore corresponds to the spectral power distribution observed when the sun's radiation is coming from an angle to overhead of about 48 degrees, since $\text{Cos } 48 = 0.67$ and the reciprocal of this is 1.5.

1.3 Solar Energy

The Sun is a very large source of energy and earth intercepts about 1.8×10^{11} MW of power, which is several thousands of times larger than the total energy rate on earth. Hence this quantity of energy consumption certainly can meet the present and future needs of this planet on a continuing basis. Thus, it is one of the most promising sources of energy. Unlike fossil fuels and nuclear energy, it is an environmentally clean source of energy. Secondly, it is free and available in adequate quantities in almost all parts of the world where people live. Solar energy is always in an advantageous position compared with depleting fossil fuels. In a tropical country like India most of the energy demands can be met by simple systems that can convert solar energy into appropriate forms. By proper application of technologies,

excellent thermodynamic match between the solar energy resources and many end-uses can be achieved.

However, there are many problems associated with its use. Major problem is that, it is a dilute source of energy. Even in the hottest regions on earth, the solar radiation flux available rarely exceeds 1 kW/m^2 and the total radiation over a day is at best about 7 kWh/m^2 . These are low values from the point of view of technological utilization. Consequently, large collecting area is required in many applications and this results in excessive cost. A second problem associated with the use of solar energy is that its availability varies with time. This occurs daily because of the day-night cycle and also seasonally because of the earth's orbit around the sun. In addition, variations occur at a specific location because of local weather conditions. Consequently, the energy collected from the sun must be stored for use during periods when it is not available. This also adds significantly to the cost of this energy. Thus, the real challenge in utilizing solar energy as an energy alternative is economic in nature [16].

1.3.1 Various Methods of Solar Energy Utilization

A broad classification of the various methods of solar energy utilization is given in Table 1.1. It can be seen that energy from the sun can be used directly or indirectly. Direct methods include thermal and photovoltaic conversion, while indirect methods include use of waterpower, wind, biomass, wave energy, and temperature differences in ocean.

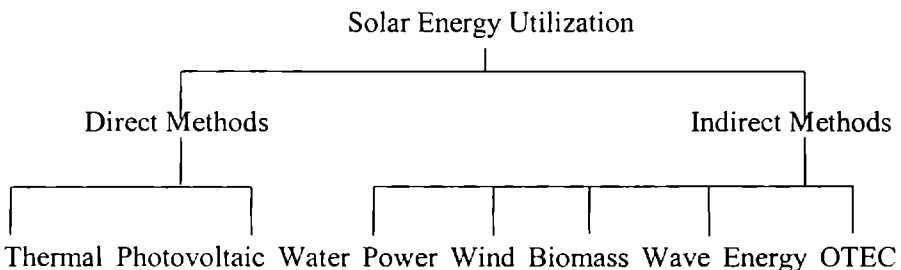


Table 1.1 Classification of methods for solar energy utilization

Solar energy can be used by three technological processes namely (i) heliochemical, (ii) helioelectrical and (iii) heliothermal. Heliochemical process, through photosynthesis, maintains life on earth by producing food on earth and converting CO_2 to O_2 . In helioelectrical process, using photovoltaic converters produces electricity and it provides power for spacecraft and is used in many industrial and domestic applications. Heliothermal process can be used to generate much of the thermal energy required for solar air heating, water heating, drying and building heating. The basic principle of a heliothermal or solar thermal conversion is that the solar radiation is converted into thermal energy. A flat plate collector is the heart of any solar energy collection system designed for operation in the low temperature range, from ambient to 90°C , or the medium temperature range, from ambient to 150°C . The flat plate collector is basically a heat exchanger, which transfers the radiant energy of the incident sunlight to the sensible heat of a working fluid (liquid or air) [17]. The term 'flat plate' slightly misleading in the sense that the surface may be truly flat – it may be combination of flat, grooved or of other shapes as the absorbing surface, with some kind of heat removal device like tubes or channels.

1.3.2 Various Applications of Solar Energy

Major application of solar energy include solar water and air heating, solar drying of agricultural products, salt production by evaporation of sea water, solar distillation on a community scale, solar cookers, solar engines for water pumping, food refrigeration, photo-voltaic conversion, solar furnace, heating and cooling of buildings, solar thermal power generation, high temperature application for industrial process heat, etc. It can be generally classified as thermal and electrical applications [18].

1.3.2.1 Direct thermal utilization

This is the most popular utilization of solar energy. In this, usually there is a collection device, which is directly exposed to the solar radiation. This can be an absorbing type or concentrating type. In the former case, there is a dark surface exposed to sun, which absorbs radiation. Absorbed energy is then transferred to a fluid (like air or water), which is in contact with the absorber. In the later case solar radiation is concentrated to a focal point and the heat energy is transferred to the fluid. There are several devices used for the direct thermal applications of solar energy. Some of these are listed below.

1.3.2.1(a) Flat-plate collector - It consists of an absorber plate on which solar radiation falls after passing through one or more transparent covers (usually made of glass). Absorbed energy is partly transferred to a liquid, flowing through tubes, which are either fixed to the absorber plate or forms an integral part of it. This energy transfer is the useful gain. Flat-plate collector is held tilted in a fixed position on a supporting structure, facing south, if located in the northern hemisphere. When the fluid is water, it is called 'liquid flat plate collector' and if air is the fluid, then it is called 'air heater' [19].

1.3.2.1(b) Focusing or concentrating collector - Solar concentrator is a device which concentrates the solar energy incident over a large surface onto a smaller surface [20-22]. The concentration is achieved by the use of suitable reflecting or refracting elements, which results in an increased flux density on the absorber surface as compared to that existing on the concentrator aperture. In order to get a maximum concentration, an arrangement for tracking the sun's virtual motion is required. An accurate focusing device is also essential. Thus, a solar concentrator consists of a focusing device, a receiver system and a tracking arrangement. Temperature

as high as 3000°C can be achieved using solar concentrators. Hence they have potential applications in both thermal and electrical utilization of solar energy at high delivery temperatures.

1.3.2.1(c) Solar pond - A novel device, which combines functions of both collection and storage of solar energy. It consists of an expanse of water about a meter or two in depth in which salts like sodium or magnesium chloride are dissolved. Because of this, bottom layer of water is denser than the surface layers even if it is hotter and natural convection does not occur. Thus, heat from the sun's rays absorbed at the bottom of the pond is retained in the lower depths, and the upper layers of water act like thermal insulation [16].

1.3.2.1(d) Space heating - The solar energy collectors are generally the air heaters or flat-plate liquid collectors for converting solar radiation into heat. In most of the solar space heating systems, the temperature requirement of the fluid is in the range of 50 to 80°C, which makes the system much simpler. In terms of fluid selection the obvious choice is either water or air and in terms of storage device the most obvious choice is water or rock bed storage system. In liquid collector based system, water is heated in the solar collector and stored in tank. Energy is transferred to air circulating in the house by means of the water-to-air heat exchanger. Two pumps provide forced circulation between the collectors and the tank, and between the tank and the heat exchanger. Provision is also made for adding auxiliary heat. Space heating is of particular relevance in colder countries where significant amount of energy is required for this purpose [23].

1.3.2.1(e) Power generation - Generation of electrical power is another application of solar energy. Here solar energy is converted into electrical energy by solar thermal cycles. Solar thermal cycles are classified as low, medium and high temperature cycles. Low temperature cycles work at maximum temperatures of about 100°C; medium temperature cycles work up

to 400°C; while high temperatures cycles work at temperatures above 400°C. Low temperatures systems use flat-plate collectors or solar ponds for collecting solar energy. Medium temperature systems use the line focusing parabolic collector technology. High temperature systems use either paraboloidal dish collectors or central receivers located at the top of towers [24-26].

1.3.2.1(f) Space cooling and refrigeration - One of the interesting thermal applications of solar energy is for the purpose of cooling. Solar energy can be used for cooling buildings (generally known as air-conditioning) or for refrigeration required for preserving food. Solar cooling appears to be an attractive proposition due to the fact that when the cooling demand is more, the sunshine is strongest. Since the energy from sun is being received as heat, the obvious choice is a system working on the absorption refrigeration cycle, which requires most of its energy input as heat.

Water heated in a flat-plate collector array is passed through a heat exchanger called generator, where it transfers heat to a solution mixture of the absorbent and refrigerant, which is rich in the refrigerant. Refrigerant vapor is boiled off at high pressure and goes to condenser where it is condensed into a high-pressure liquid. The high-pressure liquid is throttled to a low pressure and temperature in an expansion valve, and passes through an evaporator coil [27,28]. Here, the refrigerant vapor absorbs heat and cooling is therefore obtained in the space surrounding this coil. Refrigerant vapor is now absorbed by solution mixture withdrawn from the generator, which is weak in refrigerant concentration. This yields a rich solution, which is pumped back to the generator, thereby completing the cycle.

1.3.2.1(g) Distillation - Solar distillation can prove to be an effective way of supplying drinking water to large number of people. Solar distillation consists of a shallow airtight basin lined with black, impervious material, which contains saline water. Solar radiation is transmitted through the cover

and is absorbed in the black lining. Hence this water is heated to have rise of 10 to 20 degrees or more causing evaporation [29,30]. The resulting vapor rises, condenses as pure water on the inner side of the cover and flows into the condensate collection channels on the sides. An output of about 3 litres/m² with an associated efficiency of 30 to 35 percent can be obtained in a well-designed still on a good sunny day.

1.3.2.1(h) Drying - One of the traditional uses of solar energy is drying of agricultural products. Drying process removes moisture and helps in the preservation of the product. Traditionally drying is done on open ground. Major disadvantages associated with this are (1) process is slow and (2) insects/dust get mixed with the product. Use of solar dryer helps to eliminate these disadvantages. Also drying will be faster and a better quality product is obtained [31].

A cabinet-type solar dryer, is suitable for small-scale use. The dryer consists of an enclosure with a transparent cover. Material to be dried is placed on perforated trays. The absorber inside the dryer absorbs solar radiation entering the enclosure. This leads to the heating of air surrounding the absorber. The hot air is circulated through the perforated trays. As a result the moisture is removed from the product. Suitable openings at the bottom and top ensure a natural circulation. A temperature ranging from 50 to 80 degrees is usually attained, and the drying time ranges from 2 to 4 days [32]. For large-scale drying, natural circulation is replaced by forced circulation.

1.3.2.1(i) Cooking - Another important domestic thermal application is solar cooking. There are different types of designs for solar cooker. One is the 'box type' and the other is 'concentrating type' Box type cooker consists of a rectangular enclosure in which food to be cooked is placed in shallow vessels. Temperature around 100 degrees can be obtained in these cookers on sunny days. Pulses, rice, vegetables, etc., can be readily cooked with this

type of cooker [33-35]. Time taken for cooking depends on solar radiation and varies from half to two and a half hours.

In concentrating type, radiation is concentrated by a parabolic reflecting surface. Cooking vessel is placed at the focus of the parabolic mirror and is thus directly heated. These cookers require tracking. Temperatures well above 400°C can be achieved in such cookers. Various types of reflector surfaces are used for this type of cooker. These include glass mirrors, aluminum sheet and aluminum foil [36].

1.3.2.2 Electrical utilization

Photovoltaic conversion - Devices used in photovoltaic conversion is called solar cell. When solar radiation falls on this semiconductor device, it is directly converted into DC electricity. Two important steps are involved in the principle of working of a solar cell. These are, (1) Creation of pairs of positive and negative charges (called electron-hole pairs) in the solar cell by absorbed solar radiation. (2) Separation of the positive and negative charges by a potential gradient within the cell. For the first step to occur, the cell must be made of a material which can absorb the energy associated with the photons of sunlight. The only materials suitable for absorbing the energy of the photons of sunlight are semiconductors like silicon, cadmium sulphide, copper indium sulphide, Copper indium selenide, gallium arsenide, etc. [37-40]. Major advantage associated with solar cell is that it has no moving parts, require little maintenance, and work quite satisfactorily with beam and diffuse radiation. Also they are readily adapted for varying power requirements because a cell is like a 'building block' Major difficulty of solar cell is the high cost. However, significant developments have taken place in the last few years. New types of solar cells have been developed, through innovative manufacturing processes. Conversion efficiencies of existing types have increased considerably. It is obvious that in future solar

cell may become one of the most important sources of power for electrical energy.

1.4 Other Methods of Solar Energy Utilization

1.4.1 Wind Energy - Winds are caused because of two factors, (i) the absorption of solar energy on the earth's surface and in the atmosphere, and (ii) the rotation of the earth about its axis and its motion around the sun [41,42]. Because of these factors, alternate heating and cooling cycles occurs leading to differences in pressure, and the air is forced to move. Wind energy is thus an indirect manifestation of solar energy. A wind machine mainly consists of rotor, which rotates with the speed of the wind. The rotor causes mechanical energy, which is converted to electrical energy through a shaft with the help of a turbine. Advantages of using wind energy are (1) that its potential as a source of power is reasonably good (2) technology is well developed (3) suitable for large-scale power production.

1.4.2 Wave Energy - Wave arises from the interaction of winds with the surface of the oceans. Hence it is also one of the indirect ways of utilizing solar energy. The most common wave energy conversion is the oscillating water column system. Basically it consists of a chamber in the sea, exposed to the wave action through an opening on the side. The air inside the chamber is alternatively compressed or expanded due to wave action. Thus a pulsating bi-directional air movement occurs through an opening at top of the chamber. This bi-directional flow can be converted to a uni-directional flow through a system of four valves. The uni-directional flow drives an air turbine, which in turn is coupled to an electrical generator [43].

1.4.3 Ocean Thermal Energy Conversion (OTEC) - OTEC systems utilize temperature difference between water at the surface and lower level of the ocean [44]. This difference is around 20°C and covers over a few hundred meters. Temperature at the surface is fairly constant for the first few

meters because of mixing. Subsequently, it decreases and approaches a low value at the bottom of the sea. It works on closed Rankine cycle. Warm water at the surface of sea is pumped through an evaporator where the working fluid (in the form of a high-pressure liquid) absorbs heat and is converted into vapor. The vapor drives turbine-generator producing electricity. Then the vapor is condensed in condenser using a cold water pipe. The condensed liquid is pressurized before being fed into the evaporator again, thereby closing the cycle.

1.4.4 Energy from Biomass - There are a variety of ways of obtaining energy from biomass. These are broadly classified as 'direct method' and 'indirect method' In the first case the biomass is burnt and the energy is tapped. Common example is the burning of wood. In the later case, biomass is converted into a usable fuel in solid, liquid or gaseous form. These are classified into thermo chemical conversion and biological conversion. Thermo chemical conversion includes processes like destructive distillation, pyrolysis, and gasification, while biological conversion includes process like fermentation [45,46]. Biomass energy is most suitable for rural India. Interestingly this is much suitable for cities, since solid wastes can be used for energy generation.

Renewable energy technologies produce marketable energy by converting natural phenomena into useful forms. These resources represent a massive energy potential, which greatly exceeds the potential of fossil fuel resource. It is becoming increasingly evident that renewable energy technologies have a strategic role to play in the achievement of sustained economic development and environmental protection. It is virtually uninterrupted and available everywhere. Moreover, it is by and large, pollution free. Renewable energy technologies can be used for a variety of applications that can meet practically every type of energy demand.

The socio-economic benefits to be accrued from increasing the utilization of renewable are many. These include positive effects to counter rural de-population by job-creation through renewable energy efforts, improved living conditions and infrastructure in the less favored regions. For example one can consider improved quality of life through rural electrification and economic benefits through reduction of fossil fuel imports. Renewable energies are socio-economically desirable and will have to play an important role in India's energy mix. It is important to stimulate the acceleration of market uptake. A number of specific promotional measures must be adopted, to help proliferating use of this new type of energy source [47].

1.5 Flat Plate Collector (FPC)

The flat plate collector is the heart of any solar energy collection system designed for operation in the low temperature range (ambient-60°C) or in the medium temperature range (ambient-100°C). It is used to absorb solar energy, convert it into heat and then to transfer the heat to a stream of liquid or gas. It absorbs both direct and diffuse radiation, and is usually mounted on the top of a building or other structures. It does not require tracking of the sun and requires little maintenance.

Essentially the majority of flat plate collectors consist of several basic elements. These are as follows:

- (i) Absorber plate which may be flat, corrugated or fins or passages attached to it, which is normally metallic, upon which the short wave solar radiation falls and is absorbed.
- (ii) Glazing, this may be one or more sheets of glass or some other diathermanous (radiation transmitting) material.
- (iii) Thermal insulation provided at the back and sides of the absorber plate to minimize the heat losses.

- (iv) Container or casing, which surrounds the various components and protects them from dust, moisture, etc.

Flat plate collectors are basically divided in two groups according to their use, (i) water or liquid heaters, and (ii) air heaters. Flat plate collectors have the following advantages over other types of energy collectors

- (i). absorb direct, diffuse and reflected components of solar radiation,
- (ii). are fixed in tilt and orientation and, thus, there is no need of tracking the sun,
- (iii). are easy to make and are low in cost.
- (iv). have comparatively low maintenance cost and long life,
- (v). operate at comparatively high efficiency.

The principle behind a flat plate collector is simple. If a metal sheet is exposed to the solar radiation, the temperature will rise until the rate at which energy is received is equal to the rate at which heat is lost from the plate; this temperature is termed as 'equilibrium temperature'. If the back and side of the plate are protected by a heat insulating material, and the exposed surface of the plate is painted black and is covered by one or two glass sheets, then the equilibrium temperature will be much higher than that for the simple exposed sheet [12,48]. The plate may be converted into an air heater or water heater by passing air/water through the plate by ensuring sufficient heat transfer arrangement.

1.6 Solar Air Heaters

Compared to other solar collectors, solar air heaters (SAH) have some distinct advantages. The mode of heat transfer from the absorber plate and the working fluid is the main difference between liquid flat plate

collectors and air heaters. The air heaters eliminate the need to transfer heat from the working fluid to another working fluid. Air is being directly used as the working substance, the system is less complicated and is compact. The corrosion problem, which can become serious in solar water heater, is completely eliminated in solar air heaters. Hence light gauge steel or aluminium plates can easily be used. Hence, a solar air heater appears to be inherently cheaper and can last longer. Unlike liquid flat plate collectors, system is not pressurized and therefore, light gauge metal sheets can be used. In solar air heaters leakage is also not a big problem, unlike in liquid collectors [16].

One of the major problems in improperly designed air heating collectors is the poor heat transfer from the absorber plate to the air. The heat transfer coefficients can be considerably improved in several ways, and efficiencies comparable to those of liquid flat plate collectors can be obtained by properly designing the air heater [49]. Owing to the low density of air, large volume of air has to be handled, in comparison with the volume of liquid required to collect the same amount of heat. Another disadvantage is the low thermal capacity of air. The principle of solar air heater is virtually the same as that of the liquid flat plate collector. Air is circulated in contact with a black radiation-absorbing surface, which is usually over-laid by one or more transparent covers for heat loss reduction.

1.7 General Description on SAH

Conventional solar air heater consists of a flat plate collector with an absorber plate, transparent cover system at the top and insulation at the bottom and on the sides. Whole assembly is enclosed in a sheet metal container. Working fluid is air and the passage for its flow varies according to the type of air heater [50].

Materials for the construction of air heater are similar to the liquid flat plate collectors. Transmission of solar radiation through the cover system and its subsequent absorption in the absorber plate can be taken into account by expressions identical to those of liquid flat-plate collectors. In order to improve collection efficiency, selective coating on the absorber plate can be used.

1.8 Components of Solar Air Heaters

1.8.1 Absorber Plate

The absorber plate should have high thermal conductivity, adequate tensile and compressive strength, and good corrosion resistance. Copper is generally preferred because of its extremely high conductivity and resistance to corrosion. Collectors are also constructed with aluminum, steel, Galvanized Iron (GI) sheets and various thermoplastics and metal ions. Standard procedure for fabricating an absorber plate is to take a sheet of metal (like copper or aluminium) and insulate the non flow surface depending on type of solar air heater. Solar radiation absorbed by this metal sheet would heat it and some of the heat is transferred to air. This hot air is used for the practical applications. The details are given in Fig. 1.3.

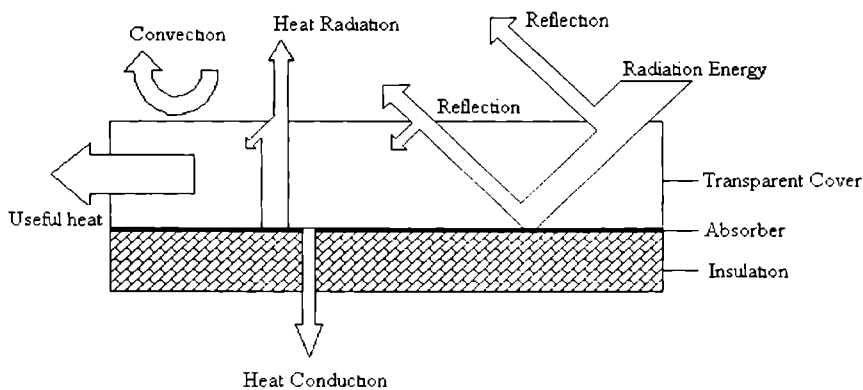


Fig. 1.3 Fundamentals of a flat plate solar air collector with flow over the absorber

1.8.2 Cover Plate

Cover plate or plates through which the solar energy must be transmitted is also extremely important part of solar air heater. Purposes of cover plates are

- to transmit as much as solar energy as possible to the absorber plate
- to minimize the loss from the absorber plate to the environment
- to shield the absorber plate from direct exposure to weathering

The most important requirements of cover plate-materials are strength, durability, non-degradability, and solar energy transmission. Glass is the most common cover material for collectors. Tempered glass has more durability than other glasses and resists thermal cycling. In selecting the glass for cover plates, mechanical strength must be adequate to resist breakage from the maximum expected wind and snow loads. Mechanical strength is proportional to the square of the thickness of the glass. Cover plates for solar collectors normally should be at least 0.33cm thick.

Thermal shock to glass cover plate also is taken into account. Several different processes cause it. For example day-by-day heating and cooling caused by variation in solar intensity on the collectors during the morning hours and subsequent decrease in the afternoon. Again in cloudy conditions, glass temperatures can rise and fall by 50 degrees or more in a matter of minutes as clouds pass overhead. Central area of the collectors is subjected to greater heating than edges. This results in thermal stress, which can cause breakage of glass covers.

Rigidity of the glass cover is important. Rigidity is proportional to the cube of the thickness of the plate. Plastic materials such as acrylic polycarbonate plastics, plastic films of Tedlar and Mylar and commercial plastics such as Lexan can be used as cover plates. However plastic material has limited lifetime because of the effect of the UV light, which reduces

transmissivity of plastic. Main advantage of plastic materials is the resistance to breakage, reduction in weight and low cost.

1.8.3 Insulation

Insulation is used to prevent loss of heat from the absorber plate due to conduction or convection. Usual insulating materials are rock wool or glass wool. Absorber plate should be insulated beneath and or in the side, depending on the type of design used. Important requirement of an insulator is that it should be heat resistant [51,52].

1.9 Classification of Solar Air Heater

Solar air heaters are of many types. In some of these, the absorber surface beneath the glazing includes overlapped, spaced, clear and black glass plates, single smooth metal sheets, stacked screens or mesh, corrugated metal plates or finned metal sheets, etc. In others air passing beneath the absorber plate or underlying air passage reduces downward heat loss; and one or two covers of glass or transparent plastic provide resistance to upward convection and radiation losses.

Depending on the absorber plate, air heaters can be classified into two types [53]; porous collector and non porous collector. Further variations may be defined by the performance improvement techniques employed and by the air flow path.

1.9.1 Nonporous Type Solar Air Heaters

1.9.1(a) Type I - In this type [Fig. 1.4] air steam does not flow through the absorber plate, but may flow above or below it [54]. No separate passage is required and air flows between transparent cover system and absorber plate. This type of air heater has a disadvantage. Due to the flow of hot air above the absorber, cover receives much of the heat and in turn losses it to the ambient.

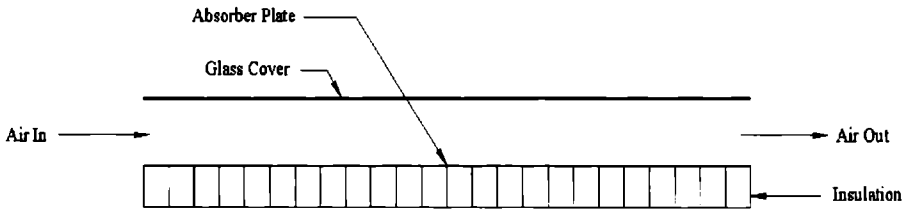


Fig. 1.4 Type I Non-porous solar air heater (flow above the absorber)

1.9.1(b) Type II - Here [Fig. 1.5] air passage is below absorber plate. A plate parallel to the absorber plate is provided in between absorber and insulation, forming the passage. Also loss of heat is minimal in this type [55,56].

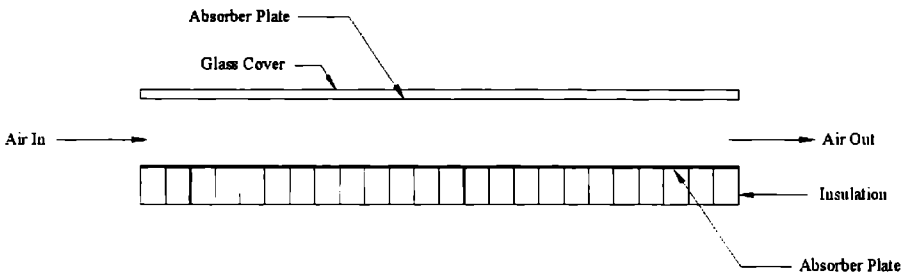


Fig. 1.5 Type II Non-porous solar air heater (flow under the absorber)

1.9.1(c) Type III In this type [Fig. 1.6] absorber plate is cooled by air stream flowing on both sides of the plate. It may be noted that heat transfer between the absorber plate and the airflow is low. This is because of low efficiency of this type of solar air heaters. Roughening the absorber surface or using corrugated plate as the absorber, improves performance [57-59]. Turbulence induced in the airflow increases convective heat transfer. Unless selective coatings are used, radiative losses from absorber plate of nonporous type are significant. Hence collection is poor. Also use of fins may result in prohibitive pressure drop, limiting the applicability of nonporous type.

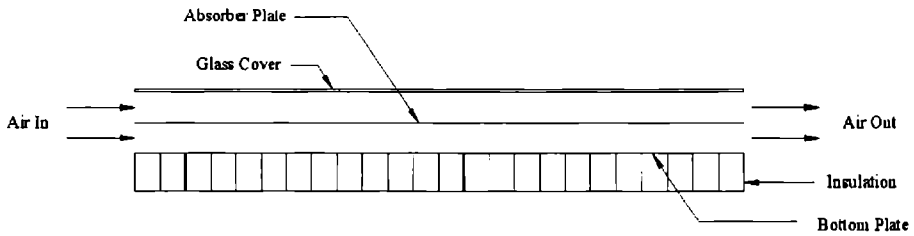


Fig. 1.6 Type III Non-porous solar air heater (flow both above and beneath the absorber)

1.9.2 Porous Type Solar Air Heaters

In porous type solar air heaters, absorber plate is porous. This type of heaters has several advantages. Solar radiation penetrates to greater depth and is absorbed along its path. As a result, radiation loss decreases. Air stream heats up as it passes through the matrix and pressure drop is usually lower than that in nonporous type. It must be, however, noted that improper choice of matrix porosity and thickness may cause reduction in efficiencies since thickness of matrix may not be sufficient enough to transfer heat to air stream. Wire meshes or porous beds formed by broken bottles are some examples of most economic porous absorbers.

1.9.2(a) Matrix type solar air heaters - This is an example of porous air heater. In matrix air heater, the fluid flows through a porous matrix on which solar radiation is directly incident. Radiation penetrates through the matrix and is gradually absorbed. Air is introduced at top and is heated as it flows down through the matrix in reverse manner. The reason is that in the first arrangement both the glass cover and the top surface of the matrix are in contact with the incoming air and are at the lowest possible temperatures [60-63]. As result, top losses are reduced. The matrices used have been made by stacking wire screen meshes or slit-and-expanded metallic foils.

1.9.2(b) Honeycomb porous-bed solar air heater - It is a variation of matrix air heater. The use of honeycomb structure [Fig. 1.7] between cover and

absorber reduces top convective losses. Air is passed through honeycomb structure. Honeycomb structure is rectangular or hexagonal shape. The honeycomb structures are attached to the matrix materials, which reduces convection and radiation to cover glass [64].

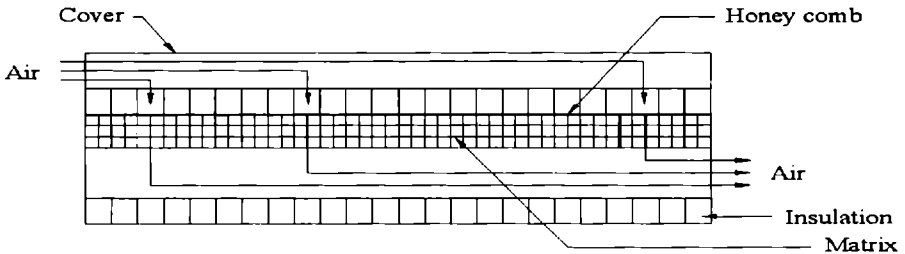


Fig. 1.7 Honeycomb porous bed air heater

1.9.3(c) Overlapped glass plate air heater - This type [Fig. 1.8] of air heater consists of a series of overlapping parallel glass plates, the lower being blackened. Air flows parallel to the glass plates and in between them. A honeycomb wall passage is used at the inlet in order to direct the air and to ensure that its velocity is uniform. Bottom of the unit is insulated [65]. Advantages of overlapped glass plate air heaters are the low-pressure drop and high collector face area.

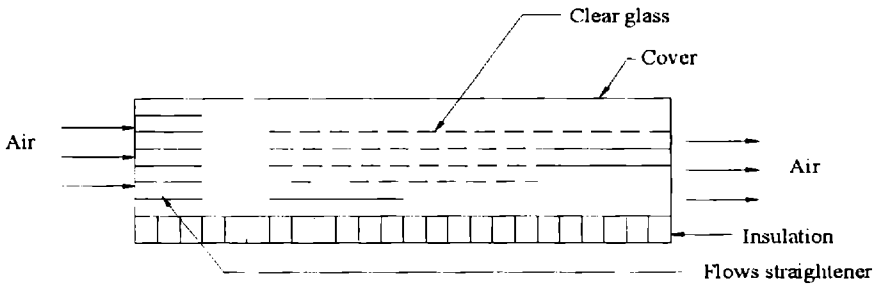


Fig. 1.8 Overlapped glass plate solar air heater

1.9.3(d) Jet plate solar air heater - In jet plate solar heater, an additional glass plate called a jet plate is introduced between the absorber and the

bottom plate [Fig. 1.9]. The jet plate has a number of equally spaced holes drilled in it. Air entering the heater flows in between the absorber plate and the jet plate as well as between the jet plate and bottom plate [66]. The impinging air jet increases value of convective heat transfer coefficient from bottom of absorber plate. This results in a significant improvement in useful heat gain and the collection efficiency.

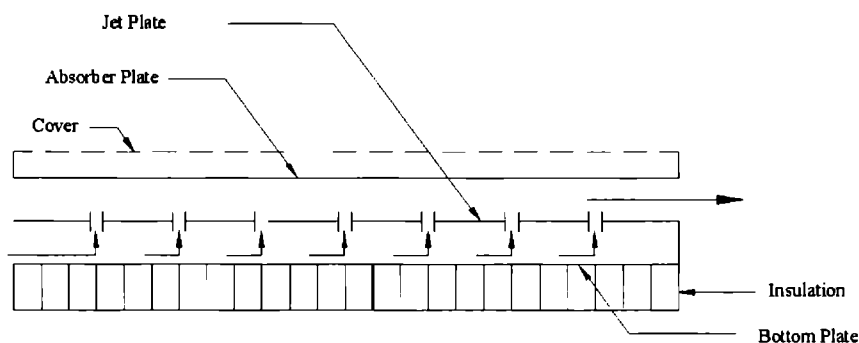


Fig. 1.9 Jet plate solar air heater

1.10 Parameters Associated with the Construction of an Air Heater

1.10.1 Heater Configuration - Heater configuration is the aspect ratio of duct and length through which air passes.

1.10.2 Airflow - Air must be pumped through the heater. Increasing the air velocity results in higher collection efficiencies.

1.10.3 Transmittance Properties of the Cover - The type and number of layers of cover material must be considered and spectral transmittance properties must be examined. In general, as temperature requirement is high, more number of covers is required. Principle underlying the use of multi-covers is that each air layer between two successive covers provides a barrier against heat loss from the absorbing surface to the surroundings. However, with a large number of covers, reflective losses increase. Covers of high

transmissivity and low reflectivity are desired to keep the amount of reflected and absorbed radiation low.

1.10.4 Absorber Plate Material Selective surfaces can improve performance of solar air heaters by increasing collector efficiency. Absorber is coated black to absorb maximum amount of incident radiation.

1.10.5 Natural Convection Barriers - Stagnant air interposes high impedance to convective heat flow between the absorber plate and the ambient air. Losses are reduced by the use of multiple covers or honeycombs.

1.10.6 Plate-to-air Heat Transfer Coefficient - Absorber can be roughened and coated to increase coefficient of heat transfer between the air and the plate. Roughness ensures high level of turbulence in the boundary layer of the flowing stream. For this reason, crumpled or corrugated sheets and wire screens are attractive as absorbing materials.

1.10.7 Insulation - Insulation is required at the absorber base to minimize heat losses through the underside of the heater.

1.10.8 Solar Radiation Data - Solar radiation data corresponding to the site are needed to evaluate heater performance [52,67].

1.11 Performance Analysis of a Conventional Solar Air Heater

Fig. 1.5 shows schematics of a conventional air heater. Air to be heated flows in a parallel passage below the absorber. The thermal performance of such a heater was first investigated by Whillier [50].

Let length and the width of the absorber plate is L_1 and L_2 respectively. Let us consider an element area $L_2 dx$ at a distance x from the inlet [Fig. 1.10].

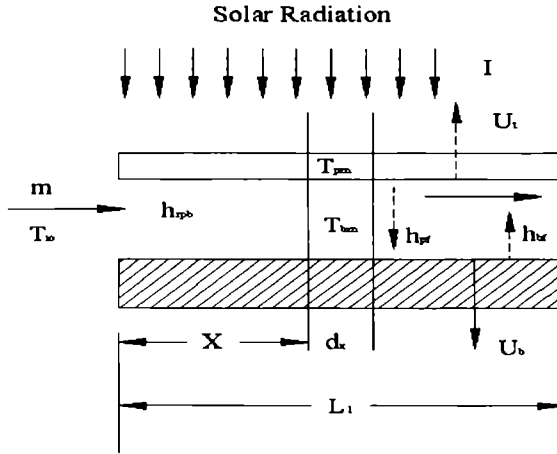


Fig. 1.10 Heat transfer process in a conventional air heater

Energy balance equations for the absorber plate, bottom plate and air stream can be written as:

For Absorber plate.

$$I(t) = U_i (T_{pmi} - T_a) + h_{pf} (T_{pmi} - T_f) + h_{rpb} (T_{pmi} - T_{bmi}) \quad (1.3)$$

For bottom plate

$$h_{rpb} (T_{pmi} - T_{bmi}) = h_{brf} (T_{bmi} - T_f) + U_b (T_{bmi} - T_a) \quad (1.4)$$

For air stream

$$m C_{air} dT_f = h_{pf} L_2 dx (T_{pmi} - T_f) + h_{brf} L_2 dx (T_{bmi} - T_f) \quad (1.5)$$

These equations can be solved for the air temperature in a way similar to that of liquid flat plate collector. Then, rise in temperature of air through the duct can be estimated, to write the useful heat gain rate of the collector (Q_u) in the following form:

$$Q_u = F_R A_p [I - U_L (T_i - T_a)] \quad (1.6)$$

Where F_R is the collector heat removal factor and is given by,

$$F_R = m C_{air} / (U_L A_p) [I - \exp [-F^1 U_L A_p / (m C_{air})]] \quad (1.7)$$

$$\text{Where } U_L = U^1 + (1/F^1) [U_b h_{brf} / (h_{rpb} + h_{brf} + U_b)] \quad (1.8)$$

$$U^1 = U_t + [h_{rpb} U_b / (h_{rpb} + h_{bf} + U_b)] \quad (1.9)$$

And the collector efficiency factor (F^1) is given by,

$$F^1 = [1 + U^1 / h_c]^{-1} \quad (1.10)$$

$$\text{with } h_c = \left[h_{pf} + \frac{h_{rpb} h_{bf}}{h_{rpb} + h_{bf}} \right] \quad (1.11)$$

The useful heat gain can be calculated from Eq. (1.6) and is in a form similar to that of liquid flat plate collectors.

1.12 Heat Transfer and Pressure Drop in a Parallel Plate Duct

In order to calculate the performance based on Eq. (1.6), we need to know the values of the convective heat transfer coefficient to the heated air. The situation corresponds to one of turbulent flow with one of the long sides heated and the other insulated. It can be considered to be fully developed if the length-to-equivalent diameter ratio exceeds a value of about 30. The following two correlations are then appropriate if the surfaces are smooth,

$$Nu = 0.0158 Re^{0.8} \quad (1.12)$$

$$Nu = \frac{0.01344 Re^{0.75}}{1 - 1.586 Re^{-0.125}} \quad (1.13)$$

Equation (1.12) is based on the Kays [68], while Eq. (1.13) has been suggested by Malik and Buelow [69]. In the above equations, the characteristic dimension is the equivalent diameter d_e given by

$$d_e = \frac{4 \times \text{Cross-sectional area of duct}}{\text{Wetted perimeter}} \quad (1.14)$$

Properties are evaluated at the arithmetic mean of the fluid inlet and outlet temperature, and the values of h_{fp} and h_{fb} are taken to be equal. Nusselt numbers calculated from Eqs. (1.12) and (1.13) agree within 10 per cent for Reynolds numbers ranging from 10000 to 20000. These values are normally obtained in solar air heater applications.

The dimensionless pressure drop in the duct can be calculated from the well-known Blasius equation which is valid for smooth surfaces.

$$f = 0.079Re^{-0.25} \quad (1.15)$$

where Nu is the Nusselt number, Re is the Reynolds number, f is the friction factor and the characteristic dimension is again the equivalent diameter d_e in meter.

1.13 Testing Procedures

ASHRAE 93-77 [70] sets forth three standard test procedures for liquid heaters and one for air heaters. A schematic diagram showing the essential features of the test set-up is shown in Figure 1.11. It is a closed loop consisting of the solar air heater to be tested, a blower and an apparatus for reconditioning the air which ensures that the air enters the air heater at the desired temperature, T_i . The essential features of the testing procedures can be summarized as follows:

- 1 Means are provided to feed the collector with fluid at a controlled inlet temperature; tests are made over range of inlet temperatures.
- 2 Solar radiation is measured by a pyranometer on the plane of the collector.
- 3 Means of measuring flow rate, inlet and outlet fluid temperatures, and ambient conditions are provided
- 4 Means are provided for measurements of pressure and pressure drop across the collector

The ASHRAE method for air collectors includes the essential features of those for liquid heaters, with the addition of detailed specifications of conditions relating to air flow, air mixing, air temperature measurements, and pressure drop measurements.

Measurements may be either outdoors or indoors. Indoor tests are made using a solar simulator, that is, a source producing radiant energy that has spectral distribution, intensity, uniformity in intensity, and direction closely resembling that of solar radiation. Means must also be provided to move air to produce wind [71,72]. There are not many test facilities of this kind available, the results are not always comparable to those of outdoor tests, and most collector tests are done outdoors. Gillet [73] has compared the results of outdoor tests with those of mixed indoor and outdoor tests and reported that diffuse fraction and long wave radiation exchange can affect the relative results of the tests.

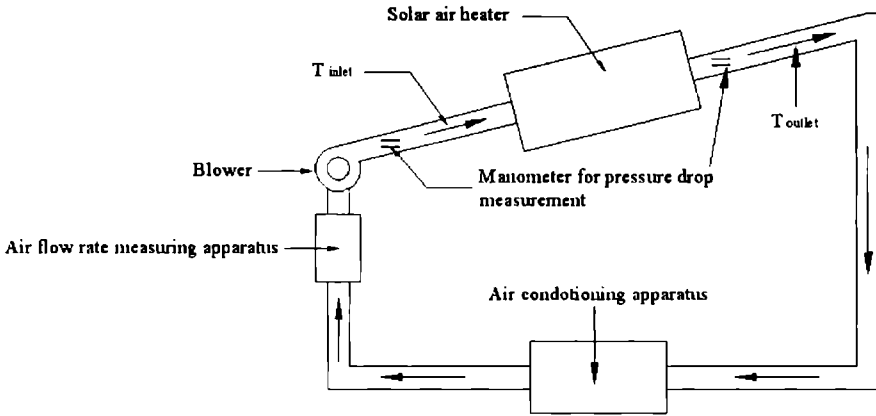


Fig. 1.11 Schematic diagram of set-up for testing solar air heaters

Since the fluid is air, it has to be ensured that it is well mixed at the exit from the air heater before its temperature is measured. Mixing is achieved with the help of vanes. As an additional precaution, temperatures at inlet and exit of air heater is measured at a number of locations across the duct cross section.

Standard specifies that collector shall be tested under clear sky conditions in order to determine its efficiency characteristics. On any given day, data is recorded under steady state conditions for fixed values of m and

at T_i . For each set of values, it is recommended that an equal number of tests be conducted symmetrically before and after solar noon.

Principal measurements made in each set are the fluid flow rate m , the fluid inlet and outlet temperatures of the collectors (T_i and T_o), solar radiation incident on the collector plane (I_T), ambient temperature (T_a), the pressure drop across the collector (ΔP), and the wind speed (V_∞). Tests are made with a range of inlet temperature conditions. To minimize effects of heat capacity of collectors, tests are usually made in nearly symmetrical pairs, one before and one after solar noon, with results of the pairs averaged.

The thermal behaviour of the collector is reported by the following equation

$$\eta = F_R \left[(\tau\alpha)_e - U_L \left(\frac{T_i - T_a}{I} \right) \right] \quad (1.16)$$

If U_L , F_R , and $(\tau\alpha)_e$ were all constant, the plots of η versus $(T_i - T_a)/I$ would be straight lines with intercept $F_R(\tau\alpha)_e$ and slope $-F_R U_L$. However, they are not, and the data scatter. U_L is a function of temperatures and wind speed, with increasing dependence as the number of covers increases. Also, F_R is a weak function of temperature and some variations of the relative proportions of beam, diffuse, and ground-reflected components of solar radiation will occur. Thus scatter in the data are to be expected, because of temperature dependence, wind effects, and angle of incidence variations. In spite of these difficulties, long-time performance of many solar heating systems, collectors can be characterized by the intercept and slope. i.e., $F_R(\tau\alpha)_e$ and $F_R U_L$.

Furthermore, considering that the performance can be expressed by another equation, containing the temperature gain produced by the collector and the Instantaneous efficiency, η are determined from

$$\eta = Q_u / (A_c I) = m C_p (T_o - T_i) / (A_c I) \quad (1.17)$$

As stated earlier, readings are recorded under steady state conditions. A collector is considered to be operating under steady state conditions, if deviation of experimental parameters is less than the following specified limits over a 15-minute period:

- Global radiation incident on collector plane $\pm 50 \text{ W/m}^2$
Ambient temperature $\pm 1^\circ\text{C}$
- Fluid flow rate $\pm 1 \%$
- Fluid inlet temperature $\pm 0.1^\circ\text{C}$
- Temperature rise across collector $\pm 0.1^\circ\text{C}$

In addition, it is specified that value of 'I' should be greater than 600 W/m^2 Wind speed should be between 3 and 6 m/s, and fluid flow rate should be set at approximately at 0.02 kg/s per square meter of collector gross area.

1.14 Applications of Solar Air Heater

It is technically feasible to use solar heated air for providing energy for almost any application that uses solar-heated liquids. The important areas of applications are the following.

1.14.1 Space Heating and Cooling of Buildings

Various air heaters have been designed and used in space heating and cooling. Air heaters are used only in actively heated and cooled buildings. Air heaters are also used with desiccant beds for solar air conditioning. Heat from air heaters can also be used to heat generator of an absorption air conditioner for cooling purpose.

1.14.2 Drying and Curing of Agricultural Products

This is a promising area of application of solar air heaters. For a developing country like India, agriculture is the backbone of the economy [31]. Importance of drying is relevant as far as the growth of the economy is concerned. Indirect drying of crops is possible with the help of solar air heaters. Main advantage of this is the hygienic condition in which it is dried. Chance of contamination of food products with dust or bacteria is very less. In indirect method of drying, hot air from solar air collector is circulated through the crop to reduce its moisture content. The air can be circulated using a fan or by natural convection. Correspondingly, the heaters are called active or passive dryers. In passive dryer the warm air rises through the air heater and enters into the drying chamber due to buoyancy effect.

1.14.3 Industrial Applications

Use of solar air heaters for industrial application is gaining momentum in these days. In timber industry, hot air is used for seasoning timber. In the case of plastic sector, solar air heaters are used for curing of plastics. Another application is the regeneration of dehumidifying agents. In industries solar air heaters are attached to industrial application on the basis of industrial cogeneration. Use of solar air heaters in industrial sector is fast increasing.

Nomenclature

A_c	area of the collector (m^2)
A_p	area of the absorber plate (m^2)
C_{air}	specific heat of air ($J/kg^\circ C$)
d_e	equivalent diameter (m)
f	friction factor
F^l	collector efficiency factor
F_R	collector heat removal factor
h_{bf}	convective heat transfer between bottom and fluid ($W/m^2^\circ C$)
h_e	effective heat transfer coefficient ($W/m^2^\circ C$)
h_{pf}	convective heat transfer coefficient between plate and fluid ($W/m^2^\circ C$)
h_{tpb}	radiative heat transfer coefficient between plate and bottom ($W/m^2^\circ C$)
I	intensity of solar radiation (W/m^2)
m	air mass flow rate (kg/s)
Nu	Nusselt number
Q_u	useful heat gain rate of the collector (W)
Re	Reynolds number
T_a	ambient temperature ($^\circ C$)
T_{bm}	mean bottom plate temperature ($^\circ C$)
T_f	fluid temperature ($^\circ C$)
T_i	inlet air temperature ($^\circ C$)
T_o	outlet air temperature ($^\circ C$)
T_{pm}	mean plate temperature ($^\circ C$)
U_b	bottom loss coefficient ($W/m^2^\circ C$)
U_L	overall heat loss coefficient of the collector ($W/m^2^\circ C$)
U_t	top loss coefficient ($W/m^2^\circ C$)
U^l	loss coefficient ($W/m^2^\circ C$)

Greek symbols

$(\tau\alpha)_e$ effective transmissivity-absorptivity product

η Instantaneous efficiency

θ_z zenith angle

References

- [1] BP Statistical Review of World Energy, 2007, [http://www.bp.com/statistical review](http://www.bp.com/statistical-review).
- [2] Bent Sorenson, Renewable Energy: Its Physics, Engineering, Use, Environmental Impacts, Economy and Planning aspects, Third Edition, Elsevier Academic Press, London, 2004.
- [3] Godfery Boyle, Renewable Energy: Power for a Sustainable Future, Second Edition, Oxford University Press, New York, 2004.
- [4] Malti Goel, Energy Sources and Global Warming, Allied Publishers Private Limited, New Delhi, 2005.
- [5] Paul Kruger, Alternative Energy Resources-The Quest for Sustainable Energy, John Wiley & Sons, New Jersey, 2006.
- [6] M. Daniel, Berman and T. John and O' Connor, Who Owns the Sun? People, Politics, and the Struggle for a Solar Economy, Chelsea Green Publishing Company, White River Junction, Vermont, 1996.
- [7] Hermann Scheer, The Solar Economy – Renewable Energy for a Sustainable Global Future, Earth Scan Publications Ltd, London, Sterling, VA, 2002.
- [8] Travis Bradford, Solar Revolution – The Economic Transformation of the Global Energy Security, The MIT Press, Cambridge, Massachusetts, London, 2006.
- [9] William James Burrougs, Climate Change: A Multidisciplinary Approach, Cambridge University Press, 2001.
- [10] Douglas Long, Global warming, Viva Books Private Limited, New Delhi, 2005.
- [11] Victor and G. David, The Collapse of the Kyoto Protocol and the Struggle to Slow Global Warming, Princeton University Press, Princeton, 2001.

- [12] J.A. Duffie, W.A. Beckman, *Solar Engineering of Thermal Processes*, John Wiley & Sons, New York, 1991.
- [13] J. Gordon, *Solar Energy- The State of the Art*, ISES Position Papers, James & James (Science Publishers) Ltd., UK, 2005.
- [14] G.N. Tiwari, *Solar Energy: Fundamentals, Design, Modelling and Applications*, Narosa Publishing House, New Delhi, 2005.
- [15] H. P. Garg and J. Prakash, *Solar Energy: Fundamentals and Applications*, Tata McGraw Hill Publishing Company Ltd., New Delhi, 2000.
- [16] S.P. Sukhatme, *Solar Energy: Principles of Thermal Collection and Storage*, Tata Mc Graw Hill Company Limited, New Delhi, 1996.
- [17] G.N. Tiwari, *Solar Energy: Fundamentals, Design, Modelling and Applications*, Narosa Publishing House, New Delhi, 2005.
- [18] B.S. Magal, *Solar Power Engineering*, Tata McGraw Hill Company Limited, New Delhi, 1990.
- [19] Indian Standard 12933 (part 2), Bureau of Indian Standards, *Solar Flat –plate collector-Specifications, Part 2- Components*, 1992.
- [20] [20] S.S. Mathur and T.C. Kandpal, *Solar Concentrators, Reviews of Renewable Energy Sources*, Vol. 2, Chapter 5, Wiley Eastern Ltd., New Delhi, 1984.
- [21] H.P. Garg, *Advances in Solar Energy Technology*, Vol. 1 D. Reidel Publishing Company, Holland, 1987.
- [22] R. Winston, *Principles of solar concentrators of novel design*, *Solar Energy* 16, 89, 1974.
- [23] C. Richard, Schubert and L.D. Ryan, *Fundamentals of Solar Heating*, Prentice-Hall, Inc., Englewood Cliffs, New Jersey, 1981.
- [24] P.De. Laquil, D. Kearney, M. Geyer and R. Diner, *Solar Thermal Electric Technology*, *Renewable Energy* (Executive Editor: Laurie Burnham), Island Press, Washington, 213-296, 1993.

- [25] F. Danials, *Direct Use of the Sun's Energy*, Yale University Press, New Haven, USA, 1929.
- [26] J. Gretz, A. Strub and W. Palz, *Thermo-mechanical Solar Power Plants*, D. Reidel Publishing Co., Dordrecht, Holland, 1984.
- [27] B.J. Brinkworth, *Refrigeration and Airconditioning, Solar Energy Engineering* (Edited A.A.M. Sayigh), Chapter 16, 341-364, Academic Press, New York, 1977.
- [28] *ASHRAE Handbook – Fundamentals*, American Society of Heating, Refrigerating, and Air Conditioning Engineers, Atlanta, GA, 1985.
- [29] G.N. Tiwari and Y.P. Yadav, *Economic analysis of large scale solar distillation plant*, *Energy Conversion and Management* 25, 423, 1985.
- [30] G.N. Tiwari, U. Singh and J.K. Nayak, *Applied Thermal Energy Devices*, Kamala Kuteer Publications, Narsapur, 1985.
- [31] M.S. Sodha, N.K. Bansal, A. kumar, P.K. Bansal and M.A.S. Malik, *Solar Crop Drying*, Vol 1, CRC Press, USA, 1987.
- [32] M.S. Sodha, A. Dang, P.K Bansal, S.B. Sharma, *An analytical and experimental study of open sun drying and a cabinet type dryer*, *Energy Conservation and Management* 25(3), 263-271, 1985.
- [33] M.K. Ghosh, *Solar Cooker*, *Bull. Inst. Engineers (India)* 14(12), 1-7, 1965.
- [34] T.C. Thulasi Das, S. Karunakar and D.P. Rao, *Solar box cooker:part II - Analysis and Simulation*, *Solar Energy* 52(3), 265-272, 1994.
- [35] S.C. Mullick, T.C. Kandpal and A.K. Saxena, *Thermal test procedure for box-type solar cookers*, *Solar Energy* 39(4), 353-360, 1987.
- [36] S.C. Mullick, T.C. Kandpal and Subodh Kumar, *Thermal test procedure for a paraboloid concentrator solar cooker*, *Solar Energy* 46(3), 139-144, 1991.
- [37] K. L. Chopra, *Thin Film Phenomena*, Mc Graw Hill, New York, 1969.

- [38] K. L. Chopra and S. R. Das, *Thin Film Solar Cells*, Plenum Press, New York, 1983.
- [39] P. Jayarama Reddy, *Science and Technology of Photovoltaics*, BS Publications, Hyderabad, 2004.
- [40] N.K. Bansal, *Photovoltaic Systems*, Omega Scientific Publishers, New Delhi, 2003.
- [41] Paul Gipe, *Wind Energy Comes of Age*, John Wiley & Sons, Inc., New York, 1995.
- [42] Richard L. Hills, *Power from Wind: A History of Windmill Technology*, Cambridge University Press, New York, 1994.
- [43] S.K. Agarwal, *Non conventional Energy Systems*, A.P.H. Publishing Corporation, New Delhi, 2005.
- [44] Maheswar Dayal, *Renewable Energy: Environment and Development*, Konark Publishers Pvt. Ltd., New Delhi, 1989.
- [45] N.H. Ravindranath and D.O. Hall, *Biomass, Energy and Environment: A Developing Country Perspective from India*, Oxford University Press, New York, 1995.
- [46] Donald L. Klass, *Biomass for Renewable Energy, Fuels, and Chemicals*, Academic Press, USA, 1998.
- [47] W. Jefferson, Tester, Elizabeth M. Drake, Michael J. Driscoll, W. Michael Golay, William A Peters, *Sustainable Energy: Choosing among Options*, The MIT Press, Cambridge, Massachusetts, 2005.
- [48] H.P.Garg, *Treatise on Solar Energy*, John Wiley, New Delhi, 1982.
- [49] K. Altfeld and W Leiner, Second law optimization of flat plate solar air heaters, *Solar Energy* 41, 127-132, 1998.
- [50] A. Whillier, Performance of black-painted solar air heaters of conventional design, *Solar Energy* 8(1), 31-37, 1964.

- [51] A.R. Shukla, H.P. Garg and R.S. Adhikari, Performance of a solar air heating collector designed as per Indian specifications, *J. of the Solar Energy Society of India* 7(2), 1997.
- [52] S. Robert Hastings and Ove Morck, *Solar Air Systems: A Design Handbook*, James & James (Science Publishers) Ltd., London, UK, 2000.
- [53] D.J. Close, Solar air heaters for low and moderate temperature applications, *Solar Energy* 7(3), 117-124, 1963.
- [54] A.K. Bhargava, H.P. Garg and V.K. Sharma, Evaluation of the performance of air heaters of conventional designs, *Solar Energy* 29(6), 523-533, 1982.
- [55] P. Biondi, L. Cicala and G. Farina, Performance analysis of solar air heaters of conventional design, *Solar Energy* 41(1), 101-107, 1988.
- [56] D.L. Loveday, Thermal performance of air heating solar collectors with thick, poorly conducting absorber plates, *Solar Energy* 41(6), 593-602, 1988.
- [57] S. Satcunanathan and S. Deonarine, A two-pass solar air heater, *Solar Energy* 15, 41-49, 1973.
- [58] H.P. Garg, V.K. Sharma and A.K. Bhargava, Theory of multiple-pass solar air heaters, *Energy* 10, 589-599, 1985.
- [59] N.E. Wijeyesundera, L.L. Ah and L.E. Tjioe, Thermal performance study of two-pass solar air heaters, *Solar Energy* 28, 363-370, 1982.
- [60] R.K. Swartman and O. Ogunlade. An investigation on packed bed collectors, *Solar Energy* 10, 106-110, 1966.
- [61] F.L. Lansing, V. Clarke and R. Reynolds, A high performance porous flat-plate solar collector, *Energy* 4, 685-694, 1979.
- [62] S.P. Sharma, J.S. Saini and H.K. Varma, Thermal performance of packed-bed solar air heaters, *Solar Energy* 47(2), 59-67, 1991.

- [63] C.L. Gupta and H.P Garg, Performance studies on solar air heaters, *Solar Energy* 11(5), 25-31, 1967.
- [64] O. Lalude and G. Buchberg, Design and application of honeycomb porous-bed solar air heaters, *Solar Energy* 13, 223, 1971.
- [65] M.K. Selcuk, Thermal and economic analysis of the overlapped glass plate solar air heater, *Solar Energy* 13, 165, 1971.
- [66] C. Choudhury and H.P. Garg, Evaluation of a jet plate solar air heater, *Solar Energy* 46, 199, 1991.
- [67] C. Richard, Schubert and L.D. Ryan, *Fundamentals of Solar Heating*, Prentice-Hall, Inc., Englewood Cliffs, New Jersey, 1981.
- [68] W.M. Kays, *Convective heat and mass transfer*, McGraw-Hill, New York, 1966.
- [69] M.A.S. Malik and F.H. Buelow, Hydrodynamic and heat transfer characteristics of heated air duct, *Heliotechnique and Development* 2(3), 1975
- [70] ASHRAE Standard 93-77, *Methods of testing to determine the thermal performance of solar collectors*, ASHRAE, New York, 1977.
- [71] R.W. Vernon and F.F. Simon, Flat plate collector performance determined experimentally with a solar simulator, NASA TMX-71602, 1974.
- [72] F.F. Simon, Flat plate solar collector performance evaluation with a solar simulation as a basis for collector selection and performance prediction, *Solar Energy* 18, 451, 1976.
- [73] W.B. Gillet, The equivalence of outdoor and mixed indoor/outdoor solar collector testing, *Solar Energy* 25, 543, 1980.

REVIEW ON SOLAR AIR HEATERS, SOLAR DRYERS AND LATENT HEAT THERMAL ENERGY STORAGE

2.1 Solar Air Heaters

Air is generally used as heat transfer fluid in many types of energy conversion systems. In drying applications, industrial process heat and for heating of buildings, solar energy can play a significant role because the warm air is also the final receiver of energy. Flat plate collectors are therefore the best candidates for heating air, but in contrast to liquid solar collectors, the technology and applications of solar air heaters have not been widely developed. The use of air as a working fluid in the solar flat plate collector further eliminates the need for a heat exchanger, which is generally employed for transferring the heat from liquid to air in a liquid flat plate collector. Solar heated air can be used more effectively for drying under controlled conditions. A solar air heater may supply hot air to a conventional dryer, or a special design combining the air heater and the drying cabinet in one package may be used.

Research and development in solar air heating commenced in the 1940s, with studies by Miller [1], Lof [2] and Telkes [3]. These works included the construction and testing of complete solar air heating systems by Lof in 1944 and Telkes in 1947, in houses located in Colorado and Massachusetts, respectively. The overlapped glass solar air heater invented by Lof has been tested by his collaborators [4,5]. Selcuk [6] conducted a quasi-steady state analysis of the overlapped glass plate air heater and tested the model experimentally. In 1950s, Bliss [7] designed, built, and tested a

solar air heating system in an Arizona house. Studies on simple flat plate collectors were conducted by Whillier [8], Close [9], and Gupta and Garg [10]. Charters [11] theoretically investigated the performance of single glazed collector designs having the flow above and below the absorber plate. Cole-Appel and Haberstroh [12] theoretically examined the flow paths for single flat plate employing two glass covers.

Solar air heaters have been made in many variations. Beneath the glazing, absorber surfaces have included overlapped, spaced, clear and black glass plates, single smooth metal sheets, flow-through stacked screens or mesh, corrugated metal plates, finned metal sheets, etc. In some collectors air passing beneath the plate or underlying air passage reduces downward heat loss. Sheven et al. [13] classified various air heating collector designs under six categories according to the type of absorbing surface. Further variations may be defined by the performance improvement techniques employed and by the air flow path.

Theoretical and experimental studies on the corrugated sheet type of solar air collectors were first conducted by Buelow [14]. The idea of a V-groove in the absorber plate for increasing the solar absorptance and the turbulence in the air was given by Hollands [15]

Close [9] examined the effect of equilateral triangular cross sectional grooves with a selective surface for the various flow paths. Charters and MacDonald [16] also examined the V-grooved absorbing surface for the various flow arrangements. Gupta and Garg [10] examined the absorber composed of two sheets of round corrugated material, transversely placed above each other and welded along the length. Cole-Appel and Haberstroh [12] used a simple linear model to compare the thermal performance of five flat plate solar air heater designs, two of which were of the straight finned type. Bevill and Brandt [17] analytically and experimentally studied the

effects of specularly reflecting fins on a single glazed collector with the air flow and the fins located above the absorber plate.

For compact heat exchangers, the corrugated surfaces, in which the air flows perpendicular to the corrugation and moves along undulating paths as it encounters successive peaks and valleys, enhance the convective heat transfer coefficient considerably [18-23]. Augmentation by a factor of 4 to 10 in the convective heat transfer coefficient was reported [20]. Wefeng Gao et al. [24] studied a cross-corrugated heater consists of a wavelike absorbing plate and a wavelike bottom plate, which are crosswise positioned to form the air flow channel. They found that cross-corrugated solar air heaters have much superior thermal performances to that of the flat-plate one.

The main hindrance to the immediate large scale proliferation of solar air heaters for different practical applications is its cost. The cost of air heating by a solar collector is dominated by the collector material cost and air pumping cost. Charters [25] examined the optimization of the aspect ratio of the rectangular flow passage from the view point of minimizing the cost for a fixed pumping power. Hollands and Scheven [26] studied the effect of the dimensions of the rectangular and triangular air flow passages on the coefficient of forced convective heat transfer from absorber to flowing air in plate type air heating collectors. The study carried out by Choudhury [27] and Choudhury and Garg [28], suggestions citing specific examples have been made on the design selection criteria at a predetermined pressure drop required to obtain design features with moderately high efficiency. Hamdan and Jubram [29] have evaluated the cost-effectiveness of bare, covered-and finned-plate air heaters for the Jordanian climate.

Chiou et al. [30] have experimentally and theoretically investigated the heat transfer and flow friction characteristics of six types of slit and expanded aluminium foil matrices. Gupta and Garg [10] examined two mesh type air heaters, one using galvanized iron and the other aluminium. Porous

matrix type air heaters were extensively analysed and tested by Beckman [31] and Hamit and Beckman [32]. These air heaters were used by Selcuk [33] and Akyurt et al. [34] in their solar drying experiments. Lalude and Buchberg [35] have theoretically examined a single glazed porous bed collector with specularly reflecting honeycomb, extending above the porous bed to just under the glass cover. Wiebelt and Thatree [36] have analytically and experimentally studied a V-groove, porous bed, single glazed collector. Lancing et al. [37] have done theoretical analysis on three types of porous flat plate solar collector. A simple analysis on matrix air heaters have been suggested by Neeper [38].

The use of crushed glass as a transpired air heating solar collector material has been suggested by Collier [39]. An investigation on packed bed collectors was conducted by Swartman and Ogunlade [40] and an evaluation of matrix solar collectors for heating air was made by Clary and Morgan [41]. Several designs of solar air heaters have been developed over the years in order to improve their performance. Later many researchers took up the design, employing inexpensive matrix materials (like stones [40], metal wool [37], wool [42] and plants [43]), mainly for application in developing countries. Packed bed solar air heaters with bed materials, slit-and expanded aluminium foil matrix [30,44], wire screen matrix [31,45,46], optically semitransparent material [47], crushed glass matrix [48] were also been investigated. Sodha et al. [49] investigated the effect of different boundary conditions on the performance of matrix air heaters. Coppage and London [50] studied the heat transfer and flow friction characteristics in the ducts using various geometries of wire mesh screen made of stainless steel. Tong and London [51] developed heat transfer and flow friction correlations for such systems. Kays and London [52] gave detailed data for heat transfer and flow friction as applicable to compact heat exchangers which use wire screens inside the heat exchanger tubes. It may, however, be noted that flow

direction in these studies was always normal to the plane of wire screens. Researchers have used wire mesh screen matrices as a heat absorbing media in the solar air heater duct in a bid to improve its performance.

Selcuk [53] suggested the use of broken glass pieces for matrix air heaters. Besides its availability in broken pieces almost without cost, glass being transparent to solar radiation can be used in three ways for absorbing the solar radiation, viz. (i) the top surface is blackened so that the radiation is absorbed at the top, (ii) the radiation is allowed to be absorbed gradually throughout the volume of the matrix, (iii) the bottom of the matrix is blackened so that the unabsorbed radiation is collected at the bottom, which is insulated from the environment.

Ramdan et al. [54] experimentally and theoretically investigated the thermal performance of a double glass-double pass solar air heater with a packed bed above the heater absorber plate with limestone and gravel as packed bed materials. It was inferred that for increasing the outlet temperature of the flowing air after sunset, one can use the packed bed materials with higher masses and therefore with low porosities. It was recommended to operate the system with packed bed with values of equal 0.05 kg/s or lower to have a lower pressure drop across the system. Thermohydraulic investigations on a packed bed solar air heater having its duct packed with blackened wire screen matrices of different geometrical parameters (wire diameter and pitch) was studied by Mittal et al. [55]. Based on energy transfer mechanism in the bed, a mathematical model was developed to compute effective efficiency. A design criterion was also suggested to select a matrix for packing the air flow duct of a solar air heater which results in the best thermal efficiency with minimum pumping power penalty. Paul and Saini [56] studied two types of packed bed collectors (one with wire mesh screen matrix bed and other with pebble bed), which were optimized on the basis of minimum cost per unit energy delivered. Tables for

optimum values of bed parameters namely number of layers, porosity, pitch to wire diameter ratio and pebble diameter have been prepared on the basis of minimum cost per unit energy delivered. These tables can be used by a designer for selecting the optimum values of bed parameters.

Emphasis on solar energy development has also promoted fundamental and applied research on solar air heaters. Heat transfer phenomena related to the absorber plate and the collector assembly was further examined. Among the publications on heat transfer from the absorber plate to the air stream are those by Hollands and Shewen [57], Yusoff and Close [58] and Garg et al. [59]. Heat losses from the collector plate to the ambient by the convection mechanism had been examined both theoretically and experimentally by Randal [60], Meyer [61], and Hollands [62]. Several simple designs were also developed and evaluated. Among several approaches, the work of Misra et al. [63] and Erb [64], using plastics, is worth mentioning. Some building-integrated designs were developed and tested by Peck and Proctor [65] and Gordan and Nerhoof [66].

Charters [11], and Ambrose and Bandopadhyay [67] have also examined the heat transfer phenomena in symmetrically heated ducts representing the flat plate solar collector. Karmare and Tikekar [68] experimentally investigated heat transfer to the airflow in the rectangular duct of an aspect ratio 10:1. The entropy generation in the duct of solar air heater having repeated transverse chamfered rib-groove roughness on one broad wall was studied numerically by Layek et al. [69]

The use of artificial roughness on heat transfer surfaces has been found to be an effective method of enhancement of heat transfer coefficient, although it is accompanied by a substantial increase in friction losses also. A number of investigators have studied the phenomenon of heat and fluid flow over rough surfaces. In one of the earliest studies, Nikuradse [70] identified three flow regions depending on variation of friction factor with roughness

Reynolds number and roughness height. Dipprey and Sabersky [71] developed a heat momentum transfer analogy for flow in tubes having sand grain roughness. The analogy has been used extensively for computation of heat transfer coefficient in flow through tubes. Webb et al. [72] extended the law of wall and the heat momentum transfer analogy to geometrically non-similar roughness and developed correlation valid for flow in circular tubes with transverse ribs and for fully rough flow. These correlations have been used by Han [73] for computation of friction factor and heat transfer coefficient in square ducts with two opposite rib roughened surfaces. Kader and Yaglom [74] developed a general relationship for coefficient of heat transfer for rough wall on the basis of general dimensional and similarity considerations. Vilemas and Simonis [75], in an experimental investigation for flow of air in an annulus (with inner tube, rectangular rib roughness, and transverse to flow) have derived correlations for heat transfer coefficient and friction factor. It has been reported that in the course of transition from partial to fully rough region, a clear kink in Nusselt number versus Reynolds number curve is observed, and the Reynolds number at which change in slope is observed, decreases with an increase in relative roughness height. The optimum operating parameters for the augmentation of heat transfer are the smaller possible height of roughness element, provided that the system operates in the region of the transition from partial to fully rough flow conditions. All these studies used circular passages or square ducts with two opposite walls having rib roughness.

However, an experimental investigation for rectangular ducts having rib roughness on one principal wall was reported by Sparrow and Tao [76]. Prasad and Mullick [77] investigated the effect of transverse wire roughness on absorber plate and have suggested a simple linear relationship between the Nusselt number and Reynolds number from their experimental data. Prasad and Saini [78], on the basis of law of wall similarity and heat

momentum analogy, proposed relationships for friction factor and heat transfer coefficient in a solar air heater duct. Dalle Donne and Meyer [79] proposed a transformation method to obtain data applicable to reactor fuel elements from annulus experiments. The transformed friction and heat transfer data were correlated by single equations. Wilkie et al. [80] proposed a procedure for the measurement of friction factor in rectangular channels which were not identically roughened, and they have shown that the absolute value of friction factor is up to 10% lower because of presence of smooth surface opposite to the rough surface. Williams et al. [81] and White and White [82] have also investigated the effect of roughness on friction factor and heat transfer in annulus flow and they have reported the effect of various roughness parameters on friction factor and heat transfer.

The comparison of effective efficiency of solar air heaters having different types of geometry of roughness elements on the absorber plate was studied by Mittal et al. [83]. The effective efficiency has been computed by using the correlations for heat transfer and friction factor developed by various investigators within the investigated range of operating and system parameters. Sahu and Bhagoria [84] studied heat transfer coefficient by using 90° broken transverse ribs on absorber plate of a solar air heater; the roughened wall being heated while the remaining three walls are insulated. The roughened wall has roughness with pitch (P), ranging from 10–30 mm, height of the rib of 1.5 mm and duct aspect ratio of 8. The air flow rate corresponds to Reynolds number between 3000–12,000. The heat transfer results have been compared with those for smooth ducts under similar flow and thermal boundary condition to determine the thermal efficiency of solar air heater.

Choudhury and Garg [85] studied a collector with air jet with the air flow rate of the device ranging from $50 \text{ m}^3 \text{ m}^{-2} \text{ h}^{-1}$ to $250 \text{ m}^3 \text{ m}^{-2} \text{ h}^{-1}$. This is compared to the collectors with two air channels without baffles. The jet air

collector proved better than the later one. The authors tested a two air channel collector without baffles with a thickness being 0.1m and 0.05m. The result confirmed that the efficiency increased as the thickness diminished. Yeh and Chou [86] investigated the efficiency of upward type baffled solar air heaters. All the absorber plates deal with clean new materials, implying high costs on the production of the very special absorber plates. Henden et al. [87] mentioned that the main barrier for large scale introduction of thermal solar systems is the high cost compared with conventional heating systems. Alvarez et al. [88] proposed an air collector with an absorber plate made of recyclable aluminium cans and achieved a maximum efficiency of 74%.

Satcunanathan and Deonarine [89] introduced the concept of two pass air heater and later considered by Caouris [90] for liquid systems. Satcunanathan and Deonarine concluded experimentally that the two pass design with air flow between the two glass covers and under the absorber plate had an efficiency which was about 10-15 % higher than single pass design. Wijayasundera et al. [91] developed two-pass flow arrangements, and the design curves for those devices over a range of variables were also presented. In order to know the effect of the pattern of fluid flow on the efficiency of the collector, Katam and Kishore [92] have studied flow configuration reversal (i.e. inlet at the top of the collector) for the collector test rig developed by the Tata Energy Research Institute, India. The experimental results showed that the reverse flow pattern reduces the collector efficiency by 9-73% in the temperature range of 35-75°C. Garg et al. [93] developed the theory of multiple pass solar air heaters. It is well known that the collector configuration will influence the fluid velocity as well as the strength of forced convection. A simple procedure for changing the fluid velocity as well as the strength of forced convection involved adjusting the aspect ratio of a rectangular flat-plate collector with constant

flow rate [94]. A logistic method to achieve considerable improvement in collector efficiency is to use an extended heat transfer area [95] by attaching fins to a flat-plate type of solar air heater.

The improvement of the heat transfer rates has been continuously performed to obtain smaller and more effective thermal systems. Many research works have been conducted on flow and heat transfer characteristics in the solar air heater. Hegazy [96] analyzed a criterion for determining the optimum flow-channel depth of conventional flat-plate solar air heaters. Toure [97] studied the characteristic temperatures in a natural convection solar air heater. Good agreement was obtained between the calculated data and measured ones. Badescu [98] presented the details about the modeling of the air heating system of an ecological building. Two different operating modes of the heating system were investigated. Thakur et al. [99] experimentally investigated the heat transfer and friction factor correlations in packed bed solar air heater for a low porosity system. Togrul et al. [100] investigated the forced convection performance of a solar air heater with a cylindrical absorber central to a conical concentrator. Gao et al. [101] numerically studied the natural convection inside the channel between the flat-plate solar cover and the sine-wave absorber in a cross-corrugated solar air heater. Karwa et al. [102] theoretically investigated a thermo-hydraulic performance of the collector arrays. Ammari [103] applied the mathematical model for predicting the thermal performance of a single pass flat-plate solar air heater with the metal studs. Effects of volume air flow rate, collector length, and spacing between the absorber and bottom plates were investigated. Abu-Hamdeh [104] developed the mathematical model for computing the thermal efficiency, heat gain, and outlet air temperature. The predicted results were validated by comparing with the measured data. Naphon and Kongtragool [105] applied the mathematical models for predicting the heat transfer characteristics and performance of the various

configurations flat-plate solar air heater. The performance and entropy generation of the double-pass flat plate solar air heater with longitudinal fins are studied numerically by Paisarn Naphon [106]. The predictions were done at air mass flow rate ranging between 0.02 and 0.1 kg/s.

2.2 Solar Dryers

Solar drying has been considered as one of the most promising areas for the utilization of solar energy, especially in the field of food preservation. Drying is an energy intensive process, which involves complex heat and mass transfer phenomena. Open sun drying is the most common method employed in tropical countries for the drying of agricultural products, food stuffs, etc. The method is simple, since it does not involve any costly equipment. The product to be dried is spread under sun and the moisture evaporates from it over a course of time. Even though the process is simple, it suffers from the disadvantages like dust contamination, insect infestation, microbial contamination, spoilage due to rains, etc. Produce dried in this way is unhygienic and sometimes unsuitable to human consumption [107-110].

Solar drying can be most successfully employed as a cost effective drying technique. It has got several attractive features. For example, energy is available free of cost and can be harnessed in the site itself. Controlled drying is also possible by this method and it enhances the quality of dried product. Solar drying systems must be properly designed in order to meet particular drying requirements of specific crops and to give satisfactory performance with respect to energy requirements [111,112].

All drying systems can be classified primarily according to their operating temperature ranges into two main groups of high temperature dryers and low temperature dryers. However, dryers are more commonly classified broadly according to their heating sources into fossil fuel dryers

(generally known as conventional dryers) and solar energy dryers. Strictly, all practically-realized designs of high temperature dryers are fossil fuel powered, while the low temperature dryers are either fossil fuel or solar-energy based systems.

Experiments conducted in many countries have clearly proved beyond doubt that solar dryers can be used successfully to dehydrate the food in less time. Moreover, it gives high quality product competing with conventional dryers with added advantage of saving fossil fuels. Szulmayer [113] has categorized solar dryers into three types. i.e., (1) the hot-box type in which the product directly collects energy from the sun, (2) the indirect-type conventional dryer in which the product is dried with warm air heated separately by solar air heaters, and (3) the mixed-type dryer in which the product is exposed to sun and also receives heat from a stream of hot air. On the other hand, Lawand [114] has broadly classified solar dryers into five main categories, i.e, Nature (or sun) dryers, direct-type dryers, indirect-type dryers, mixed mode dryers and solar timber dryers. Many other classifications also have been proposed. Malik et al. [115] classified dryers as (1) direct-mode, (2) indirect-mode, (3) mixed-mode, (4) structure-integrated, (5) solar timber dryers, and (6) others (which include freeze drying, osmovac drying, and desiccant drying, etc.)

In india, Kapoor and Agarwal [116] designed and tested a combination collector dryer; Pattanayak et al. [117] developed a continuous solar grain dryer whereas Singhal [118] imparted a good deal of knowledge on grain drying. Significant contribution has been made in this direction by Garg and Krishnan [119], Biswas [120], Moy [121], Bose [122], Exell [123] and many others.

Using glass to trap the heat along with dull-black-painted, galvanized-iron absorber, Johnson [124] successfully dried cherry and white

oak of 2.5 cm thickness. Similar studies have been made by Peck [125], Plumtre [126], and Tshernitz and Simpson [127].

The simplest type of solar dryers introduced for drying grain and fruit is the one in which heating the incoming ambient air and removing the moisture from the produce take place in the same unit. In this category, cabinet, tunnel and shelf-type dryers have been developed. The preliminary model cabinet-type solar dryer conceived at the Brace Experimental Station of McGill University, Montreal, was field tested in Syria by Lawand [128]. Several designs of similar configuration have been developed. Among them are dryers developed by Garg and Krishnan [119] and a simple design (made out of locally available materials such as bamboo, sticks, rope, etc.) developed by the Development Technology Centre, Bandung, Indonesia. Wagner [129] developed an unusual cabinet dryer which has double exposure, flat plate collectors with vertical and horizontal mirrors to expose the drying produce to sunlight on both sides. Shri A.M.M. Murugappa Chettiar Research Centre of Madras, India has also developed a simple cabinet for drying fish [130]. It is reported that in general, a cabinet-type dryer reduces the drying period by one half in comparison to open-sun drying. Improved product quality in some cases is, of course, an additional benefit.

In an attempt to increase the drying capacity and reduce the drying time associated with the cabinet-type dryers, shelf-type dryers were developed. In the shelf type of dryers, warm air is flown through the produce for which an air heater is attached. A vertical cassava stick dryer made by Roa et al. [131] is an example of it. Others who developed such dryers were Richard and Vincent [132] for cocoa, and Van Dresser [133] for orchard drying.

Large scale industrial drying usually is accomplished using tunnel-type dryers. Retrofitting such structures with solar-heat supply requires only

less capital investment. Fuel savings as a result of using solar energy make the operation of the dryer cost effective. In another study undertaken by the team from the Midwest Research Institute, cost and performance were analyzed for alfalfa drying plant in which solar energy partly supplied the energy need.

An industrial soybean drying system developed by Teledyne Brown Engineering and reported by Fisher [134] used flat-plate, solar air heating collectors: the collectors of area 1208 m² operate an annual average efficiency of 52 % and collect heat at the rate of 3.9 million MJ/year. Heid [135] studied the performance and costs of eight experiments on farm solar collectors designed to dry corn. It was concluded that further research, large-scale production, and increasing energy costs should enhance the economic feasibility of solar grain drying.

An indirect type cabinet dryer with a transparent cover and forced convection flow has been considered favorable since such dryer is able to produce high quality product without discoloration. A wide variety of direct and indirect solar dryer has been developed so far [108, 136-146]. Low capital cost, production of hygienic and better quality products and zero or marginal running costs are also important parameters for the large-scale adoption of solar dryers.

Properly designed solar drying systems must take into account drying requirements of specific crops, energy efficiency requirements, and cost effectiveness [147]. Simulation models are needed in the designs and operations of solar dryers. Several researchers have developed simulation models for natural and forced convection solar drying systems [123, 148-151].

In a different way, Ratti and Mujumdar [110] developed a model and simulation code of a solar dryer, using heat and mass balances, applied to solid and gas phases with time varying air conditions. The results compared

well with experimental ones. The effect of several parameters and shrinking were presented. Pangavhane and Sawhney [152] have given technical and economical results on the use of solar drying for grapes. It was found that the use of a solar dryer is feasible. However, its acceptance by the farmers was limited due to its small capacity and too long a pay back period. Jain and Tiwari [153] evaluated the convective heat transfer coefficient for some crops (green chillies, green peas, white gram, onions, potatoes, and cauliflower) under solar drying and developed a mathematical model for predicting the drying parameters. Jain and Tiwari [154] further studied the dependence of convective heat transfer coefficient on the drying time during complete solar drying process of green peas and cabbage. The convective heat transfer coefficient of jaggery under solar drying has been evaluated by Tiwari et al. [155].

Ait Mohamed et al. [156] conducted studies on single layer solar drying behaviour of *Citrus aurantium* leaves under forced convection. An indirect forced convection solar dryer consisting of a solar air collector, an auxiliary heater, a circulation fan, and a drying cabinet were used for the experiments. The air temperature varied from 50 to 60°C; the relative humidity from 41% to 53%; and the drying air flow rate from 0.0277 to 0.0833m³/s. Many researches on the mathematical modeling and experimental studies have been conducted on the thin layer solar drying processes of various vegetables and fruits, such as grapes [157], apricots [158], green pepper, green bean and squash [159], eucalyptus globulus [160], mint, pistachio [161,162], red pepper [163] and prickly pear fruit [164].

Azharul Karim and Hawlader [165] reported the performance study on v-groove solar air collector for drying applications and indicated better thermal efficiency for this type of collector, compared to a flat plate collector. Most fruits and vegetables contain more than 80% water and are,

therefore, highly perishable. Losses of fruits and vegetables in developing countries are estimated to be 30–40% of production and, in India alone, yearly losses worth more than US \$1.5 billion [166]. Prospect of solar drying applications in the ASEAN region is enormous. A large volume of fruits is produced in the vast rural areas of Thailand, Malaysia, and Indonesia.

Amir et al. [167] reported a multipurpose solar tunnel dryer for use in humid tropics. It reported that, compared to sun drying, the drying time of cocoa, coffee and coconut could be reduced by up to 40%. Collector efficiency was reported to be in the range of 23.5–36%. Significant improvement in product quality was also reported. Gauher et al. [168] developed a tunnel dryer suitable for small farmers and cooperatives. The economic study of the dryer revealed a payback period of just two years. Tarigan et al. [169] reported a solar dryer with perforated collector for tea wilting. The collector efficiency was reported to be about 54% at very high flow rate, when collector outlet temperature was about 30°C. In all the above studies, emphasis was placed on the dryer performance and product quality. The main component of the solar dryer, the collector, was thus ignored. The design of efficient and suitable air collectors is one of the most important factors controlling the economics of solar drying. The majority of the solar dryers are equipped with flat plate collectors. The heat transfer coefficient of a surface in contact with air is considerably lower than that with water.

Palaniappan and Subramanian [170] developed a solar air heating system for tea processing and detailed economic analysis was carried out. The system has reduced specific fuel consumption for tea production from 0.932 to 0.71 kg/kg dmt (dryer mouth tea), which represents a fuel savings of approximately 25%.

Several solar energy drying systems have been designed as alternatives to the traditional open-sun drying. The construction details and operational principles of such dryers have been reviewed by Ekechukwu and

Norton [171]. Schirmer et al. [172] and Hossain and Bala [173] evaluated a multi-purpose transparent solar tunnel dryer with fans, powered by PV modules. In these systems, the product to be dried receives energy from both the hot air supplied by the collector and direct exposure to solar radiation; also the product being dried is protected from rain, insects, and dust. They found the product to have high-quality in terms of flavor, color, and texture. In all cases, the use of a solar tunnel dryer considerably reduced drying time in comparison to open-sun drying. Supranto et al. [174] carried a study on an experimental solar assisted dryer consisting of a collector, a dryer, an auxiliary burner, and a fan. Tiris et al. [175] developed a dryer where a fan controlled by a manual valve was used to force the drying air through the collector and the drying chamber. Bena and Fuller [176] demonstrated a direct-type natural convection solar dryer combined with a simple biomass burner to provide a drying technology suitable for small scale drying of fruits and vegetables in non-electrified areas.

Specifically, drying methods affect properties such as color, texture, density, porosity, and sorption characteristics of dehydrated materials. It has been pointed out that dehydrated products do not keep their visco-elastic behavior after dehydration due to structural damages that occur during drying [177]. Gallalia et al. [178] found that solar dryers alter the sugars and vitamin C level more than open-sun drying because of relatively higher temperature inside the solar drying chamber.

A thermal performance analysis derived from the second law of thermodynamics of the solar drying process was reported by Torres-Reyes et al. [179]. The results from the studies on modeling and thermal performance of the collector of a semi-cylindrical solar tunnel dryer (STD) have been presented by Garg and Kumar [180]. The tunnel can be used for air heating in many applications including drying. Earlier, the tunnel as air heater was used by Pyrko [181] at Warsaw Agricultural University in Poland. In air

tunnel dryer, the air is forced in the tunnel either by an air blower or natural circulation. Some studies on multi-purpose solar tunnel dryer (STD) have been carried out at the Institute of Agricultural Engineering, University of Hohenheim [182,183]. Some experimental results on the field performance of the STD under forced circulation mode have been reported by Lutz et al. [184]. Fuller [185] has also reported some experimental study on tunnel dryer and a comparison of its performance with conventional dryer. Condori et. al. [186] developed a new low cost design for a forced convection tunnel greenhouse dryer for sweet pepper and garlic drying.

Active solar drying systems depend only partly on solar-energy. They employ solar energy and/or electrical or fossil-fuel based heating systems and motorized fans and/or pumps for air circulation. All active solar dryers are, thus, by their application, forced-convection dryers. A typical active solar dryer depends solely on solar energy as the heat source but employs motorized fans and/or pumps for forced circulation of the drying air. Other major applications of active solar dryers are in large-scale commercial drying operations in which solar air heaters supplement conventional fossil-fuel fired dehydrators [187-196], reducing the overall conventional energy consumption, while maintaining control of the drying conditions. If warm enough, the solar-heated air could be used directly for the drying process, otherwise the fossil-fuel fired dehydrator would be used to raise the drying air temperature to the required level (for example during night time drying operations or periods of low insolation levels), thus avoiding the effects of fluctuating energy output from the solar collector, since the fossil-fuel system can be controlled automatically to provide the required optimum drying conditions. These active solar dryers that incorporate dehydrators for supplemental heating are commonly known as "hybrid solar dryers"

Since high temperature drying requires high air flow rates (due to the requirement of limited exposure of the product to the very hot drying air), all high temperature solar drying applications would, of necessity, employ active solar dryers (requiring forced circulation of air by fans and/or pumps). Thus, all practically-realized designs of continuous-flow solar energy drying systems [117,197] are of the active type. A variety of active solar energy dryers exist which could be classified into either the integral-type, distributed-type or mixed-mode dryers.

A distributed-type active solar dryer is one in which the solar collector and drying chamber are separate units. A typical design would be comprised of four basic components, namely; i) the drying chamber; ii) the solar air heater; iii) the fan and/or pump; and iv) the ducting. For conventional drying systems, drying efficiencies increase with temperature, thus encouraging drying at temperatures as high as the product can withstand. However, for distributed-type active solar dryers, the maximum allowable temperature may not yield an optimal dryer design, as the efficiencies of solar collectors decrease with higher outlet temperatures. Thus, a critical decision in the design of distributed active solar dryers would be either to choose high drying air temperatures and, consequently, accommodate lower air-flow rates (implying the use of smaller fans and requiring high levels of insulated ducting) or to employ low temperature drying, minimizing the cost of insulation, since heat losses are low. However, the efficiency of high-temperature distributed active solar dryers is significantly improved by high air-flow rate. Thus a balance has to be made between the size of fans used and the level of insulation for a cost effective design. Most of the distributed-type active solar drying systems have similar structural designs comprising the basic components. Modifications to the typical design have tended to be based on the following features:

a) The solar air heaters - Most air heaters make use of metal absorbers (with appropriate surface treatment). A few designs employ black polythene absorbers to minimize the overall cost of dryer construction [198,199].

b) Air re-circulation - The re-circulation of the drying air employed in some known designs [61,199,200] is another distinguishing feature. This ensures a low exhaust air temperature, thereby increasing efficiency. In non-recirculation drying, the existing air may still be containing some considerable heat. Re-circulation of the drying air implies a higher total temperature and that the warm air is not discarded until it carries an appreciable quantity of moisture, thereby ensuring an efficient use of energy.

c) Fan/pump location – Most of the designs fans are located between the air heater and the drying chamber [61,170,201]. This keeps the collector under negative pressure, ensuring that all air leakages and the additional heat generated by the pump is into the system. Locating a pump and/or fan at the air inlet of the collector involves less elaborate construction details and ensures that each component can be easily de-coupled from the system for maintenance and repair. For systems employing air recirculation, the pump should be located appropriately. Conventional distributed active solar energy dryers are batch-type designs mostly. However, some continuous-flow designs have been built [61,202,203].

To achieve more efficient energy use, some active solar dryers are equipped with thermal storage devices, mostly rock bed or gravel storage [204-207]. This improves drying during night time or periods of low insolation levels. Desiccants are incorporated in some designs [128,208-210] to reduce the relative humidity of the drying air to very low level so as to improve its moisture carrying capacity. The use of desiccants would only be appropriate for forced-convection systems, as their incorporation into the system increases the resistance to air flow. Finally, as indicated earlier, large-scale commercial active solar dryers employ mostly air-heating solar

collectors as supplements to electricity or fossil-fuel fired dehydrators to reduce the overall conventional energy consumption. The requirement of fossil-fuel driven fans and/or the use of auxiliary heating sources improve the efficiency of these dryers, but it renders their capital, maintenance and operational costs to be prohibitively high for small scale farming operations.

2.3 Solar PCM Thermal Storage

Solar drying can be most successfully employed as a cost effective drying technique. It has got several attractive features. For example, energy is available free of cost and can be harnessed in the site itself. Controlled drying is also possible by this method and it enhances the quality of dried product. Solar drying systems must be properly designed in order to meet particular drying requirements of specific crops and to give satisfactory performance with respect to energy requirements. Perishable crops like fruits and vegetables require continuous drying; otherwise the product may be vulnerable to insect attack. In order to prevent this, some sort of auxiliary heating mechanisms should be incorporated with a solar dryer. Escalating prices of fossil fuels prevent the large-scale adoption of fossil fuel or electrical based dryer among small or marginal farmers. Hence it is essential to develop some mechanism that could be able to supply energy requirements during cloudy and non-solar hours. Thus the intermittent, variable and unpredictable nature of solar energy make it necessary to incorporate a storage system with a solar dryer. The advantage of using storage system is that it stores excess energy and supplies when the collected amount is inadequate. Among latent and sensible heat storage material for thermal energy requirements, the energy density of latent heat material is much higher than that of the latter. Much work has been reported using Phase Change Material (PCM) for solar thermal applications, particularly for cooking [211,212]. Experimental and theoretical efforts have been made to

incorporate PCMs into flat plate collectors for storing solar energy by Bansal and Buddhi [213,214]. Some other researchers [215-221] analyzed various material properties of different types of PCMs under various conditions and its applications in solar energy storage.

The study on incorporation of PCM storage with solar dryer is in its infancy and very few published works are there in the literature. Enibe [222] studied the performance of a natural circulation solar air heating system with phase change material energy storage for crop drying and egg incubation. In that study, PCM was prepared in modules with the modules equispaced across the absorber plate. No work has been performed on forced circulation solar dryers with PCM thermal energy storage. In the present study, the feasibility of latent heat thermal energy storage in forced circulation solar dryer was investigated. A PCM container was fabricated similar to a shell and tube heat exchanger. The fabricated container was placed in a solar cabinet dryer and studies were conducted on with and without loading the product in the dryer. The charging and discharging of PCM has also been investigated.

References

- [1] K.W. Miller, Solar heat collector, US Pat. 2680327, 1954.
- [2] G.O.G. Lof, Solar energy utilization for house heating, Office of the Publication Board, Washington, PB 25375, 1946.
- [3] M. Telkes and E. Raymond, Storing heat in chemicals-a report on the Dover House, Heat. Vent. 80, 1949.
- [4] G.O.G. Lof, Performance of solar energy collectors of overlapped glass plate type, Proc. course symp. Space heating by Solar Energy, MIT, 72-83, 1950.
- [5] G.O.F. Lof and T.D. Neves, Heating of air by solar energy, Ohio J. Sci. 53, 272-280, 1953.
- [6] M.K. Selcuk, Thermal and economic analysis of the overlapped glass plate solar air heaters, Solar Energy 13(2), 165-191, 1971.
- [7] R.W. Bliss, Design and performance of the nations only fully solar heated houses, Air condit. Heat Vent. 82, 1955.
- [8] A.F. Whillier, Performance of black painted solar air heaters of conventional design, Solar Energy 8(1), 31-37, 1964.
- [9] D.J. Close, Solar air heaters for low and moderate temperature applications, Solar Energy 7(3), 117-124, 1963.
- [10] C.L. Gupta and H.P. Garg, Performance studies on solar air heaters, Solar Energy 11(1), 25-31, 1967.
- [11] W.W.S. Charaters, Some aspects of flow duct design for solar air heater applications, Solar Energy 13(2), 282-288, 1971.
- [12] B. Cole-Appel and R.D. Haberstroh, Performance of air cooled flat plate collectors, Proc. ISES Conf., American Section, Winnipeg, Canada, 2, 94-106, 1976.

- [13] E.C. Sheven, A.R. Balakrishnan and J.F. Origill, Development of a solar air heater, Waterloo Research Institute, Report No. 77-04, Final report-Phase I, 1977.
- [14] F.H. Buelow and J.J. Boyd, Heating air by solar energy, *Agri. Engineering* 38(1), 28-30, 1957.
- [15] K.G.T. Holands, Directional selectivity, emittance and absorptance properties of Vee-corrugated specular surfaces, *Solar Energy* 7(3), 108-116, 1963.
- [16] W.W.S. Charters and R. MacDonald, Heat transfer effects in solar air heaters. *COMPLES, Revue Internationale d' Heliotechnique* 1, 29-38, 1974.
- [17] V Bevil and H. Brandt, A solar energy collector for heating air, *Solar Energy* 12 (1), 19-36, 1968.
- [18] M.M. Ali and S. Ramadhyani, Experiments on convective heat transfer in corrugated channels, *Experimental Heat Transfer* 5(3), 175-193, 1992.
- [19] M. Molki and C.M. Yuen, Effect of interwall spacing on heat transfer and pressure drop in a corrugated-wall duct, *Int. j. Heat and Mass Transfer* 29(7), 987-997, 1986.
- [20] W.W Focke, J. Zachariades and I. Olivier, The effect of the corrugation inclination angle on the thermo hydraulic performance of a plate heat exchanger, *Int. J. Heat Mass Transfer* 28(8), 1469-1479, 1985.
- [21] E.M. Sparrow and L.M. Hossfeld, Effect of rounding of protruding edges on heat transfer and pressure drop in a duct, *Int.J.Heat Mass Transfer* 28(10), 1715-1723, 1984.
- [22] E.M. Sparrow and J.W. Comb, Effect of interwall spacing and fluid flow inlet conditions on a corrugated-wall heat exchanger, *Int. J. Heat and Mass Transfer* 26(7), 993-1005, 1983.

- [23] J.E. O'Brien and E.M. Sparrow, Corrugated-duct heat transfer, pressure drop, and flow visualization, *Trans. ASME-J. Heat Transfer* 104, 410-416, 1982.
- [24] Wenfeng Gao, Wenxian Lin, Tao Liu and Chaofeng Xia, Analytical and experimental studies on the thermal performance of cross-corrugated and flat-plate solar air heaters, *Applied Energy* 84(4), 425-441, 2007.
- [25] W.W.S. Charters, Some aspects of flow duct design for solar air heater applications, *Solar Energy* 13, 283, 1971.
- [26] K.G.T. Hollands and E.C. Scheven, Optimization of flow passage geometry for air heating plate type solar collector, *J. Solar Energy Engineering, Trans. ASME* 103, 323, 1981.
- [27] C. Choudhury, A corrugated plate solar air heater: trade offs between efficiency and pressure drop, Report 88-15, ISSN 0332-5571, Institute of Physics, University of Oslo, Norway, 1988.
- [28] C. Choudhury and H.P. Garg, Design analysis of corrugated and flat plate solar air heaters, *Renewable Energy* 1, 595, 1991.
- [29] M.A. Hamdan and B.A. Jubram, Thermal performance of three types of solar air collectors for the Jordanian climate, *Energy* 17, 173, 1992.
- [30] J.P. Chiou, M.M. El-Wakil and J.A. Duffie, A slit and expanded aluminium-foil matrix solar collector, *Solar Energy* 9(2), 73-80, 1965.
- [31] W.A. Beckman, Radiation and convection heat transfer in a porous bed, *J. Eng. Power, ASME*, 51-54, 1968.
- [32] Y.H. Hamit and W.A. Beckman, Transpiration cooling and radiatively heated porous bed, ASME Paper No. 69-WA/Sol-6, 1969.
- [33] M.K. Selcuk, Solar air preheater and fruit dryer, *Complex Bull.* 10, 79-82, 1966.

- [34] M. Akyurt and M.K. Selcuk, A solar dryer supplemented with auxiliary heating systems for continuous operation, *Solar Energy* 14(3), 313-320, 1973.
- [35] O.A. Lalude and H. Buchberg, Design and application of honeycomb porous bed solar air heaters, *Solar Energy* 13(2), 223-242, 1971.
- [36] J.A. Wiebelt and N. Thatree, Design and experimental evaluation of V-grooved solar collector, ASME paper, 76-HT-53, 1976.
- [37] F.L. Lansing, V Clarke and R. Reynolds, A high performance porous flat plate solar collector, *Energy* 4(4), 685-694, 1979.
- [38] D.A. Neeper, Analysis of matrix air heaters. Report No. LA-UR-79-1318 of Los Alamos Scientific Laboratory, New Mexico, 1979.
- [39] R.K. Collier, The characterization of crushed glass as a transpired air heating solar collector material. Report No. LA-UR-79-1336 of Los Alamos Scientific Laboratory, New Mexico, 1979.
- [40] R.K. Swartman and O. Ogulande, An investigation on packed bed collectors, *Solar Energy* 10(3), 106-110, 1966.
- [41] B.L. Clery and R.G. Morgan, Evaluation of matrix-solar collector for heating air, Proc. solar crop drying conf. North Carolina State University at Raleigh, 44-66, 1977.
- [42] M.M. Sorour and M.A. Hassab, A screen type solar air heater, In proc. of the Eighth International Heat Transfer Conference 6, pp. 3097 – 3103, 1986.
- [43] M.A. Hasab and M.M. Sorour, Heat transfer studies in matrix-type solar air heaters, *Journal of Solar Energy Engineering* 111, 82-87, 1989.
- [44] M.J. Shoemaker, Notes on a solar collector with unique air permeable media, *Solar Energy* 5, 138-141, 1961.
- [45] S.P. Sharma, J.S. Saini and H.K. Varma, Thermal performance of packed-bed solar air heaters, *Solar Energy* 47(2), 59-67, 1991.

- [46] A. Ahmad, J.S. Saini and H.K. Varma, Effect of geometrical and thermo physical characteristics of bed materials on the enhancement of thermal performance of packed bed solar air heaters, *Energy Conversion and Management* 36(12), 1185-1195, 1995.
- [47] M. Hasatani, Y. Itaya and K. Adachi, Heat transfer and thermal storage characteristics of optically semi transparent material packed bed solar air heater, *Current Researches in Heat and Mass Transfer, India, IIT Madras*, pp. 61-70, 1985.
- [48] R.K. Collier, The characterization of crushed glass as transpired air heating solar collector material, *Proceedings of the International Solar Energy Society, Atlanta*. pp. 264-268, 1979.
- [49] M.S. Sodha, N.K. Bansal and R.S. Mishra, *Energy Conservation and Management* 24, 281, 1984.
- [50] J.E. Coppage and A.L. London, Heat transfer and flow friction characteristics of porous media, *Chemical Engineering Progress* 52, 57F-63F, 1956.
- [51] L.S. Tong and A.L. London, Heat transfer and flow friction characteristics of woven-screen and cross-rod matrixes 79, 1558-1570, 1957.
- [52] W.M. Kays and A.L. London, *compact heat exchangers*, McGraw-Hill, New York, 1964.
- [53] M.K. Selcuk, *Solar thermal engineering* (edited by A.A.M. Sayigh), 155-183, Academic Press, New York, 1977.
- [54] M.R.I. Ramadan, A.A. El-Sebaili, S. Aboul-Enein and E. El-Bialy, Thermal performance of a packed bed double-pass solar air heater, *Energy* 32(8), 1524-1535, 2007.
- [55] M.K. Mittal and L. Varshney, Optimal thermohydraulic performance of a wire mesh packed solar air heater, *Solar Energy* 80(9), 1112-1120, 2006.

- [56] B. Paul and J. S. Saini, Optimization of bed parameters for packed bed solar energy collection system, *Renewable Energy* 29(11), 1863-1876, 2004.
- [57] K.G.T. Hollands and E.C. Shewen, Optimization of flow passage geometry for air heating solar collectors, *ISES Proc.* 302-306, 1979.
- [58] M. Yusoff and D.J. Close, Transient studies of solar air heaters, *Int. Sympto. on solar energy for development*, Tokyo, Japan, 1979.
- [59] H.P. Garg, Usha Rani and Ram Chandra, Finite difference analysis of transient behaviour of flat plate solar collector, *Int. J. of Energy Research*, 1980.
- [60] K.R. Randal, Natural convection characteristics of flat plate collectors, *Proc. ISES*, 4-20, 1977.
- [61] B.A. Meyer, An interferometric investigation of heat transfer in flat collector cells, *Proc. ISES*, 635-639, 1978.
- [62] K.G. Hollands, Dimensional relations for free convective heat transfer in flat plate collectors, *Proc. ISES*, 207-213, 1978.
- [63] R.N. Misra and H.M. Keener, Solar grain drying for Ohio, *Proc. Solar Drying Conf.*, Purdue University, 13-28, 1978.
- [64] R.A. Erb, The unitary solar collector, A new approach to low cost flat plate systems, *Proc. ISES*, 269-391, 1979.
- [65] M.K. Peck and D. Proctor, Design and performance of a roof integrated solar air heater, *Proc. ISES*, 269-391, 1979.
- [66] H.T. Gordan and R.A. Nearhoof, A fan assisted vertical wall hybrid solar collector system, *Proc. ISES*, 274, 1979.
- [67] C.W. Ambrose and P.C. Bandopadhyay, Asymmetrical heating in non circular ducts, *Proc. Inst. Solar Energy Society Conf. Melbourne*, Paper No. 7/17, 1970.
- [68] S.V. Karmare and A.N. Tikekar, Heat transfer and friction factor correlation for artificially roughened duct with metal grit ribs,

- International Journal of Heat and Mass Transfer 50(21-22), 4342-4351, 2007.
- [69] A. Layek, J.S. Saini and S.C. Solanki, Second law optimization of a solar air heater having chamfered rib-groove roughness on absorber plate, *Renewable Energy* 32(12), 1967-1980, 2007.
- [70] J. Nikuradse, *Laws of flow in rough pipes*, NASA TM 1292, 1950.
- [71] D.F. Dipprey and R.H. Sabersky, Heat and momentum transfer in smooth and rough tubes at various Prandtl numbers, *Int. J. Heat and Mass Transfer* 6, 329-353, 1963.
- [72] R.L. Webb, E.R.G. Eckert and R.J. Goldstein, Heat transfer and friction in tubes with repeated rib roughness, *Int. J. Heat and Mass Transfer* 14, 601-617, 1971.
- [73] J.C. Han, Heat transfer and friction in channels with two opposite rib roughened walls, *Trans. ASME, J. Heat Transfer* 106, 774-781, 1984.
- [74] B.A. Kader and A.M. Yaglom, Turbulent heat and mass transfer from a wall with parallel roughness ridges, *Int. J. Heat Mass Transfer* 20, 345-357, 1977.
- [75] J.V. Vilemas and V.M. Simonis, Heat transfer and friction of rough ducts carrying gas flow with variable physical properties, *Int. J. Heat Mass Transfer* 28(1), 59-68, 1985.
- [76] E.M. Sparrow and W.Q. Tao, Enhanced heat transfer in a flat rectangular duct with stream wise periodic disturbances at one principal wall, *Trans. ASME. J. Heat Trans.* 105, 851-861, 1983.
- [77] K. Prasad and S.C. Mullik, Heat transfer characteristics of a solar air heater used for drying purposes, *Applied Energy* 13, 83-93, 1983.
- [78] B.N. Prasad and J.S. Saini, Effect of artificial roughness on heat transfer and friction factor in a solar air heater, *Solar Energy* 41, 555-560, 1988.

- [79] M. Dalle Donne and L. Meyer, Turbulent convection heat transfer from friction factor rough surfaces with two-dimensional ribs, *Int. J. Heat and Mass Trans.* 22, 583-620, 1979.
- [80] D. Wilkie, M. Cowan, P. Burnett and T. Burgoyone, Friction factor measurements in a rectangular channel with walls of identical and non-identical roughness, *Int. J. Heat Trans.* 10, 611-621, 1967.
- [81] F. Williams, M.A.M. Pirie and C. Warburton, Heat transfer from surfaces roughed by ribs, In: *Augmentation of convective heat and mass transfer*, ASME, New York, 35-43, 1970.
- [82] W.J. White and L. White, The effect of rib profile on heat transfer and pressure loss properties of transversely ribbed roughened surfaces, In: *Augmentation of convective heat and mass transfer*, ASME, New York, 4454, 1970.
- [83] M.K. Mittal, Varun, R.P. Saini and S.K. Singal, Effective efficiency of solar air heaters having different types of roughness elements on the absorber plate, *Energy* 32(5), 739-745, 2007.
- [84] M.M. Sahu and J.L. Bhagoria, Augmentation of heat transfer coefficient by using 90° broken transverse ribs on absorber plate of solar air heater, *Renewable Energy* 30 (13), 2057-2073, 2005
- [85] C. Choudhury and H.P. Garg, Evaluation of jet plate solar air heater, *Solar Energy* 46, 199-209, 1991.
- [86] H.M. Yeh and W.H. Chou, Efficiency of solar air heaters with baffles, *Energy* 16(7), 983-987, 1991.
- [87] L. Henden, J. Rekstad and Meir, Thermal performance of combined solar systems with different collector efficiencies, *Solar Energy* 72(4), 299-305, 2002.
- [88] G. Alvarez, J.I. Arce, L. Lira and M.R. Heras, Thermal performance of a solar collector with an absorber plate made of recyclable aluminium cans, *Solar Energy* 77, 107-113, 2004.

- [89] S. Satcunanathan and S. Deonaraine, A two-pass solar air heater, *Solar energy* 15, 41-49, 1973.
- [90] Y. Caouris, A novel solar air collector, *Solar Energy* 21, 157-160, 1978.
- [91] N.E. Wijeyesundera, L.L. Ah and L.E. Tjioe, Thermal performance study of two-pass solar air heaters, *Solar Energy* 28, 363-370, 1982.
- [92] S. Katam and V.V.N. Kishore, Effect of flow reversal on the performance of flat plate collectors, *Energy options for the 90s, Proc. of the national Solar Energy Convention, IIT, New Delhi*, pp. 28-31, 1987.
- [93] H.P. Garg, V.K. Sharma and A.K. Bhargava, Theory of multiple-pass solar air heaters, *Energy* 10, 589-599, 1985.
- [94] H.M. Yeh and T.T. Lin, The effect of collector aspect ratio on the collector efficiency of flat-plate solar air heaters, *Energy* 20, 1041-1047, 1995.
- [95] H.M. Yeh and Y.C. Ting, Effect of free convection on collector efficiencies of solar air heaters, *Applied Energy* 22, 145-155, 1986.
- [96] A.A. Hegazy, Comparative study of the performances of four photovoltaic/thermal solar air heater, *Renewable Energy* 18, 283-304, 1999.
- [97] S. Toure, Characteristics temperature in a natural convection solar air heater, *Energy Conversion and Management* 42, 1157-1168, 2001.
- [98] V. Badescu, Model of a space heating system integrating a heat pump, photothermal collectors and solar cells, *Renewable Energy* 27, 489-505, 2002.
- [99] N.S. Thakur, J.S. Saini and S.C. Solanki, Heat transfer and friction factor correlations for packed bed solar air heater for a low porosity system, *Solar Energy* 74, 319-329, 2003.
- [100] I.T. Torgul, D. Pehlivan and C. Akosman, Development and testing of a solar air heater with conical concentrator, *Renewable Energy* 29, 263-275, 2004.

- [101] W. Gao, W. Lin and E. Lu, Numerical study on natural convection inside the channel between the flat-plate cover and sine-wave absorber of a cross-corrugated solar air heater, *Energy Conversion and Management* 41, 145-151, 2000.
- [102] R. Karwa, S.N. Garg and A.K. Arya, Thermo-hydraulic performance of a solar air heater with n-subcollectors in series and parallel configuration, *Energy* 27, 807-812, 2002.
- [103] H.D. Ammari, A mathematical model of thermal performance of a solar air heater with slats, *Renewable Energy* 28, 1597-1615, 2003.
- [104] N.H. Abu-Hamdeh, Simulation study of solar air heater, *Solar Energy* 74, 309-317, 2003.
- [105] P. Naphon, B. Kongtragool, Theoretical study on heat transfer characteristics and performance of the flat plate solar air heaters, *Int Commun. Heat Mass Transfer* 30, 1125-1136, 2003.
- [106] Paisarn Naphon, On the performance and entropy generation of the double-pass solar air heater with longitudinal fins, *Renewable Energy* 30(9), 1345-1357, 2005.
- [107] M.S. Sodha, A. Dang, P.K. Bansal and S.B. Sharma, An analytical and experimental study of open sun drying and a cabinet type dryer, *Energy Conservation and Management* 25(3), 263-271, 1985.
- [108] M.S. Sodha, N.K. Bansal, A. Kumar, P.K. Bansal and M.A.S. Malik, *Solar Crop Drying Vol. I*, CRC Press, USA, 1987.
- [109] M.S. Sodha and R. Chandra, Solar drying and their testing procedures: A review, *Energy Conservation and Management* 35, 219-267, 1994.
- [110] C. Ratti and A.S. Mujumdar, Solar drying of foods: Modeling and numerical simulation, *Solar Energy* 60, 151-157, 1997.
- [111] H.P. Garg, *Advances in solar energy technology*, Vol. 3, D. Reidel Publishing Company, Holland, 1987.

- [112] M.A. Karim and M.N.A. Hawlader, Development of solar air collectors for drying applications, *Energy Conservation and Management* 45(3), 329-344, 2004.
- [113] W. Szulmayer, Thermodynamics of sun-drying, Paper No. V24, in: *Sun in the Service of Mankind*, UNESCO Conf., Paris, 1973
- [114] T.A. Lawand, Agriculture and other low temperature applications of solar energy, in *Solar Energy Handbook*, McGraw-Hill, Chapter 18, New York, 1980.
- [115] M.A.S. Malik, M.S. Sodha, P.K. Bansal, N.K. Bansal and A. Kumar, Solar crop drying, United Nation Development Programme Global Project (GLO/80/003), on 'Studies on Testing and Demonstration of Renewable Energy Technologies', World Bank, Washington, D.C., 1983.
- [116] S.G. Kapoor and H.C. Agarwal, Solar dryers for Indian conditions, Proc. ISES congress, *The Sun in the Service of Mankind*, Paper No. V-29, Paris, 1973.
- [117] S. Pattanayak, P. Sengupta and B.C. Raychaudhuri, Continuous solar grain dryer, In Proc. ISES, New Delhi, pp.1449-1452, 1978.
- [118] O.P. Singhal, Utilization of solar energy for parboiling and drying of paddy, PhD Thesis, IIT, Kharagpur, 1979.
- [119] H.P Garg and A. Krishnan, Solar drying of agricultural products. 1. Drying of chillies in a solar cabinet dryer, *Ann. Arid Zone*, 13(4), 285, 1974.
- [120] D.K. Biswas, Design of solar dehydrator for fruits and vegetables, Symposium on Dehydrated Food Industry in India, at Food Corporation of Indian Auditorium, New Delhi, 1977.
- [121] J.H. Moy, Testing some concepts of freeze drying and osmovac drying with solar energy, Proc. National Conference on Energy Use and Management, Vol. III/IV, 529-530, 1977.

- [122] S.C. Bose, Commercial solar energy dryers-Indian Experience, Proc. Solar Drying Workshop, Bureau of Energy Development, Manila, 1978.
- [123] R.H.B. Exell, Basic design theory for a simple solar rice dryer, Renewable Energy Review Journal I(2), 1-14, 1980.
- [124] C.L. Johnson, Wind-powered solar heated lumber dryer, South Lumberman, 203 (2532), 1961.
- [125] E.C. Peck, Drying 4/4 red oak by solar heat, For. Prod. Journal 12(3), 1962.
- [126] R.A. Plumtre, Simple solar heated timber dryers: Design, performance and commercial viability, Commonwealth for Rev 58(4), 243-251, 1979.
- [127] J.L. Tschernitz, W.T. Simpson, Solar-heated forced-air lumber dryer for tropical latitudes, Solar Energy 22, 563-566, 1979.
- [128] T.A. Lawand, A solar cabinet dryer, Solar Energy 10, 154-164, 1966.
- [129] C.J. Wagner, R.L. Coleman and R.E. Berry, A low cost, small scale solar dryer for Florida fruits and vegetables, Proc. Florida State Hort Soc. (U.S.A.) 92, pp. 180-183, 1979.
- [130] Anon, Solar Dryers, Shri A.A.M. Murugappa Chettiar Research Centre, Algal Division, Tharaumani, Madras, India, 1978.
- [131] Roa, Kluppel and Abreu, Res. Rep. No. T-99, Brace Research Institute, Quebec, 1975.
- [132] M. Richard and M. Vincent, See-saw dryer (Ivory Coast), in Res. Rep. No. T-99, CS/EC-G-1, Brace Research Institute, Quebec, 1975.
- [133] P. Van Dresser, Solar fruit and vegetable dryer, in Res. Rep. No. T-99, Quebec CS/EC-J-4, Brace Research Institute, 1975.
- [134] P.N. Fischer, Final design report for applications of solar energy to industrial drying of soybeans, Rep. No. ORO/5122-1, U.S. Department of Energy, Washington DC., 1977.

- [135] W.G. Heid, The performance and economic feasibility of solar grain drying systems, Agricultural Economic Rep. No. 396, U.S. Department of Agriculture, Washington DC., 1978.
- [136] B.K. Bala, M.R.A. Mondol, B.K. Biswas, B.L. Chowdury and S. Janjai, Solar drying of pineapple using solar tunnel dryer, Renewable Energy 28,183-190, 2003.
- [137] P. Schimer, S. Janjai, A. Esper, R. Smitabhindu and W. Muhlbauer, Experimental investigation of the performance of the solar tunnel dryer for drying bananas, Renewable Energy 7,119-129, 1996.
- [138] S. Chirarattananon, C. Chinporncharoenpong and R. Chirarattananon, A steady state model for the forced convection solar cabinet dryer, Solar Energy 41, 349-360, 1988.
- [139] H.P. Garg and J. Prakash, Solar energy fundamentals and application, Tata McGraw-Hill Publishing Company, New Delhi, 2000.
- [140] S.A. Lawrence, A. Pole and G.N. Tiwari. Performance of solar crop dryer under PNG climatic conditions, Energy Conversion and Management 30, 333-342, 1990.
- [141] N.M. Khattab, Development of an efficient family size solar dryer, Energy Sources 18, 85-93, 1996.
- [142] A.S. Majumdar, Innovation and R&D needs in industrial drying technologies. In: Asia Pacific Drying Conference. Allied Publishers Pvt. Ltd., New Delhi, 2005.
- [143] G.J. Thuesen, W.J. Fabrycky, Engineering Economics, Prentice Hall, New York, 2001.
- [144] C. Ratti and A.S. Mujumdar, Solar drying of foods: Modeling and numerical simulation, Solar Energy 60,151-157, 1997.
- [145] V.K. Sharma, A. Colangelo and G. Spagna, Experimental investigation of different solar dryers suitable for fruits and vegetables drying, Renewable Energy 6, 413-424, 1995.

- [146] L. Ait Mohamed, M. Kouhila, A. Jamali, S. Lahsasni, N. Kechaou and M. Mahrouz, Single layer solar drying behaviour of Citrus aurantium leaves under forced convection, *Energy Conversion and Management* 46, 1473-1483, 2005.
- [147] A. Steinfeld and I. Segal, A simulation model for solar thin layer drying process, *Drying Technology* 4, 535–542, 1986.
- [148] G.R. Gamea, A.H. Amer and A. Lotfy, The thin layer drying behavior of apricots by indirect natural convection solar dryer, In: the 10th conference of the Miser J. Agri. Eng. 'Development of Agriculture Engineering Technology in the Arab and Islamic World', Faculty of Agriculture, Al-Azhar University, Egypt, pp. 251–272, 2002.
- [149] C. Tiris, N. Ozbalta, M. Tiris and I. Dincer, Performance of solar dryer, *Energy* 19, 993–997, 1994.
- [150] O. Yaldiz, C. Ertekin and H.I. Uzun, Mathematical modeling of thin layer solar drying of sultara grapes, *Energy* 26, 457–465, 2001.
- [151] M. Zaman and B.K. Bala, Thin layer solar drying of rough rice, *Solar Energy* 42, 167, 1989.
- [152] D.R. Pangavhane and R.L. Sawhney, Review of research and development work on solar dryers for grape drying, *Energy Conversion and Management* 43, 45–61, 2002.
- [153] D. Jain and G.N Tiwari, Thermal aspect of open sun drying of various crops, *Energy* 28, 37–54, 2003.
- [154] D. Jain and G.N Tiwari, Effect of greenhouse on crop drying under natural and forced convection I: evaluation of convective mass transfer coefficient, *Energy Conversion and Management* 45, 765–783, 2004.
- [155] G.N Tiwari, S. Kumar and O. Prakash, Evaluation of convective mass transfer coefficient during drying of jaggery, *Journal of Food Engineering* 63, 219–227, 2004.

- [156] L. Ait Mohamed, M. Kouhila, A. Jamali, S. Lahsasni, N. Kechaou and M. Mahrouz, Single layer solar drying behaviour of Citrus aurantium leaves under forced convection, *Energy Conversion and Management* 46, 1473–1483, 2005.
- [157] O. Yaldiz, C. Ertekin and H.I. Uzun, Mathematical modeling of thin layer solar drying of sultana grapes, *Energy* 26, 457–465, 2001.
- [158] T.I. Togrul and D. Pehlivan, Mathematical modelling of solar drying of apricot in thin layers, *J. Food Eng.* 55(3), 209–216, 2002.
- [159] O. Yaldiz and C. Ertekin, Thin layer solar drying of some vegetables, *Drying Technology* 19(3&4), 583–597, 2001.
- [160] M. Kouhila, N. Kechaou, M. Otmani, M. Fliyou and S. Lahsasni, Experimental study of sorption isotherms and drying kinetics of Moroccan Eucalyptus globules, *Drying Technology* 20(10), 2027–2039, 2002.
- [161] A. Midilli and H. Kucuk, Mathematical modeling of thin layer drying of pistachio by using solar energy, *Energy Conversion and Management* 44(7), 1111–1122, 2003.
- [162] A. Midilli, Determination of pistachio drying behaviour and conditions in a solar drying system, *Int. J. Energy Res.* 25(8), 715–725, 2001.
- [163] E.K. Akpınar, Y. Bicer and C. Yildiz, Thin layer drying of red pepper, *J. Food Eng.* 59, 99–104, 2003.
- [164] S. Lahsasni, M. Kouhila, M. Mahrouz and J.T. Jaouhari, Drying kinetics of prickly pear fruit (*Opuntia ficus indica*). *J. Food Eng.* 61(2), 173–179, 2003.
- [165] Md Azharul Karim, M.N.A. Hawlader, Performance evaluation of a v-groove solar air collector for drying applications, *Applied Thermal Engineering* 26, 121–130, 2006.

- [166] K.S. Jayaraman and D.K. Gupta, Drying of fruits and vegetables, Handbook of industrial drying, Marcel Dekker Inc., pp. 643–690, 1995.
- [167] J.E. Amir, K. Grandegger, A. Esper, M. Sumarsono, C. Djaya and W. Muhlbauer, Development of a multi-purpose solar tunnel dryer for use in humid tropics, *Renewable Energy* 1(2), 167–176, 1991.
- [168] A. Gauher, M. Mastekbayeva, M. Augustus and S. Kumar, Performance evaluation of solar tunnel dryer for chili dryer, ASEAN Workshop on Drying Technology, Solar Energy Research and Training Center, Pitsanulok, Thailand, pp. 15–26, 1998.
- [169] I.I. Tarigan, Y.S. Utomo, Sugiyatno, E.E.H. Hawala, A. Brojonegoro and Abdurrachim, Tea wilting using perforated solar collector, The 4th ASEAN Science and Technology Week, ASEAN Committee on Science and Technology, Bangkok, Thailand, pp. 277–288, 1995.
- [170] C. Palaniappan and S.V. Subramanian, Economics of solar air pre-heating in South Indian tea factories: A case study, *Solar Energy* 63 (1), 31–37, 1998.
- [171] O. Ekechukwu and B. Norton, Review of solar energy drying systems II and overview of solar drying technology, *Energy Conversion & Management* 40, 615–655, 1999.
- [172] P. Schirmer, S. Janjal, A. Esper, R. Smitabhindu and W. Muhlbauer, Experimental investigation of the performance of the solar tunnel dryer for drying bananas, *Renewable Energy* 7 (2), 119–129, 1996.
- [173] M.A. Hossain and B. Bala, Drying of hot chilli using solar tunnel dryer, *Solar Energy* 81, 85–92, 2007.
- [174] S.K. Supranto, W. Daud, M. Othman and B. Yatim, Design of an experimental solar assisted dryer for palm oil fronds, *Renewable Energy* 16, 643–646, 1999.

- [175] C. Tiris, M. Tiris and I. Dincer, Experiments on a new small-scale solar dryer, *Applied Thermal Engineering* 16 (2), 183–187, 1996.
- [176] B. Bena and R. Fuller, Natural convection solar dryer with biomass back-up heater, *Solar Energy* 72 (1), 75–83, 2002.
- [177] M. Krokida, C. Kiranoudis and Z. Maroulis, Viscoelastic behaviour of dehydrated products during rehydration, *Journal of Food Engineering* 40, 269–277, 1999.
- [178] Y. Gallalia, Y. Abujnaha and F. Bannanib, Preservation of fruits and vegetables using solar dryer: a comparative study of natural and solar drying, III; chemical analysis and sensory evaluation data of the dried samples (grapes, figs, tomatoes and onions), *Renewable Energy* 19, 203–212, 2000.
- [179] E. Torres-Reyes, J.J. Navarrete-Gonzalez and B.A. Ibarra-Salazar, *Renewable Energy* 26, 649–660, 2002.
- [180] H.P. Garg and R. Kumar, Studies on semi-cylindrical solar tunnel dryers: thermal performance of collector, *Applied Thermal Engineering* 20, 2000.
- [181] J. Pyrko, Tubular plastic solar collector for crop drying, Special Rep. 118, Department of Farm Buildings (LBT), Lund, Sweden.
- [182] A. Esper and W. Muhlbauer, Development and dissemination of solar tunnel dryers, in: *Proc. of Workshop-Drying and Conservation with Solar Energy*, ISES Solar World Congress, Budapest, 1993.
- [183] W. Muhlbauer, A. Esper and J. Muller, Solar energy in agriculture, in: *ISES Solar World Congress*, Budapest, August 23-27, 1993.
- [184] K.U. Lutz and W. Muhlbauer, Solar tunnel dryer with integrated collector, *Drying Technology* 4, 583-603, 1986.
- [185] R.J. Fuller, Comparison between solar tunnel dryers and conventional fuel dehydrators for on-farm drying, *Drying Technology* 13(5-7), 1487-1502, 1995.

- [186] M. Condori, R. Echazu and L. Saravia, Solar drying of sweet pepper and garlic using the tunnel greenhouse dryer, *Renewable Energy* 22, 447-460, 2001.
- [187] R.G. Bowrey, K.A. Buckle, I. Hamey and P. Pavenayotin, Use of solar-energy for banana drying. In: *Food Technol. Aust.* 32(6), 290-291, 1980.
- [188] M.W. Bassey, Design and performance of hybrid crop dryer using solar-energy and sawdust. In: *Proc ISES Cong INTERSOL 85*, Montreal, Canada, Pergamon Press, Oxford, pp. 1039-1042. 1985.
- [189] B.K. Huang and M. Toksoy, Design and analysis of greenhouse solar systems in agricultural production. *Energy in Agric.* 2, 115-136, 1983.
- [190] M.N. Ozisik, B.K. Huang and M. Toksoy, Solar grain drying, *Solar Energy* 24, 397-401, 1980.
- [191] B.K. Huang, M.N. Ozisik and M. Toksoy, Development of greenhouse solar drying of farm crops and processed products, *Agric. Mech. Asia, Africa and Latin America* 12(1), 47-52, 1981.
- [192] B.K. Huang and M. Toksoy, Greenhouse solar system for effective year-round solar-energy utilization in agricultural production, *Agric Energy* 1, 152, 1981.
- [193] O.P. Singhal and G.P. Gupta, Use of solar-energy for par-boiling and drying of paddy, *ISES Conf New Delhi, India*, pp. 1958-1963, 1978.
- [194] B.D. Mclendon and J.M. Allison, Solar-energy utilization in alternate grain systems in the southeast, *Trans ASAE* 23, 1289-1292, 1980.
- [195] J. Sohns, N. Fisch, A. Haug and Y. Tanes, Performance of a solar heated drying plant, *ISES Solar World Forum, Brighton, UK.*, Pergamon Press, Oxford, 10, pp. 112-117, 1981.
- [196] A. Chakraverty, S.K. Das, Design and testing of an integrated solar-cum-husk fired paddy dryer of one tonne per day capacity. *Int. Drying Symp.*, *Drying* 86, Cambridge, U.S.A., pp. 692-702, 1986.

- [197] T.A. Reddy, D. Pushparaj and G.L. Gupta, A design procedure for convective solar dryers, In: Solar Energy Symp., The Utilization of Solar Heat in Industry and Agric. Nice, France, pp. 101-111, 1979.
- [198] R.D Piacentini, R. Gaspar, M.A. Lara, A and Cortes, Experiments on solar grain drying in Argentina, In: Proc Solar Energy Symp on The Utilization of Solar Heat in Industry and Agric. Nice, France, pp. 133-138, 1979.
- [199] H.R. Bolin, A.E. Stafford and C.C. Huxsoll, Solar heated fruit dehydrator, Solar Energy 20, 281-291, 1978.
- [200] K.A. Leiner and M. Fiebig, Second law optimization of flat-plate solar air heaters, Part I: the concept of exergy flow and the modeling of solar air heater, Solar Energy 41, 127-132, 1988.
- [201] S.K. Kalra and K.C. Bharadwaj, Use of simple dehydrator for drying fruit and vegetables products, Journal of Food Science Technology 18, 23-26, 1981.
- [202] B.K. Bala and J.L Woods, Optimization of a natural convection solar drying system, Energy 20(4), 285-294, 1995.
- [203] M.A. Rehman and O.P. Chawla, Seasoning of timber using solar energy, Indian Forest Bulletin, No. 229, Forest Research Institute, Dehradun, India, 1961.
- [204] Y Tao and O.E. Hsia, Lumber solar drying experiment at Taichung, Bull. No. 63-N-490/C. Taiwan Provincial Chung Hsing University, Taichung, 1964.
- [205] R.A. Plumptre, Solar timber kilns: their suitability for developing countries in technology for solar energy utilization, Development and Transfer of Technology, Ser. No. 5. ID/202. UNIDO, New York, 1978.
- [206] H.E. Troxwell and L.A. Mukker, Solar lumber drying in the central Rocky Mountain region, Forest Pro. J. 18(1), 19, 1968.

- [207] S.N. Sharma, P. Nath and B.I. Bali, A solar timber seasoning kiln. *J. Timber Dev. Assoc. India* 18(2), 10, 1972.
- [208] M. Bedel and P. Gueneau, Lumber dryer (Madagascar), in Res. Rep. No. T-99, Brace Research Institute. Quebec, CS/EC-X-1, 1975.
- [209] J.L. Tschernitz and W.T. Simpson, Solar heated forced air lumber drying for tropical latitudes, *Solar Energy* 22, 563, 1977.
- [210] R.H. Wagner, Applications of solar energy to continuous belt dehydration, Final report, Phase 1, Rep. No. ORO/5119-1, U.S. Department of Energy, Washington, DC., 1977.
- [211] D. Buddhi, S.D. Sharma and A. Sharma, Thermal performance evaluation of a latent heat storage unit for late evening cooking in a solar cooker having three reflectors, *Energy Conversion and Management* 44, 809-817, 2003.
- [212] S.D. Sharma, T. Iwata, H. Kitano and K. Sagara, Thermal Performance of solar cooker based on an evacuated tube solar collector with a PCM storage unit, *Solar Energy* 78, 416-426, 2005.
- [213] N.K. Bansal and D. Buddhi, An analytical study of a latent heat storage system in a cylinder, *Energy Conversion and Management* 33(4), 235-242, 1992a.
- [214] N.K. Bansal and D. Buddhi, Performance equation of a collector cum storage system using phase change materials, *Solar Energy* 48, 185-194, 1992b.
- [215] A. Abhat, Low temperature latent heat thermal energy storage: Heat storage materials, *Solar Energy* 30(4), 313-332, 1983.
- [216] Ahmet Sari, Thermal reliability test of some fatty acids as PCMs used for solar thermal latent heat storage applications, *Energy Conversion and Management* 44, 2277-2287, 2003.
- [217] A. Hasan, Phase change material energy storage system employing palmitic acid, *Solar Energy* 52(2), 143-154, 1994.

- [218] S.D. Sharma, D. Buddhi and R.L. Sawhney, Accelerated thermal cycle test of latent heat storage materials, *Solar Energy* 66(6), 483-490, 1999.
- [219] C. Tuncbilek, A. Sari, A. Tarhan, G. Ergunes and K. Kaygusuz, Lauric and palmitic acids eutectic mixture as latent heat storage material for low temperature heating applications, *Energy* 30, 677-692, 2005.
- [220] R. Nikolic, New materials for solar thermal storage-solid/liquid transitions in fatty acid esters, *Solar Energy Materials and Solar Cells* 79, 285-292, 2003.
- [221] Z. Liu, Z. Wang and C. Ma, An experimental study on heat transfer characteristics of heat pipe heat exchanger with latent heat storage, Part I: Charging only and discharging only modes, *Energy Conversion and Management* 47, 944-966, 2006.
- [222] S.O. Enibe, Performance of a natural circulation solar air heating system with phase change material energy storage, *Renewable Energy* 27(1), 69-86, 2002.

DESIGN AND DEVELOPMENT OF VARIOUS TYPES OF SOLAR AIR HEATERS

3.1 Introduction

Flat plate solar air heaters have been used with success for many industrial and domestic applications such as drying farm produce, dehydrating industrial products, and space heating [1-4]. Solar energy is important in low-temperature thermal applications because it replaces considerable amounts of conventional fuels.

Several types of solar air heaters have been developed over the years, the flat plate type being the most common because it is simple to construct, easy to operate, and inexpensive to maintain. Since air is the working fluid, the problems of freezing or boiling of the fluid are obviated. However, the low density, low thermal capacity, and low heat conductivity of air requires larger ducts to transport the required energy. These are probably the important drawbacks of air panels. However, low cost and reliability makes them an attractive alternative. A conventional solar air heater generally consists of an absorber plate with a parallel plate below, forming a passage of high aspect ratio through which the air to be heated flows. A transparent sheet covers the absorber plate, while a sheet-metal container filled with insulating material is attached underneath and to the sides [5-7]. There are two possible alternatives to maximize the collection of useful energy from air heaters, namely (a) to maximize the collector area by lengthening the absorber plate while keeping channel depth and mass flow rate constants and (b) to make the channel deeper while keeping the surface area constant. However, for a system with design constraints on fan power

and collector length, the only practical alternative is to increase the volume of air by making the channel deeper.

In order to increase the thermal efficiency of solar air heaters, the absorbed heat must be transferred to the air flowing above, underneath, both above and underneath or through the absorber plate. Different configurations of the absorber plate have been designed toward this end. Choudhury et al. [8] designed a corrugated absorber, Garg et al. [9] introduced the absorber plate with fins attached, and Mohamad [10] proposed a metal matrix absorber plate. Choudhury and Garg [11] studied a collector with an air jet. The air flow rate of the device ranged from $50 \text{ m}^3\text{m}^{-2}\text{h}^{-1}$ to $250 \text{ m}^3\text{m}^{-2}\text{h}^{-1}$. When compared to the collectors with two air channels without baffles, the air jet collector proved better. The authors tested two versions of the collector without baffles: one 10 cm deep and the other 5cm deep. The result confirmed that the efficiency increases as the depth decreases.

Many designs of the solar air heating system with different construction materials and different configurations of the heat transfer passage are described in literature. The performance of these designs has been assessed both by analytical methods and numerical simulation techniques. Buelow [12], Whillier[13], and Close [14] derived performance equations for flat plate collectors analytically. Close considered the effect of selective paints, vee-corrugations and fins. Performance equations were also derived by Gupta and Garg [15] for a solar air heating system with a non-porous absorber. Conventional single and double exposure air heating systems have been analysed by Suri and Saini [16]. Later studies included the effect of conduction along the direction of air flow and of radiative heat exchange between the absorber and the rear plate. The results confirmed that conduction along the direction of air flow is not significant in the case of metallic absorbers. Reddy and Gupta [17] presented a graphical method of

determining, under different operating conditions, the design data for a system using air heaters.

Swartman and Ogulande [18] modified the simple absorber flat plate for a solid matrix. Yeh and Chou [19] investigated the efficiency of upward-type baffled solar air heaters. All absorber plates are made with clean, new materials, which increase their cost of production. Henden et al. [20] considered high cost to be the main barrier to large-scale introduction of thermal solar systems. Alvarez et al. [21] proposed an air collector with the absorber plate made of recyclable aluminium cans and achieved a maximum efficiency of 74%.

In the present work, a detailed technical study was performed in all types of solar air heaters. Five types of solar air heaters were developed and performance evaluation was carried out in every model and compared with each other. The various types of solar air heaters designed and tested are listed below and are discussed with the help of engineering/mechanical drawings.

- (1) Underflow collector-copper as absorber plate
- (2) Overflow collector-aluminium as absorber plate
- (3) Overflow collector-corrugated Galvanized Iron (GI) as absorber plate
- (4) Double flow collector-aluminium as absorber plate
- (5) Matrix collector-Galvanized Iron mesh as absorber plate

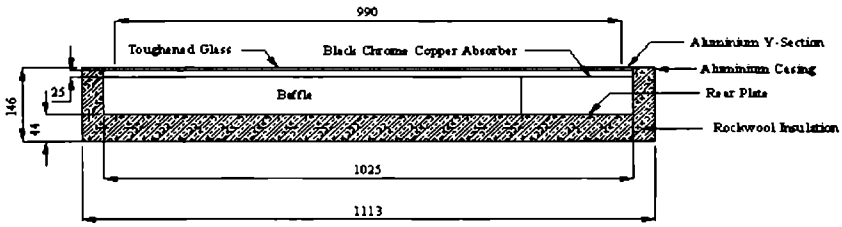
Studies were carried out separately for the collectors with and without baffles in the air channel.

3.2 Solar Air Heaters Developed

As mentioned above, mainly 5 types of solar air heaters were developed. The design details of all the collectors are described exhaustively.

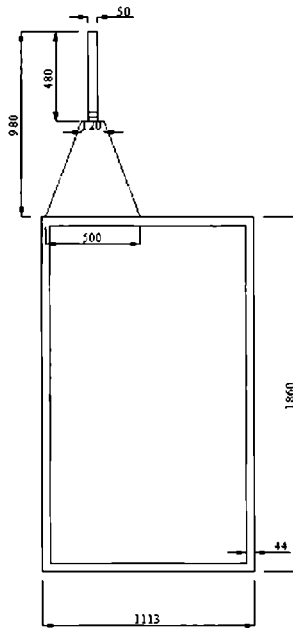
3.2.1 a) Underflow Copper Collector with Baffles

The gross area of the collector was 2.1 m^2 with a collector aperture area of 1.82 m^2 . The developed solar air heater was of the 'underflow' type. The structural frame of the air heater was made of aluminium extrusions. The absorber plate was made of a 38 SWG black chrome copper sheet, fitted to the aluminium frame with screws. The absorber plate and the rear plate (bottom plate), with a gap of 77 mm separating them, formed a rectangular air duct. An air gap of 25 mm was provided between the absorber plate and the glazing. The bottom plate was a 24-SWG aluminium sheet. Rockwool insulation was packed along the sides of the copper sheet and underneath and along the sides of the aluminium sheet. The insulation was 44 mm thick throughout. A 4 mm thick sheet of toughened glass was mounted 25 mm above the absorber plate. Design details of the copper collector are presented in Table 3.1. Fig. 3.1 is a sectional view and Fig. 3.2 is a schematic diagram of the features of the solar air heater with baffles. Two baffles were placed along the air passage to increase the air fill factor. Each baffle was 72.5 cm long and occupied 71% of the width of the collector. The passage of air inside the collector with baffles is shown in Fig. 3.3. The baffles were attached to the bottom plate. The baffles were 76 mm tall, positioned vertically pointing to the absorber plate. The baffles made the air to follow a winding path, thereby doubling the length of the air passage through the collector. The baffles create turbulence, which forces the air to come in close contact with hot surface of the absorber and decreases the thermal sub layer. The space between the absorber and the glass reduces the convective losses from the front. The outer body of the whole structure is covered with aluminium sheet, and a trapezoid was provided to the air outlet of the air heater through which the air is sucked by a centrifugal blower. All possible leaks from the side and the bottom were sealed with silicon sealant.



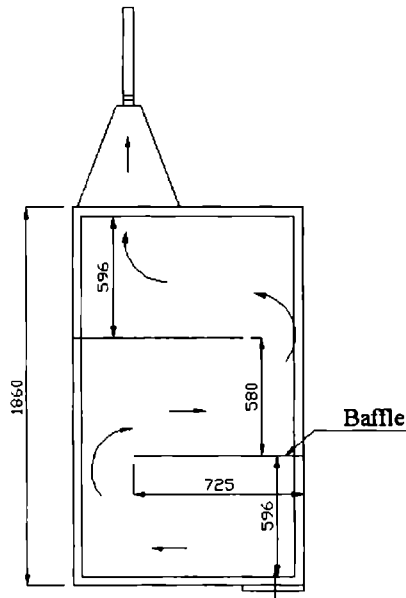
ALL DIMENSIONS IN MM

Fig. 3.1 Sectional view of the underflow copper solar air heater with baffles



ALL DIMENSIONS IN MM

Fig. 3.2 Schematic diagram of the underflow solar air heater



ALL DIMENSIONS IN MM

Fig. 3.3 Air flow distribution in the collector fitted with baffles

Table 3.1 Design details of underflow copper air heater

Gross collector area	1860 mm x 1113 mm x 146 mm
Aperture area	1772 mm x 1025 mm
Absorbing material	Black chrome copper (38 SWG)
Rear plate	Aluminium
Working fluid	Air
Insulation material	Rock wool
Insulation thickness (side and bottom)	44 mm
Collector tilt angle	12°
Cover plate material	Toughened glass
Dimensions	1730 mm x 990 mm
Thickness	4 mm
Number of cover glass	One
Mode of air flow	Underflow
Centrifugal blower	335 W
Air inlet area	300 mm x 77 mm
Air outlet area	: 300 mm x 77 mm

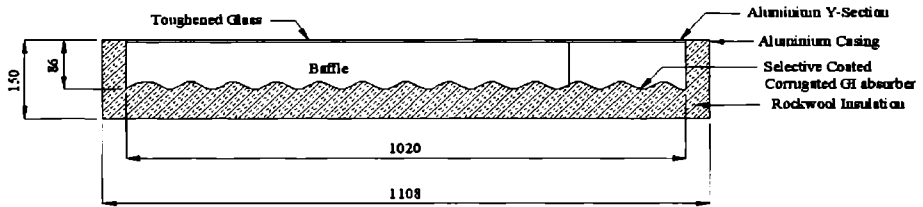
3.2.1 b) Underflow Copper Collector without Baffles

A parallel study was also conducted on a similar solar air heater without baffles to compare the underflow copper collector with baffles. All the design parameters are same as that of collector with baffles, except that the baffles were not fitted to the absorber.

3.2.2 a) Overflow Galvanized Iron (GI) Collector with Baffles

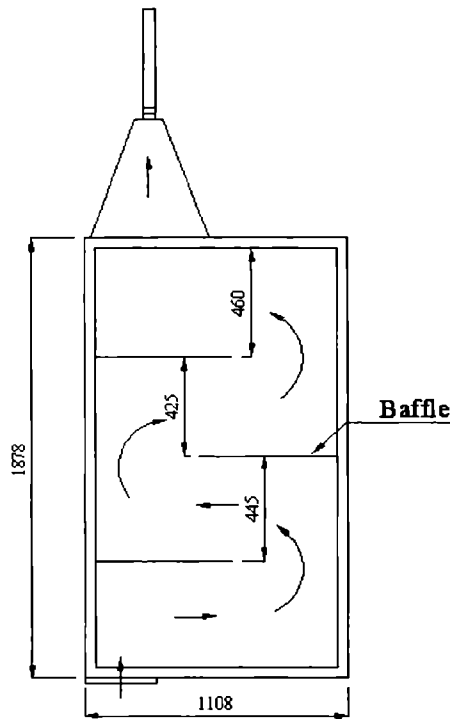
The experimental set up consists of a GI collector having a gross collector area of 2.1 m^2 with a collector aperture area of 1.82 m^2 . The total height of the collector was 150 mm (from glass plate to bottom). The developed solar air heater was an 'overflow' type. The structural frame of the air heater was made of aluminium extrusions. Absorber plate used was 22 SWG selective coated corrugated GI sheet, it was screwed with aluminium square tubes. Rockwool insulation was tightly packed bottom and sides of the absorber plate. The whole set up was encapsulated in an aluminium casing. 4-mm toughed glass was used as glazing material. A rectangular air duct of 86 mm was formed in between the absorber plate and transparent cover. Three baffles were provided in the air flowing area in order to increase the air fill factor. The baffles were attached to the corrugated absorber plate after it was made in the required shape. Fig. 3.4 shows the sectional view of the corrugated solar air heater with baffles. The length of the baffle was 58 cm and it occupied 57% of width of the collector. The air flow passage of the collector with baffles is given in Fig. 3.5. The baffles were positioned vertically upward pointing to the glass plate. The height of the baffles was 85 mm and the other end was placed very near to the top glass plate. The effect of the baffles is the creation of turbulence, in such a way as to make the air, licking the hot surface of the absorber and to decrease the thermal sub layer. A Plenum chamber was provided at the outlet of the collector to stabilize the air flow out and it was connected to a

centrifugal blower having a capacity of 335 W. All the possible air leakage from the side and bottom was prevented by silicon sealant.



ALL DIMENSIONS IN MM

Fig. 3.4 Sectional view of the corrugated overflow collector with baffles



ALL DIMENSIONS IN MM

Fig. 3.5 Air flow distribution in GI collector with baffles

The air was made to flow normal to the corrugation waves, i.e., across the peaks and valleys. The corrugation pitch was 75 mm and it contained 13 hills and valleys along the width of the collector. The height difference between the peak and valley was 20 mm. The characteristic dimensions of the corrugation shape is shown in Fig. 3.6. As described earlier, duct height of flow passages (H) was 86 mm. This height corresponds to duct aspect ratio of 1.15. The corrugation aspect ratio, AR_c is

$$AR_c = \frac{\text{Corrugated duct height (H)}}{\text{Corrugation cycle length (L}_c\text{)}}$$

In a solar air heater using corrugated absorber plate, the corrugation inclination angle, β , is a major parameter determining the efficiency. The pressure drop and the heat transfer are fully dependent on the flow structure that is largely affected by the inclination angle (β) [22]. The study conducted by Focke et al. [23] recommended the use of β between 30° and 60° for an acceptable compromise between enhancement of the heat transfer coefficient and the accompanied increase in the pressure drop. The corrugation inclination angle for the present absorber was 30° . Design details of baffled GI collector investigated experimentally are presented in Table 3.2.

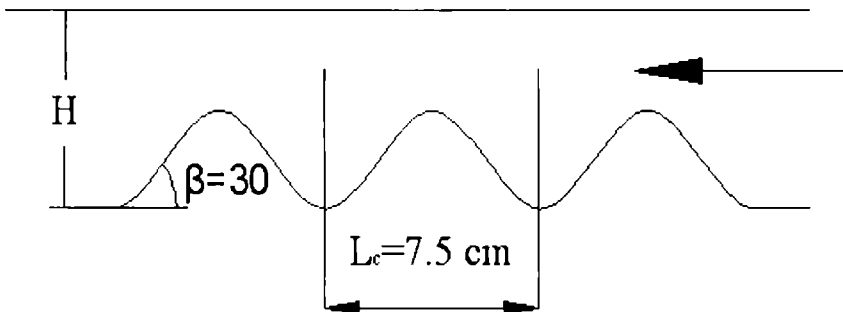


Fig. 3.6 Dimensions of simple cycle of the corrugated duct

Table 3.2 Design details of corrugated GI air heater

Gross collector area	1878 mm x 1108 mm x 150 mm
Area of absorber	1790 mm x 1020 mm
Absorbing material	Selective coated corrugated GI sheet (22 SWG)
Working fluid	Air
Insulation material	Rock wool
Insulation thickness (side and bottom)	44 mm
Collector tilt angle	12°
Cover plate material	Toughened glass
Dimension	1734 mm x 980 mm
Thickness	4 mm
Number of cover glass	One
Mode of air flow	Overflow
Centrifugal blower	335 W
Air inlet area	440 mm x 45 mm
Air outlet area	: 440 mm x 45 mm

3.2.2 b) Overflow Galvanized Iron (GI) Collector without Baffles

A similar air heater without baffles and all other design features exactly same as that of the above was also developed. This enabled the comparison of overflow GI collector with and without baffles.

3.2.3 a) Overflow Aluminium Collector with Baffles

Fig. 3.7 shows the sectional view of the overflow baffled solar air heater. The air is passed through the solar air heater having a rectangular channel size of 1790 x 1020 x 97 mm³. Selective coated 24 SWG plane aluminium sheet acted as absorber plate and rock wool insulation was packed bottom and sides of the absorber plate to suppress the heat losses. 4-mm toughed glass was used as glazing material. The air channel was formed

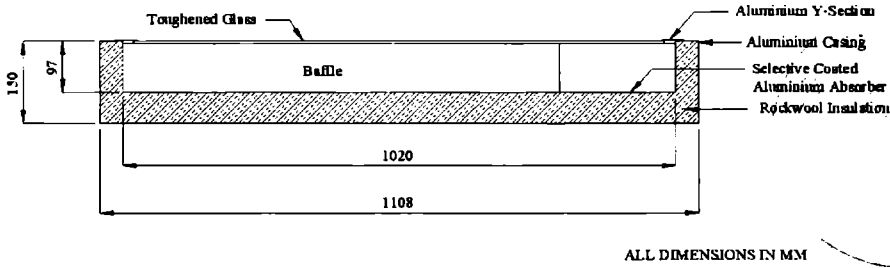
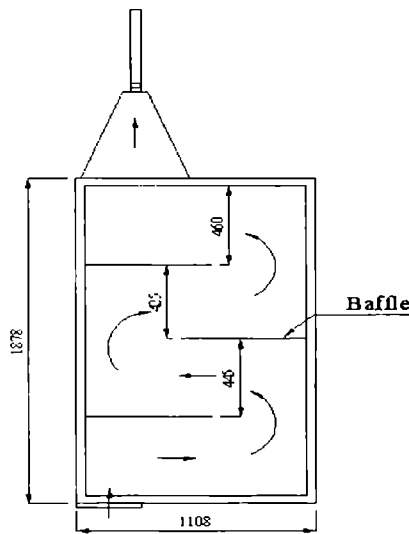


Fig. 3.7 Sectional view of the overflow solar air heater with baffles

in between the absorber plate and transparent cover. Three baffles were positioned in the air passage and it was attached to absorber plate. The length of the baffle was 58 cm and it occupied 57% of collector's width. The air flow passage of the collector with baffles is given in Fig. 3.8. The height of the baffles was 96 mm and it was positioned vertically upward pointing to the glass plate. A plenum chamber was provided at the outlet of the collector to stabilize the air flow out and it was connected to a centrifugal blower having a capacity of 335 W. Design details of baffled aluminium collector investigated experimentally are presented in Table 3.3



T
621 383 51 664
CRE

Fig. 3.8 Air flow distribution inside the overflow solar air heater with baffles

Table 3.3 Design details of overflow aluminium solar air heater

Gross collector area	1878 mm x 1108 mm x 150 mm
Area of absorber	1790 mm x 1020 mm
Absorbing material	Selective coated aluminum sheet (24 SWG)
Working fluid	Air
Insulation material	Rock wool insulation
Insulation thickness (side and bottom)	44 mm
Collector tilt angle	12°
Cover plate material	Toughened glass
Dimension	1734 mm x 980 mm
Thickness	4 mm
Number of cover glass	One
Mode of air flow	Overflow
Centrifugal blower	335 W
Air inlet area	440 mm x 45 mm
Air outlet area	440 mm x 45 mm

3.2.3 b) Overflow Aluminium Collector without Baffles

In order to compare the efficiency of the aluminium collector with baffles, another collector was also fabricated with same materials and design features. The performance of the collector was investigated and compared with each other.

3.2.4 a) Double Passage Solar Air Heater with Baffles

An aluminium sheet of 24 SWG and 1900 mm x 900 mm size was used as absorber plate with the top surface painted black. The gross area of the collector was 2 m² and the collector aperture area was 1.71 m². The passage of air was both above and underneath of the absorber. Above the absorber plate, air passage was in between the glazing and absorber plate, while it was in between the bottom plate and absorber plate, when it was passing beneath the plate. The air enters from the top of the collector and

flows over the absorber plate and passes down through the duct, which provided on the bottom portion. Air leave the collector through the top after it passes beneath the absorber plate. The depth of air channel was same for both above and below the absorber plate and it was 5cm. The total air channel depth of the collector was 100 mm (50 mm equally above and below the absorber plate). 24 SWG aluminium sheet was used as bottom plate and rockwool insulation was packed sides and beneath the bottom plate. The thickness of insulation was 5 cm both at the bottom and sides. 4 mm toughened glass was mounted on the top as glazing. The space between the absorber and the glass reduces the convective losses at the front side. The outer body of the whole structure was covered with aluminium sheet.

Two baffles were provided in the air flowing area above the absorber plate. Fig. 3.9 shows a sectional view of the double passage solar air heater with baffles. The length of the baffles was 76 cm and distance between the baffles was 63.3 cm. Baffle occupied 84% of collector's width. The baffles were attached to the absorber plate and it was pointed towards the top glass. The schematic diagram of solar air heater with baffles is given in Fig. 3.10.

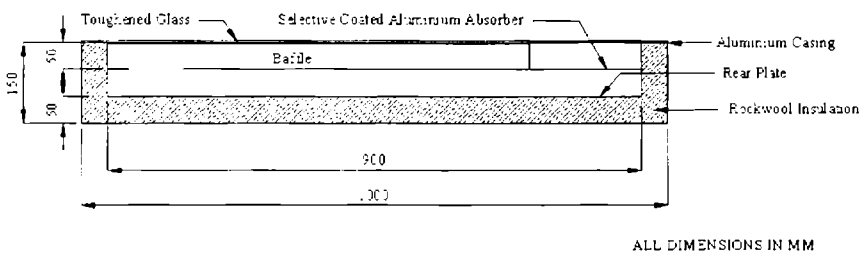
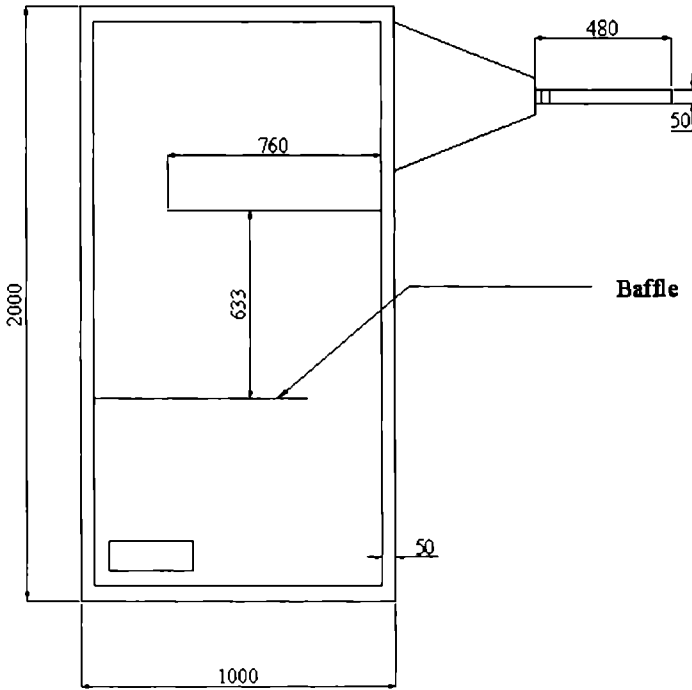


Fig. 3.9 Sectional view of the double pass solar air heater with baffles



ALL DIMENSIONS IN MM

Fig.3.10 Schematic diagram of the double flow solar air heater with baffles

A plenum chamber was provided at the outlet of the collector to stabilize the air flow out and it was connected to a centrifugal blower having a capacity of 335 W. All possible air leakage from the side and bottom was prevented by silicon sealant. Design details of double flow collector with baffles investigated experimentally are presented in Table 3.4.

3.2.4 b) Double Passage Solar Air Heater without Baffles

In addition to the above type, a parallel study was also performed on a similar double passage solar air heater without baffles. The dimensions of the two collectors were exactly made identical.

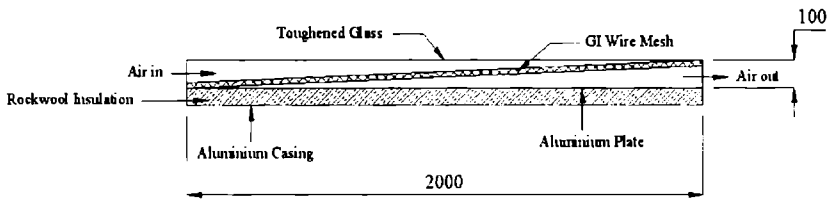
Table 3.4 Design details of double flow air heater

Gross collector area	2000 mm x 1000 mm x 150 mm
Area of absorber	1900 mm x 900 mm
Absorbing material	Selective coated Aluminium sheet (24 SWG)
Working fluid	Air
Insulation material	Rock wool
Insulation thickness (side and bottom)	50 mm
Collector tilt angle	12°
Cover plate material	Toughened glass
Dimension	2000 mm x 1000 mm
Thickness	4 mm
Number of cover glass	One
Mode of air flow	Double flow
Centrifugal blower	335 W
Air inlet area	150 mm x 50 mm
Air outlet area	: 150 mm x 50 mm

3.2.5 Matrix Collector

The matrix collector was covered by a single, highly transparent 4 mm solar toughened glass plate, in order to reduce convective and long wave radiative losses to the atmosphere. The choice of single glazing was because of maximizing the radiation impact on the absorber surface and also to reduce cost. The gross area of the collector was 2 m² and the collector aperture area was 1.74 m². Rock wool was used as insulation material and the thickness of insulation was 4.4 cm at the bottom and sides. The size of the air channel was 191 x 91 x 10 cm. The inner side surface and bottom wall were covered by 24 SWG aluminium sheet. The air channel depth of the collector was 10 cm. Selective coated G.I. wire mesh was used as absorber. The position of absorber was diagonally inside the box and air enters through the top of the absorber, and leaves through the bottom. Fig. 3.11 shows the schematic diagram of the matrix air heater. The outlet of the

solar air heater was connected through a trapezium to a centrifugal blower. The absorber matrix consisted of two parallel sheet of G.I. mesh (20 meshes per linear inch) of known physical characteristics (Table 3.5). The spacing between the layers was 8 mm. The solar radiation transmitted through the cover glass is absorbed mainly on the surface of the black painted mesh and transferred by convection to the air flowing through it. Considerable advantage of this type of material is that the geometry as well as the material is free to be chosen from a wide range of commercially available material, yielding ideal prerequisites for absorber materials. Design details of matrix collector investigated experimentally are presented in Table 3.6.



ALL DIMENSIONS ARE IN MM

Fig. 3.11 Schematic diagram of the matrix solar air heater

Table 3.5 Physical properties of absorber matrix with specifications

Absorber Matrix	Meshes per in.	Meshes per cm	Wire diameter painted (d)	Porosity of bed (p) (mm)	Packing surface area (A_p) (m^2)
GI mesh	20 x 20	7.8 x 7.8	0.27	0.946	3.24

Table 3.6 Design details of matrix solar air heater

Gross collector area	2000 mm x 1000 mm x 150 mm
Area of absorber	1912 mm x 912 mm
Absorbing material	Selective coated GI wire mesh (20 mesh)
Matrix thickness	8 mm
Working fluid	Air
Insulation material	Rock wool
Insulation thickness (side and bottom)	50 mm
Collector tilt angle	12°
Cover plate material	4 mm Toughened glass
Dimension	2000 mm x 1000 mm
Thickness	4 mm
Number of cover glass	One
Mode of air flow	Downward through the matrix
Centrifugal blower	335 W
Air inlet area	150 mm x 100 mm
Air outlet area	150 mm x 100 mm

3.3 Other Materials/Components Used

3.3.1 Selective Coating

For efficient collection of solar energy, it is desirable that the absorber surface should absorb maximum amount of incident solar radiation while emit less radiation. A selective surface has high absorptance for short wave radiation (less than 2.5 μm) and low emittance for long wave radiation (more than 2.5 μm). In the present work, black chrome selective coating, the most successful and stable selective surface was used for absorber coating in copper collector. The reported absorptivity and emissivity of the material is 0.95 and 0.08 respectively. Except for copper collector, the composition of selective paint used in all other collectors tested is Copper oxide (CuO), Ferric Oxide (Fe₃O₄), and Manganese dioxide (MnO₂) and its absorptivity is 0.93.

3.3.2 Cover Plate

The characteristics of cover plate through which the solar energy is transmitted are extremely important in the functioning of solar collector. The functions of cover plate are: (1) to transmit maximum solar energy in the absorber plate; (2) to minimize upward heat loss from the absorber plate to the environment; (3) to shield the absorber plate from direct exposure to weathering. The most critical factors for the cover plate materials are the strength, durability, non-degradability and solar energy transmittance. Tempered glass of 4-mm thickness was used as the glazing material in all the collectors fabricated and its transmissivity is 92%. Tempered glass is the most common cover material for collectors because of its proven durability and stability when exposed to UV radiation. A properly mounted tempered glass cover is highly resistant to breakage both from thermal cycling and natural events. Glass cover also reduces the radiation loss from the absorber plate because it is opaque to the longer wavelength IR radiation emitted by the hot absorber plate. The space between the absorber and the glass reduces the convective losses at the front side.

3.3.3 Insulation

Insulation is an important factor playing a very significant role in minimizing the heat losses from lower surface of the collector plate and from the lateral edges of the collector. Rock wool was used as insulation material by packing beneath and sides of absorber plate of all the collectors tested. The thickness of insulation used was 44 mm and 50 mm. The desired characteristics of an insulating material are: low thermal conductivity, stability at high temperature (up to 200°C), no degassing upto around 200°C, ease of application, etc. The density of rock wool insulation is 48 kg/m³ and its thermal conductivity is 0.044 W/m°C.

3.4 Performance Equation

The performance of a flat-plate collector operating under assumed steady-state conditions can be described by the following relationship [13, 24].

$$\frac{Q_u}{A_c} = I(\tau\alpha)_e - U_L (T_p - T_a) \quad (3.1)$$

If one introduces the parameter called collector heat removal factor, F_R [7], Eq. (3.1) can be rewritten as

$$\frac{Q_u}{A_c} = F_R I(\tau\alpha)_e - F_R U_L (T_i - T_a) \quad (3.2)$$

Then the collector efficiency, η , can be written from Eq. (3.1) and Eq. (3.2), as

$$\eta = \left[(\tau\alpha)_e - U_L \left(\frac{T_p - T_a}{I} \right) \right] \quad (3.3)$$

or

$$\eta = F_R \left[(\tau\alpha)_e - U_L \left(\frac{T_i - T_a}{I} \right) \right] \quad (3.4)$$

However, for solar air heaters taking in air at ambient temperature ($T_i = T_a$), it is advantageous to utilize the following equation for thermal efficiency [7, 24]

$$\eta = F_0 \left[(\tau\alpha)_e - U_L \left(\frac{T_o - T_i}{I} \right) \right] \quad (3.5)$$

where A_c is the area of the collector (m^2), Q_u is the useful heat gain rate of the collector (W), F_0 is the heat removal factor referred to the outlet temperature, η is the overall efficiency of the collector, F_R is the heat

removal factor related to the inlet temperature, τ is the transmittance of the glass cover for direct radiation at normal incidence, α is the solar absorptance of the absorber plate for direct radiation at normal incidence, $(\tau\alpha)_e$ is the effective transmissivity-absorptivity product, U_L is the collector heat loss coefficient between the absorber plate and the atmosphere (W/m^2k), including allowances for side and rear losses, I is the intensity of solar radiation (W/m^2) T_a is the ambient temperature ($^{\circ}C$), T_i is the inlet temperature of air ($^{\circ}C$), T_o is the outlet temperature of air ($^{\circ}C$) and T_p is the average temperature of the absorber surface of the solar collector ($^{\circ}C$)

Eq. (3.5) indicates that a plot of efficiency against $\left(\frac{T_o - T_i}{I}\right)$ will result in a straight line whose slope is $F_0 U_L$ and ordinate axis-intercept is $F_0 (\tau\alpha)_e$; if F_0 , U_L and $(\tau\alpha)_e$ are not very strong functions of operating parameters like mass flow rate, intensity of solar radiation, ambient temperature, and wind velocity variations. This approach, similar to the one conventionally used for solar flat-plate collectors, undoubtedly, assumes that the dependence of F_0 on mass flow rate which positively exists, is weak.

Furthermore, considering that the performance can be expressed by another equation, containing the temperature gain produced by the collector and expressed as

$$\eta = \frac{m C_p (T_o - T_i)}{I} \quad (3.6)$$

Where m is the mass flow rate per unit collector area (kg/m^2h) and C_p is the specific heat of air ($kJ/kg^{\circ}C$). Thus, by measuring the air flow rate, solar intensity at the inclined plane, outlet and inlet air temperatures of the heater, one can find the efficiency.

Thus Eq. (3.5) and (3.6) can be represented on a single diagram having the same quantities as the abscissa and ordinates [17]. For a given collector, this diagram shows the typical performance parameters, η and $\left(\frac{T_o - T_i}{I}\right)$ as a function of mass flow parameter m to represent Eq. (3.6)

and as a single regression straight line plot to represent Eq. (3.5)

The pumping power can be calculated from the measured pressure drop across the system using the following equation.

$$PP = \frac{m}{\delta_f} \Delta P \quad (3.7)$$

where ΔP is the pressure drop (Pa) and δ_f is the density of fluid (kg/m^3)

3.5 Instrumentation and Measurement of Various Thermo physical Parameters

The measured variables in all the experimental set-ups include solar flux normal to the absorber surface, ambient air temperature, inlet and outlet temperature, top glass temperature as well as the temperature of the absorber plate at various points. The air mass flow rate was calculated from the output air velocity. The pressure drop across the collector was monitored for different air mass flow rate. The air was supplied to the units by centrifugal blower.

Solar radiation intensity was measured with a calibrated 'Solarimeter', locally named Suryamapi (Central Electronics Limited, India), having a least count of 2 mW/cm^2 with $\pm 2\%$ accuracy on the full scale range of $0\text{-}120 \text{ mW/cm}^2$. Air velocity was measured with a 'Digital thermo-anemometer' (model. TA 35 made by Airflow, UK) with a range of 0.25 to 20 m/s . The accuracy of the anemometer is $\pm 0.1 \text{ m/s}$. A 0.5-HP centrifugal fan was used to make the air flow through the collector. The velocity of the

centrifugal blower was adjusted using an externally controlled regulator. The temperatures of air at the inlet, outlet and at the top glass and absorber plate were monitored using an LM 35 sensor. The sensor was connected to a computer using an RS 232 interface through a 16-channel data logger, which records the temperatures at the required points for every minute. The pressure drop across the collector was measured by using a U-tube manometer filled with water.

3.6 Experimental Procedure

The experiments were conducted on the terrace of Dept. of Physics, Cochin University of Science and Technology, Kochi ($9^{\circ}57'N$ and $76^{\circ}16'E$). The materials and the methods for performance evaluation are as follows. The tests were conducted between 9.00 a.m to 5.00 p.m solar time. During the experimental period, the following quantities were measured: ambient air temperature, T_a ; hot air outlet from the collector, T_o temperature of the top glass, T_g ; solar radiation, I ; inlet air temperature, T_i ; and air velocity through the panel and mass flow rate, m

For every model of solar air heaters, two types of collectors - with baffles and without baffles - were used for testing. In collector with baffles, the air was made to flow in a zig-zag pattern. A 0.5-HP centrifugal fan was used to make the air flow through the collector. The blower was connected to the outlet of the solar air heater through a triangular section and duct. The velocity of the centrifugal blower was adjusted using a manually controlled regulator. The air mass flow rate was calculated from the measured velocity at the output of the collector and the experiment was repeated with different mass flow rates each day. The maximum and average temperatures were recorded for each mass flow rate. The instantaneous and average efficiency over the day for a particular mass flow rate was calculated.

All the parameters were recorded in every 10 minutes. The experiments were conducted for different mass flow rates for the two types of experimental set up. The pressure drop across the collector was examined for all the mass flow rates studied. Pumping power was calculated from the measured value of pressure drop. Tests were conducted outdoors for all the collectors under identical conditions on clear days. The flow rate was kept constant for all the collectors during the experiment. The collector was subjected to different mass flow rates like 20, 45, 70, 80, 100, and 130 kg/m² h, which cover the normal range of air flow rates [25,26]. An experimental set up is shown in Fig. 3.12



Fig. 3.12 Experimental set up on copper collector

3.7 Performance Test, Results and Discussion

3.7.1 Underflow Copper Collector

The experimentally observed thermal performance of the copper solar air heater with and without baffles during the month of March to May 2006 in

Kochi is presented here. The tests were conducted between 9.00 a.m to 5.00 p.m solar time. Variation in the extent of increase in air temperature as a function of air mass flow rate for copper collector with baffles is shown in Fig. 3.13. As the mass flow increased, the gain in temperature decreased. Maximum temperature at the outlet was 87.6°C for a flow rate of 45 kg/m²h. The intensity of solar radiation varied from 120 W/m² to 970 W/m² during the day, the average was 4.92 kWh/m²day. The appreciable rise in temperature (54.1°C above ambient) was remarkable in this collector. Ambient temperature varied between 29.9°C and 33.8°C during the experimental period. Fig. 3.14 shows the diurnal variation in ambient, inlet, and outlet temperatures along with the intensity of solar radiation incident at an angle 12°, for a mass flow rate of 45 kg/m²h. Table 3.7 gives the various environmental and performance parameters of the copper air heater with baffles. Maximum outlet temperatures were monitored for all the mass flow rates, among which minimum temperature was observed for a mass flow rate of 130 kg/m²h, at which the average efficiency attained its maximum value of 63%. The average rise in temperature was above 10°C even at the higher mass flow rates.

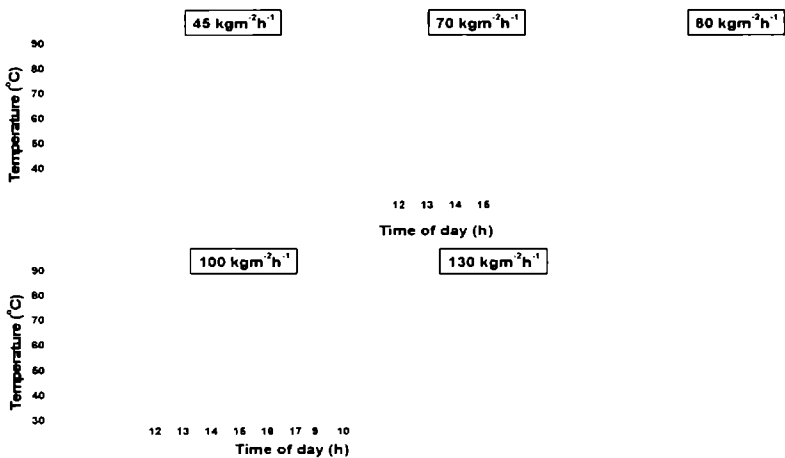


Fig. 3.13 Variation of air temperature as a function of mass flow rate

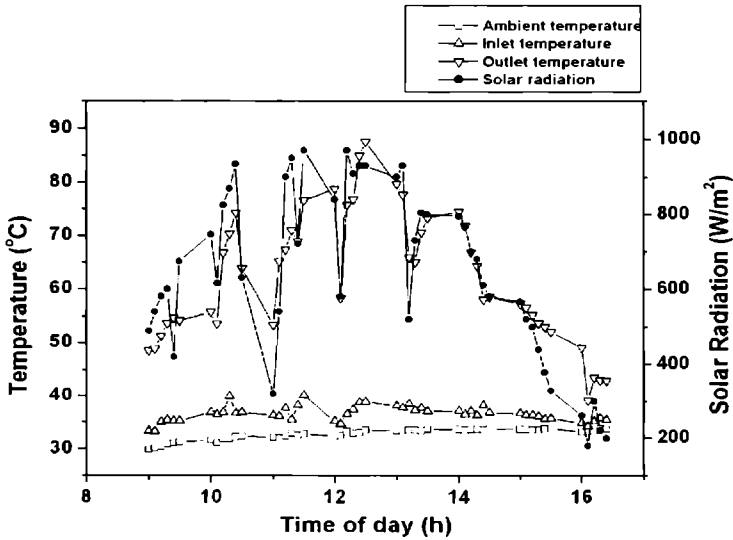


Fig. 3.14 Performance curve of copper collector with baffles for a mass flow rate of 45 kg/m²h

Table 3.7 Environmental and performance parameters of copper air heater with baffles

Flow rate (kg/m ² h)	Ambient temp (°C)	Inlet air temp (°C)	Max. rise in temp (°C)	Overall efficiency (%)	Pressure drop (Pa)
45	29.9-33.8	33.2-40.1	54.1	55	28
70	28.9-34.3	32.8-39.6	34	57	34
80	29.2-32.9	30.6-35.8	22.4	59	65
100	28.4-32.8	31.4-37.5	21.1	60	95
130	30.2-32.6	31.7-34.7	18.2	63	100

The results showed a substantial enhancement of thermal performance of the collector with baffles. It is seen from Fig. 3.15 that

the efficiency of air heater without baffles increased from 26% to 46% as mass flow rate increased from 45 kg/m²h to 130 kg/m²h, whereas that with baffles the corresponding increase was from 55% to 63%, a nearly twofold increase particularly at lower mass flow rates. At higher flow rates, the increase in efficiency was less, being only 37% more at a mass flow rate of 130 kg/m²h. The high performance of the collector was due to the provision of baffles, which increased the air fill factor: the winding flow of air due to the baffles nearly doubles the distance over which the air has to flow depending upon the number and dimension of baffles, while in contact with a heated surface.

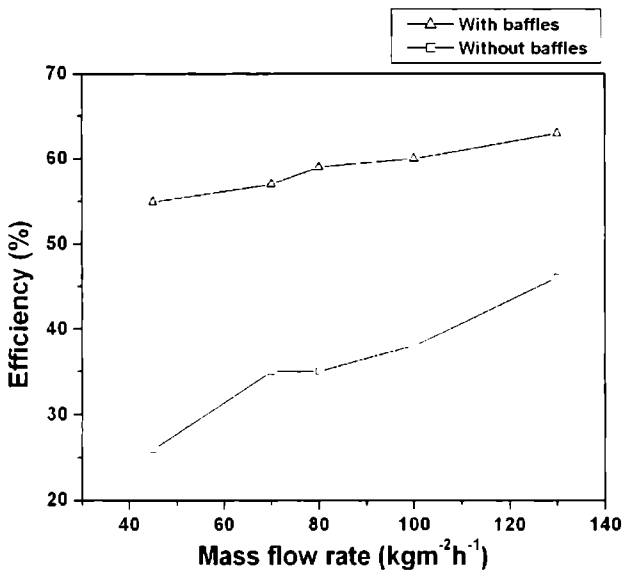


Fig. 3.15 Efficiency as a function of mass flow rate in collectors with and without baffles

The average temperature difference between the two types of collectors is shown in Fig. 3.16. It can be seen that the average temperature difference was more at low mass flow rates; as the mass flow rate increased, the difference tended to be nominal. This was due to the

increased convective heat transfer between the absorber plate and air at high flow rates, which explains why the baffles made little difference at high flow rates. The pressure drop across the collector was studied and the pumping power required to operate the system was calculated. The study showed that the difference in pressure drop between the two types of collector was marginal (Fig. 3.17). It is obvious from the figure that as the mass flow rate increases the pressure drop across the collector also increases. The pumping power required to operate the system is represented in Fig. 3.18. It is evident from the figure that pumping power increases with pressure drop. The drop in pressure and the extent of pumping power were comparable in both the collectors.

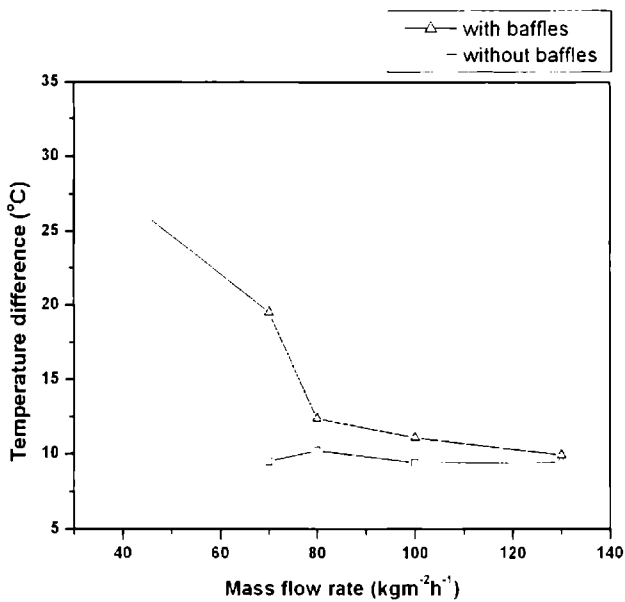


Fig. 3.16 Average rise in temperature as a function of mass flow rate

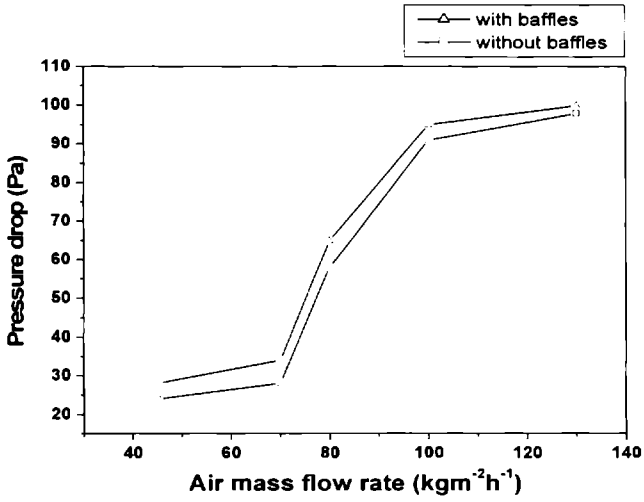


Fig. 3.17 Pressure drop across the collector as a function of air flow rates

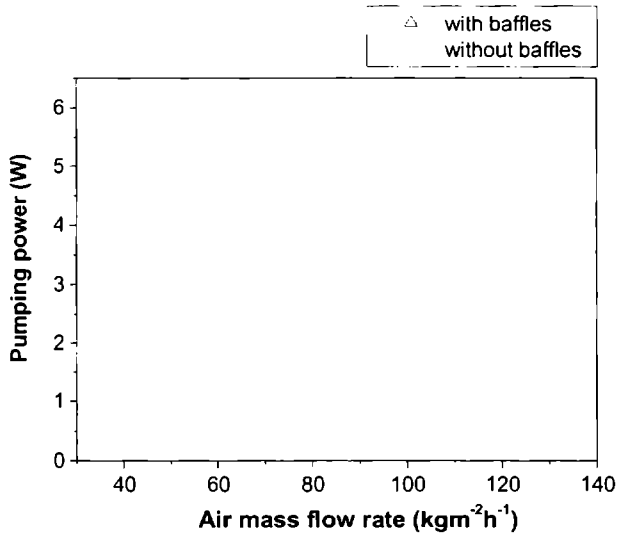


Fig. 3.18 Pumping power required as a function of mass flow rate

3.7.2 Overflow Collector-Corrugated GI Sheet as Absorber Plate

The collector was subjected to different mass flow rates of 20, 40, 55, 80, 90 kg/m²h. The outlet air temperature for different mass flow rate is represented in Fig. 3.19. Among the different mass flow rate studied, the maximum temperature of 69.8°C was recorded for baffled collector for a flow rate of 55 kg/m²h. The solar radiation reached a peak value of 1000 W/m² during the same experimental period. The rise in temperature was 37.7°C above ambient. Fig. 3.20 shows the diurnal variation of ambient, inlet, and outlet temperature along with solar radiation intensity for a mass flow rate of 55 kg/m²h. Ambient temperature varied between 30.1°C and 32.9°C during the day. The maximum value of temperature found to be decreased when the mass flow rate was above 55 kg/m²h. Table 3.8 represents the various environmental and performance parameters of the collector. Minimum highest temperature was observed for a mass flow rate of 90 kg/m²h, in which the average efficiency attained its maximum value of 67%. The average rise in temperature over the day was 19.53°C for a mass flow rate of 55 kg/m²h.

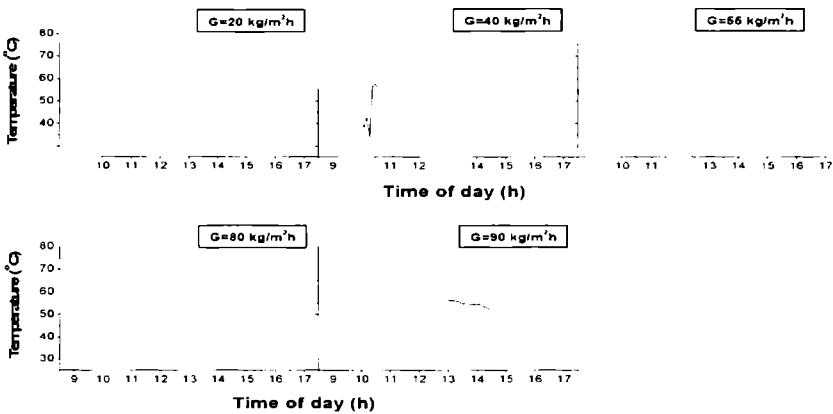


Fig. 3.19 Variation of temperature gain as a function of different mass flow rates

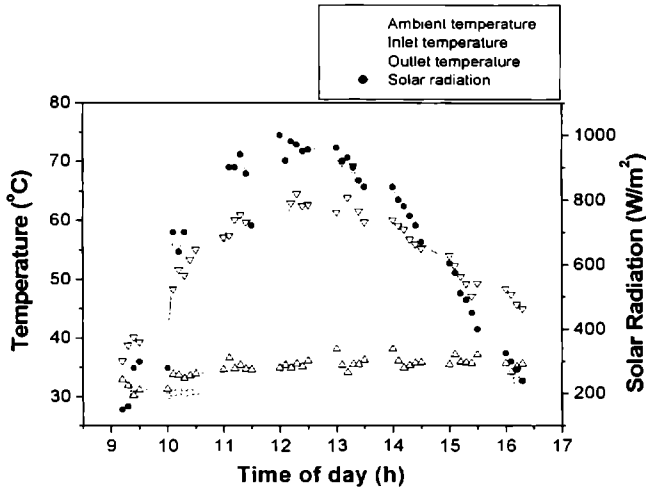


Fig. 3.20 Performance curve of corrugated collector with baffles for a mass flow rate of 55 kg/m²h

Table 3.8 Environmental and performance parameters of corrugated GI air heater with baffles

Flow rate (kg/m ² h)	Ambient temp (°C)	Inlet air temp (°C)	Max.Rise in temp (°C)	Overall efficiency (%)	Pressure drop (Pa)
20	29.5-33.1	30.9-39.8	37.1	17.54	15
40	28.1-32.9	28.8-42.1	27.7	22.68	56
55	30.1-32.9	30.2-38.1	37.7	44	69
80	28.1-31.3	31.6-40	27.7	47	89
90	29.7-31.5	31.8-42.6	22.0	67	90

Comparison of corrugated GI collector with and without baffles and identical design features were investigated in the same test facility. The evaluation of the results of collector with and without baffles showed a

substantial enhancement in the thermal performance of the collector with baffles. An efficiency curve with varying mass flow rate for corrugated collector with and without baffles is given in Fig. 3.21. It is seen from the above Figure that the efficiency of air heater without baffles increased from 17.2% to 43% as mass flow rate increased from 20 kg/m²h to 90 kg/m²h. But in the case of collector with baffles, corresponding increase was from 17.5% to 67%. At low mass flow rates, the difference in efficiency was comparable but it was found that a remarkable increase in efficiency for collector with baffles over without baffles at high mass flow rates. The average efficiency value of collector without baffles took a linear growth but there was a sharp increase in efficiency for collector with baffles, when the mass flow rate increased beyond 40 kg/m²h.

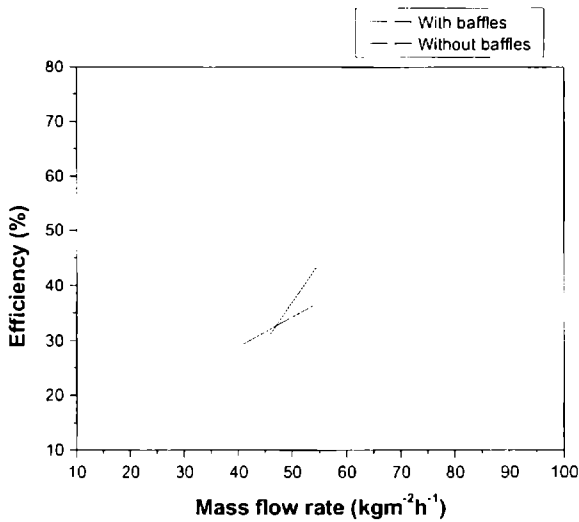


Fig. 3.21 Efficiency as a function of mass flow rate for corrugated collector with and without baffles

Fig. 3.22 shows the comparison results of maximum hot air outlet temperatures of both the collectors. The maximum temperature rise of 62°C

was monitored for collector without baffles, which was at a mass flow rate of $20 \text{ kg/m}^2\text{h}$. The reduction in temperature with increase in mass flow rate was not substantial for collector with baffles and it was a noted advantage of the designed collector. This was mainly due to the increase in convective heat transfer due to the provision of baffles. The outlet temperature drop as a function of increase in mass flow rate was rapid in the case of collector without baffles.

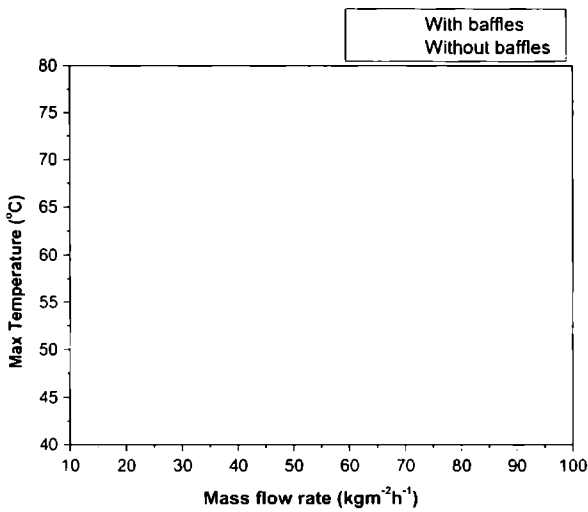


Fig. 3.22 Maximum temperature recorded for different mass flow rates for collector with and without baffles

Study was conducted to find out the pressure drop across the collector and the required pumping power to operate the system was calculated out of it. Fig. 3.23 gives the variation of pressure drop in mm of water versus the flow rate of both the collectors. It was obvious from the figure that, as the mass flow rate increased, the pressure drop across the collector also increased. From the measured pressure drop, the pumping power required to operate the system was calculated and it is represented in Fig. 3.24. It is evident from the Figure that pumping power

increases with pressure drop. It was noticed from the present study that, the pressure drop of both the collectors at low and high flow rates, i.e., 20&90 kg/m²h, was almost equal. The pressure drop for collector with baffles increased considerably in the low mass flow rate region, while the rise in pressure drop in the high flow region was comparable to the collector without baffles. The temperature output and efficiency of the collector with baffles was considerably good over without baffles with equal pumping power.

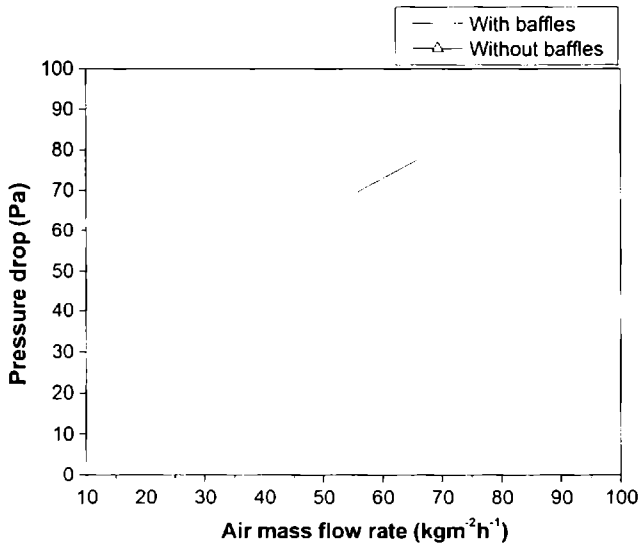


Fig. 3.23 Variation of pressure drop with air mass flow rates

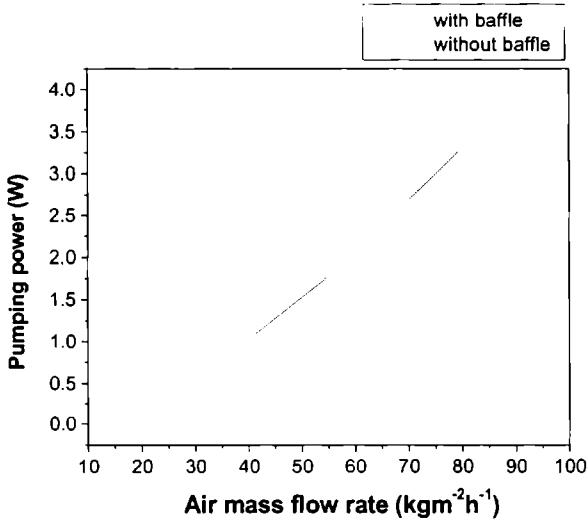


Fig. 3.24 Pumping power required as a function of mass flow rates

3.7.3 Overflow Collector-Aluminium as Absorber Plate

The different mass flow rates studied were, 20, 40, 55, 90 kg/m²h. The temperature output of the collector was studied for different air mass flow rates and the variation in air temperature gain as function of mass flow is represented in Fig. 3.25. As expected, it was revealed from the study that as the mass flow increased, efficiency of the collector increased. Among the four mass flow rate studied, the maximum temperature of 70.9°C was recorded for collector with baffles at a flow rate of 20 kg/m²h. The rise in temperature was 37.8°C above ambient.

The solar radiation reaches a peak value of 980 W/m² during the same experimental period. Fig. 3.26 shows the diurnal variation of ambient, inlet and outlet temperature along with solar radiation intensity, incident at an angle 12° for a mass flow rate of 20 kg/m²h, in which the collector achieved its maximum temperature. Ambient temperature varied between 29.5°C and 33.1°C during the day. The maximum rise in temperature came

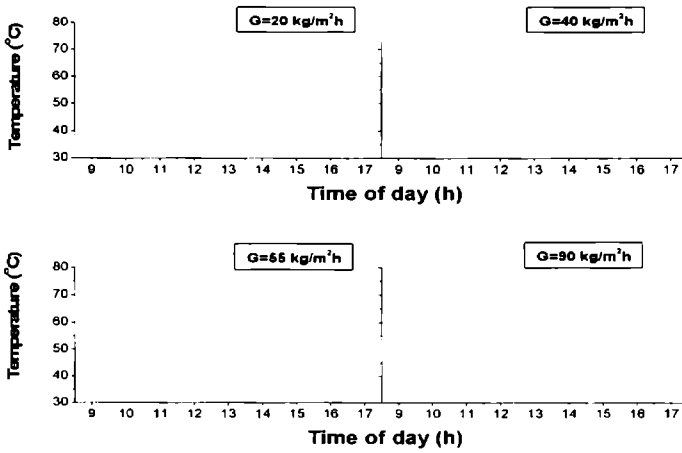


Fig. 3.25 Variation of temperature gain as a function of different mass flow rate

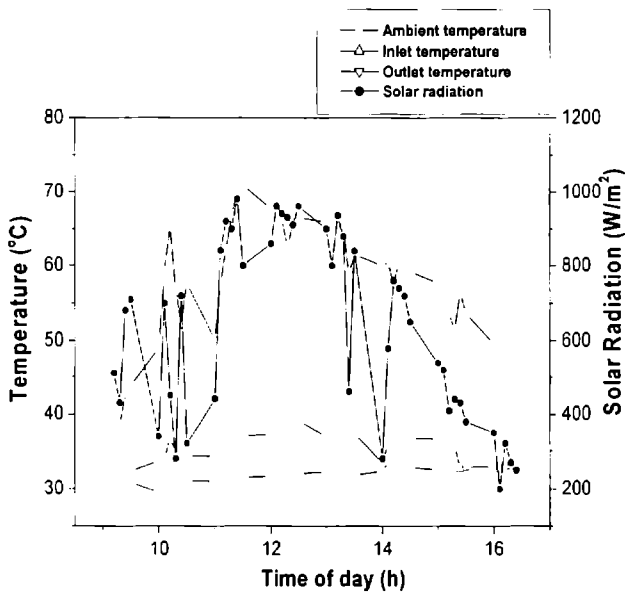


Fig. 3.26 Performance curve of overflow collector with baffles for a mass flow rate of 20 kg/m²h

down when the mass flow rate kept above 20 kg/m²h. Table 3.9 represents the various environmental and performance parameters of the overflow

aluminium collector. Maximum temperature output for all the mass flow rate was monitored, among which minimum temperature was observed for a mass flow rate of 90 kg/m²h, in which the average efficiency attained its maximum value of 45.1%. The average rise in temperature over the day was 25.33°C corresponding to the mass flow rate of 20 kg/m²h. The evaluation of the results of overflow collector with baffles than that of without baffles showed a significant enhancement in the thermal performance of collector with baffles. The provision of baffles caused an increased thermal performance.

Table 3.9 Environmental and performance parameters of overflow aluminium solar air heater with baffles

Flow rate (kg/m ² h)	Ambient temp (°C)	Inlet air temp (°C)	Max. rise in temp (°C)	Overall efficiency (%)	Pressure drop (Pa)
20	29.5-33.1	30.9-39.8	37.8	18.9	10
40	28.7-32.9	33.1-42.1	30.9	23.9	32
55	28.1-31.3	31.6-40.0	28.9	33.2	48
90	29.7-31.5	31.8-42.6	27.6	45.1	93

Efficiency curves with varying mass flow rate for the two collectors tested are given in Fig. 3.27. It is seen from the above Figure that the efficiency of overflow solar air heater without baffles increased from 18.14% to 40.21% as mass flow rate increased from 20 kg/m²h to 90 kg/m²h. But in the case of collector with baffles, corresponding increase was from 18.9% to 45.1%. The enhancement in efficiency of collector with baffles over without baffles collector was 12.21% at higher flow rate.

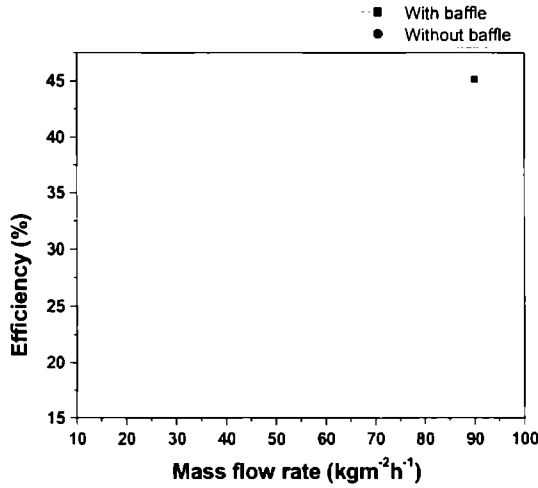


Fig. 3.27 Efficiency vs. mass flow rate for overflow aluminium collector

Fig. 3.28 shows the comparison results of maximum hot air outlet temperatures of baffled and unbaffled collectors. Maximum outlet hot air temperature of 62.9°C was monitored for unbaffled collector, which was at the same mass flow rate of baffled collector attained its maximum temperature.i.e., 20 kg/m²h. The maximum temperature obtained for overflow collector with baffles was higher than that of collectors without baffles for high and low mass flow rates. As seen in the earlier case, the reduction in temperature with increase in mass flow rate was not appreciable for collector with baffles. It finds a wide variety of application in the industries for producing more thermal energy without significant reduction in hot air temperature. This was mainly due to the increase in convective heat transfer due to the provision of baffles. The outlet temperature drop as a function of increase in mass flow rate was abrupt in the case of collector without baffles.

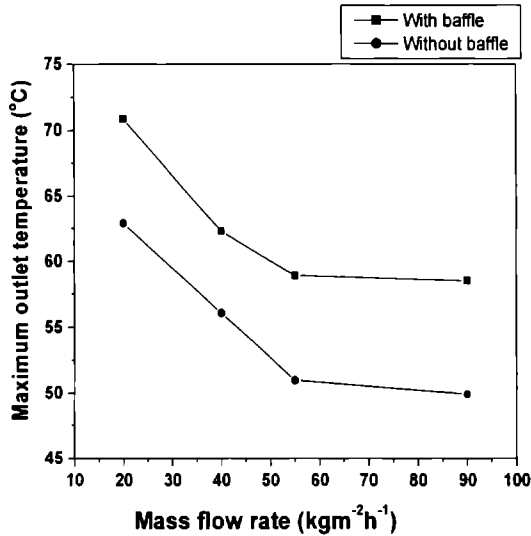


Fig. 3.28 Maximum temperature recorded for different mass flow rates for both collectors with and without baffles

A study was carried out to find out the pressure drop across the collector and the required pumping power to operate the system was calculated out of it. At lower mass flow rates, the pressure drop for both the cases was same and at high mass flow rates, the pressure drop of collector with baffles was higher than that of without baffles. Fig. 3.29 gives the pressure drop (in mm of water) for different mass flow rates of both the collectors. The pressure drop across the collector increased with increase in air mass flow rate. From the measured pressure drop, the pumping power required to operate the system was calculated and it is represented in Fig. 3.30. It is evident from the figure that pumping power increased with pressure drop. It was noticed from the present study that the pressure drop of both the collectors for both the low and high flow rates, i.e., 20&90 kg/m²h, was almost equal. The noted feature is that the temperature output and efficiency of collector with baffles were considerably good over collector without baffles with equal pumping power in the lower mass flow rate. This implies that without any

additional expenses for pushing external air through the air heater, the collector with baffles can be replaced by collector without baffles for low air mass flow rate in order to achieve its best performance.

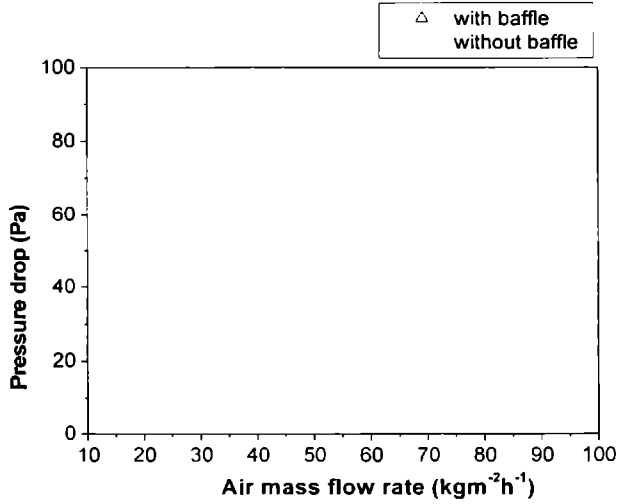


Fig.3.29 Pressure drop as a function of air flow rate

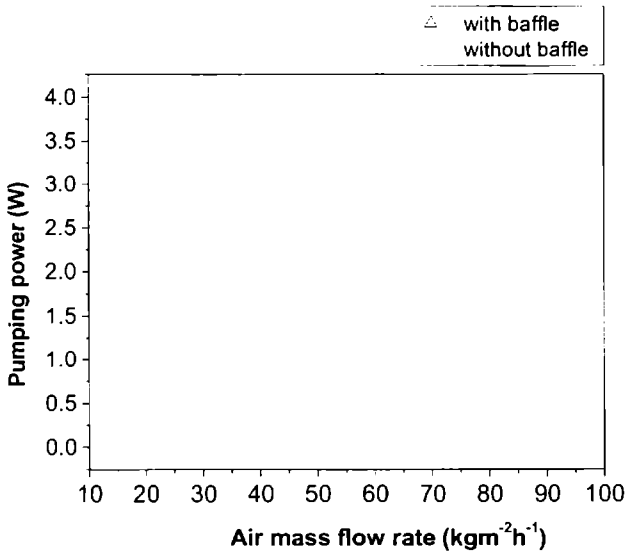


Fig. 3.30 Pumping power required as a function of mass flow rate

3.7.4 Double Flow Collector-Aluminium as Absorber Plate

The different mass flow rates studied were, 40, 55, 72, 95, 120 kg/m²h. The temperature output of the collector was monitored for different mass flow rates and the variation in air temperature gain as function of mass flow is represented in Fig. 3.31. Among the different mass flow rate studied, the maximum temperature of 70.4°C (35.6°C above ambient) was recorded for a flow rate of 72 kg/m²h. The solar radiation reached a peak value of 1040 W/m² during the same experimental period. The maximum rise in outlet temperature of the collector was 35.6°C above ambient. Fig. 3.32 demonstrates the diurnal variation of ambient, inlet and outlet temperature along with solar radiation intensity incident at an angle 12° for a mass flow rate of 72 kg/m²h. Ambient temperature varied between 31.3°C and 34.8°C

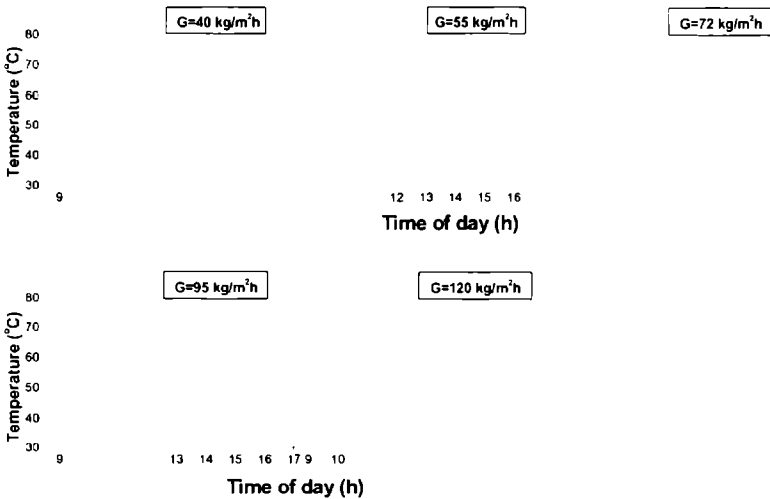


Fig. 3.31 Variation in air temperature gain as a function of different mass flow rate

during the day. The maximum value of temperature decreased when the mass flow rate was above and below 72 kg/m²h. Table 3.10 represents the

various environmental and performance parameters of the double flow solar air heater. Minimum highest temperature was observed for a mass flow rate of $120 \text{ kg/m}^2\text{h}$, in which the average efficiency attained its maximum value of 80.5 %. The average rise in temperature over the day was 21°C for a mass flow rate of $72 \text{ kg/m}^2\text{h}$. The average rise in temperature was above 15°C even for the higher mass flow rate studied.

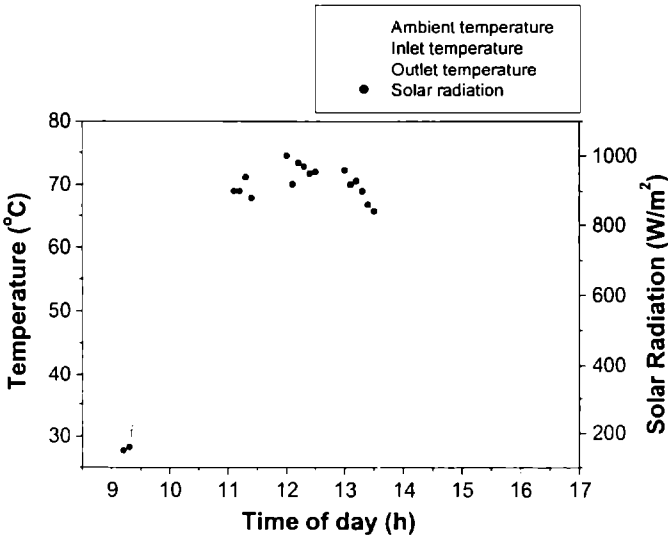


Fig. 3.32 Performance curve of double pass air heater with baffles for a mass flow rate of $72 \text{ kg/m}^2\text{h}$

A comparison of baffled double pass solar air heater with a similar one without baffles and identical design features were investigated in the same test facility. The thermal performance of the collector with baffles was better compared to collector without baffles. Efficiency curves with varying mass flow rates are given in Fig. 3.33. The efficiency of double pass solar air heater without baffles increased from 30% to 54% as mass flow rate increased from $45 \text{ kg/m}^2\text{h}$ to $120 \text{ kg/m}^2\text{h}$ and while that of collector with baffles, corresponding increase was from 42% to 81%. The enhancement in efficiency of baffled air heater over unbaffled collector was 50% at high

mass flow rate. Fig. 3.34 shows the comparison results of maximum rise of air temperature above ambient that recorded at the outlet of both the collectors tested.

Table 3.10 Environmental and performance parameters of double pass solar air heater with baffles

Flow rate (kg/m ² h)	Ambient temp (°C)	Inlet air temp (°C)	Max. temp (°C)	Overall efficiency (%)	Pressure drop (Pa)
40	30.0-32.7	30.6-35.3	65.4	41.65	30
55	30.2-32.6	31.7-34.7	63.2	43.63	35
72	31.3-34.8	31.8-37.7	70.4	60.43	55
95	29.2-32.9	30.6-35.8	57.6	70.34	68
120	28.4-32.8	31.4-37.5	56.5	80.50	80

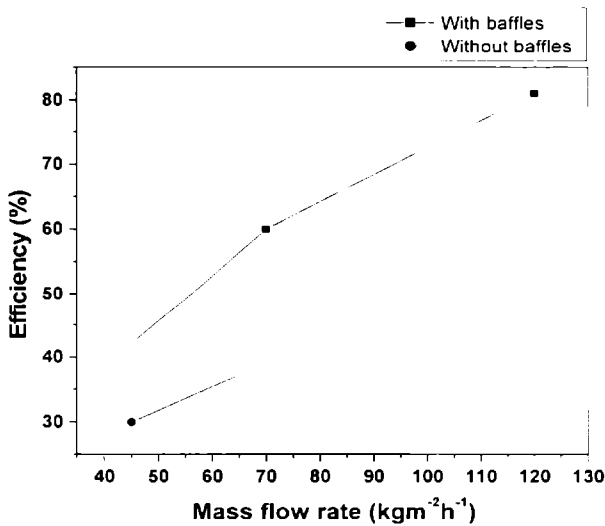


Fig. 3.33 Efficiency vs. mass flow rate for the solar air heaters tested

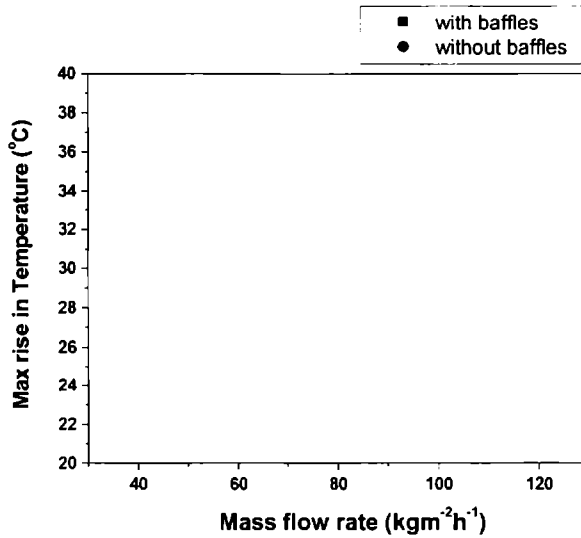


Fig. 3.34 Maximum rise in temperature as a function of mass flow rate

The pressure drop across the collector and the required pumping power to operate the system was calculated for both the collectors. The pressure drop measurement was carried out for 40, 55 and 95 kg/m²h. Fig. 3.35 gives the pressure drop across the collector in mm of water versus the mass flow rate of both collectors. It was obvious from the figure that as the mass flow rate increased, the pressure drop across the collector also increased. At low mass flow rates, the pressure drop of double passage collector with and without baffles was comparable and at higher flow rates the difference was sizeable. From the measured pressure drop, the pumping power required to operate the system was calculated and it is represented in Fig. 3.36. It is evident from the figure that pumping power increases with pressure drop. From the study it was revealed that the temperature output and efficiency of the collector with baffles was considerably good over without baffles with equal pumping power. The pumping power in the case

of collector with baffles was more compared to without baffles. The difference was more at high mass flow rates.

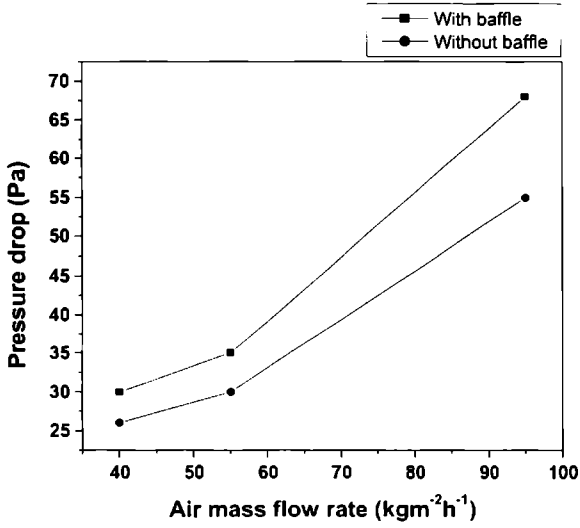


Fig. 3.35 Pressure drop as a function of air mass flow rate

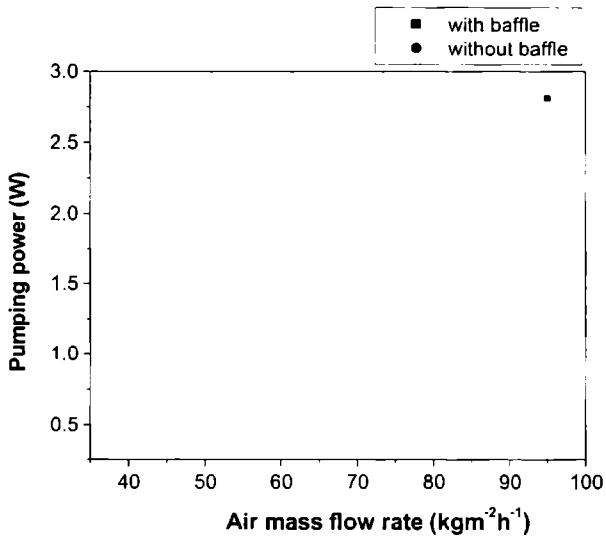


Fig. 3.36 Pumping power required as a function of mass flow rate

3.7.5 Matrix Collector-GI Mesh as Absorber Plate

Tests were conducted outdoor under identical conditions on clear days. The collector was subjected to different mass flow rates of 45, 60, 70, 80, 100 kg/m²h.

Among different mass flow rate analyzed, the maximum outlet temperature of 76.6°C was recorded for 45 kg/m²h, which was the lowest mass flow rate studied. The peak value of solar radiation monitored during the test was 970 W/m². The maximum and average difference in outlet temperature of the collector was high for the same mass flow rate. The diurnal variation of outlet air temperature of matrix collector for all the mass flow rate is given in Fig. 3.37. The appreciable temperature rise above ambient (43.3°C at noon for $m = 45$ kg/m²h) was the noticeable feature of the collector. Fig. 3.38 represents the diurnal variation of ambient, inlet and outlet temperature along with solar radiation intensity incident at an angle 12° for a mass flow rate of 45 kg/m²h, in which the collector reached its

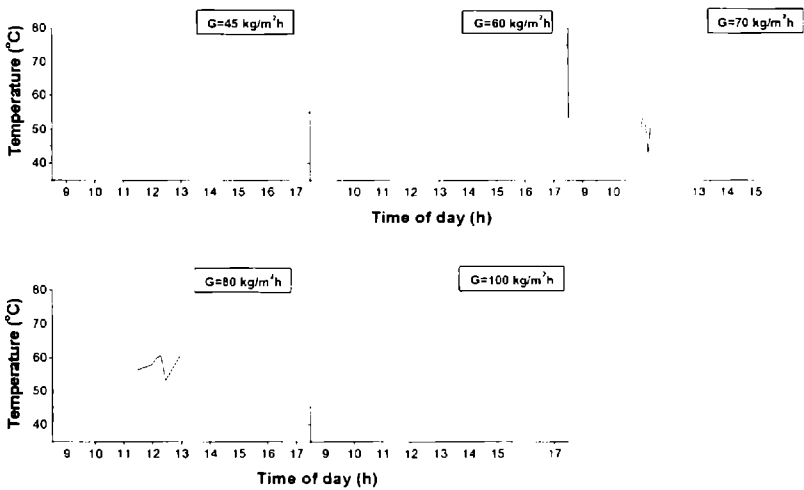


Fig. 3.37 Temperature outlet of matrix collector for different mass flow rate

maximum outlet temperature. Table 3.11 represents the various environmental and performance parameters of the matrix heater. Minimum highest temperature was observed for a mass flow rate of $100 \text{ kg/m}^2\text{h}$, in which the average efficiency attained its maximum value of 71%. From the data, it was obvious that as the mass flow rate increased, the temperature output decreased. The average rise in temperature was above 15°C for all the mass flow rates.

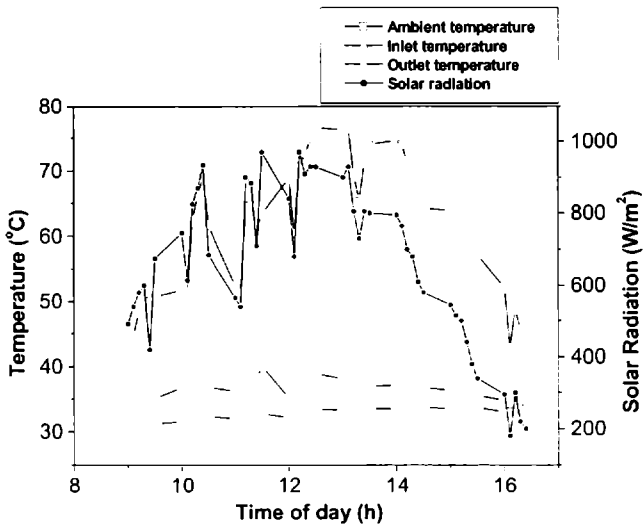


Fig. 3 38 Performance curve of matrix collector for a mass flow rate of $45 \text{ kg/m}^2\text{h}$

It was observed from the Fig. 3.39 that the efficiency of the collector increased from 53% to 71% as air mass flow rate increased from $45 \text{ kg/m}^2\text{h}$ to $100 \text{ kg/m}^2\text{h}$. A sharp increase in efficiency was observed with mass flow rate beyond a particular value. The good performance of the matrix collector was due to the geometrical parameters of absorber. The difference in performance of these absorber was attributed to difference in values of effective volumetric thermal capacity, $[\alpha\rho C_p]$ of packing materials absorbing direct solar radiation, heat transfer area, A (resulting

from diameter of wires and mesh number), per unit volume of packing materials and convective heat transfer coefficient.

Table 3.11 Environmental and performance parameters of matrix air heater

Flow rate (kg/m ² h)	Ambient temp (°C)	Inlet air temp (°C)	Max. Rise in temp (°C)	Overall efficiency (%)	Pressure drop (Pa)
45	29.9-33.8	36.5 – 40.1	43.3	52.55	24
60	28.9-34.3	32.8-39.6	31.3	49.61	31
70	30.2-34.1	31.4-39.2	29.6	53.10	38
80	29.5-33.4	33.1-39.0	28.3	60.88	48
100	29.6-33.6	31.0-37.8	7.3	71.31	85

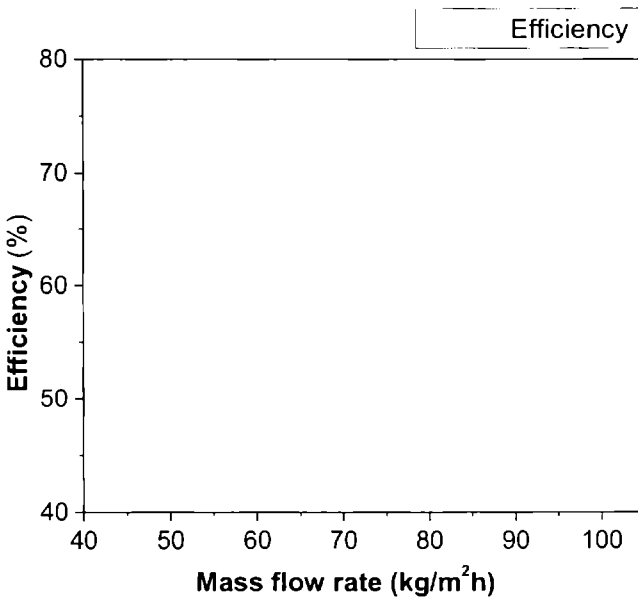


Fig. 3.39 Efficiency as a function of mass flow rate

Comparison of maximum temperature rise over the day for different mass flow rate is shown in Fig. 3.40. Maximum temperature rise was above 25°C even for the high mass flow rate studied, i.e., 100 kg/m²h. Pressure drop across the system was monitored and the corresponding pumping power was also calculated from it. Fig. 3.41 gives the pressure drop versus mass flow rate of the matrix collector. It was obvious from the figure that, as the mass flow rate increased the pressure drop across the collector also increased. A steep rise in pressure drop for matrix collector was found, when the mass flow rate increased from 80 kg/m²h to 100 kg/m²h. However, the pressure drop for matrix collector was considerably less than conventional collector at low mass flow rates. From the measured pressure drop, the pumping power required to operate the system was calculated and it is represented in Fig. 3.42. It was evident from the figure that pumping power increased with pressure drop.

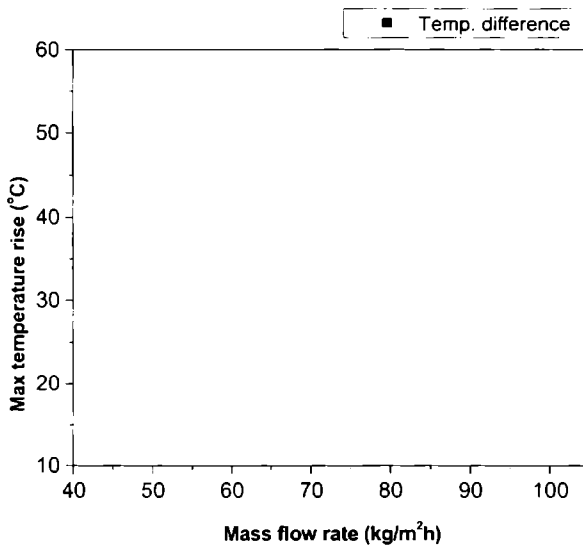


Fig. 3.40 Maximum rise in temperature as function of mass flow rates

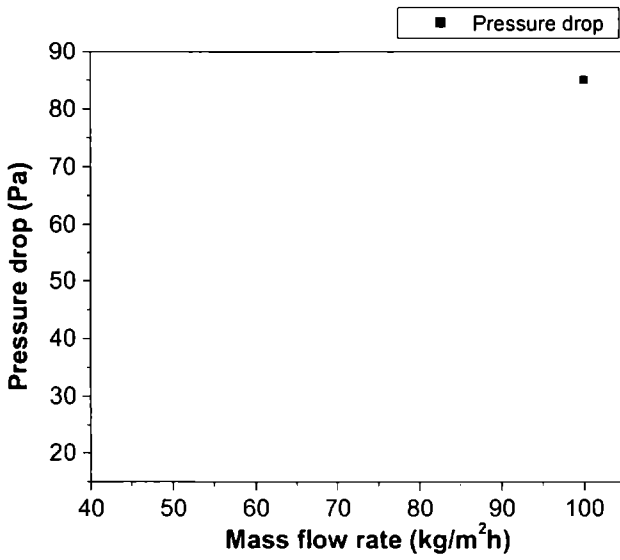


Fig. 3.41 Variatiorn of pressure drop as a function of mass flow rate

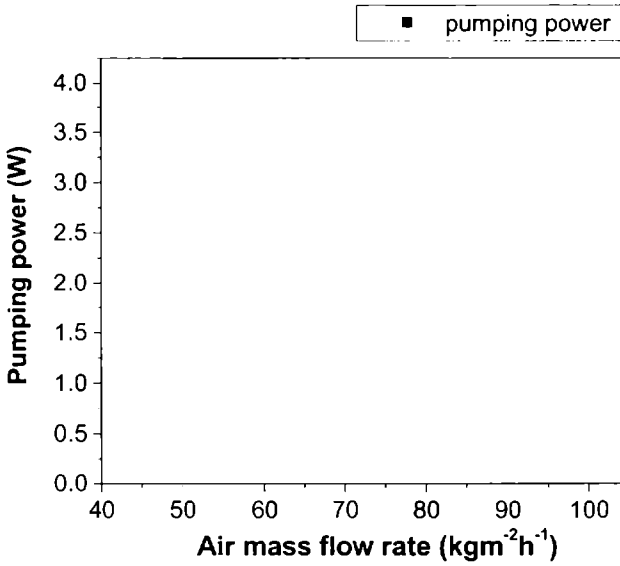


Fig. 3.42 Pumping power required as a function of mass flow rate

3.8 Comparison of all Types of Solar Air Heaters Developed

The experimentally observed thermal performance of all the solar air heaters developed with baffles is depicted in Fig. 3.43. In the figure, diurnal variation of temperature for a mass flow rate in which the collector attained its maximum temperature is shown. Among the different types of solar air heaters tested, maximum outlet temperature was observed for copper collector. The temperature attained was 87.6°C at 12.50 p.m for a mass flow rate of 45 kg/m²h. The rise in temperature for copper collector of 54.1°C (above ambient) was remarkable in this study. The average efficiency for the same mass flow rate was 55%. The better thermal performance of copper collector is probably due to the better convective heat transfer between the copper absorber plate and air. The absorber plate was 'selective coated black chrome copper sheet' which has high absorptivity. Besides, since the collector was underflow type, the heated air flows out from the air heater is not in contact with the glazing. Hence, there is little chance of the dissipation of heat through glazing, which consequently brings down the air temperature.

The second highest maximum temperature was recorded for matrix collector, which was for the same mass flow rate in which the copper collector attained its maximum temperature. i.e., 45 kg/m²h. The maximum temperature attained was 76.6°C, which was above 43.3°C above ambient. The overall efficiency calculated for this mass flow rate was 52.55%.

As seen from the above Figure, the maximum temperature attained for overflow aluminium collector, corrugated GI collector and double passage collector was 70.9°C, 69.8°C and 70.4°C, respectively. This temperature was for corresponding flow rates of 20, 55 and 72 kg/m²h. Low temperature output of the overflow collector compared to the underflow

collector is due to the high heat losses through the transparent cover to the ambient.

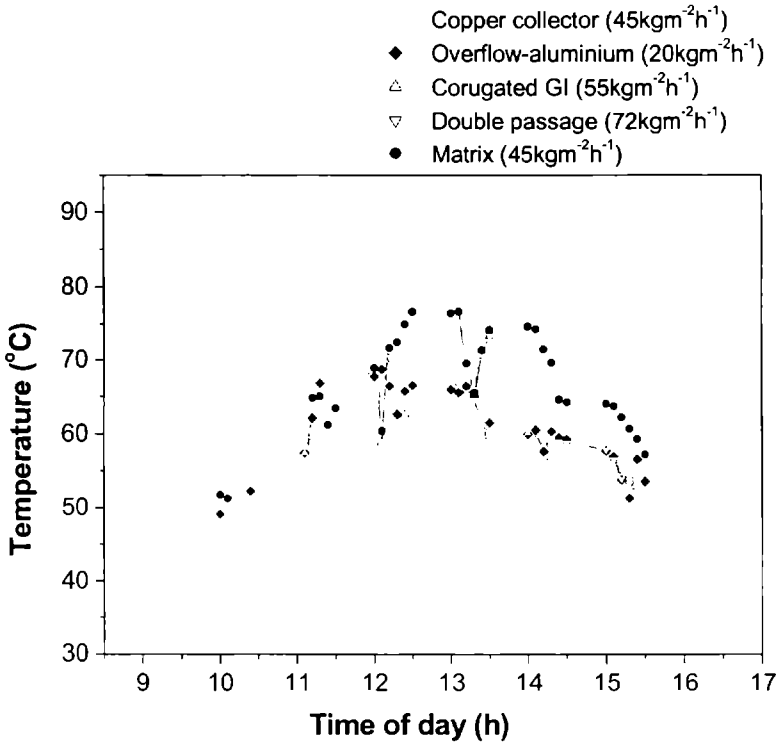


Fig. 3.43 Maximum outlet temperature for all the collectors with baffles

The average efficiency calculated for three specific mass flow rates is given in Fig. 3.44. At low mass flow rate studied, say $45\text{ kg/m}^2\text{h}$, the highest value of efficiency was calculated for underflow copper collector while double flow collector with baffles scored maximum efficiency at high flow rates ($120\text{ kg/m}^2\text{h}$). Overflow collector without baffles proved to be the least efficient for both low and high mass flow rates. The efficiency of both low and high mass flow rates for overflow corrugated GI collector and overflow aluminium collector was almost equal. The efficiency of matrix collector was always on the higher side for low and high mass flow rates and

matrix collector emerged as the second highest efficient collector, after copper collector for both low and high mass flow rates.

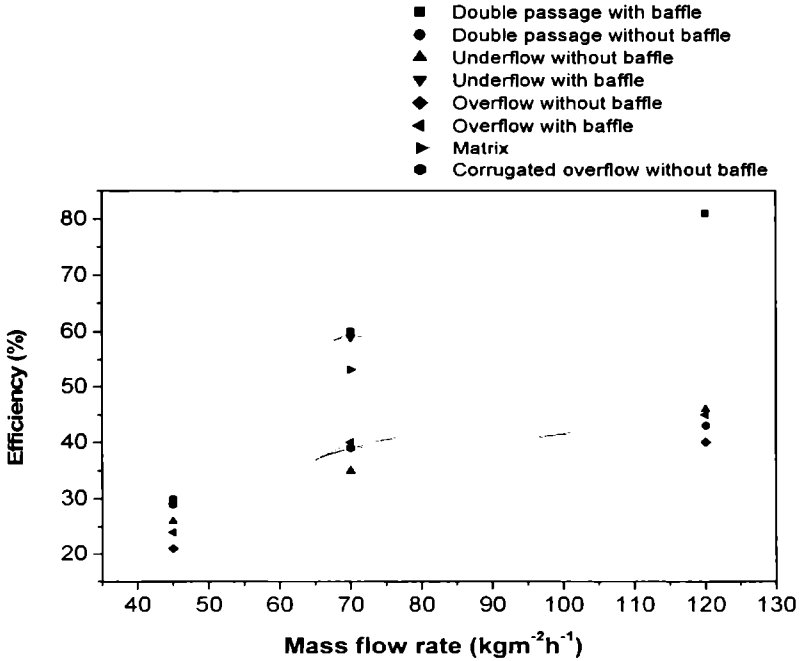


Fig. 3.44 Efficiency of the collector with mass flow rates

The diurnal variation of cover glass temperature of all the collectors tested is depicted in Fig. 3.45. The graph is plotted for collector with baffles for a flow rate of 80 kg/m²h. The average glass temperature recorded was least for underflow copper collector, and double flow collector, it was second least. The average temperature of cover glass of underflow copper and double flow collectors were 36.7°C and 40.50°C, respectively. Temperature monitored for matrix, overflow aluminium and overflow GI collectors were almost equal and the value was around 44°C. The minimum glazing temperature recorded for underflow copper collector was due to flow of hot air beneath the absorber plate and not in contact with the top glass. But in the case of overflow collector, since the air flows between the

absorber plate and the transparent cover, the cover receives much of the heat and in turn, losses it to the ambient. A substantial amount of heat is lost to the ambient in this collector and reduces overall performance. In double flow solar air heater, the absorber plate is cooled by air stream flowing on both sides of the plate and top heat loss is reduced.

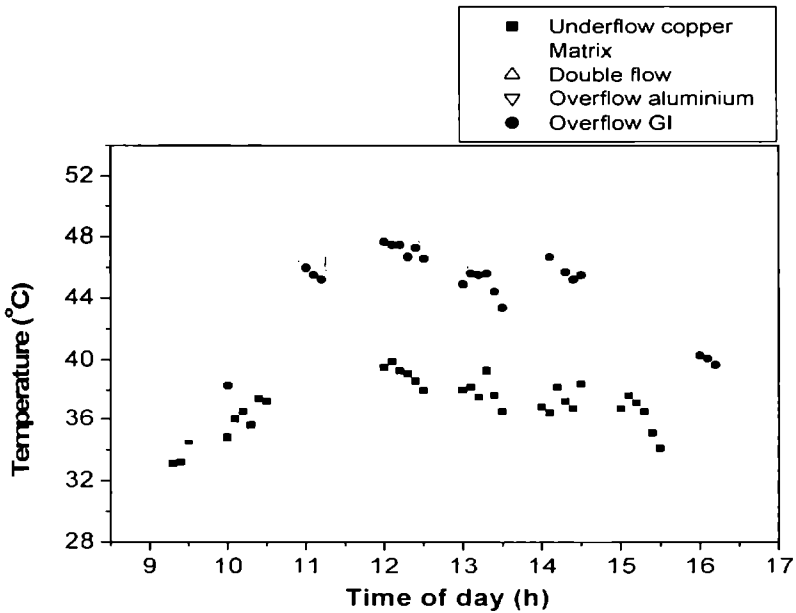


Fig. 3.45 Diurnal variation in top glass temperature of all the collectors tested for a mass flow rate of $80 \text{ kg/m}^2\text{h}$

3.9 Conclusion

The study proved that solar air heaters with copper as absorber plate and two air channels [one for flowing air and the other for still air] with the provision of baffles efficiently to promote turbulence, exhibited high heat transfer coefficient and efficiency. For the same air flow rate ($45 \text{ kg/m}^2\text{h}$), the average efficiency of the collector without baffles was 26%, whereas that of the collector with two baffles was 55%. The instantaneous efficiency recorded while the collector reached its maximum temperature, was 88%.

The maximum temperature difference was 54.1°C for a flux of 930 W/m^2 . The results exemplified, as expected, that a collector with longer air path having air flow under the absorber plate performed better. The additional electrical power required to push the air through the copper collector fitted with baffles was minimal, proving that the collector with baffles scored on every count.

Comparison of the results of matrix collector with plane collectors except underflow collector with baffles, showed a substantial enhancement in thermal efficiency as a result of using selective coated double layered GI wire mesh as absorber. The maximum rise in temperature above ambient was 43.3°C , when the system was subjected a flow rate of $45\text{ kg/m}^2\text{h}$ and the temperature recorded was appreciably high. The study conducted to determine the pressure drop and corresponding pumping power showed that both the values were smaller for matrix collector. The matrix collector exhibited an improved thermal performance with higher heat transfer rates to the air flow and lower friction losses compared to flat plate air collectors of conventional design.

The enhancement in efficiency of double passage air heater with baffles over without baffles was above 50% at high mass flow rate and it was nearly double than that of overflow collector for all the mass flow rates. The study revealed that the overflow collector, the maximum rise in temperature was least for all the mass flow rates. The experiment on all other solar air heaters developed in the facility proved that the provision of baffles in solar air heater is a simple method to enhance thermal efficiency.

References

- [1] I.A. Abbud, Simulation of solar air heating at constant temperature, *Solar Energy* 54, 75-83, 1995.
- [2] M.S. Sodha and R. Chandra, Solar drying and their testing procedures: A review, *Energy Conservation and Management* 35, 219-267, 1994.
- [3] C. Jallut, A. Jemni and M. Lallemand, Steady state and dynamic characterization of an array of air flat-plate collectors, *Solar and Wind Technology* 5, 573-579, 1988.
- [4] R.S. Pawar, M.G. Takwale and V.G. Bhide, Solar drying of custard powder, *Energy Conversion and Management* 36, 1085-1096, 1995.
- [5] H.P. Garg and H. Prakash, *Solar Energy Fundamentals and Applications*, Tata McGraw-Hill, New Delhi, 2002.
- [6] S.P. Sukhatme, *Solar Energy: Principles of Thermal Collection and Storage*, Tata McGraw-Hill Limited, New Delhi, 1998.
- [7] J.A. Duffie and W.A. Beckman, *Solar Engineering of Thermal Processes*, Wiley intersciences, New York, 1991.
- [8] C. Choudhury, S.L. Anderson and J. Rekstand, A solar air heater for low temperature application, *Solar Energy* 40, 335-344, 1988.
- [9] H.P. Garg, C. Choudhury and G. Datta, Theoretical analysis of a new finned type solar collector, *Energy* 16, 1231-1238, 1991.
- [10] A.A. Mohamad, High efficiency solar air heater, *Solar Energy* 60, 71-76, 1997.
- [11] C. Choudhury and H.P. Garg, Evaluation of jet plate solar air heater, *Solar Energy* 46, 199-209, 1991.
- [12] F.H. Buelow, Heating air by solar energy, *Solar Energy* 3(2), 39, 1959.
- [13] A. Whillier, Performance of black-painted solar air heaters of conventional design, *Solar Energy* 8(1), 31-37, 1964.

- [14] D.J. Close, Solar air heaters for low and moderate temperature applications, *Solar Energy* 7 (3), 117-124, 1963.
- [15] C.L. Gupta and H.P Garg, Performance studies on solar air heaters, *Solar Energy* 11 (1), 25-31, 1967.
- [16] R.K. Suri and J.S Saini, Performance prediction of single and double exposure solar air heaters, *Solar Energy* 12 (4), 525-530, 1969.
- [17] T.A. Reddy and C.L. Gupta, Generating application design data for solar air heating systems, *Solar Energy* 25, 527-530, 1980.
- [18] R.K. Swartman and O. Ogunlade, An investigation on packed-bed collectors, *Solar Energy* 10(3), 106-110, 1966.
- [19] H.M. Yeh and W.H. Chou, Efficiency of solar air heaters with baffles, *Energy* 16(7), 983-987, 1991.
- [20] L. Henden, J. Rekstad and Meir, Thermal performance of combined solar systems with different collector efficiencies, *Solar Energy* 72(4), 299-305, 2002.
- [21] G. Alvarez, J.I. Arce, L. Lira and M.R. Heras, Thermal performance of a solar collector with an absorber plate made of recyclable aluminium cans, *Solar Energy* 77, 107-113, 2004.
- [22] M.N. Metwally, H.Z. Abou-Ziyan and A.M. EL-Leathy, Performance of corrugated-duct solar air collector compared with five conventional designs, *Renewable Energy*, 10(4), 519-537, 1997.
- [23] W W Focke, J. Zachariades and I. Olivier, The effect of the corrugation inclination angle on the thermohydraulic performance of plate heat exchanger, *Heat and Mass transfer* 28(8), 1469-1479, 1985.
- [24] R.W Bliss, The derivation of several 'plate efficiency factor' useful in design of flat-plate solar heat collectors, *Solar Energy* 3, 55-64, 1959.
- [25] P. Biondi, L. Cicala and G. Farina, Performance analysis of solar air heaters of conventional design, *Solar Energy* 41, 101-107, 1988.

- [26] M.A. Bernier and E.G. Plett, Thermal performance representations and testing of solar air solar collectors, *J. of Solar Energy Engineering* 110, 74-81, 1988.
- [27] W.A. Beckman, S.A. Klein and J.A. Duffie, *Solar heating design by the f-chart method*, Wiley, New York, 1979.

DESIGN AND PERFORMANCE STUDY OF A SOLAR AIR HEATING SYSTEM FOR FOOD PROCESSING INDUSTRIES

4.1 Introduction

Food preservation can reduce wastage of a harvest surplus, allow storage for food shortages, and in some cases facilitate export to high-value markets. Preservation of fruit and vegetables is essential for storing them for a long time without deterioration. Preserving fruits, vegetables, grains, meat, spices, etc. has been practiced in many parts of the world for thousands of years. Methods of preservation includes: canning, refrigeration, curing (smoking or salting), chemical treatment and drying. Drying is perhaps the oldest and most common method of preserving the food materials. Drying or the removal of moisture is an energy intensive operation applied in both agriculture and industrial sectors of any economy. Drying of various feedstocks is needed for one or several of the following reasons: easiness to handle free-flowing solids, preservation and storage, reduction in cost of transportation, achieving desired quality of product, etc. In many processes, improper drying may lead to irreversible damage of product quality and hence a non salable product. Drying is an essential operation in the chemical, agricultural, biotechnology, food, polymer, ceramics, pharmaceutical, pulp and paper, mineral processing, and wood processing industries [1].

Drying is a complicated process involving simultaneous heat and mass transfer. Drying of farm produce is an energy intensive operation, and improving energy efficiency by only 1% could increase the profits by 10% [2]. It has been a topic of many research studies necessary for process

design, optimization, energy integration, and control. Drying of solids commonly describes a process of thermally removing volatile substances (moisture) to yield solid product. When a wet product is subjected to drying, two processes occur simultaneously: a) transfer of energy from the drying medium to the material to be dried and b) transfer of moisture from the material to the drying medium [3]. Drying of fruits and vegetables demands a special attention, as these are important sources of vitamins and minerals. Fruits and vegetables have gained commercial importance and their growth on a commercial scale has become an important sector of agriculture industry. Production of processed fruits and vegetables is also increasing. Most fruits and vegetables contain more than 80% water and these are, therefore, highly perishable. Post-harvest losses in the developing countries like India are estimated to be 30%–40% in the case of fruits and vegetables [4]. The need to reduce post harvest losses is of paramount importance as far these countries as concerned. This calls for innovation of adequate preservation method.

Artificial drying of foodstuffs is an important method of preservation and production of a wide variety of products. Such materials are generally characterized by high initial moisture content, high temperature-sensitivity (i.e., colour, flavour, texture and nutritional value subject to thermal deterioration), high susceptibility to microbial attack and presence of a 'skin' (e.g. fruits like grapes or tomato) which has poor permeability for water or moisture. It is clear from the above list that drying of foodstuffs is necessarily a slow energy consuming process carried out under gentle drying conditions leading to large dryers for a given throughput [5].

Open sun drying is practiced widely in tropical countries since ancient times. Considerable savings can be obtained with this type of drying since the source of energy is free and renewable. In traditional open sun drying where the product is directly exposed to sun in the open air, the

necessary heat required for moisture removal is supplied from the sun and a little from the ambient air and wind and the natural convection disperse water vapour. However, this process is unhygienic and extremely weather dependent. Moreover it has the problem of contamination, infestation, microbial attack, spoilage due to rain, etc. Also, the required drying time for a given commodity can be quite long [6]. As a result, new drying methods with conventional heat sources have been widely developed and used in order to solve these problems. The high operating cost of the drying system based on fossil fuel and electrical energy makes them less attractive to many users.

Wherever feasible, solar drying often provides the most cost-effective drying technique. Solar drying is considered as one of the most promising techniques for food preservation [7]. Escalating price of petroleum products and the shortage of fossil fuels have led to increased emphasis on using solar energy as an alternative energy source especially in developing countries like India. Apart from the rise in energy costs, legislation on pollution and sustainable/eco-friendly technologies have created greater demand for energy efficient drying processes in food industries. The food processing industries can have economic savings by avoiding wastage of costlier energy. The solutions involving solar energy collection devices or solar dryers have been proposed to utilize free, renewable and non-polluting energy provided by the sun. Solar dryers can reduce crop losses and significantly improve the quality of the dried product [8]. However, solar drying systems must be properly designed to match particular drying requirements of specific crops, which can increase the efficiency of a system. In recent years, several designs of solar dryers have been proposed in the developing countries and a good deal of work is still in progress [9-18].

4.2 Classification and Selection of Dryers

Drying techniques may be divided into six general categories based on the way the food is heated. *Open air* or unimproved, solar drying takes place when food is exposed to the sun and wind by placing it in trays, on racks, or on ground. Although the food is rarely protected from predators and weather, in some cases screens are used to keep out insects, or a clear roof is used to shed rain. *Direct sun* dryers enclose food in a container with a clear lid, such that sun shines directly on the food. In addition to the direct heating of the solar radiation, the green house effect traps heat in the enclosure and raises the temperature of the air. Vent holes allow for air exchange. *Indirect sun* dryers heat fresh air in a solar collector separate from the food chamber, so the food is not exposed to direct sunlight. This is of particular importance for foods which lose nutritional value when exposed to direct sunlight. *Mixed mode* dryers combine the aspects of direct and indirect types; a separate collector pre-heats air and then direct sunlight adds heat to the food and air. *Hybrid* dryers combine solar energy with a fossil fuel or biomass fuel such as rice husks. *Fueled* dryers use conventional fuels or utility supplied electricity for heat and ventilation.

4.3 Comparing Solar Drying with other Options

When one considers solar drying, it has to be compared with other options available. In some situations open-air drying or fueled dryers may be preferable to solar. Solar drying will only be successful if it has a clear advantage over the current practice. Table 4.1 lists the primary benefits and disadvantages of solar drying when compared with traditional open-air drying, and then with the use of fueled dryers.

The above comparison will assist in deciding among solar, open-air, and fueled dryers. The local site conditions will also play an important role

in this decision. Some indicators that solar dryers may be useful in a specific location include

1. Conventional energy is unavailable or unreliable
2. Plenty of sunshine
3. Quality of open-air dried products needs improvement
4. Land is extremely scarce (making open sun drying unattractive)
5. Introducing solar drying technology will not have harmful socio-economic effects

Table 4.1 Solar dryers compared with open-air and fuel drying

Type of drying	Benefits (+) & Disadvantages (-) of Solar Dryers
Solar vs. Open-air	<ul style="list-style-type: none"> + Can lead to better quality dried products, and better market prices + Reduces losses and contamination from insects, dust and animals + Reduces land required (by roughly 1/3) + Some dryers protect food from sunlight, better preserving nutrition and colour + May reduce labour required + Faster drying time reduces the chances of spoilage + More complete drying allows longer storage + Allows more control (for example, sheltered from rain) - Comparatively more expensive <li style="padding-left: 20px;">In some cases, food quality is not significantly improved <li style="padding-left: 20px;">In some cases, market value of food will not be increased
Solar vs. Fueled	<ul style="list-style-type: none"> + Prevents fuel dependence + Operating cost is almost zero + Often less expensive + Reduced environmental impact - Requires adequate solar radiation - Hot & dry climates preferred <li style="padding-left: 20px;">In some models, greater difficulty in controlling process, may result in lower quality product

Some useful criteria for selecting solar dryers- If the use of solar dryers appear favourable, the next step is to consider which type of solar dryer is to be used. Table 4.2 presents four general categories of solar dryers along with advantages and disadvantages of each. The decision of whether solar, open-air, or fueled dryers are best may be made according to the criteria in Table 4.1. If solar drying is the best option, Table 4.2 and the selection criteria given may be used to choose a dryer.

Table 4.2 Advantages and disadvantages of the four types of solar food dryers

Classification	Advantages	Disadvantages
Direct Sun	Least expensive Simple	UV radiation can damage food
Indirect Sun	Products protected from UV Less damage from temperature extremes	more complex and expensive than direct sun
Mixed Mode	Less damage from temperature extremes	UV radiation can damage food more complex and expensive than direct sun
Hybrid	ability to operate without sun reduces chance of food loss allows better control of drying fuel mode may be up to 40 times faster than solar	expensive may cause fuel dependence

4.4 Basic Principles

Drying is a complex operation involving transient transfer of heat and mass along with several rate processes, such as physical or chemical transformation, which, in turn, may cause changes in product quality as well as the mechanisms of heat and mass transfer. Physical changes that may occur include: shrinkage, puffing, crystallization and glass transitions. In

some cases, desirable or undesirable chemical or biochemical reactions may occur leading to changes in colour, texture, odour or other properties of the solid product [3].

Drying occurs by effecting vaporization of the liquid by supplying heat to the wet feedstock. As noted earlier, heat may be supplied by convection (direct dryers), by conduction (contact or indirect dryers), radiation or volumetrically by placing the wet material in a microwave or radio frequency electromagnetic field. Over 85 percent of industrial dryers are of the convective type with hot air or direct combustion gases as the drying medium. Over 99 percent of the applications involve removal of water.

Transport of moisture within the solid may occur by any one or more of the following mechanisms of mass transfer [19]:

1. Liquid diffusion, if the wet solid is at a temperature below the boiling point of the liquid
2. Vapour diffusion, if the liquid vaporizes within material
3. Knudsen diffusion, if drying takes place at very low temperatures and pressures, e.g., in freeze drying
4. Surface diffusion (possible although not proven)
5. Hydrostatic pressure differences, when internal vapourization rates exceed the rate of vapour transport through the solid to the surroundings
6. Combinations of the above mechanisms

Note that since the physical structure of the drying solid is subjected to changes during drying, the mechanisms of moisture transfer may also change with elapsed time of drying.

4.5 Design Consideration

Strictly speaking, no design procedure that can apply to several of the dryer variants is possible. It is essential to revert to the fundamentals of

heat, mass and momentum transfer coupled with knowledge of the material properties (quality) when attempting design of a dryer or analysis of an existing dryer. Mathematically speaking, all process involved, even in the simplest dryer, are highly nonlinear and hence scale-up of dryers is generally very difficult. Experimentation at laboratory and pilot scales coupled with field experience and know-how is essential to the development of a new dryer application.

The principal objective in a drying operation is to supply the required heat in an optimum manner to yield the best quality product with a minimum overall expenditure of energy. It is known that relatively modest increase in ambient temperature and air flow in the produce will reduce the drying duration and give high quality product. A properly designed solar dryer can successfully be used to produce hygienic and quality food product that can compete with conventional dryer products with the added advantage of saving fossil fuel. A number of designs of natural/forced convection solar dryers are now available, but the market penetration of solar dryers is very poor. Some of the barriers of the large scale deployment are due to the non-awareness of the various technicalities involved and lack of good design to satisfy the requirement. Also the commercial units available are few, often badly designed with no parametric optimization. It needs an urgent measure of designing solar dryers which are cost effective, gives satisfactory performance and meets the particular requirements of different types of produce. Keeping all the design constraints in mind, a solar air heating system for drying 200 to 250 kg fresh fruits/vegetables was fabricated and installed at a Food Processing Centre in Kerala. The courses of investigations carried out on pilot model air heaters described in chapter 3 helped to undertake and materialize of the project. The drying system installed essentially consisted of three components viz., solar air heater to collect the energy from the sun, a drying chamber to hold the material to be

dried and a duct for the passage of hot air from the solar air heater to the dryer. The design and fabrication details are illustrated with the help of engineering drawings. Through this design, an attempt has been made for

1. Identification and selection of various materials and their integration to build an ideal solar drying system
2. The selection of component to meet the best collector design requirements and best fabrication techniques.
3. The most economic, efficient, and operating mechanism
4. Large scale proliferation of solar air heating technology for drying applications

To make a solar dryer techno economically feasible one must take into account the thermo-physical aspects of the system. These refer to all heat, mass and humidity calculations and fix the major parameters like the quantity of air required, mass of moisture removed from the produce, rise and fall of air temperature, amount of energy required, etc. The mechanical design consideration concentrates on fixing the mechanical details of the drying chamber and collector. Mechanical design studies are regarding materials for solar air heater fabrication, cabinet size, tray volume, number of trays, size of ducting and cladding, etc. The other design parameters that should be taken into account are geographical location, local climatic conditions, types of materials to be dried, available solar flux, etc. The design consideration for the drying system i.e., the solar air heater used to supply hot air, drying chamber and ducting are discussed here separately.

4.5.1 Design Consideration for Solar Drying Chamber

The major design parameters of a drying chamber are

- a) quantity of product to be dried per batch or day and size of the drying cabinet to hold the material
- b) capacity of the dryer (kg/batch)

- c) system for loading and unloading the material
- d) materials for dryer cabinet and tray construction
- e) arrangement to pass hot air through the material to be dried
- f) effective circulation and recirculation of hot air through the dryer
- g) a vent through which the warm moist air to remove from the drying chamber

4.5.1.1 Thermodynamical aspects

Based on the thermodynamical aspects, the quantity of air needed for drying a specified mass of the product was evaluated in this section. Two different methods are employed here for these calculations. They are listed below:

(i) The psychrometric charts

The capacity of air for moisture removal depends on its humidity and temperature. The study of relationships between air and its associated water is called psychrometry. On the psychrometric chart, various properties of moist air like dry and wet bulb temperature, dew point temperature, relative humidity, humidity ratio and enthalpy become evident. When any two of the three temperatures are known, i.e., dry-bulb, wet-bulb, or dew-point, all other properties can be determined from the psychrometric chart.

In this chart (Fig. 4.1), the humidity ratio is the ordinate and dry bulb temperature is the abscissa. The upper curve of the chart is labeled wet bulb and dew point temperatures. The other curves on the psychrometric chart that are similar in shape to the wet bulb lines are lines of constant relative humidity (%). The straight lines sloping gently downward to the right are lines of constant wet bulb temperature. The intersection of a dry bulb and a wet bulb line gives the state of the air for a given moisture content and relative humidity. The amount of air needed for drying a particular quantity of produce can be calculated using psychrometric chart.

(ii) The energy balance equation for drying

The energy balance is an equation that expresses the following idea

mathematically: The energy available from the air going through the food inside the dryer should be equal to the energy needed to evaporate the amount of water to be removed from the crop. The removal of water from a surface by evaporation requires an amount of heat equal to the latent heat of evaporation of water plus a current of air moving over the surface to carry away the water vapour produced. Hence the task in solar dryer is to calculate and then achieve optimum temperature, T_f and air flow, m_a to remove the specified amount of water, m_w . So we have

$$m_w L = (T_f - T_i) m_a C_p \quad (4.1)$$

where m_w = mass of water evaporated; L = latent heat of evaporation; m_a = mass of air circulated; C_p = specific heat of air; T_f , T_i = final and initial temperatures. The quantity of water to be evaporated is calculated from the initial and desired final moisture content with the help of the following equation

$$m_w = \frac{M_i (m_i - m_f)}{(100 - m_f)} \quad (4.2)$$

where M_i = initial mass of the sample,

m_i , m_f = initial and final moisture content

After these, the volume of air can be determined by using the gas laws

$$\frac{V_{air}}{m_v} = \left(\frac{m_a}{m_v} \right) \left(\frac{RT}{P} \right) \quad (4.3)$$

$$\text{i.e. } V_{air} = \frac{m_a RT}{P} \quad (4.4)$$

where m_w , the amount of water evaporated can be read from moisture ratio scale or can be calculated from the energy balance equation.

Because the vapour pressure of bound water in hygroscopic material is less than saturation, the effect of bound water is also to be taken into account.

Again, the latent heat value should be chosen to correspond to a very low vapour pressure.

The equations can be employed for evaluating various parameters as mentioned above. Here, these are made use of in calculating the quantity of air needed for drying (m_a) for various materials to be dried as given below.

4.5.1.1 (a) The quantity of air needed for drying

Pineapple was used for drying test in the developed system. The quantity of air needed for drying pineapple by means of dehydration process was estimated, both by using energy balance equation as well as by psychrometric chart. The calculation details are discussed below:

a) From the psychrometric chart: The amount of air required to dry 1 kg of pineapple from an initial moisture content of 80% (wet basis) to a final moisture content of 10% was calculated using the psychrometric chart (Fig. 4.1). The ambient air is at a temperature of 30°C (T_1) and Relative Humidity (RH) of 50%. Ambient air is shown as point A on the psychrometric chart. As the ambient air (Point A) is heated in the solar air heater, the air heats up to 60°C (T_2) and the RH drops to 15%, which is point B on the psychrometric chart. The path A-B represents the heating of the air in the solar collector, keeping a constant humidity ratio and hence moving parallel to the dry bulb temperature axis. As the heated air passes through the drying chamber, it picks up moisture from the pineapple and cools down, moving along the curve of wet bulb temperature. The path B-C represents the change in the state of the air as it passes through the drying material. The point D, with temperature 36.4°C (T_3) and humidity ratio 0.0240, represents the end of the process. The humidity ratio rose from 0.0135 (point B) to 0.024 (point D). The difference ($0.024 - 0.0135 = 0.0105$) is the amount of water (kg water vapour per kg of dry air) carried away from the pineapple by the air.

The amount of water to be extracted from 1 kg of pineapple, calculated from Eq. (4.2) is 0.777 kg.

The mass of air needed = $0.777/0.0105 = 74$ kg

The weight of dry air (m_a) can be transformed to volume (V) using the following expression

$$PV_{\text{air}} = m_a RT \quad (4.5)$$

Where $P = 101.3$ kPa (normal barometric pressure at sea level), and $T = 309^\circ\text{K}$ (36°C), $R = 0.291$ kPa $\text{m}^3/\text{kg K}$, $m_a = 74$ kg, then

$$V_{\text{air}} = \frac{m_a RT}{P}$$

where R is a constant factor, equal to 0.291 kPa $\text{m}^3/\text{kg}^\circ\text{K}$; T is the Temperature ($^\circ\text{K}$); V_{air} is the volume of air (m^3); P is the pressure (Pa)

$$= \frac{74 \times 0.291 \times 309}{101.3} = 65.68 \text{ m}^3$$

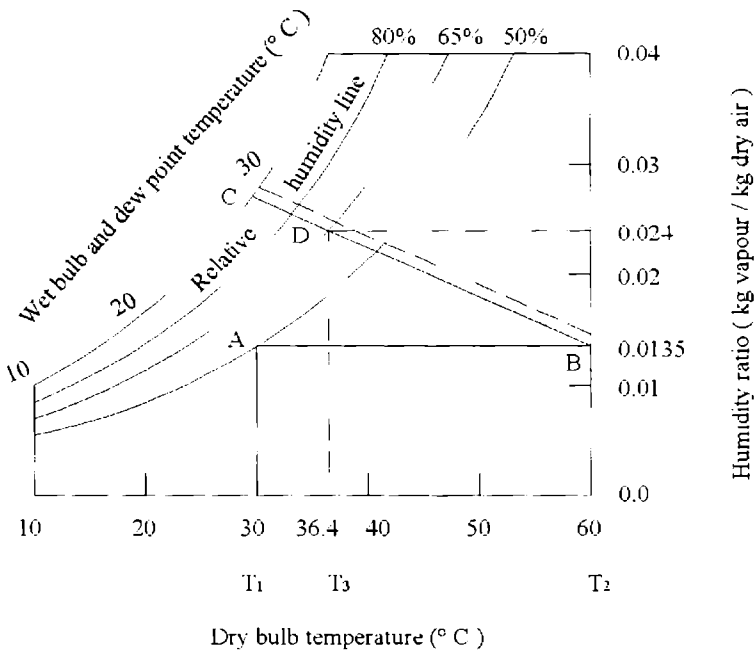


Fig. 4.1 Psychrometric chart: Drying process for Pineapple

(b) From the energy balance equation: It is based on the concept that the energy available from the air going through the food inside a dryer should be equal to the energy needed to evaporate the amount of water to be removed from the crop.

The task in solar dryer design is to calculate and then achieve optimum temperature (T_f) and air flow (m_a per time) to remove the specified amount of water (m_w). The calculation of the volume of air needed for drying from the energy balance equation (4.2), in the above case, is as follows.

Amount of water to be extracted=0.777 kg

Latent heat of vapourization=2.8 MJ/kg

Specific heat capacity=1.02 kJ/kg°C

Then by using the same data, we get the mass of air needed is 71.1 kg. The corresponding volume of air, calculated as before, using the expression $PV_{air} = m_aRT$, is 63.11 m³

4.5.1.2 Mechanical Aspects

The mechanical details of the drying chamber involve detailed studies regarding cabinet size, tray volume, number of trays, depth of drying material in the tray, clearance between two trays, plenum chamber height, top clearance area, ventilation holes, etc.

(a) Tray volume

It is defined as the capacity of the drying chamber to the loading rate. Once the tray area is known, the number of trays and the amount of product in the trays can be determined. The depth of loading in each tray can be calculated as follows:

$$\text{Depth of loading} = \frac{\text{Volume}}{\text{Area}}$$

But,

$$\text{Volume} = \frac{\text{Mass}}{\text{BulkDensity}}$$

and Volume = Length x Breadth x Height of the material

Hence,

$$L_1 \times B \times H = \frac{M_i}{\rho} \quad (4.6)$$

where M_i = Mass of the material

ρ = Bulk density

L_1 = Length

B = Breadth

H = Height

If the depth of the loading is calculated, say, as H_1 cm and small clearance above the product is H_2 cm then total depth of the tray is (H_1+H_2) cm. So total volume of tray is $L_1 \times B \times (H_1+H_2)$ cm³ So total height required for trays = (No. of gaps x distance between two successive trays) + (No. of trays x height of each tray)

4.6 Description of the Solar Air Heater

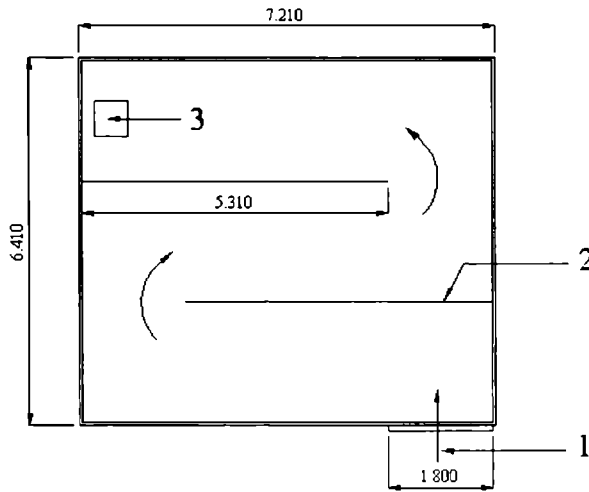
The solar drying system was designed, fabricated and installed at Food Processing Centre, Alapuzha district (9°31'N and 76°20'E), Kerala. The solar air heating system was integrated with the roof of the building. A south-facing asbestos roof was constructed on the terrace of the building using truss, pillars and beams. The solar air heater was fabricated and mounted over the asbestos roof. The installed system was a forced convection indirect type. The hot air generated from the solar air heater was sucked by a centrifugal blower and it was applied to the dryer through a duct. The designs can be broken into its components for the

sake of analysis. The identification of the possible material candidate and selection of the components, which can meet the requirements of the air heater play an important role. Overall description of the components such as absorber plate, glazing, insulation, and cover structure are depicted.

The solar air heater fabricated was of 'underflow' type. The dimension of the collector was 6.41m long and 7.21m wide, giving a gross collector area of 46 m². The structural frame of the heater was made of extruded aluminium. The absorber plate used was 38 SWG black chrome copper sheet, which was screwed to the aluminium frame. The reported absorptivity and emissivity of the material is 0.95 and 0.08 respectively. The solar radiation incident on the absorber plate raises its temperature. This thermal energy is transferred to the working fluid.

The copper absorber plate was 0.3 m wide and was joined each other by using rivets and supported in aluminium square tubes. A rectangular air duct underneath the absorber was formed by providing a rear plate (bottom plate) at a spacing of 10 cm to each other. Three baffles were provided in the air flowing area in order to increase the air fill factor. Each baffle was 5.31 m long, and thus extended to occupy 75% of the collector's width. The baffles were fixed to the bottom plate and their top edge was in contact with the absorber plate. The baffle was made up of 22 SWG aluminium sheet. The baffles caused the flowing air to follow a winding path, effectively doubling the length of its passage through the collector. The baffles created turbulence, making the air to flow in close contact with the absorber and decreasing the thermal sublayer. The outer body of the whole structure was covered with aluminium sheet. Fig. 4.2 is a schematic diagram of the air flow through the solar air heater. 24 SWG aluminium sheet was used as bottom plate. The size of the single sheet was 8' x 4' and the whole area was covered by jointing individual sheet. Rock wool insulation was packed on sides as

well as below the aluminium sheet and on the sides of copper sheet. On the bottom sides it was spread in between the asbestos sheet and aluminium sheet. The thickness of insulation was 4 cm at the bottom and sides.



1. Air inlet 2. Metal partition 3. Air outlet to the duct

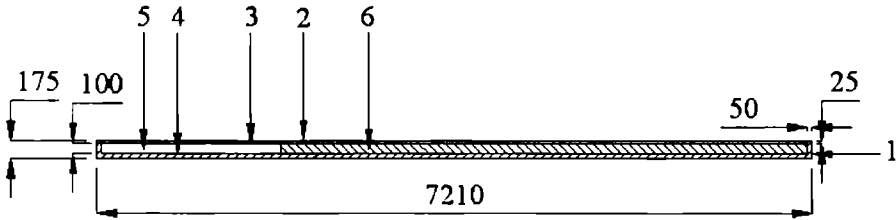
ALL DIMENSIONS IN METER

Fig. 4.2 Schematic diagram of the air flow passage in the air heater

The whole structure was placed above the asbestos roof. A sectional view of solar air heater is shown in Fig. 4.3. The tempered glass having thickness of 4 mm was mounted using aluminium sections and frames at a height of 25.4 mm from the absorber plate. The space between the absorber and the glass reduces the convective losses at the front side. All the possible air leakage from the side and bottom was prevented by silicon sealant. Fig. 4.4 shows the front view of the 46 m² solar air heater.

The hot air outlet of the air heater was connected to a 0.75 kW centrifugal blower through a double-walled Galvanized Iron duct insulated with a thick layer of glass wool in between. The size of the duct was 300 mm

x 300 mm. The material used for the duct fabrication was 24 SWG GI sheet and it was fully covered with 50 mm rock wool insulation. Again the rock wool insulation was enclosed by 24 SWG aluminium sheet, which formed the cladding.



1. Insulation 2. Transparent glass 3. Copper sheet 4. Aluminium sheet 5. Air channel 6. Metal partition

ALL DIMENSIONS IN METER

Fig. 4.3 Sectional view of the solar air heater

4.7 Description of the Dryer

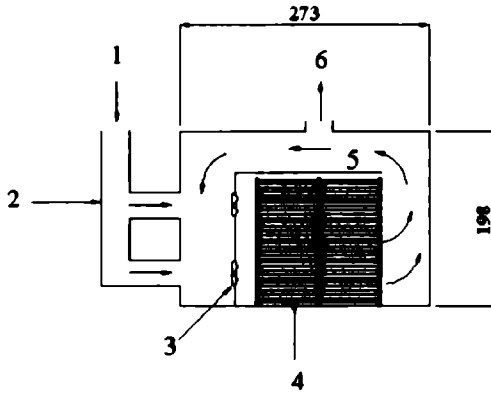
The centrifugal blower outlet was connected to the dryer, in which the material to be dried was loaded. The dryer was a batch type, with a drying capacity of 200-250 kg of fresh fruit/vegetables (Fig. 4.5). The total volume of the dryer was 6.54 m³. The frame of the dryer was fabricated using CR square tubes and its inner and outer walls were made up of Stainless Steel (SS) sheets, separated with an insulating layer of rock wool slab to prevent heat loss through the walls of the dryer. A schematic diagram of the dryer is shown in Fig. 4.6.



Fig. 4.4 A 46 m² solar air heater installed in the food processing industry



Fig. 4.5 Solar fruits and vegetables dryer (capacity - 200 to 250 kg)



**1.Hot air from solar collector 2.Insulated duct 3.Axial fans 4.Perforated trays
5.Air plenum chamber 6.Moist air out**

ALL DIMENSIONS IN METER

Fig. 4.6 Schematic diagram of the dryer

The whole inner, outer walls and trays of the dryer were fabricated using SS to make the process hygienic and corrosion free. The dryer consisted of 128 perforated trays in 4 partitions to spread the product into thin layer. Each tray was 560 mm x 560 mm and the diameter of the perforations was 3 mm with a pitch of 5 mm. Trays were supported using SS angles, welded with SS square tubes. The drying chamber was divided into loading area and the plenum area. The hot air was circulated and recirculated with four axial fans fitted in the dryer, each with a volume flow rate of 4000 m³ per hour. The axial fans sucked hot air from the solar air heater through the insulated duct and hot air enters the plenum chamber, from where it was distributed uniformly in the dryer. Quantity of air inside the drying chamber was nearly eight times more than that of the air coming from the solar panels. Moist air from the dryer escapes through the exhausts provided at the top of the dryer and two dampers was fitted here for controlling the airflow rate. The size of both the dampers was same and it was 150 mm x 300 mm. The temperature inside the dryer was set to 70°C using an actuator control mechanism. Whenever the temperature rose beyond the preset value, the

damper coupled with the actuator positioned in the duct opened, allowing the ambient air to enter in the duct and caused lower the temperature. The design detail of the solar drying system is illustrated in Table 4.3.

Table 4.3 Design details of solar drying system

Solar Air Heater	
Gross collector area	:6.41 m x 7.21 m
Aperture area	:6.31 m x 7.11 m
Absorbing material	:Black chrome copper (38 SWG)
Rear plate	:Aluminium
Working fluid	:Air
Insulation material	:Rock wool
Insulation thickness (side and bottom)	:50 mm
Collector tilt angle	:12°
Cover plate material	:Toughened glass
Thickness	:4 cm
Number of cover glass	:One
Mode of air flow	:Underflow
Centrifugal blower	:0.75 kW
Air inlet area	:1.8 m x 0.1 m
Air outlet area	:0.3 m x 0.3 m
Solar Drying Chamber	
Gross dimensions	:2.73 m x 1.98 m x 1.21 m
No. of trays	:128
Size of tray	:560 mm x 560 mm
Material for tray	:Stainless Steel
Spacing between two trays	:4 cm
Insulation material	:Rock wool
Insulation thickness	:40 mm
Air plenum chamber dimensions	:118 cm x 46 cm x 121 cm
No. of axial fans	:4
Volume flow rate of individual fan	:4000 m ³ /h
Ducting and Cladding	
Dimension of ducting	:300 mm x 300 mm
Material for ducting	:24 SWG GI sheet
Insulation material	:Rock wool
Insulation thickness (side and bottom)	:50 mm
Material for cladding	:24 SWG Al sheet
Dimension of cladding	:350 mm x 350 mm

4.8 Working

Sunlight is made of shortwave radiation, which penetrates the toughened glass of the collector, absorbed by the black chrome copper sheet, and thereby converted into thermal energy. i.e., long wave radiation. However, the long wave radiation emitted from the absorber plate strikes the glass and bounces back, the glass does not let any long wave radiation to pass through it. The heat absorbed by the absorber plate is transferred convectively to the air passing under the absorber plate.

The fan sucks ambient air and pushes underneath of the absorber plate. The heat absorbed by the absorber plate is transferred convectively to the air passing over the absorber plate. The hot air then enters the drying chamber through the insulated duct. As hot air passes through the chamber, it draws moisture from the product loaded in the trays and the warm moist air goes out through the vent provided on the top of the dryer.

4.9 Attractive Design Features

Since the dryer does not expose the product directly to solar radiation, the product retains its colour even when fully dry. It also preserves nutrition and resulted in a high quality product. The black chrome copper absorber plate enhances the efficiency of the overall system. The baffles by forcing the air to traverse a longer path, raises air temperature further. The four axial fans within the drying cabinet circulate and recirculate the hot air within the cabinet, which accelerates the overall drying processes, while the actuator controlling mechanism prevents the temperature from rising beyond the set point. The stainless steel perforated trays preclude staining and enhance the product quality.

4. 10 Investigation of the Performance of the Dryer

The performance of the system was monitored continually during the year 2005 and 2006. The instruments, materials, and the method of performance evaluation are described below.

4.10.1 Instruments

Various measuring devices were used for investigating the effects of environmental and operating parameters on the performance of the solar drying system. Solar radiation flux on a horizontal surface was measured by using a Solarimeter (Central Electronics Limited, India). Air velocity was measured with a Digital thermo-anemometer (Model No. TA 35, made by Airflow, UK) which has a range of 0.25 to 20 m/s, with an accuracy of ± 0.1 m/s. The ambient temperature, inlet temperature, outlet temperature and temperature inside the drying chamber were monitored with an LM 35 sensor connected to a computer with RS 232 interface through a 16-channel data logger. The temperatures were recorded every minute. Relative humidity of ambient air and of that inside the drying chamber was measured periodically with a digital hygrometer. Samples of the product being dried were weighed at hourly intervals using an electronic digital balance. At the end of the drying process, the moisture content of the sample was determined by drying the sample in a hot air oven at 108°C for 24 hours.

4.10.2 Materials and Methods

Pineapple was used for the drying tests, which available in abundance in Kerala. The fruit rich in sugars is a perishable product. Dried pineapple also enjoys a very good market. For the drying tests, each batch consisted of 200 kg ripe pineapples. The initial moisture content of the product was 82%. The fruit was sliced horizontally into 5 mm thick discs before loading the drying trays, no other pretreatment was involved. Other

materials processed in the dryer were bitter gourd, banana, and tapioca (cassava).

4.10.3 Economic Analysis

The dried products are available in the market as both branded and unbranded items. The unbranded product is cheaper, but it is often of inferior quality and produced under unhygienic conditions. The product has a short shelf life and is often unfit for consumption. Branded products are usually manufactured under hygienic conditions, and find a ready market despite the higher price. The economic analysis done here assumes that the cost of solar-dried product sells at a price comparable to that of a branded product.

Three methods were used for the economic analysis. The first one is 'annualized cost method' [20]. This compares the cost of drying of unit weight of the product with the solar dryer to that of drying it using an electric dryer. The total annualized cost of the dryer is divided by the amount of product dried in a year to obtain the cost of drying per unit weight of the dried product. The drawback of this method is that the cost of drying does not fully capture the economics of the solar dryer because the cost of drying varies little over the entire life of the dryer, say 20 years (only cost incurred is the cost required to operate the blower and axial fans), while the case of dryers using conventional energy, the increasing cost of conventional energy increases the cost of drying. Therefore, for assessing the economic benefits of the solar dryer, it is essential to determine the savings over the life of the dryer-which is what the second method, namely the 'life cycle savings' does. In this method, the first step is to determine the savings per drying day for the solar dryer in the base year. The present worth of annual savings over the life of the system is calculated next [21]. If the payback period of the system is short, people will come forward to procure the system, if it is long, even when substantial long-term savings are possible, they will not [22].

Therefore, the third method, namely ‘payback period’, was also used. A similar approach was also followed by Singh et al. [23] with relevant equations for economic analysis of a solar dryer for domestic use.

4.10.3.1 Annualized cost method

The cost of drying is calculated using the annualized cost method to compare the cost with the drying by using other conventional energy sources. In this method, the annualized cost of the dryer is divided by the quantity of product dried per year to obtain the cost of drying per unit weight of the dried product.

Annualized cost. The annualized cost of a dryer is calculated by Eq. (4.7)

$$C_a = C_{ac} + C_m - V_a + C_{rf} + C_{re} \quad (4.7)$$

In Eq. (4.7), the C_{ac} is the annualized capital cost and V_a is the salvage value and these are given by Eq. (4.8) and Eq. (4.9).

$$C_{ac} = C_{cc}F_c \quad (4.8)$$

$$V_a = VF_s \quad (4.9)$$

where F_c is the capital recovery factor and F_s is the salvage fund factor and these two terms are defined by Eqs. (4.10) and (4.11), respectively.

$$F_c = \frac{d(1+d)^n}{(1+d)^n - 1} \quad (4.10)$$

$$F_s = \frac{d}{(1+d)^n - 1} \quad (4.11)$$

In Eq. (4.7), C_m is the annualized maintenance cost calculated as a fixed percentage of the annualized capital cost. The cost of drying per kilogram of dried product is then calculated by using Eq. (4.12)

$$C_s = \frac{C_a}{M_y} \quad (4.12)$$

(i) **Solar dryer** - The quantity of product dried in the solar dryer per year, M_y is calculated using Eq. (4.13)

$$M_y = \frac{M_d D}{D_b} \quad (4.13)$$

Normally the annual running fuel cost of the solar dryer is zero.

C_{re} is the running cost for fans in the dryer.

$$C_{re} = R \times W \times C_e \quad (4.14)$$

R is the number of hours the blower and fans working in a year, W is the rated power consumption of fans, and C_e is the unit charge for electricity.

(ii) **Electric dryer** - The annual running fuel cost of using an electric dryer to dry the same quantity of product dried by the solar dryer is calculated. The annual running fuel cost, C_{rf} , of the electric dryer is given in Eq. (4.15)

$$C_{rf} = M_y \left[\left(\frac{m_1}{100} \right) \frac{LC_e}{\eta_e \times 3600} \right] \quad (4.15)$$

where m_1 is the moisture content in dry basis and is given by Eq. (4.16)

$$m_1 = \left(\frac{M_f - M_d}{M_d} \right) \times 100 \quad (4.16)$$

Here also, the operating cost of fans is taken into account.

4.10.3.2 Life cycle savings

In the life cycle saving method, the first step is to determine the savings per drying day for the solar dryer in the base year; the present worth of annual savings over the life of the system is calculated next.

4.10.3.2 (a) **Savings per day** The cost of fresh product per kilogram of dried product is calculated using Eq. (4.17)

$$C_{dp} = C_{fp} \times \frac{M_f}{M_d} \quad (4.17)$$

The expense required to dry 1 kg of product (C_{ds}) in the solar dryer is the sum of the cost of fresh product (C_{dp}) and the cost of drying (C_s) per kilogram of dried product.

$$C_{ds} = C_{dp} + C_s \quad (4.18)$$

The quality of the dried product in a solar dryer is equivalent to the quality of branded products available in the market. Therefore, the saving per kilogram of dried product (S_{kg}) in the base year due to use of the solar dryer is calculated using Eq. (4.19). The saving per batch (S_b) and the saving per day (S_d) in the base year are then calculated using Eqs. (4.20) and (4.21) respectively.

$$S_{kg} = C_b - C_{ds} \quad (4.19)$$

$$S_b = S_{kg} \times M_d \quad (4.20)$$

$$S_d = \frac{S_b}{D_b} \quad (4.21)$$

4.10.3.2 (b) Present worth of annual savings - For the life of the system, the annual savings (S_j) for drying the typical product in the j^{th} year are obtained using Eq. (4.22). The present worth of annual savings in the j^{th} year is obtained from Eq. (4.23).

$$S_j = S_d \times D \times (1 + i)^{j-1} \quad (4.22)$$

$$P_j = F_{pj} \times S_j \quad (4.23)$$

where the present worth factor for the j^{th} year is given by Eq. (4.24)

$$F_{pj} = \frac{1}{(1 + d)^j} \quad (4.24)$$

The cumulative present worth of the savings for the life of the system, i.e., the life cycle savings, was obtained by adding the present worth of the annual savings over the life of the system.

4.10.3.3 Payback period

The payback period (N) is calculated from Eq. (4.25)

$$N = \frac{\ln\left(1 - \frac{C_{cc}}{S_1} (d - i)\right)}{\ln\left(\frac{1+i}{1+d}\right)} \quad (4.25)$$

4.11 Results and Discussion

The mass flow rate of air through the dryer was kept constant throughout the study. All the experiments were conducted from 9.30 a.m to 4.30 p.m. The dryer was loaded with 200 kg pineapple to study the drying behaviour. The parameters monitored (such as ambient temperature, inlet air temperature, dryer outlet temperature, temperature in the solar dryer, and intensity of solar radiation) are shown in Fig. 4.7. The experiment was conducted with the centrifugal blower and four axial fans in operating condition. The maximum temperature of air monitored at the outlet of the solar air heater was 76.6°C, which was at 12.40 p.m. During the study, the air flow rate was maintained at 43 kgm⁻²h⁻¹. The high temperature output from the air heater, despite moderately high air mass flow rate, was due to the copper sheet used as absorber material and the provision of baffles to increase the air fill factor. In this experiment, no attempt was made to control the temperature because we wanted to find out the maximum temperature that the collector can attain. Apart from this, all other processing was carried out at a set temperature of 70°C and with a fixed mass flow rate of 43 kgm⁻²h⁻¹. The intensity of solar radiation was 930 W/m² when the collector achieved its maximum temperature. The maximum temperature monitored in the drying chamber was 67.3°C and it was obviously at the time that the solar output temperature was maximum. Ambient temperature varied from

29.9°C to 33.8°C. The average efficiency of the solar air heater over the day was calculated as 52.55%.

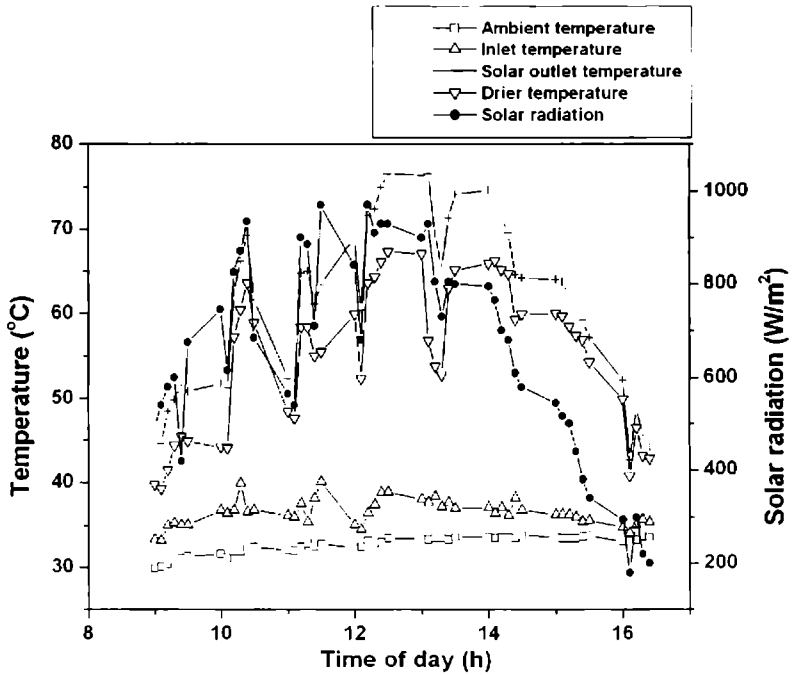


Fig. 4.7 Variation of temperature at the solar air heater outlet and in the drying chamber with solar radiation

Loading the product had no effect on the solar outlet temperature, because the air heater and dryer were two separate entities connected only by a duct. The maximum rise in temperature (above the ambient) achieved by the solar air heater was 43.3°C. Relative humidity of the air flowing into the dryer varied from 51% to 82% during the study period. The average velocity of air inside the dryer was monitored as 1.2 m/s. The drying test revealed that the moisture content of pineapple reduced from the initial level of 82% (w.b) to the final level of 9.7% (w.b) within about 8 hours (Fig. 4.8). The energy required for removing the moisture from 200 kg of the product was calculated at 435 MJ. The samples were collected from different trays to

analyze the uniformity of drying and it was found that the reduction in moisture in all the trays was uniform, the variation was negligible. Drying was rapid initially but gradually decreased because the surface moisture evaporated quickly at the beginning of the process. It is known that as the moisture content of a product is reduced, more energy is required to evaporate the same amount of moisture from the product. The moisture content at the end of the experiment on the first day was 12.02%. The product was kept in the dryer overnight and the doors were tightly closed to prevent air infiltration. Drying continued the next day and the final moisture content was achieved after 2 hours. Thus, the total drying duration was 8 hours. The colour of the dried product is an important parameter to determine the quality of the product. The product retained its original colour in the solar dryer, even after it was completely dry.

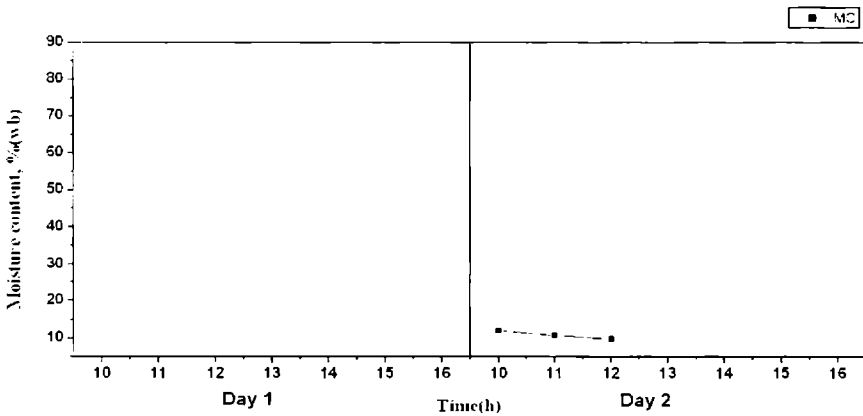


Fig. 4.8 Reduction in moisture content of pineapple with time

4.11.1 Economic Analysis

The economic parameters are based on the economic situation in India as shown in Table 4.4. The economic analysis done by the three

methods, namely annualized cost, life cycle savings, and payback period are summarized below.

Table 4.4 Cost and economic parameters of solar dryer

1. Material and labour cost for the construction of the solar dryer	Rs 550,000
2. Interest rate	8%
3. Rate of inflation	5%
4. Real interest rate	3%
5. Life span of the dryer	20 years
6. Electricity cost	Rs. 4.00/kWh
7. Cost of fresh pineapple	Rs. 10/kg
8. Selling price of dried pineapple	Rs. 200/kg

4.11.1.1 Annualized cost method

The annual capital cost was calculated first and annual maintenance cost of the solar dryer was taken as 10% of the annual capital cost. The salvage value was also assumed to be 10% of the annual capital cost. The annual capital cost of the solar dryer worked out to Rs. 55,990. A solar dryer can be easily operated for 290 days in a year in countries like India, although number of solar days was taken as 250 for the purpose of the calculation.

The dryer was provided with four axial fans, and the running cost of the fans was also taken into account for economic analysis. Annual electricity charge for running the dryers was calculated as Rs. 12000 for the solar dryer and Rs. 8000 for the electric dryer. The high running cost of the solar dryer was due to the additional consumption of electric power by the

blower required to suck hot air from the solar air heater, which is absent in the case of electric dryer. The total amount of dried product processed annually in the solar dryer was 6666.66 kg and the cost of drying of 1 kg of pineapple slices turned out to be Rs. 11 for the solar dryer and Rs. 19.73 for the electric dryer. The capital cost of the electric dryer, electricity cost per unit, and the efficiency of the electric dryer were assumed as Rs. 275,000, Rs. 4 /kWh, and 0.75% respectively.

4.11.1.2 Life cycle savings

The cost required for drying 1 kg pineapple in the solar dryer and electric dryer was calculated. The current saving per day turned out to be Rs. 4773. Table 4.5 shows the calculated annual savings, present worth of the annual savings and cumulative present worth of annual savings for each year of life of the solar dryer. The cumulative present worth turned out to be approximately 17 million rupees. The investment on solar dryer was Rs. 550,000. Thus, by investing Rs. 550,000 in a solar dryer today, we can save roughly 17 million rupees. This calculation assumed the life span of the dryer to be 20 years; however the savings were extended over the life of the system.

4.11.1.3 Payback period

Payback period is the time needed for the cumulative fuel savings to equal the total initial investment. It is clear from the Table 4.5 that the total investment, i.e. Rs. 550,000 is recovered within the first year of operation. The payback period was calculated to be 0.54 year (equivalent to 191 drying days), which is very short compared to the life of the dryer (20 years). Thus, the dryer will dry the product free of fuel cost with a marginal running cost for almost its entire life period.

Table 4.5 Economics of the solar dryer – Annual saving, present worth of annual saving and present worth of cumulative annual saving for each year during the life of the solar dryer for drying pineapple and 250 days of use of solar dryer

Year	Annualized cost of dryer (Rs.)	Annual savings (million rupees)	Present worth of annual saving (million rupees)	Present worth of cumulative saving (million rupees)
1	0.073	1.19	1.10	1.10
2	0.073	1.25	1.07	2.18
3	0.073	1.32	1.04	3.22
4	0.073	1.38	1.01	4.24
5	0.073	1.45	0.99	5.23
6	0.073	1.52	0.96	6.19
7	0.073	1.60	0.93	7.12
8	0.073	1.68	0.91	8.03
9	0.073	1.76	0.88	8.91
10	0.073	1.85	0.86	9.77
11	0.073	1.94	0.83	10.60
12	0.073	2.04	0.81	11.41
13	0.073	2.14	0.79	12.20
14	0.073	2.25	0.76	12.96
15	0.073	2.36	0.74	13.70
16	0.073	2.48	0.72	14.43
17	0.073	2.60	0.70	15.13
18	0.073	2.73	0.68	15.81
19	0.073	2.87	0.67	16.48
20	0.073	3.02	0.65	17.13

4.12 Conclusion

A roof integrated solar air heater with a batch dryer was developed and installed in a Food Processing Centre. The project funded by State Government under a scheme called “Kudumbasree” The major task of the scheme was the income generation of poor rural women group through sustained technology. The drying system proved to be efficient and economic for drying fruits/vegetables. The experiments were conducted on pineapple, having large content of water. The solar air heater was 46 m² and recorded a maximum temperature of 76.6°C. The hot air generated from the roof mounted solar air heater was sucked by a blower through an insulated duct and circulated in the dryer located in a room below. Since the product was not directly exposed to solar radiation, the colour of the product was retained even after complete drying. The dryer was loaded with 200 kg of fresh pineapple slices of 5 mm thick. The initial moisture content of 82% was reduced to the desired level (<10 %) within 8 hours. The performance of the dryer was analyzed in detail by three methods namely annualized cost, present worth of annual savings, and present worth of cumulative savings. Economic analysis showed that the cumulative present worth of annual savings for drying pineapple over the life of the solar dryer turned out to be approximately 17 million rupees. The capital investment of the dryer was Rs. 550,000 and the payback period of the dryer was found to be 0.54 year, which is very short considering the life of the system. The cost of drying pineapple in the solar dryer was only about 20 % of drying cost when dried in electric dryer. The life of the system was expected to be 20 years, because the material used in the construction was corrosion proof. The dryer continues to work in the food processing centre to produce dried food and the performance is quite satisfactory.

Nomenclature

C_a	annualized cost of dryer (Rs.) (US\$1 \approx Rs. 45)
C_{ac}	annual capital cost (Rs.)
C_b	selling price of branded dried product (Rs./kg)
C_{cc}	capital cost of dryer (Rs.)
C_{de}	cost of drying per kg of dried product in electric dryer (Rs./kg)
C_{dp}	cost of fresh product per kg of dried product (Rs./kg)
C_{ds}	cost per kg of dried product for domestic solar dryer (Rs./kg)
C_e	cost per kWh of electric energy (Rs./kWh)
C_{fp}	cost per kg of fresh product (Rs./kg)
C_m	annualized maintenance cost (Rs.)
C_p	specific heat of air (kJ/kg $^{\circ}$ C)
C_{rf}	annual running fuel cost (Rs.)
C_{re}	annual electricity cost of fans (Rs.)
C_s	cost of drying per kg of dried product in dryer (Rs./kg)
d	rate of interest on long term investment
D	number of days of use of domestic dryer per year
D_b	number of drying days per batch
F_c	capital recovery factor
F_s	salvage fund factor
F_p	plate efficiency factor
F_{pj}	present worth factor for j^{th} year
F_R	collector heat removal factor
I	intensity of solar radiation (W/m 2)
i	rate of inflation
L	latent heat of evaporation (kJ/kg)
m_a	mass of air circulated (kg)
m_f	final moisture content of the product

m_i	initial moisture content of the product
m_1	moisture content (dry basis) (%)
m	mass flow rate ($\text{kgm}^{-2}\text{h}^{-1}$)
m_w	mass of water evaporated (kg)
M_d	mass of dried product removed from solar dryer per batch (kg)
M_f	mass of fresh product loaded in solar dryer per batch (kg)
M_i	initial mass of the product (kg)
M_y	mass of product dried in the dryer per year (kg)
n	life of solar dryer (year)
N	payback period (year)
P	pressure (Pa)
P_j	present worth of annual saving in j^{th} year (Rs.)
R	annual running hours of blower and axial fans
S_b	saving per batch for solar dryer (Rs./kg)
S_d	saving per day for domestic solar dryer in the j^{th} year (Rs.)
S_j	annual savings for domestic solar dryer in the j^{th} year (Rs.)
S_1	saving during first year for solar dryer (Rs.)
S_{kg}	savings per kg compared to branded product for solar dryer (Rs./kg)
T_i	inlet temperature ($^{\circ}\text{C}$)
T_f	outlet temperature ($^{\circ}\text{C}$)
T_a	ambient temperature ($^{\circ}\text{C}$)
T_p	plate temperature ($^{\circ}\text{C}$)
U_L	collector heat loss coefficient ($\text{W}/\text{m}^2\text{ }^{\circ}\text{C}$)
V	salvage value (Rs.)
V_{air}	volume of air (m^3)
V_a	annualized salvage value (Rs.)
W	rated power of electric blower and axial fans (kW)

Greek symbols

η overall efficiency of the collector

η_e efficiency of electric dryer

τ transmittance of the glass cover

α solar absorptance

$(\tau\alpha)_e$ effective transmittance absorptance product

References

- [1] K. Lutz and W. Muhlbauer, *Drying Technology* 4, 583, 1986.
- [2] M. Beedie, Energy savings-a question of quality, *South African Journal of Food Science and Technology* 48(30), 14-16, 1995.
- [3] R.B. Keey, *Introduction to Industrial Drying Operations*, Pergamon Press, Oxford, 1978.
- [4] K.S. Jayaraman and D.K. Gupta, *Drying of fruits and vegetables*. In: *Handbook of industrial drying*, 643–690, Marcel Dekker, New York, 1995.
- [5] A.S. Mujumdar and A.S. Menon, *Drying of Solids*, In: A.S. Mujumdar (Ed.) *Handbook of Industrial Drying*, 2nd Edition, 1- 46, Marcel Dekker, New York, 1995.
- [6] S.I. Anwar and G.I. Tiwari, Evaluation of convective heat transfer coefficient in crop drying under open sun drying, *Energy Conversion and Management* 42, 627, 2001.
- [7] M.S. Sodha, N.K. Bansal, A. Kumar, P.K. Bansal and M.A.S. Malik, *Solar Crop Drying Vol.I*, CRC Press, USA, 1987.
- [8] M.S. Sodha, A. Dang, P.K. Bansal and S.B. Sharma, An analytical and experimental study of open sun drying and a cabinet type dryer, *Energy Conservation and Management* 25(3), 263-271, 1985.
- [9] C. Ratti and A.S. Mujumdar, Solar drying of foods: Modeling and numerical simulation, *Solar Energy* 60, 151-157, 1997.
- [10] B.K. Bala, M.R.A. Mondol, B.K. Biswas, B.L. Chowdury and S. Janjai, Solar drying of pineapple using solar tunnel dryer, *Renewable Energy* 28, 183-190, 2003.
- [11] P. Schimer, S. Janjai, A. Esper, R. Smitabhindu and W. Muhlbauer, Experimental investigation of the performance of the solar tunnel dryer for drying bananas, *Renewable Energy* 7, 119-129, 1996.

- [12] S.A. Lawrence, A. Pole and G.N. Tiwari, Performance of solar crop dryer under PNG climatic conditions, *Energy Conversion and Management* 30, 333-342, 1990.
- [13] C. Ratti and A.S. Mujumdar, Fixed-bed batch drying of shrinking particles with time varying drying air conditions, *Drying Technology* 11, 1311-1335, 1993.
- [14] A.S. Majumdar, Innovation and R&D needs in industrial drying technologies, In: *Asia Pacific Drying Conference*, Allied Publishers Pvt. Ltd, New Delhi, 2005.
- [15] L. Ait Mohamed, M. Kouhila, A. Jamali, S. Lahsasni, N. Kechaou and M. Mahrouz, Single layer solar drying behaviour of Citrus aurantium leaves under forced convection, *Energy Conversion and Management* 46, 1473-1483, 2005.
- [16] D. Jain and G.N Tiwari, Effect of greenhouse on crop drying under natural and forced convection I: evaluation of convective mass transfer coefficient, *Energy Conversion and Management* 45, 765–783, 2004.
- [17] G.N Tiwari, S. Kumar and O. Prakash, Evaluation of convective mass transfer coefficient during drying of jaggery, *Journal of Food Engineering* 63, 219–227, 2004.
- [18] T.I. Togrul and D. Pehlivan, Mathematical modelling of solar drying of apricot in thin layers, *J. Food Eng.* 55(3), 209–216, 2002.
- [19] D. Marinos-Kouris and Z.B. Maroulis, Transport properties in the drying of solids, In: A.S. Mujumdar (Ed.) *Handbook of Industrial Drying*, 2nd Edition, 113-159, Marcel Dekker, New York, 1995.
- [20] M.S. Sodha, Ram Chandra, Kamna Pathak, N.P. Singh and N.K. Bansal, Techno-economic analysis of typical dryers, *Energy Conversion and Management* 31, 503-513, 1991.

- [21] J.A. Duffie and W.A. Beckman, Solar engineering of thermal processes, Wiley, New York, 1991.
- [22] S.P. Sukhatme, Solar Energy – Principles of Thermal Collection and Storage, Tata McGraw-Hill Limited, New Delhi, 1998.
- [23] P.P. Singh, S. Singh and S.S. Dhaliwal, Multi-shelf domestic solar dryer, Energy Conversion and Management 47, 1799-1815, 2006.

PERFORMANCE OF AN INDIRECT SOLAR CABINET DRYER WITH THERMAL ENERGY STORAGE

5.1 Introduction

Some industries related to tea, textiles, ceramics, milk powder, edible starch, baking powder, food, sugar, paper, raisins, pharmaceuticals etc. consumes large quantity of energy for drying processes. Though mechanical dryers have been introduced, increasing oil prices along with high investment and operational costs restrict their use in industry. Solar drying has been considered as one of the most promising drying processes for the utilization of solar energy. A properly designed solar dryer can alleviate the drawbacks associated with open sun drying and upgrade quality of the dried product. This in turn causes high returns to the producers [1-5]. Low capital cost, production of hygienic and better quality products and zero or marginal running costs are also important parameters for the large-scale adoption of solar dryers. However, many of the solar dryers, presently available in the market, do not satisfy these criteria. Hence development of an efficient and low cost solar dryer has very much economic importance.

Solar drying systems are classified primarily according to their heating modes and the manner in which the solar heat is utilized. Broadly, they can be classified into two major groups, namely active solar energy drying systems (most of which are often termed hybrid or forced circulation solar dryers) and passive solar energy drying systems (conventionally termed natural circulation solar drying systems). A typical active solar dryer depends solely on solar energy as the heat source but employs motorized

fans and/or pumps for forced circulation of the hot air through the drying chamber.

Taylor et al. [6] designed a forced circulation cabinet solar timber dryer, in which the material absorbs solar radiation directly. Other active solar cabinet dryers reported in literature were a transparent roof solar bans [7] and some small scale forced convection dryers [8-10]. All these dryers, the product to be dried was directly exposed to solar radiation, and the product itself acts as an absorber. Temperature of the product rises, which helps to release the moisture. The fan provided in the system either pushes the air out or sucks air from the ambient to the drier. These dryers had the following drawbacks. The product cannot be made thicker because the solar radiation heats only the top thin layer. Further in some products, direct exposure to sunlight leads to discoloration and vitamin loss. Also, direct absorption of solar radiation by the product causes an unacceptable local temperature rise in the top thin layer of the product. An indirect type cabinet dryer with forced convection flow has been considered favorable since such a dryer is able to produce high quality product without discoloration with minimal drying duration. However, so far, indirect forced circulation solar cabinet dryers have not been reported in literature. The objective of the present work was to develop an efficient solar cabinet dryer, and to investigate its performance so as to optimize the design parameters. The feasibility of Phase Change Material (PCM) based latent heat thermal energy storage in solar drying was also brought under study.

5.2 Energy Storage

Solar energy is a time-dependent energy resource. Energy needs of different applications are also time dependent. But this is not coinciding with that of the solar energy supply. Consequently, the storage of energy in a solar process is necessary if solar energy is to meet substantial portions of

these energy needs. Energy storage is essential whenever the supply of consumption of energy varies independently with time. Hence, energy storage can reduce the time or mismatch between energy supply and energy demand, thereby playing a vital role in energy conservation [11].

The optimum capacity of an energy storage system depends on the expected time dependence of solar radiation availability, the nature of loads in the process, the degree of reliability needed for the process, the manner in which auxiliary energy is supplied, and an economic analysis that determines how much of the annual load should be carried by solar and how much by the auxiliary energy source. The size of storage is related to the 'energy density', or the amount of energy stored per unit mass (or per unit volume) of storage material. An important characteristic of the storage material is its 'volumetric energy capacity' or the amount of energy stored per unit volume. The energy density may be expressed in kJ/kg, MJ/kg or kWh/kg, while the volumetric energy capacity may be expressed per cubic meter as kJ/m³, MJ/m³, or kWh/m³. Denser materials have smaller volume, and correspondingly an advantage of larger energy capacity per unit volume.

Basically, there are three methods of storing thermal energy: sensible, latent, and thermochemical heat storage. They differ in the amount of heat that can be stored per unit weight or volume of storage medium, in the time-temperature history of the medium during heat storage and retrieval, and in the relative state of development of storage technology at the present time.

5.2.1 Sensible Heat Storage

In sensible heat storage, thermal energy is stored by changing the temperature of the storage medium. The amount of heat stored depends on the heat capacity of the medium, the temperature change, and the amount of storage material.

$$Q = \int_{T_1}^{T_2} m C_p dT \quad (5.1)$$

$$= m C_p (T_2 - T_1) \quad (5.2)$$

where m is the mass of heat storage medium (kg), C_p is the specific heat (J/kg°C), and T_1 and T_2 represent the lower and upper temperature levels (°C) between which the storage operates. The difference ($T_2 - T_1$) is referred to as the temperature swing. A wide variety of substances have been used as sensible heat materials. These include liquids like water, heat transfer oils and certain inorganic molten salts, and solids like rocks, pebbles and refractories. In the case of solids, the material is invariably in the porous form and heat is stored or extracted by the flow of a gas or a liquid through the pores or voids.

5.2.2 Latent Heat Storage

In latent heat storage, thermal energy is stored by means of a reversible change of state, or phase change, in the storage medium. Solid-liquid transformations are most commonly utilized, though solid-solid transitions have been investigated. Liquid-gas or solid-gas phase changes involve the most possible energy in latent storage methods. Storage of gas phase is difficult and bulky. Steam accumulators are one feasible example.

In practice, latent heat storage systems also make use of some sensible heat capacity in the system and so we must add this contribution also. The amount of energy stored in this case depends on the mass and the latent heat of fusion of the material. Thus,

$$Q = m \lambda \quad (5.3)$$

where λ is the latent heat of fusion (kJ/kg). In this case, the storage system operates isothermally at the melting point of the material. If isothermal operation at the phase change temperature is difficult, the system operates over a range of temperatures T_1 to T_2 which includes the melting point. Then

sensible heat contributions have to be considered and the amount of energy stored is given by

$$Q=m \left[\left\{ \int_{T_1}^{T_m} C_{ps} dT \right\} + \lambda + \left\{ \int_{T_m}^{T_2} C_{pl} dT \right\} \right] \quad (5.4)$$

where C_{ps} and C_{pl} represent the specific heats of the solid and liquid phases (J/kg°C) and T_m is the melting point (°C).

5.2.3 Thermochemical Heat Storage

In a thermo chemical storage system, the solar energy to be stored is used to produce a certain endothermic chemical reaction and the products of the reaction are stored. When the energy is to be released, the reverse exothermic reaction is made to take place. Both reactions take place at different temperatures, the forward reaction occurring at a higher temperature than the reverse reaction. Thermochemical storage systems are suitable for medium or high temperature applications only. In this case, the heat stored depends on the amount of storage material, the endothermic heat of reaction, and the extent of conversion.

$$Q = a_r m \Delta h_r \quad (5.5)$$

where a_r is fraction reacted and Δh_r is the heat of reaction per unit mass.

5.3 PCM in Solar Drying

Latent heat thermal energy storage in phase change materials (PCMs) is considered as a developing energy technology, and there has been increasing interest in using this essential technique for thermal applications such as drying, hot water, air conditioning and so on. This type of thermal energy storage offers the advantage of storing a large amount of energy in a small mass/volume. In a latent heat storage system, when a PCM is subjected to phase change process (melting or solidification) at an almost

constant temperature, it absorbs or releases a quantity of heat as much as latent heat [12-14].

Perishable crops like fruits, vegetables, etc. require continuous drying; otherwise the product may be vulnerable to insect attack. In order to prevent this some sort of auxiliary heating mechanisms should be incorporated with a solar dryer. Escalation of cost of fossil fuels prevent the large-scale adoption of fossil fuel or electrical based dryer among farmers of low or medium income. Hence it is essential to develop some mechanism that could be able to supply energy during cloudy and non-solar hours. Thus the intermittent, variable and unpredictable nature of solar energy make it necessary to incorporate a storage system with a solar dryer. Advantage of using storage system is that it stores excess energy and supplies when the collected amount is inadequate. Amongst the various heat storage techniques, latent heat storage is particularly attractive due to its ability to provide a high energy storage density and to store heat at a constant temperature corresponding to the phase transition temperature of the heat storage substance. Much work has been reported using Phase Change Material (PCM) for solar thermal applications, particularly for cooking [15-16]. Experimental and theoretical efforts have been made to incorporate PCMs into flat plate collectors for storing solar energy by Bansal and Buddhi [17]. Some other researchers [18-22] analyzed the material properties of different types of PCMs under various conditions and their applications in solar energy storage.

As stated earlier, study on incorporation of PCM storage with solar dryer is in its infancy and very few published works are there in the literature. Enibe [23] studied the performance of a natural circulation solar air heating system with phase change material energy storage for crop drying and egg incubation. In that study, PCM was prepared in modules with the modules equispaced across the absorber plate. No work has been performed

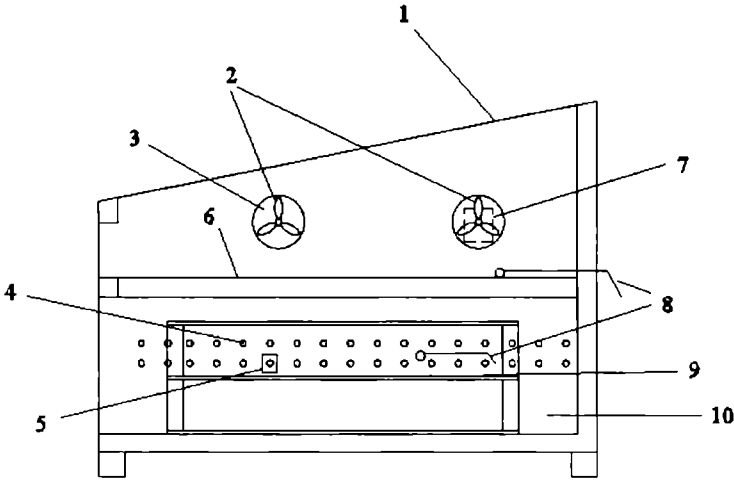
on forced circulation solar dryers with PCM thermal energy storage. In the present study, the feasibility of latent heat thermal energy storage in forced circulation solar dryer has been investigated. A PCM container was fabricated similar to a shell and tube heat exchanger. The fabricated container was placed in a solar cabinet dryer and studies were conducted with and without loading the product in the dryer. The charging and discharging of PCM has also been investigated.

5.4 Experimental Set-up

5.4.1 Description of the Solar Dryer

The experimental set up, shown in Fig. 5.1, consists of an indirect forced circulation solar drier provided with two axial fans and drying cabinet. The aperture area of the dryer was 1.27 m². This dryer consists of two parts: top collector and bottom drying chamber. The reason for the separate sections for energy collection and drying area was for avoiding the direct exposure of the product to sun and to retain the original colour of the dried product even after the complete drying. The top section of the solar dryer was the absorber area. The structural frame of the dryer was made up of (38.1 x 38.1 x 1.6 mm thick) aluminium square tube. The absorber plate used was 24 SWG aluminium sheet coated with selective black paint. All the sidewalls and bottom wall were packed with rock wool insulation. In between the inner and outer aluminium walls rock wool insulation was filled to suppress the heat losses. A double-layered door packed with rock wool insulation was provided in front of the dryer. A 4-mm thick clear glass was mounted on the top of the dryer in a slanting position, with an angle of 12^o, to transmit solar radiation. This angle was selected as the dryer was designed for Kochi (9^o57'N and 76^o16'E). Height of the front, back sections of the absorber region was 10.5 cm, 31 cm, respectively. Two axial fans (20W each) were provided in one side to admit fresh air. Flow rate of each fan was

95 m³/h. Positions of the fans were at a height of 4 cm from the absorber plate. An air duct of area 0.0896 m² was provided in the absorber to pass the hot air through the drying chamber. The location of the air duct was just opposite to the axial fan.



1-Glazing; 2-Fans; 3-Air inlet; 4-Exit of air; 5-Humidity probe; 6-Drier absorber plate; 7-Velocity probe; 8-Temperature sensors; 9-Perforated tray; 10-Drying cabinet

Fig. 5.1 Schematic representation of solar drier

The total volume of the drying chamber was 0.272 m³ and it was located underneath of the absorber plate. It consists of six perforated trays to load the material to be dried. The material used to make the tray was 22 SWG aluminium sheet. The size of the single tray was 0.333 m². All the trays were separated into two compartments each having 3 trays. The perforated trays were arranged at three different levels, one above the other. Aluminium 'L' angle was fitted all the corners of the tray to support it. Space between two consecutive trays was 10.2 cm. The diameter of the perforation was 6 mm and the distance between the holes was 70 mm. The surrounding wall of the drying chamber was also insulated with rock wool. A double-layered door filled with rockwool insulation was fitted in the

drying cabinet for loading and unloading the material. Photograph of the dryer is shown in Fig. 5.2

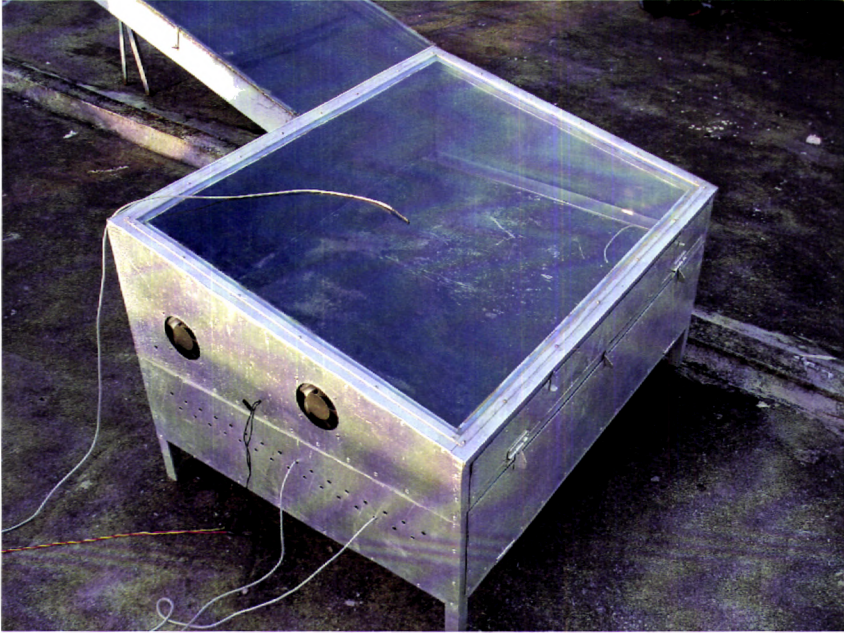


Fig. 5.2 solar cabinet dryer

Two rows of holes, having sixteen holes per row facilitated the exhaust of warm moist air from the dryer. Diameter of individual hole was 12 mm. Two consecutive rows were separated by a distance of 2.5 cm and distance between the holes was 4 cm. The total area of the exhaust was 0.362 m²

5.4.2 PCM Container

The prototype was moreover similar to that of a shell and tube heat exchanger. The whole body of the container was made up of 26 SWG stainless steel (SS) sheet and it was supported by SS square tubes in all the four sides. Ten number of aluminium tubes were inserted in the container

with its both ends kept open. The diameter of the tube was 8 mm and its volume was 25.12 cm^3 . The tubes were positioned equidistant from each other with a distance of 4 cm between the tubes. The total area of the PCM container was 0.25 m^2 with equal length and width of 0.50 m each. The total volume of the PCM container was 5250 cm^3 and the filling area was 5054 cm^3 . Tubes were positioned in centre of the container. Fig. 5.3 shows the schematic diagram of the PCM container. On the top surface of the tube a small pipe was fitted to fill the PCM into the container. Black selective coating was applied all over the container surface. Initial filling of PCM was done by melting it in a gas burner and then pouring it into the container. The PCM occupied entire volume inside the container surrounding the heat transfer tubes. PCM container was placed very close to the air duct area of the dryer and the heat exchanger pipe was parallel to the air inflow. Airflow passage in the PCM container is depicted in Fig. 5.4. A schematic diagram of the solar dryer integrated with PCM storage is given in Fig. 5.5

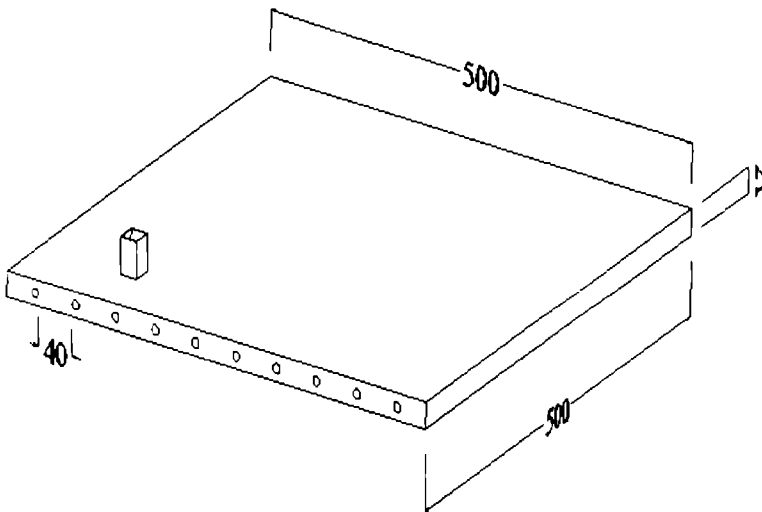


Fig. 5.3 Schematic diagram of the PCM container

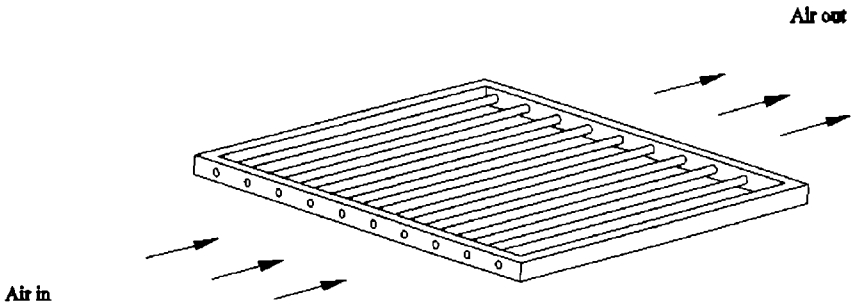


Fig. 5.4 Air flow passage in the PCM container

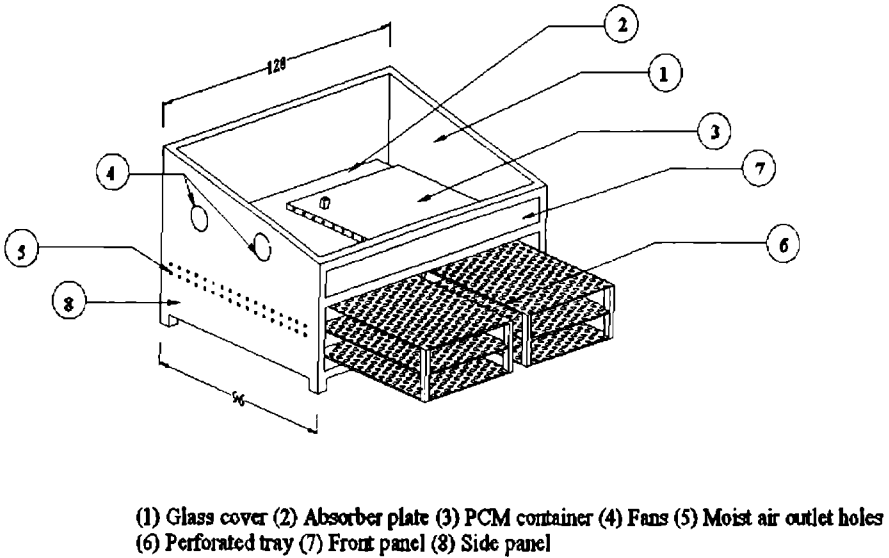


Fig. 5.5 Schematic diagram of the PCM integrated solar cabinet dryer

5.4.3 Phase Change Material (PCM) Investigated

Sharma et al. [16] reported that the PCM used for low temperature applications like water heating, baking and drying should have a melting / freezing cycle in the range of 45 – 90°C. Various materials suitable for energy storage in a temperature range of 50 – 100°C have been reported in

literature [18,24]. Commercial grade acetamide (CH_3CONH_2) was chosen as the PCM in the present work due to its low cost (Rs. 300/kg) and large-scale availability in the Indian market. The calculated melting temperature of acetamide was 76.56°C (reported 81°C in literature) and it favoured the application in drying since the recommended drying temperature required for most of the agricultural crops were around 60°C . Acetamide used in the present work was procured from Nice Chemicals Pvt. Ltd., India; its thermo-physical properties were measured using Differential Scanning Calorimeter (DSC) and is shown in Fig. 5.6. Another reason for the selection of acetamide is that its stability over large number of melting/freezing cycle.

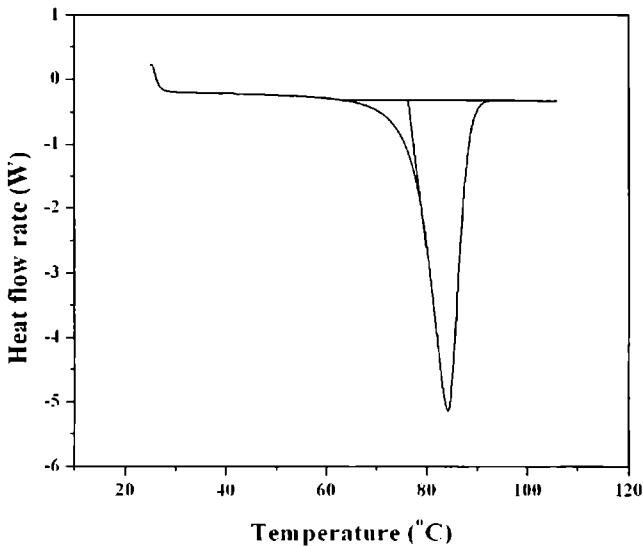


Fig. 5.6 DSC measurement of the latent heat of fusion and melting temperature of acetamide

Sharma et al. [19] conducted a detailed study on accelerated thermal cycle test of acetamide to investigate the changes in melting point, latent heat of fusion and the specific heat for 300 repeated melt/freeze cycles. The study revealed that the latent heat of fusion of acetamide has a variation of -1 to $+14\%$ from their zero cycle valued during 300 cycles. There were no

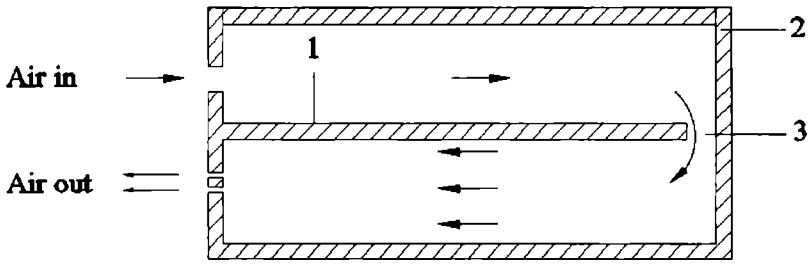
major changes in the melting point of the material. Melting point in the 0th, 100th, 200th, and 300th cycle were 82°C, 83°C, 82°C, and 82°C, respectively. Hence they concluded that acetamide show reasonably good stability throughout the cycling process and can be considered as a promising PCM.

5.5 Working

The solar radiation penetrates through the toughened glass of the drier and is absorbed by the selective coated aluminium sheet and thereby converted into thermal energy, i.e., long wave radiation. However, the long wave radiation is not allowed to escape through the glass.

The fan pushes ambient air through the absorber plate. The heat absorbed by the absorber plate is transferred convectively to the air passing over it. The hot air is allowed to pass through drying chamber along the duct provided in the absorber plate. Airflow passage in the solar dryer is depicted in Fig. 5.7. As hot air passes through the chamber, it draws moisture from the product loaded in the trays and warm moist air escapes out through the outlet holes.

The PCM with whole surface painted black was placed in good thermal contact with the absorber plate to ensure maximum conductive heat transfer. It was heated due to the direct absorption of solar radiation and the heat conducted from the absorber plate. As the temperature of the container increases, it transfers heat to the PCM, which is filled inside. PCM begins to melt at 76.56°C and the solid PCM will be converted to liquid. The process continues if the intensity of solar radiation is good and when the intensity decreases, the reverse phenomenon will start. The melted PCM will transfer heat through the heat transfer pipes and the container surface and it solidifies. As the air passes through the container, heat is transferred to the air and this hot air is used for drying during adverse weather conditions.



1-Absorber plate; 2-Insulation; 3-Air duct

Fig. 5.7 Airflow passage in the solar dryer

5.6 Attractive Design Features

As compared to other conventional solar dryers, the present solar dryer has got some special advantages. Most of the solar dryers commercially available are direct type. It may be of two types. In the first one, the product is loaded in perforated trays above the absorber plate. So part of the absorber region is used for spreading the product. It causes a reduction in efficiency because the products itself shades the absorber area even though it absorbs direct solar radiation. In another type, the above problem is mitigated by increasing the area of the solar dryer. i.e., by having separate sections for energy production and spreading area of the product. In this type, the efficiency of the process may increase, but it adds up the total material cost of the unit. The common disadvantage associated with both the types is the possibility of product discoloration.

In the present solar dryer, the product was loaded beneath the absorber area and absorber plate shaded the product from sunshine. Moreover, the entire area of the absorber plate was used for thermal energy production. It also protected the product from discoloration. The heated air was pushed by using two axial fans above the absorber plate and this hot air passed through the perforated trays, where the product to be dried was

loaded. The spacing between the individual trays was also more. This resulted in better heat transfer from the hot air to the product, due to large contact area, making the drying uniform. Two rows of hot air exhaust holes were provided to remove the warm moist air.

5.7 Investigation of the Performance of the System

The experiments were conducted on the terrace of Dept. of Physics, Cochin University of Science and Technology, Kochi (9°57'N and 76°16'E). All the experiments were conducted from 9.30 a.m to 4.30 p.m and continued till 7.00 p.m, when the drier was integrated with PCM storage. Basically three types of studies were done on the solar dryer: no load with axial fans switched off, no load with axial fans in operating condition and axial fans operated with load. Charging and discharging of PCM and its effect on solar drying was also carried out separately. Performance of the system was monitored for number of days. Details of the experiments, instruments, materials and methods for the performance evaluation are described below.

5.7.1 Instruments

During the study, various devices were used to measure the effects of environmental and operating parameters of the solar dryer cum thermal energy storage. The solar radiation intensity was measured by using a Solarimeter (Make – Central Electronics Limited). Digital thermo anemometer Mod. TA35 (Make-Airflow) was used for measuring air velocity in the dryer. Ambient temperature, along with the temperatures in the drying chamber, absorber plate, dryer outlet, PCM container, outlet of the heat exchanger pipe, cover glass, and inlet were monitored using LM 35 sensor. The sensor was connected to a computer using RS 232 interface through a 16-channel data logger. It recorded the temperature at the required points at every minute. Temperature of the PCM was recorded by using PT

100 sensors. A differential Scanning calorimeter (DSC) manufactured by Mettler Toledo – DSC 822e (Temperature range – 150°C to 700°C and temperature accuracy - $\pm 0.2^\circ\text{C}$) was used for measuring the latent heat of fusion and the melting temperature of the solid phase change material. Relative humidity of the ambient air and drying air were periodically monitored with a digital hygrometer. Samples of products in the dryer were weighed at 1 hour interval using an electronic digital weighing balance. At the end of the drying process, the moisture content of the sample was determined by drying the sample in hot air oven and kept the temperature at 108°C for 24 hours.

5.7.2 Materials

Acetamide was used as phase change material and it was filled in a container. The products used in the drying tests were bitter gourd and banana. Bitter gourd (*Momordica charantia*), is one of the most popular vegetables in Southeast Asia. It is a member of the cucurbit family along with cucumber, watermelon and muskmelon. Native of China or India, the fast-growing vine is grown throughout Asia and is becoming popular worldwide. These are abundantly available in Kerala State. It has also got medicinal importance. The oil-fried bitter gourd produced from dried bitter gourd is a valuable dish. For the drying tests 4 kg bitter gourd was loaded in the dryer. The fresh bitter gourd was cut into 5 mm slices before loading the dryer. The product was dried without doing any type of pretreatment.

Banana is an abundantly available fruit item in the Kerala state. Drying is essential for banana to prevent the wastage and preservation of it for long-term storage. The better quality-dried banana is also having very good market. Banana was peeled and sliced into pieces of 5 mm thick. For the drying tests 4 kg product was loaded in the dryer. The initial moisture content of the product was 78%. Dried banana make a delicious and

inexpensive snack. If dried properly, none of the nutrients is lost. Selling dried bananas as snacks is a good way to make money using a local food. Dried bananas can also be soaked and cooked, or added to dishes such as porridge before cooking. The banana was dried without using any type of pretreatment.

5.7.3 Methods

5.7.3.1 Design of PCM container

The quantity of PCM required for drying the product was calculated using the following relation

$$Q = mC_{ps} (T_m - T_i) + m\lambda + mC_{pl} (T_f - T_m) \quad (5.6)$$

where Q is the total heat stored in the PCM (kJ), T_i is the initial temperature of PCM ($^{\circ}\text{C}$), T_m is the melting temperature of PCM ($^{\circ}\text{C}$), T_f is the final temperature of PCM ($^{\circ}\text{C}$) C_{ps} is the average specific heat between T_i and T_m ($\text{J}/\text{kg}^{\circ}\text{C}$), C_{pl} is the average specific heat between T_m and T_f ($\text{J}/\text{kg}^{\circ}\text{C}$), and λ is the heat of fusion of PCM (kJ/kg)

The energy required to evaporate water from a product is calculated with the help of the following equation

$$Q = \frac{M_i (m_i - m_f)}{(100 - m_f)} \times L \quad (5.7)$$

Let the initial moisture content, m_i = 78 %

The final desired moisture content, m_f = 15 %

The quantity of the product to be dried, M_i = 4 kg

Latent heat of evaporation, L = 2800 kJ/kg

Therefore, Q = 8301 kJ

The total energy required for drying 4 kg banana from an initial moisture content of 78% to a final desired moisture content of 15% was estimated as 8.3 MJ. It was also assumed for calculation that 80% (6.64 MJ)

of the energy requirement should be met from solar energy and the remaining 20% (1.66 MJ) from storage medium. The quantity of PCM required to meet this energy supply was calculated from Eq. (5.6) as follows. The excess volume during the phase change was also taken into account in the calculation. Time required for drying the given quantity of the product for the applied mass flow rate is assumed to be 10 hours. Total time requirement is distributed to solar and PCM drying. Then 8 hours (9.00 a.m to 5.00 pm) of the total time duration met by solar energy and the remaining 2 hours by PCM storage during off sunshine/night time.

The storage capacity of the Latent Heat Storage (LHS) with a PCM medium is given by

$$Q = mC_{ps} (T_m - T_i) + m \lambda + mC_{pl} (T_f - T_m)$$

The quantity of energy required to dry the product	=	8301 kJ
The quantity of energy required for drying per hour	=	830 kJ/h
The energy to be delivered by the PCM storage	=	830 x 2
	=	1660 kJ

Acetamide (CH_3CONH_2) was used as PCM for the calculation, its properties in the solid and liquid state are given below.

Density of acetamide in the solid state	=	1159 kg/m ³
Density of acetamide in the liquid state	=	998 kg/m ³
Fusion temperature of acetamide, t_f	=	81°C
Initial temperature of PCM, t_o	=	30°C
End temperature of PCM, t_f	=	105°C
Latent heat of fusion of acetamide, λ	=	241 kJ/kg
Specific heat of acetamide, C_p	=	1.9 kJ/kg °K

Initial and end temperature of PCM are assumed value.

$$\begin{aligned}
 Q &= D \times V \times C_{ps} (T_m - T_i) + D \times V \times \lambda + D \times V \times C_{pl} (T_f - T_m) \text{ kJ} \\
 &= V [1.23 \times 10^5 + 2.4 \times 10^5 + 0.73 \times 10^5] \\
 1660 &= V \times 3.975 \times 10^5
 \end{aligned}$$

$$\begin{aligned}
 \text{Volume of the PCM, } V &= 1660/3.975 \times 10^5 \\
 &= 4.176 \times 10^{-3} \text{ m}^3
 \end{aligned}$$

This is the actual volume of the PCM. But there would be a change in volume in the conversion of the PCM from the solid phase to liquid phase. This change in volume is also to be taken into account while designing the container.

Mass of the PCM required to store 1660 kJ energy

$$\begin{aligned}
 &= \text{volume} \times \text{density} \\
 &= 4.50 \text{ kg}
 \end{aligned}$$

For 1kg mass of PCM,

$$\begin{aligned}
 V_1 &= m/\rho_{\text{solid}} \\
 &= 1/1159 = 8.628 \times 10^{-4} \text{ m}^3 \\
 V_2 &= m/\rho_{\text{liquid}} \\
 &= 1/998 = 1.002 \times 10^{-3} \text{ m}^3
 \end{aligned}$$

$$\begin{aligned}
 \text{Volume expansion of PCM during phase change} &= (V_2 - V_1)/V_1 \\
 &= 16.13\%
 \end{aligned}$$

$$\begin{aligned}
 \text{The excess volume to be considered} &= V_1 + 0.16 V_1 \\
 &= 8.628 \times 10^{-4} + 0.16 \times 1.002 \times 10^{-3} \\
 &= 8.78 \times 10^{-4}
 \end{aligned}$$

$$\begin{aligned}
 \text{Total volume} &= \text{Actual volume} + \text{Excess volume} \\
 &= 4.176 \times 10^{-3} + 8.78 \times 10^{-4} \\
 &= 5.054 \times 10^{-3} \text{ m}^3
 \end{aligned}$$

$$\begin{aligned}
 \text{Total volume of the container} &= 5054 \text{ cm}^3 \\
 \text{for the storage of 4.5 kg PCM}
 \end{aligned}$$

Hence, it was calculated that the volume requirement of the PCM container to release 1660 kJ of thermal energy is 5054 cm³ and it had the capacity to hold 4.5 kg PCM.

5.8 Experimental Procedure

The analysis was done on the drier with and without PCM storage. A brief description of the study is as follows:

5.8.1 Test without PCM

This study was done without integrating PCM in the solar drier. Various investigation carried out are described as follows. An economic analysis was also done without consideration of PCM unit.

5.8.1.1 Test of the dryer without load and axial fans switched off (Condition -1)

The experiment at no load was conducted for 5 days to measure the maximum temperature achieved by the absorber plate of the dryer and the drying cabinet. During the study, the outlet holes were kept open and both the axial fans did not operate throughout the day. Intensity of solar radiation on the aperture of the dryer, temperatures of ambient, absorber plate and cover glass were recorded at every 5 minutes during the study period.

5.8.1.2 Test without load and axial fans in operating condition (Condition -2)

All parameters were monitored as described above except that both the fans operated throughout the day.

5.8.1.3 Test with product loaded in the dryer (Condition -3)

In this test, the dryer was loaded with fresh bitter gourd having initial moisture content of 95%. The total quantity loaded was 4 kg. The product was equally loaded in all the six trays uniformly. The axial fans were in running throughout the experimental period. The temperature of the absorber plate, ambient and drying chamber temperature were monitored at

every 5 minutes along with solar radiation. The weight of the product being dried was recorded every 1 hr interval.

5.8.1.4 Economic analysis

The profit from solar dried products is certainly higher than open sun dried products. Hence, the solar dried product can be sold as branded items and its financial attractiveness is superior to that of products dried in the open sun, which sell as unbranded items. Traditional sun drying is commonly used for the production of unbranded product. Such product has poor quality and low shelf life, sometimes even unable to consume. People are prepared to buy the branded product, which is usually processed in hygienic condition, even if the price is a bit more. The economic analysis done here by assuming the cost of solar dried product is comparable to that of branded items available in the market.

5.8.2 Test with PCM

Here, the performance of the dryer was evaluated after placing PCM container in the dryer.

5.8.2.1 Test on dryer with PCM (Condition-4)

This study was aimed at analyzing charging / discharging behaviour of PCM. Heat retention inside the dryer was studied when the axial fans in idle condition. Temperatures of the PCM, its container and outlet of the heat exchanger pipe were monitored along with other parameters described above. The experimental time period was from 9.30 a.m to 7.00 p.m.

5.8.2.2 Test on dryer with PCM, product loaded and axial fans in running condition (Condition-5)

In this test the dryer was loaded with 4 kg banana having initial moisture content of 78%. Banana was cut into 5 mm thick slices before loading in the dryer. The product was equally loaded in all the six trays uniformly. The experiment was conducted from 9.30 a.m to 7.00 p.m when

the dryer was integrated with PCM storage. The experimental period was from 9.30 a.m to 4.30 p.m when it was done without PCM storage.

Three methods were adopted here for the economic analysis as discussed in chapter 4. The methods used for the analysis were 'annualized cost method' [25], 'life cycle analysis' [26] and 'Payback Period' [27]

5.9 Results and Discussion

5.9.1 Condition -1

The parameters monitored [such as ambient temperature, temperature in the solar dryer and solar radiation intensity] are shown in Fig. 5.8. In this study, both the axial fans did not operate throughout the experimental period and it was conducted without loading the product. Fig. 5.9 shows the variation of temperatures of absorber plate and top glass cover of the dryer with solar radiation. The maximum temperature monitored in the absorber plate was 97.2°C, which was at 12.40 p.m. The intensity of solar radiation was 870 W/m² at that time. The high temperature of the absorber plate was due to the coating of selective paint, which has an absorptivity of ~ 0.93. The maximum temperature of air in the dryer was monitored as 78.1°C at 2.00 p.m. The maximum temperature of top glass cover was 56°C at the same time when the absorber plate achieved its maximum temperature. The solar radiation reached its high value (910 W/m²) during the study period at 11:50 a.m. The small difference in incident radiation resulted in a slight difference of air temperature in the drier. Ambient temperature varied from 31.1°C to 33.7°C. It was observed that the temperature rise above that of the ambient was in the range of 12.3°C to 45°C during the study period.

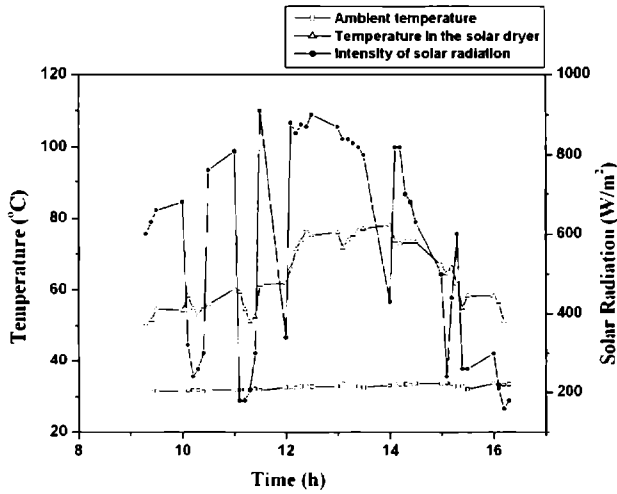


Fig. 5.8 Variation of temperature in the solar dryer and ambient temperature with solar radiation under no load and axial fans switched off condition

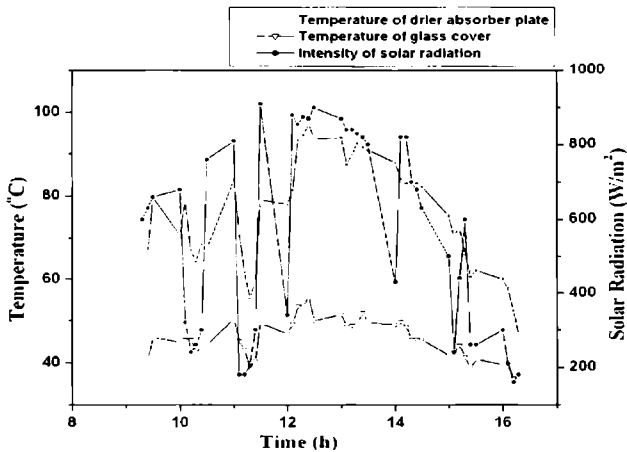


Fig.5.9 Variation of absorber plate temperature and glass cover temperature with solar radiation under no load and axial fans switched off condition

5.9.2 Condition -2

In contrast to the earlier study, in this case, both the fans operated all over the day. All the parameters monitored in the earlier study were

measured here also. Fig. 5.10 & Fig. 5.11 show the performance of the dryer. The maximum temperature attained by the absorber plate and the temperature of air flowing over the absorber plate were, 80.5°C and 56.6°C, respectively. The reduction in both the temperature compared to the earlier study was due to the operation of fans. As fans pushed air through the absorber plate, convective heat transfer took place between absorber plate and flowing air. However, it was observed that the temperature rose above the ambient air in the range of 2.7 – 23.7°C during 9.30 a.m to 4.30 p.m. The maximum temperature recorded in the top glass cover was 44.6°C while the corresponding value, when the fans in idle condition was 56°C. i.e., heat loss through the glass cover was minimum when the fans were in running condition. The air flowing over the absorber plate took away maximum heat from the absorber plate and it was used for drying purpose.

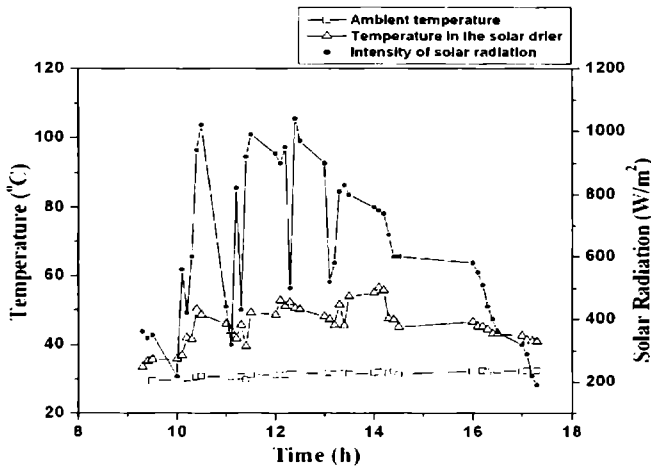


Fig. 5.10 Variation of temperature in the solar dryer and ambient temperature with solar radiation under no load and the axial fans in operating condition

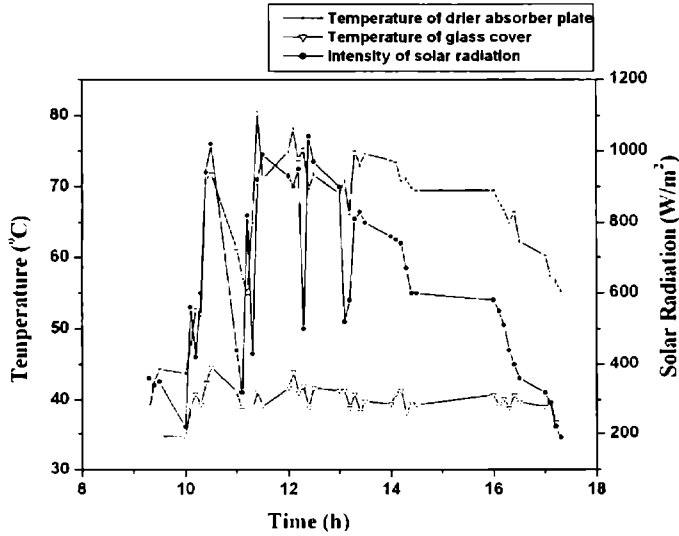


Fig. 5.11 Variation of absorber plate temperature and glass cover temperature with solar radiation under no load and the axial fans in operating condition

5.9.3 Condition -3

In this experiment, the dryer was loaded with 4 kg fresh bitter gourd to study the drying behaviour. The solar radiation incident on the aperture of the dryer, ambient temperature and rise in air temperature inside the dryer above the ambient temperature are shown in Fig. 5.12. The loading of the product did not cause any drop in absorber plate temperature of the dryer, since it was spread beneath the absorber plate. Rise in air temperature varied from 10.8°C to 39.8°C during 9.30 a.m to 4.30 p.m. Relative humidity of the air flowing into the dryer varied in the range of 51% to 72% during the study period. The average velocity of air inside the dryer was 1.2 m/s and it was monitored in the air duct and suction point of the fans.

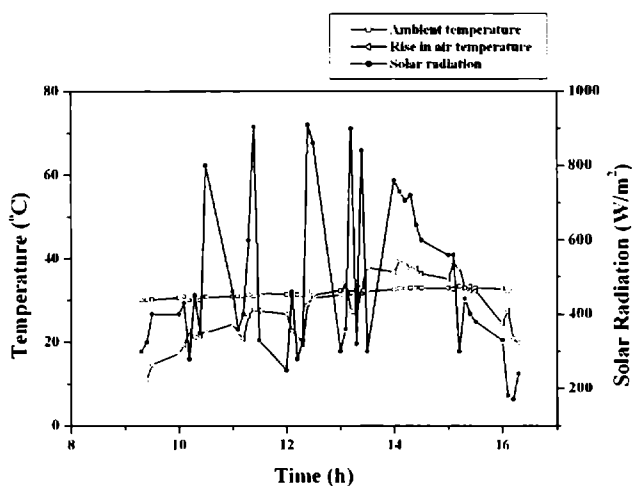


Fig. 5.12 Rise in temperature of the solar dryer above ambient temperature (dT), ambient air temperature and solar radiation during a drying day when the dryer was loaded with 4 kg bitter gourd

For a fluctuating radiation intensity level, the moisture content of the bitter gourd reduced from an initial moisture content of 95% (w.b) to the final value of 5% (w.b) within one day with an effective drying time of 6 hours as shown in Fig. 5.13. The solar energy required for the removal of the moisture from 4 kg product was calculated as 10.6 MJ/batch. The samples were collected from different trays to analyze the uniformity of drying and it was found that the reduction in moisture in all the trays were almost same with negligible variations. Drying was very fast in the initial hours of operation and then it gradually decreased. This was because of the evaporation of surface moisture at the beginning of the process. It was known that as the moisture content of the product reduced, more energy was required to evaporate the same amount of moisture from the product. The result obtained was compared with the bitter gourd dried in the open sun. The drying duration in the case of open sun drying was 2 days with an effective drying time of 11 hours. The moisture content at the end of the

experiment in the first day was 9.7% for open sun drying, but the entire moisture was removed from the product loaded in the solar dryer in the first day itself. The drying continued in the next day with the open dried sample and the moisture evaporation was in a very slow rate. The final desired moisture of 5% was attained after 5 hours of drying the sample in the next day. The colour of the dried product is an important parameter to determine the quality of the product. The product could retain its original green colour in the solar dryer, even after it was completely dried. But the colour completely lost under open sun and turned to be a brownish appearance. This corresponds to a high-quality dried bitter gourd in the solar dryer.

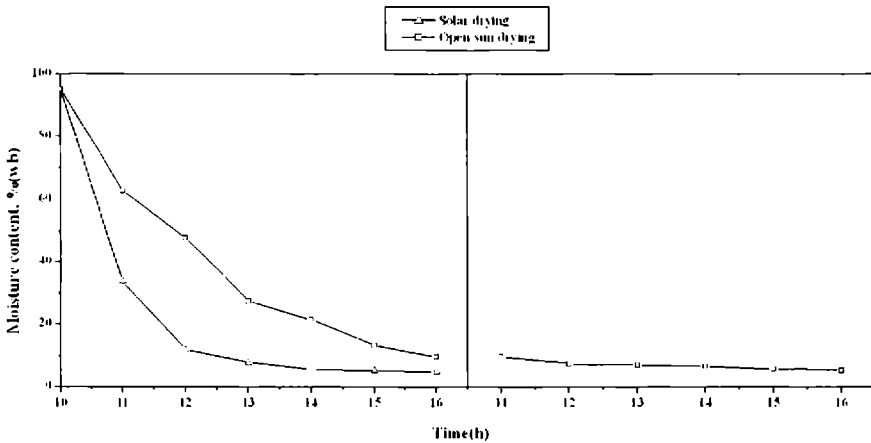


Fig. 5.13 Reduction of moisture content of bitter gourd with time of the drying test under solar drying and open sun drying

5.9.4 Economic Analysis

The economic parameters are based on the economic situation in India as shown in Table 5.1. The economic analysis done by three methods such as annualized cost method, life cycle savings and payback period are summarized below.

Table 5.1 Cost and economic parameters

1. Material and labour cost for the construction of the dryer	Rs. 6500
2. Interest rate	8%
3. Rate of inflation	5%
4. Real interest rate	3%
5. Life span of the dryer	20 years
6. Electricity cost	Rs 4/kWh
7. Cost of fresh bitter gourd	Rs 10/kg
8. Selling price of dried bitter gourd	Rs 250/kg

5.9.4.1 Annualized cost method

The annual maintenance cost of the solar dryer is low, and it was taken as 3% of annual capital cost. The salvage value was assumed as 10% of the annual capital cost. The annual capital cost of the solar dryer was calculated to be Rs. 661.70. The number of solar drying days was taken here as 250 days for calculation. The dryer was provided with two axial fans and the running cost of the fan was also taken into account for economic analysis. The quantity of dried product processed in this solar dryer per year was 52.5 kg and the cost of drying 1 kg bitter gourd turned out to be Rs. 17.52. The corresponding cost of drying in electric dryer was calculated as Rs. 41.35 per kg of dried product. The capital cost of electric dryer, electricity cost for unit charge and the efficiency of the electric dryer were assumed as, Rs. 3500, Rs. 4 /kWh and 80%, respectively.

5.9.4.2 Life cycle savings

The saving due to drying the bitter gourd in the solar drier vis-à-vis commercially dried branded product was calculated. The current saving per day turned out to be Rs. 23.8. Table 5.2 shows the calculated value of annual

saving, present worth of annual saving, and cumulative present worth of annual saving for each year of life of the solar dryer in the case of bitter gourd drying. The cumulative present worth of annual savings for drying bitter gourd over the life of the solar dryer turned out to be Rs. 31660. The investment for solar dryer is Rs. 6500. It means that by investing Rs. 6500 to procure a solar dryer today, we are saving Rs. 31,660 today, although the savings are spread over the life of the system.

5.9.4.3 Payback period

As per the definition, the payback period is the time needed for the cumulative fuel savings to become equal to the total initial investment. It is clear from the Table 5.2 that the total investment i.e., Rs. 6500 lies in between 3rd and 4th year. To get the exact value, the following equation was used to calculate the payback period, n_p

$$n_p = \frac{\ln \left[1 - \frac{C}{S_1} (d - i) \right]}{\ln \left(\frac{1 + i}{1 + d} \right)}$$

Where 'C' is the capital cost in Rupees, 'S₁' is the savings during first year for solar dryer in Rupees, 'd' is the rate of interest on long term investment and 'i' is the rate of inflation.

The payback period was calculated to be 3.26 years (equivalent to 815 drying days), which is small compared to the life of the dryer (20 years). Hence the dryer will dry product free of cost for almost its entire life period.

Table 5.2 Economics of the solar dryer – Annual saving, present worth of annual saving and present worth of cumulative annual saving for each year during the life of the solar dryer for drying bitter gourd and 250 days of use of solar dryer

Year	Annualized cost of dryer (Rs.)	Annual savings (Rs.)	Present worth of annual saving (Rs.)	Present worth of cumulative saving (Rs.)
1	920.11	2205	2041.66	2041.66
2	920.11	2315.25	1984.95	4026.61
3	920.11	2431.01	1929.81	5956.42
4	920.11	2552.56	1876.20	7832.62
5	920.11	2680.19	1824.09	9656.71
6	920.11	2814.20	1773.42	11430.13
7	920.11	2954.91	1724.16	13154.29
8	920.11	3102.65	1676.26	14830.55
9	920.11	3257.78	1629.70	16460.25
10	920.11	3420.67	1584.43	18044.68
11	920.11	3591.71	1540.42	19585.10
12	920.11	3771.29	1497.63	21082.73
13	920.11	3959.86	1456.03	22538.76
14	920.11	4157.85	1415.58	23954.34
15	920.11	4365.74	1376.26	25330.60
16	920.11	4584.03	1338.03	26668.63
17	920.11	4813.23	1300.86	27969.49
18	920.11	5053.90	1264.73	29234.22
19	920.11	5306.59	1229.60	30463.82
20	920.11	5571.92	1195.44	31659.26

5.9.5 Condition -4

The PCM container was placed in good thermal contact with the absorber plate of the solar dryer. In addition to the parameters monitored above, temperatures of PCM container plate, heat exchanger pipe and PCM temperature at different locations in the container were monitored. There was not any appreciable difference in temperature values at different points of PCM inside the container. This was due to the reason that the thickness of the PCM container was minimum to ensure uniform melting of the material filled in the container. If the container is not thin enough, during heat extraction process, the storage material first solidifies the container surface. As a result the thermal resistance to the flow of heat increases during the heat extraction process. A trial run was conducted on 9 May 2006 to study the performance of the system. Fig. 5.14 shows the temperature profile on the day. The experiment was performed to determine the maximum temperature of PCM when it was filled in a black selective coated container and placed in the absorber plate of the dryer. The PCM container was also exposed to solar radiation and there was no forced movement of air over the PCM container. The maximum temperature of PCM recorded in the set up was 91.8°C, which was 15.2°C higher than melting point. The maximum temperatures of the PCM container and outlet of the heat exchanger pipe were, 103.7°C and 95.1°C, respectively. But the absorber plate temperature was 61.2°C, which was very less compared to the earlier study. The appreciable reduction in the absorber plate temperature was due to the high heat transfer from the plate to the PCM through the container. The recorded maximum temperature of the PCM was an indication of the occurring of phase change, as the measured melting point of acetamide is 76.6°C. The experiment was continued till 7.00 p.m in the night and the temperatures of PCM, container and heat exchanger pipe were, 58.6°C, 55.8°C, and 59.4°C, respectively. The reduction of temperatures was in a very slow mode. While

the absorber plate temperature reduced to 39.2°C. Ambient temperature varied from 30.3°C to 33.9°C during 9.30 a.m to 7.00 p.m.

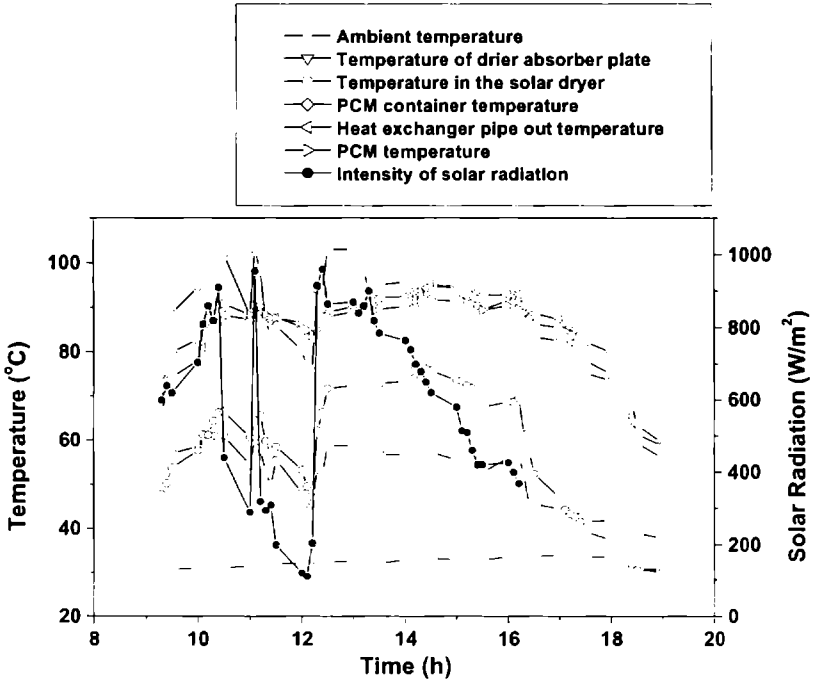


Fig. 5.14 Temperature profile of the PCM integrated solar dryer without forced circulation of air

5.9.6 Condition -5

The experiment was conducted on two consecutive days from 14 May 2006 with 4 kg ripe banana loaded in the dryer. The PCM container was placed on the absorber near the air duct. Variations of temperatures of the PCM and dryer on the first day of operation are shown in Fig. 5.15. The maximum temperature attained by the PCM was 88.8°C while it was 91.8°C when the fan was in idle condition. It was observed that the difference in maximum temperature of PCM was comparable under natural and forced convection. It was due to the low airflow rate of the fan; in this condition, the conductive heat transfer from plate to PCM container was predominant

than the convective heat transfer from plate to flowing air. The airflow rate was maintained at 0.11kg/s. Relative humidity of air flowing into the dryer varied in the range of 45% to 73% during the study period. The experiment was continued from 9.30 a.m. to 7.00 p.m. The temperature of hot air at outlet, recorded just before entering the drying chamber reached its maximum value of 72.5°C at 2.10 p.m, which was above 39.8°C than corresponding ambient temperature.

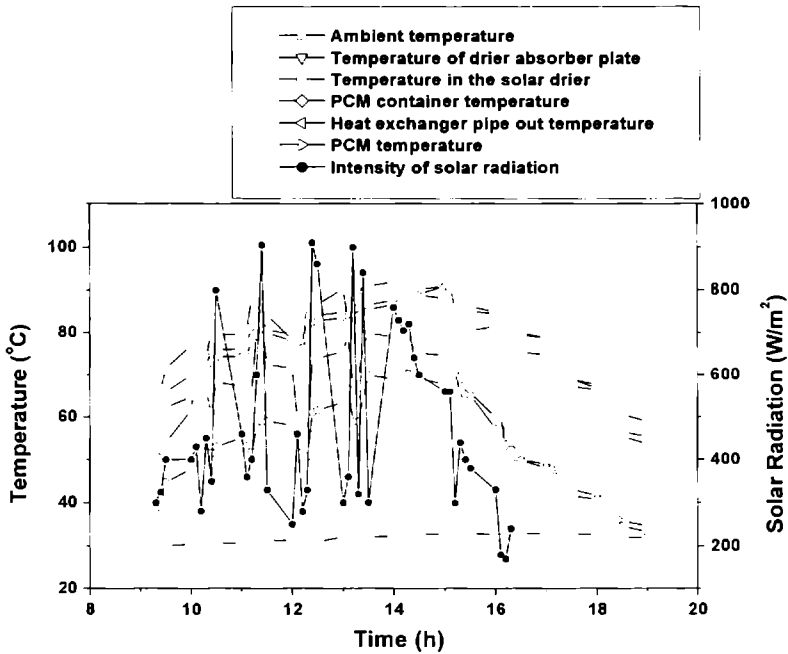


Fig. 5.15 Variation of dryer and PCM temperatures with product loaded in the dryer

The product was equally distributed in all the six trays to ensure uniform drying. The initial moisture content of banana was 78% and reached the desired value of 15% in 12.5 hours as shown in Fig. 5.16. The samples were collected from different trays to analyze the uniformity of drying and it was found that the reduction in moisture content in all the trays were almost same with negligible variations. The drying was very fast during the initial

hours of operation and then gradually decreased. This was because of the evaporation of surface moisture at the beginning of the drying process and as the moisture content reduced, more energy was required to evaporate the same amount of moisture from the product. Drying was continued till 7.00 p.m on the first day of study. The percentage reduction of moisture content between 5.30 p.m and 7.00 p.m was 3.21%. The reduction in moisture content during the evening hours was only due to the provision of thermal energy storage, even if the intensity of solar radiation was meager or zero. After 7.00 p.m the product were kept in the dryer without operating the fans throughout the night hours. The weight of the sample was taken on the next day morning and it was found that there was a reduction of moisture content of 2.41%. Thus the total reduction of moisture content during the non-solar hours was 5.62%. Apart from the small reduction of moisture content during the night hours, the provision of PCM produced a warm environment in the solar dryer. It helps for not only reducing the moisture content but also prevent deterioration of the product even though the solar radiation intensity is abysmal.

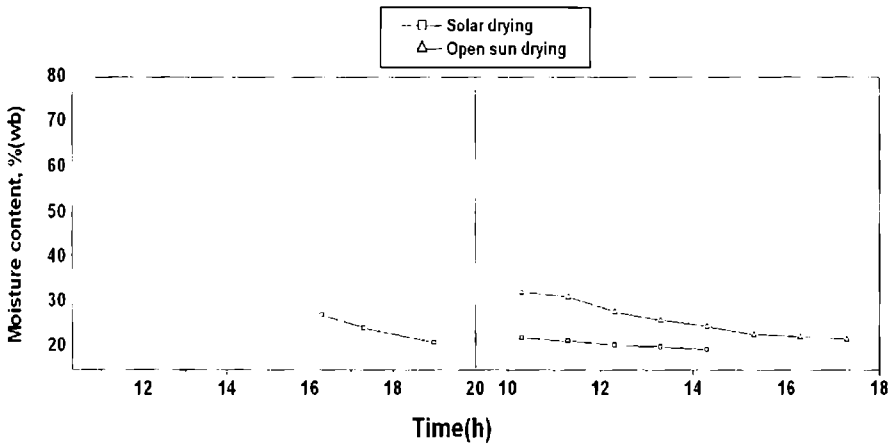


Fig. 5.16 Reduction of moisture content of banana with time of the drying test in the solar dryer with PCM

A study was also performed by keeping the sample in the open sun to compare the drying performance with solar dryer. The moisture content measured at the end of first day of operation, with an effective drying duration of 7 hours, was 30.87%, while that of the sample loaded in the solar dryer was 24.18%. The experiment was continued on the next day with the open dried sample and the value of moisture content after 14 hours of operation was 18.23%. This showed that the final desired moisture content could not be achieved even after 2 days of operation [with an effective drying duration of 14 hours] as the sample was dried in open sun.

5.10 Conclusion

An efficient solar cabinet dryer was designed, fabricated and its performance was analyzed. The product was loaded beneath the absorber plate and not exposed to direct sunshine. This retained original colour of the product. Since the drying took place in a closed chamber, the product was protected from insects and dust. Hence it is possible to get good quality product from the dryer. The axial fans provided in the dryer accelerated the drying process. Economic analysis was also performed in the dryer and it was found that the cumulative present worth of annual savings for drying bitter gourd over the life of the solar dryer turned out to be Rs. 31,660. The capital investment of the dryer was Rs. 6500 and the payback period of the dryer was found to be 3.26 years, which was very less considering the life of the system. The cost of drying bitter gourd in the solar dryer was 42% less than that of an electric dryer. The life of the system was expected to be 20 years, because it had no corrosive material. The designed dryer was integrated with a Phase Change Material to extend the use of dryer in the evening/night hours. The study revealed that there was a 5.62% reduction of moisture due to the incorporation of storage material during evening/night. The drying experiment conducted with banana and it was found that the

complete drying process could be attained with 12.5 hours, which was much less than that of open sun drying. It was also established that acetamide is a promising PCM in solar drying applications. The system can be adopted by medium and low income farmers and the present set up will reduce the use of conventional energy sources upto a very large extent. The developed system is well adaptable to perishable crops and some sensitive products, which require continuous drying. Otherwise these are susceptible to the attack of insects and microorganisms. The study conducted in the open sun drying revealed that the drying time was much larger than that of solar drying. Hence the arrangement would help to reduce the usage of other conventional energy sources/back up used to meet energy requirement during non-sunshine hours to some extent.

References

- [1] M.S. Sodha, N.K. Bansal, A. Kumar, P.K. Bansal and M.A.S. Malik, Solar crop drying, Vol.1, Boca Raton, Florida, CRC Press, USA, 1987.
- [2] H.P. Garg and A. Krishnan, Solar drying of agricultural products, *Annals of arid zone* 13, 285 – 292, 1974.
- [3] T.A. Lawand, A solar cabinet dryer, *Solar Energy* 10, 158-164, 1966.
- [4] B.K. Bala, M.R.A. Mondol, B.K. Biswas, B.L. Chowdury and S. Janjai, Solar drying of pineapple using solar tunnel dryer, *Renewable Energy* 28, 183-190, 2003.
- [5] P. Schimer, S. Janjai, A. Esper, R. Smitabhindu and W. Muhlbauer, Experimental investigation of the performance of the solar tunnel dryer for drying bananas, *Renewable Energy* 7, 119-129, 1996.
- [6] U.J. Taylor and A.D. Weir, Simulation of a solar timber dryer, *Solar Energy* 34(3), 249-255, 1985.
- [7] G.C. Shove, G.W. Barton, M.D. Hall and W.H. Peterson, Field studies of solar grain drying, ASAE paper, 81-4037, 1981.
- [8] P.H. Bailey and W.F. Williamson, Some experiments on drying grain by solar radiation, *J. Agric Engng Res* 10. 191-196, 1965.
- [9] G.G. Umarov and A.I. Ikramov, Features of the drying of fruit and grapes in solar radiation drying apparatus, *Applied Solar Energy* 14(6), 55-57, 1978.
- [10] M.W. Basseyy, Design and performance of hybrid crop dryer using solar energy and sawdust, In: Proc. ISES Cong INTERSOL 85, Montreal, Canada, Pergamon Press, Oxford, pp. 1039-42, 1985.
- [11] R.C. Schubert and L.D. Ryan, *Fundamentals of Solar Heating*, Prentice-Hall, Inc., Englewood Cliffs, New Jersey, 1981.
- [12] H.P. Garg, S.C. Mullick and A.K. Bhargava, *Solar Thermal Energy Storage*, D. Reidel Publishing Company, Dordrecht, Holland, 1985.

- [13] K. Kaygusuz, The viability of thermal energy storage, *Energy Sources* 21, 745-756, 1999.
- [14] A. Sari and K. Kaygusuz, Thermal performance of palmitic acid as a phase change energy storage material, *Energy Conversion and Management* 43, 863-876, 2002.
- [15] D. Buddhi, S.D. Sharma and A. Sharma, Thermal performance evaluation of a latent heat storage unit for late evening cooking in a solar cooker having three reflectors. *Energy Conversion and Management* 44, 809-817, 2003.
- [16] S.D. Sharma, T. Iwata, H. Kitano and K. Sagara, Thermal Performance of solar cooker based on an evacuated tube solar collector with a PCM storage unit, *Solar Energy* 78, 416-426, 2005.
- [17] N.K. Bansal and D. Buddhi, Performance equation of a collector cum storage system using phase change materials, *Solar Energy* 48, 185-194, 1992b.
- [18] A. Abhat, Low temperature latent heat thermal energy storage: Heat storage materials, *Solar Energy* 30(4), 313-332, 1983.
- [19] S.D. Sharma, D. Buddhi and R.L. Sawhney, Accelerated thermal cycle test of latent heat storage materials, *Solar Energy* 66(6), 483-490, 1999.
- [20] C. Tuncbilek, A. Sari, A. Tarhan, G. Ergunes and K. Kaygusuz, Lauric and palmitic acids eutectic mixture as latent heat storage material for low temperature heating applications, *Energy* 30, 677-692, 2005.
- [21] R. Nikolic, New materials for solar thermal storage-solid/liquid transitions in fatty acid esters, *Solar Energy Materials and Solar Cells* 79, 285-292, 2003.
- [22] Z. Liu, Z. Wang and Chongfang Ma, An experimental study on heat transfer characteristics of heat pipe heat exchanger with latent heat

- storage, Part I: Charging only and discharging only modes, *Energy Conversion and Management* 47, 944-966, 2006.
- [23] S.O. Enibe, Performance of a natural circulation solar air heating system with phase change material energy storage, *Renewable Energy* 7(1), 69-86, 2002.
- [24] Ahmet Sari, Thermal reliability test of some fatty acids as PCMs used for solar thermal latent heat storage applications, *Energy Conversion and Management* 44, 2277-2287, 2003.
- [25] M.S. Sodha, R. Chandra, K. Pathak, N.P. Singh and N.K. Bansal, Techno-economic analysis of typical dryers, *Energy Conversion and Management* 31, 503-513, 1991.
- [26] J.A. Duffie and W.A. Beckman, *Solar Engineering of Thermal Processes*, John Wiley and Sons, Newyork, 1980.
- [27] S.P. Sukhatme, *Solar energy: Fundamentals of thermal collection and storage*, Tata McGraw-Hill Publishing Company Limited, New Delhi, 1998.

DESIGN AND DEVELOPMENT OF A SOLAR GREENHOUSE FOR INDUSTRIAL DRYING

6.1 Introduction

Solar energy, which is abundant, clean and safe, is an attractive option for drying applications. Drying is a complex process involving heat and mass transfer between the drying material surface/within the material and its surrounding medium. It can be conducted and/or enhanced with the help of a renewable energy source such as solar energy. Greenhouse easily transmits short wave radiation, which means that it exhibits little interference to incoming solar energy, but it has very poor transmittance for long wave radiation. Once the sun's energy passed through the transparent windows and has been absorbed by the material loaded inside, the heat will not be reradiated. Glass/polythene sheet therefore, acts as a heat trap, a phenomenon that has been recognized for the construction of greenhouses.

In solar greenhouse, not only the light which is maintained at a desired level but also the heat is to be stored for use at night and for cloudy days and therefore, it differs from the ordinary glass house. The solar energy is collected and stored in a variety of ways and therefore, solar greenhouses differ in their designs. Moreover, the solar collection and storage system depends on many factors like climate, greenhouse size, orientation, and economics. Further, design differences arise due to whether the energy collection, storage and distribution are based on passive or active systems. The greenhouses where thermal energy is stored directly in heavy brick walls or rock walls and/or water pools or water containers exposed to solar radiation and is distributed inside the greenhouse by natural means are

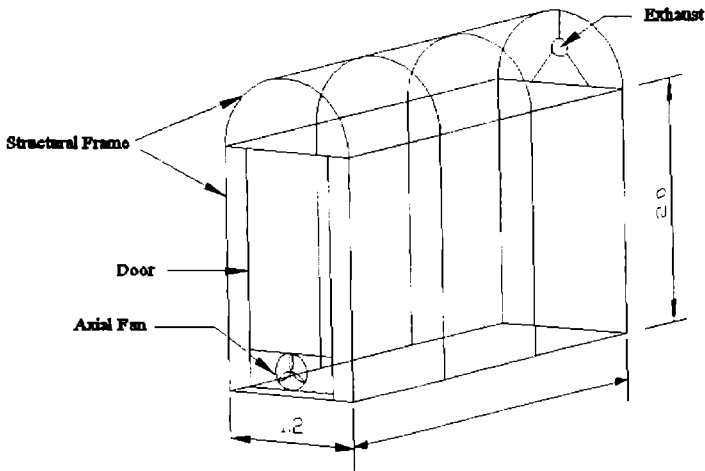
known as passive greenhouses. Greenhouses in which solar energy is collected, stored and distributed by employing some auxiliary energy are the active type. Generally, a combination of both active and passive features is employed in solar greenhouses with an objective to minimize the use of auxiliary energy either for heating the greenhouse or for collection-storage distribution system. Another class of greenhouse is known as the attached-greenhouse where a greenhouse is integrated with the structure of a house and a free exchange of air takes place between residence and greenhouse. This maintains a comfortable room temperature and reducing the heat loss from the greenhouse.

Experimental and simulation models for the energy balance of more conventional greenhouses are frequently reported subjects. Design and thermal performance of many types of solar green house have been carried out for different applications by many researchers [1-12]. Rachmat and Hoibe [13] presented a mathematical model to predict the air temperature inside the greenhouse on the basis of ambient conditions. In the present work, a greenhouse was constructed for drying the effluents of a Zinc manufacturing industry. This company, a custom zinc smelter, is designed to produce 30,000 MT of special high-grade zinc annually from imported zinc concentrate. Effluent generated in this process contains 75% copper (as report given by company), which has to be separated out. Initial moisture content of the effluent is nearly 40% and has to be brought down to 10%, for the recovery of copper from it. Presently, the effluent is loaded in a shed, having asbestos roof and it takes one to two months for complete drying. Hence large area is required for storing and this forced the company to go for a suitable system, mainly to reduce the drying duration and prevent environmental pollution. This chapter describes the details of fabrication and testing of the solar greenhouse, specifically fabricated for the waste material drying.

6.2 Description of the Greenhouse

The experiments were conducted on the terrace of Dept. of Physics, Cochin University of Science and Technology, Kochi. The experiments were conducted from 13 March to 6 April 2004.

A pilot model solar greenhouse was fabricated and installed on the terrace of Department of Physics. The greenhouse was oriented in the east west direction. Total floor area of the greenhouse was 4.64 m^2 , total roof area was 7.29 m^2 and wall area was 20.28 m^2 . Volume of the greenhouse was 11.48 m^3 . Height, width and length of the solar greenhouse were 2 m, 1.2 m, and 3.9 m respectively. The roof of the greenhouse was arch shaped with a radius of 0.6 m. Half-inch MS square tube was used for making the skeleton of greenhouse. A replaceable door was fitted in the front portion for loading and unloading the material. A schematic diagram of the solar greenhouse is shown in Fig. 6.1.



ALL DIMENSIONS IN MM

Fig. 6.1 Schematic diagram of the solar greenhouse

Clear polythene sheet (Thickness-0.3 mm, transmissivity-0.68) was used to cover all the sidewalls and roof of the greenhouse to permit maximum solar radiation. The transparent cover was screwed on the frame.

Greenhouse floor was the concrete terrace of the building. An axial flow fan was provided in the bottom region (at a height of 5 cm from bottom surface) of the greenhouse for air circulation and an exhaust was given in the opposite top portion for the escape of warm moist air. A photograph of the solar greenhouse loaded with copper cake is shown in Fig. 6.2.



Fig. 6.2 Solar greenhouse loaded with 550 kg copper cake

6.3 Theoretical Analysis

The greenhouse traps solar energy in the form of heat within the cover and reduces the convective heat losses. The fraction of trapped energy will be received partly by the substrate (effluent) and floor and the remaining solar radiation will heat the enclosed air inside the greenhouse. The temperature difference between the greenhouse air and ambient air and the vapour pressure difference between the substrate and the greenhouse air, respectively, are responsible for the natural draft and the moisture evaporation from the interior of the effluent. In order to analyze greenhouse climate, through heat and mass balance, the system was divided into four main parts, the floor, the substrate, internal air, and the roof. The roof of the greenhouse is characterized by the area, reflectance, and transmittance for short wave radiation. Chaibi et al. [11] developed a simulation model to predict the performance of a roof-integrated desalination in greenhouse. A similar approach was adopted here for deriving energy balance.

6.3.1 The Substrate

For the substrate (copper cake) the steady state heat balance is given in the following equation.

$$C_{\text{sub-ai}} + R_{\text{sub-net}} + E_{\text{sub-ai}} = I_{\text{abs}} \quad (6.1)$$

In Eq. (6.1), the terms from left to right represent heat convection from the substrate to the internal air, net thermal radiation flow from the substrate to the envelope and the floor, latent heat flow to the air associated with the evaporation from the substrate and finally absorbed solar radiation in the substrate.

The following set of equations describe the left hand term given in Eq. (6.1)

$$C_{\text{sub-ai}} = h_{\text{sub-ai}} (T_{\text{sub}} - T_{\text{ai}}) (A_{\text{sub}} / A_{\text{g}}) \quad (6.2)$$

$$R_{\text{sub-net}} = (R_{\text{sub-ci}} - R_{\text{ci-sub}}) + (R_{\text{sub-g}} - R_{\text{g-sub}}) \quad (6.3)$$

Solar radiation is the energy input to the greenhouse. More elaborated models of the transmission of solar radiation into the greenhouse space such as those of Takakura et al. [12], Kosai [14], Kimball [15] and Wang and Boulard [16] have earlier been compiled. Based on these types of models very detailed and extensive analyses of the influence or orientation, latitude, season, and hour of the day on the solar radiation transmission are possible. Global solar radiation transmitted through a specific surface with a slope β is calculated with the following equation.

$$I_{tr} = \tau_D I_D + \tau_d I_d \quad (6.4)$$

$$I_D = I_c - I_d \quad (6.5)$$

where I_d and I_D are the external diffuse and direct solar radiation (W/m^2) and I_c and I_{tr} are the external and internal global solar radiation (W/m^2). Transmission coefficient for diffuse radiation and direct radiation are denoted as τ_d and τ_D respectively.

6.3.2 The Floor

The heat balance for the top layer of the floor is written:

$$C_{g-ai} + R_{g-net} = I_{g-abs} \quad (6.6)$$

where these terms from left to right represent the heat convection to the internal air, the net thermal radiation emitted from the floor to the substrate and cover and the solar radiation absorbed by the floor.

The following equations describe the left hand term in Eq. (6.6)

$$R_{g-net} = (R_{g-sub} - R_{sub-g}) + (R_{g-ci} - R_{ci-g}) \quad (6.7)$$

$$C_{g-ai} = h_{g-ai} (T_g - T_{ai}) \quad (6.8)$$

6.3.3 The Greenhouse Air

Heat and mass balance of the greenhouse air are given in the following equation.

$$C_{sub-ai} + C_{g-ai} = C_{ai-ci} + C_v \quad (6.9)$$

Where terms from left to right represent heat convection from the substrate respectively the substrate to the internal air, the heat convection from the air to the internal surface of the cover material in the envelope and the ventilation heat loss including air infiltration through the envelope and the air exchange through ventilation openings.

Equations describing the various convection and mass flows are

$$C_{ai-ci} = h_{ai-ci} (T_{ai} - T_{ci})(A_c / A_g) \quad (6.10)$$

$$C_v = h_v (T_{ai} - T_a)(1/A_g) \quad (6.11)$$

$$E_{ai-ci} = ((h_{ai-ci} / C_p) L (H_{ai} - H_{s-ci}))(A_c/A_g) \quad (6.12)$$

$$E_v = \eta_v V \rho L (H_{ai} - H_a)(1/A_g) \quad (6.13)$$

6.3.4 The Greenhouse Envelope

Following two equations describe heat balance of the envelope

$$R_{ci-net} + C_{ai-ci} - E_{ai-ci} = (\lambda/e)(T_{ci} - T_{ce}) \quad (6.14)$$

$$R_{ce-net} + C_{ce-a} = (\lambda/e)(T_{ci} - T_{ce}) \quad (6.15)$$

Eq. (6.14) represents heat balance equation at the internal cover surface. First term on LHS represents net thermal radiation flow to the internal cover surface. Second and third terms on LHS describe the sensible and latent heat flow from the internal air to the cover surface. The term on RHS is the conduction heat flow through the cover material layer. In a similar way Eq. (6.15) is written for the heat balance at the external cover surface. The first and second term in LHS describes the radiation and convection heat flow from the surface to the ambient environment.

Equations for the thermal radiation and the convection heat flows above are the following.

$$R_{ce-net} = (R_{ce-sk} - R_{sk-ce}) + R_{ce-sg} \quad (6.16)$$

$$R_{ci-net} = (R_{sub-ci} - R_{ci-sub}) + (R_{g-ci} - R_{ci-g}) \quad (6.17)$$

$$C_{ce-a} = h_{ce-a}(T_{ce} - T_a)(A_c/A_g) \quad (6.18)$$

6.4 Instrumentation and Experimental Procedure

Solar radiation flux on a horizontal surface was measured by using a Solarimeter (Central Electronics Limited, India). Air velocity was measured with a Digital thermo-anemometer (model. TA 35 made by Airflow, UK) with a range of 0.25 to 20 m/s. The ambient temperature, temperatures at three different regions of greenhouse and inlet temperature were monitored using Type K thermocouple. An axial flow fan of flow rate 2000 m³/h was used to provide airflow through the greenhouse. Two courses of studies were undertaken in the fabricated solar greenhouse. In the first phase, around 60kg copper cake was loaded in the green house. Thickness of sample loaded was 5cm. The sample completely covered the floor area of the greenhouse. Manual shuffling was done at daily two times to expose all portions of the sample to solar radiation.

The axial fan was operated for 10 minutes at an interval of two hours to push the hot warm moist air from the system. As the solar radiation penetrates through the polythene sheet, the substrate, which is black in colour, absorbs radiation and temperature rises. Parameters monitored were temperature at three different regions of the system (at heights of 60cm, 120cm, 180cm from the sample) and intensity of solar radiation. All the parameters were recorded at an interval of 10 minutes. In the second phase, 550kg sample was loaded. The thickness of the material was 35cm. All the parameters monitored were same as that of first phase.

6.5 Results and Discussion

Variations of greenhouse temperature with solar radiation are given in Fig. 6.3. The graph was plotted to indicate the change in temperature at bottom region (at a height of 60 cm from the sample) with solar radiation at different time interval. But it was observed from the thermocouple readings

that there was no appreciable difference in temperature at the three different heights inside the green house. Maximum temperature recorded in the system was 46.8°C, which was 13.8°C higher than ambient temperature. The ambient temperature varied from 29.5°C to 34.2°C. The intensity of solar radiation when the temperature reached its maximum value was 870 W/m². The mean thickness of the sample was 9 cm. Moisture content of sample at the time of loading was measured as 40% and it reduced to the desired level of 10% after seven days.

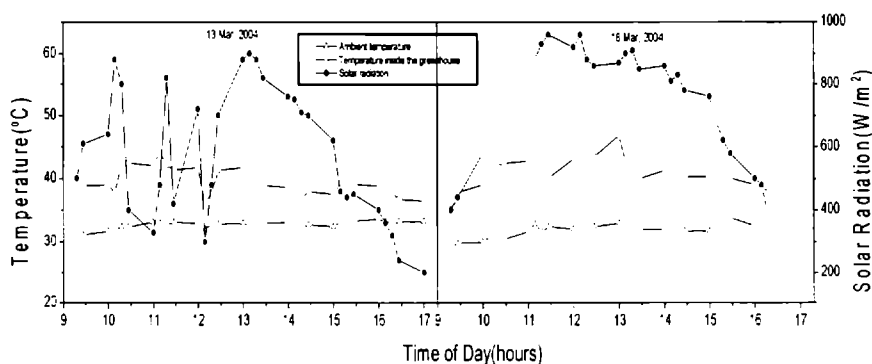


Fig. 6.3 Variation of indoor air temperature of greenhouse with solar radiation when the greenhouse was loaded with 60 kg copper cake. The temperature readings are above 60 cm from the bottom layer of the system

In the second phase of study, all the parameters monitored were same as that of the first phase. Fig. 6.4 indicates the performance of the system analyzed during the study period (which is arbitrarily taken from all readings). The quantity of sample loaded in the system was around 550 kg and it took nearly ten days to reduce the moisture content from 40% to 10%. The mean thickness of the sample loaded in this study was 35 cm. Maximum temperature recorded in the system was 50.6°C, which was 18.6°C higher than ambient temperature (which was on 29. 03. 2004). The average and maximum solar radiation on that day was 587 W/m², 830 W/m² respectively.

Minimum highest temperature recorded in the system was (on 05.04.2004) 40°C, which was 10.1°C higher than ambient temperature. The velocity of air monitored inside the greenhouse with the fan switched on was below the detectable limit. Moisture content was analyzed from top, middle, and bottom layers of the sample and it was recorded as 3.8%, 7.1% and 9.4% respectively. The desired moisture content for the industry was only 10% and the value obtained on the tenth day of continuous drying was considerably less than 10%. The longer drying duration in this case was due to rainy and cloudy days during the study period. Even then the drying duration was very less compared to the normal time experienced in the industry. The drying duration in the industry, where material was loaded in an asbestos shed, was more than forty five to sixty days.

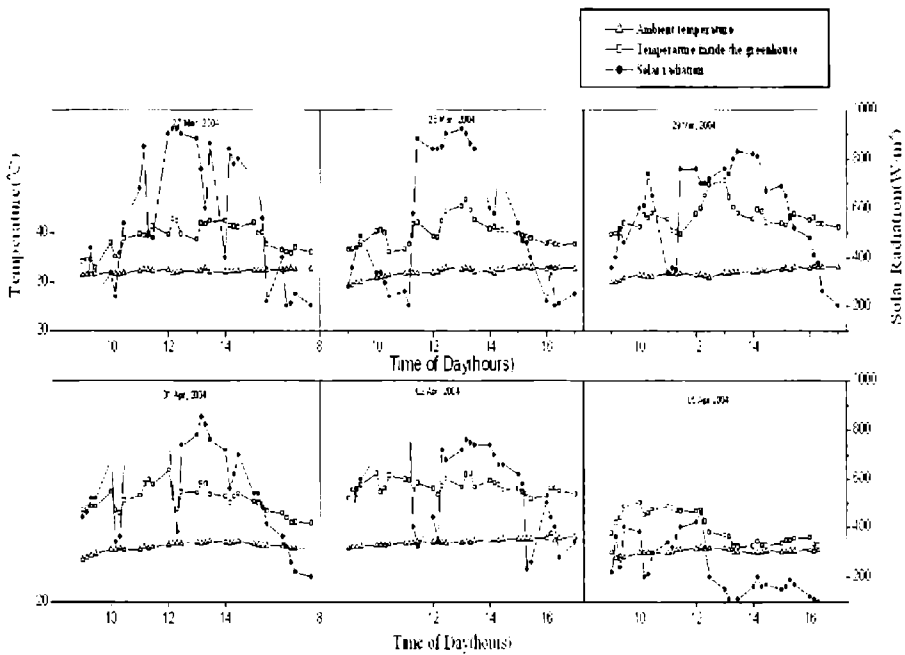


Fig. 6.4 Variation of indoor air temperature of greenhouse with solar radiation for different days of operation when the greenhouse was loaded with 550 kg copper cake. The temperature readings are above 60 cm from the bottom layer of the system

6.6 Conclusion

From the study, it was revealed that the solar greenhouse finds relevant application in industries; particularly for low temperature heating. Maximum temperature recorded in the present study was 50.6°C, which was approximately 18.6°C higher than ambient temperature. Further increase in temperature is possible by adequate improvements in the system fabricated. The fabricated system used polythene sheet of low transmissivity to solar radiation compared to glass. In order to obtain high efficiency, solar toughened glass is recommended. Further improvements in the performance can be achieved by the provision of an absorber plate below the glass (as in the solar air heating system) and a fan to push the hot air inside the greenhouse. But it suffers from disadvantages like more capital investment and high operating expenditure.

Nomenclature

A_i	effective area for air infiltration and ventilation, m^2
C	heat flow through convection, W/m^2
C_p	specific heat of air, $J/Kg-K$
e	cover material thickness, m
E	latent heat flow, W/m^2
h	heat transfer coefficient, W/m^2
H	absolute humidity in air, Kg/Kg
L	latent heat of vaporization of water, J/Kg
R	heat flow through thermal radiation, W/m^2
I	solar radiation, W/m^2
T	temperature, K or $^{\circ}C$
V	green house volume, m^3

Subscripts

a	ambient
abs	absorption
ai	internal air
c	cover
ce	external cover surface
ci	internal cover surface
d	diffuse solar radiation
D	direct (beam) solar radiation
e	external
g	green house floor
net	net thermal radiation from or to a surface
s	shortwave radiation
sg	surrounding ground
sk	sky

sub substrate
tr transpiration or transmitted
v ventilation

Greek Symbols

ρ density of air, Kg/m³
 η view factor for thermal radiation, dimensionless
 λ thermal conductivity, W/m-K
 τ transmission coefficient, dimensionless

References

- [1] D. Jain and G.N. Tiwari, Modelling and optimal design of ground air collector for heating in controlled environment greenhouse, *Energy Conversion and Management* 44(8), 1357-1372, 2003.
- [2] M. Dj. Pucar, Enhancement of ground radiation in greenhouses by reflection of direct sunlight, *Renewable Energy* 26, 561-586, 2002.
- [3] G.N. Tiwari and N.K. Dhiman, Design and optimization of a winter greenhouse for the Leh-type climate. *Energy Conversion and Management* 26(1), 71-78, 1986.
- [4] M. Condori and L. Saravia, Analytical model for the performance of the tunnel-type greenhouse dryer, *Renewable Energy* 28(3), 467-485, 2003.
- [5] J.G. Pieters and J.M. Deltour, Modeling solar energy input in greenhouses, *Fuel and Energy Abstracts* 42(1), 41-42, 2001.
- [6] A.M Hasson, A study of solar energy and its components under a plastic greenhouse, *Energy Conversion and Management* 31(1), 1-5, 1991.
- [7] G. Papadakis, A. Frangoudakis and C. Kyritsis, Theoretical and experimental investigation of thermal radiation transfer in polyethylene covered greenhouses, *Agricultural Engineering Research* 44(2), 97-111, 1989.
- [8] Govind, Rashmi, N.K. Bansal and I.C. Goyal, An experimental and theoretical study of a plastic film solar greenhouse, *Energy Conversion and Management* 27(4),395-400,1987.
- [9] C. Von Zabeltitz, Greenhouse heating with solar energy, *Energy in Agriculture* 5(2), 111-120,1986.
- [10] J. Maghsood, A study of solar energy parameters in plastic-covered greenhouses, *Agricultural Engineering Research* 21(3), 305-312, 1976.

- [11] M.T. Chaibi and T. Jilar, System design, operation and performance of roof-integrated desalination in greenhouses, *Solar Energy* 76(5), 545-561, 2003.
- [12] T. Takakura, K.A. Jordan and L.L. Boyd, Dynamic simulation of plant growth and the environment, *Trans. ASAE* 14, 964-971, 1971.
- [13] R. Rachmat and K. Hoibe, Solar heat collector characteristics of a fiber reinforced plastic drying house, *Transactions of ASAE* 42 (1), 149-157.
- [14] T. Kosai, Direct solar light transmission into single-span greenhouses, *Agriculture Meteorology* 18, 327-338, 1977.
- [15] B.A. Kimball, Simulation of the energy balance of a greenhouse, *Agriculture meteorology* 11, 243-260, 1973.
- [16] S. Wang and T. Boulard, Measurement and prediction of solar radiation distribution in full-scale greenhouse tunnels, *Agronomy* 20, 41-50, 2000.

NUMERICAL SIMULATION STUDY ON SOLAR AIR HEATERS

7.1 Introduction

Design and fabrication of all types of solar air heaters is rather tedious process. “Computational Fluid Dynamics (CFD)” method is a clear solution to alleviate the mentioned problem. CFD has distinct advantages like as cost, turn around time, detailed information and ability to simulate real condition to name few. Numerical simulation of solar air heater is helpful to check the accuracy of the experimental data. In the present study, detailed analysis was made on underflow copper collector and the simulation results were compared with the experimental data. It helped to analyze the maximum temperature output for solar air heater with and without baffles under different mass flow rates and in turn facilitated to optimize the flow path. The aim of various investigations done under the present work were 1) to know the maximum temperature for different mass flow rates, 2) attempt to enhance collector outlet temperature in relation with number of baffles, 3) pressure drop and corresponding pumping power required.

The educational/commercial version of the software “Fluent” was used for the numerical simulations. Typical CFD analysis involves pre-processing (building 3D model, grid generation, and assigning boundary conditions), solving for given accuracy and post-processing of the results. A 3D model was generated in PRO/E in pre-processor Gambit as CAD data. Model was solved to get the prediction of flow path and heat transfer using solver of Fluent. Finally results from Fluent was post processed to visualize

flow path, pressure drop, rise in temperature with different baffle configuration and mass flow rates of air.

7.2 Advantages of the Numerical Simulation on Solar Air Heaters

Obviously, it is unpractical to carry out a theoretical analysis or experimental study in every single model on solar air heaters. Computational Fluid Dynamics (CFD) has changed the traditional design process. Because CFD programme can show the detail of the flowing and heat transfer of the fluid, it can not only predict the collectivity performance of the solar air heating system, but can also easily find the problems of the product design by flow field analysis. So the use of CFD tool can broaden the research field and strengthen the research profundity at the same time.

By using CFD tools one can make many of the “experiment samples” by computer, that is many types of “dummy experiment samples” by the CFD programme. It can effectively reduce the experiment workload. The selection of the precept is based on scientific analysis and hence it is easy to insure the success of the design and the stabilization of the product quality. Performance can be predicted before real experimental research. Hence the cost of research can be reduced and the success ratio as well as research efficiency can be increased. In addition, CFD can intensify the research profundity of solar air heater, by simulation; we can see the inner flow field and temperature field which is much more detailed than the experimental research. On the basis of CFD simulation, better improvement can be done on the structure of the collector.

7.3 Geometry Model

Starting point for the CFD model was a PRO/E part file representing the volume occupied by the fluid, i.e., the volume bounded by the inner

walls of the actual part and the inflow/outflow boundaries. In order to help result interpretation, the different parts should be assigned name corresponding to the boundaries. Atmospheric air was pumped from inlet at one end of solar air heater which passed through the diffuser and entered the box of air heater. Here it made to flow in zigzag manner using baffles to enhance heat transfer. Finally hot air comes out of the air heater and can be used for applications like drying of agricultural products, industrial process heat or space heating etc. The flow path inside the solar air heater is shown in Fig. 7.1.

7.4 CFD Model

7.4.1 Grid Generation

The easiest way to obtain a grid for solar air heater was to use a tool such as GAMBIT and create a tetrahedral grid. However, experience suggested that better results are obtained with hexahedral grids. Hence it was decided to use hexahedral grid in inlet and box portion of the solar air heater and tetrahedral grid in diffuser to maintain the mesh quality. The typical grid size used had around 0.19 million cells with skewness equal to 0.79. CFD grid used in simulation is shown in Fig. 7.2. Skewness is a measure of mesh quality of the given grid and represents how bad is grid from ideal one (0 is best and 1 is worst).

7.4.2 Physical Model

The flow was assumed to be incompressible (small density variation with pressure and temperature) and turbulent. Air was assumed to be the working fluid, with properties such as density and viscosity evaluated at atmospheric conditions. For turbulence modeling, the K-Epsilon model available in Fluent with standard wall functions was considered due to its robustness.

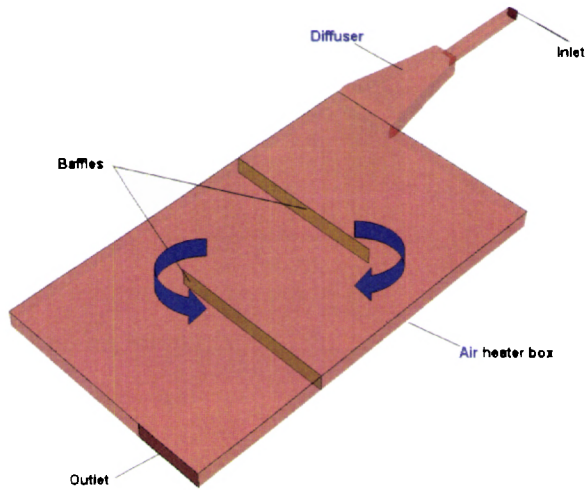


Fig. 7.1 Flow path inside air heater

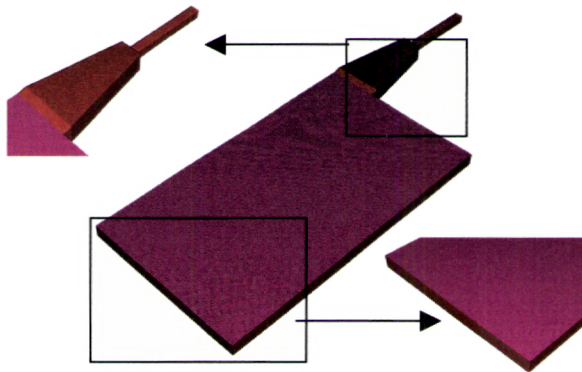


Fig. 7.2 CFD grid used in simulation

7.4.3 Boundary Conditions

Calculations were done using a mass flow inlet boundary condition at the inlet and an imposed atmospheric static pressure at the exit. Results at different flow rates (mass flux) viz, 45, 70, 80, 100, and 130 $\text{kgm}^{-2}\text{h}^{-1}$ was studied with and without baffles configuration. Solar radiation was modeled

as heat flux (considered 642.5 W/m^2) through heat input wall on the top of the air heater box. Rest of the walls was assumed to be adiabatic considering the insulation wrapped around to minimize the loss to surrounding. For turbulence, in the absence of more adequate information, the inlet turbulence intensity was assumed to be 1% with turbulent viscosity ratio of 10. Turbulence at the outlet was handled in a similar manner to deal with potential backward flow.

7.4.4 Solver Settings

The equations solved were Continuity, Momentum, Turbulence and Energy. The default solver settings in FLUENT were usually adequate to ensure solution robustness and sufficient accuracy, assuming that the grid was good enough. This means that a first order numerical scheme should be adequate for good results. But for better prediction of the pressure drop, momentum equation was solved for second order accuracy. It was recommended that residuals be allowed to decrease by 1 or 2 orders of magnitude below the default settings, particularly for the continuity equation. In addition, for the set of boundary conditions described above, one should monitor convergence by tracking quantities such as the inlet mass flow rate, area-averaged static temperature on baffle wall and the area-averaged exit total pressure.

7.5 Results and Discussion

The design details of the solar air heater used for the experimental study is given in Section 3.2.1 a. of chapter 3. The dimension of the collector used for the numerical simulation was also exactly identical to the collector fabricated. The solar air heater was subjected to different mass flow rates, viz, 45, 70, 80, 100, and 130 $\text{kg/m}^2\text{h}$. Outlet temperature of the collector and pressure drop for all the mass flow rates was investigated. The analysis was carried out separately for with and without the provision of baffles to the air

flow passage area. Interestingly, the effect of collector performance with three and four baffles was also carried out.

7.5.1 Flow Field

Fig. 7.3 to Fig. 7.10 represents the series of simulation on solar air heaters with two, three and four baffles. Velocity field, temperature distribution in the air heater was shown along with contours of total pressure. Though simulation was carried out for five different mass flow rates, the figure included here were for two mass flow rates, i.e., 45 kg/m²h and 130 kg/m²h. It was useful to look at the flow field in order to get a better understanding of flow details and identify potential improvements. The following information was useful in thorough analyze of the simulation model.

- i) Total pressure plots: Sudden decreases in total pressure usually indicate potential pressure losses (recirculation zones). Downstream of a low total pressure region, mixing usually occurs, resulting in an overall drop in total pressure. Total pressure is total energy content in the flow which is sum of static and dynamic pressure. Static is due to position of fluid and dynamic is due to the motion of the fluid.
- ii) Velocity plots: Velocity plots help to identify regions of flow separation or regions of high flow acceleration. Contour plots were used to locate low velocity zone (dead zones) and high velocity zones. High velocity zones are the region where heat transfer coefficient will be higher and mainly responsible for the heat transfer. Both vector plots and contour plots can be used.
- iii) Static temperature plots: It is complement the velocity plots by indicating low temperature regions which could be an indication of poor performance of air heater. This also tells us the region which is not effectively used for the heat transfer.

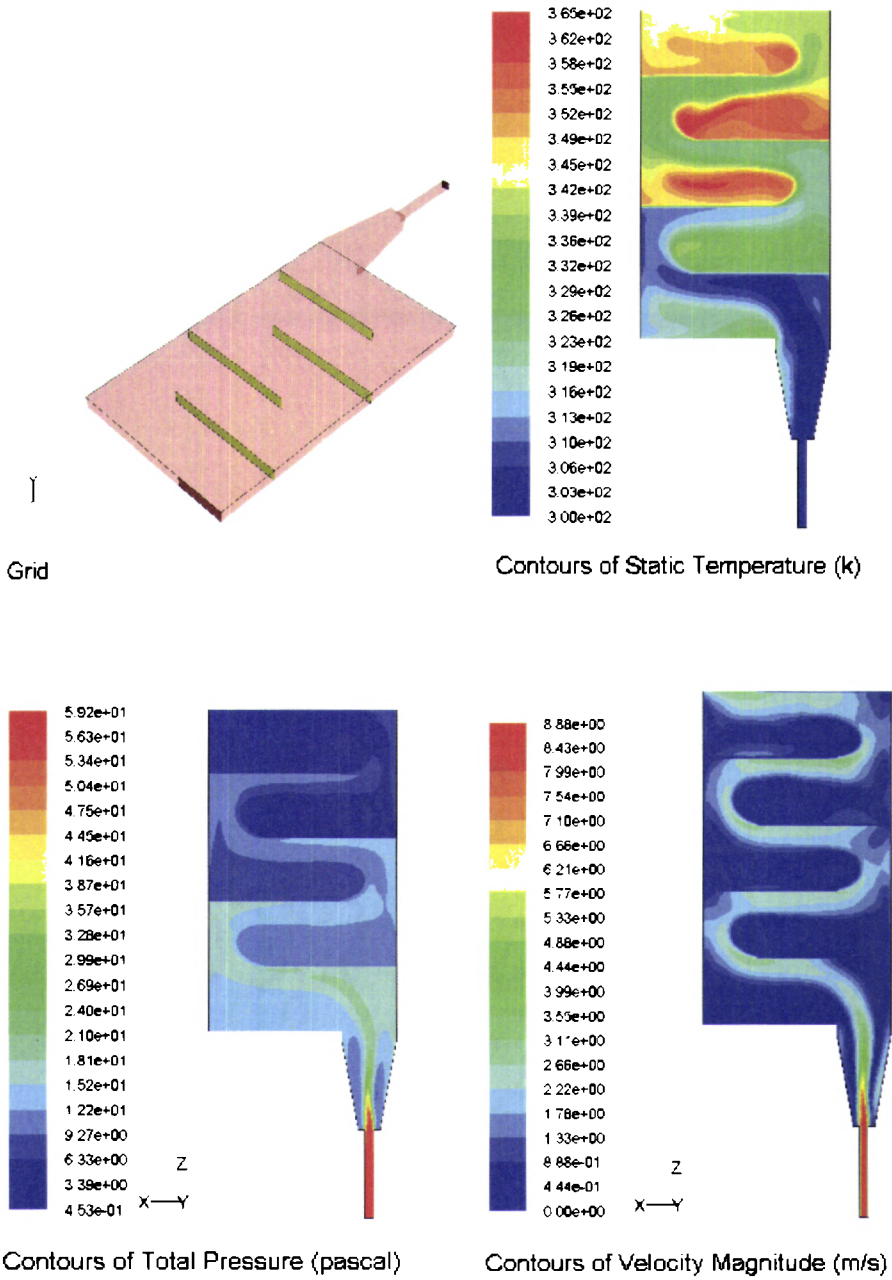
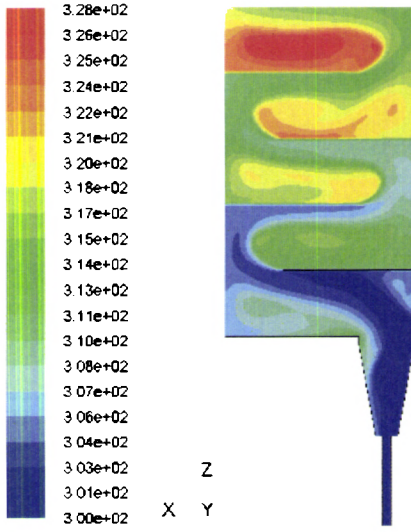
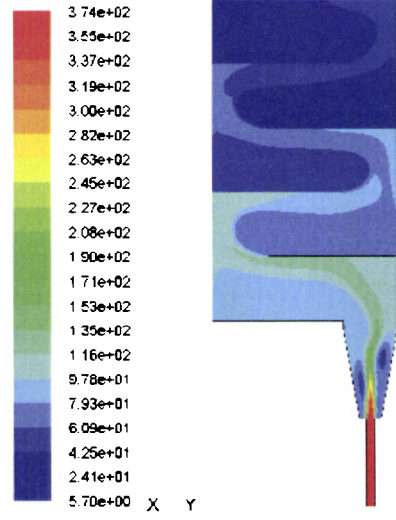


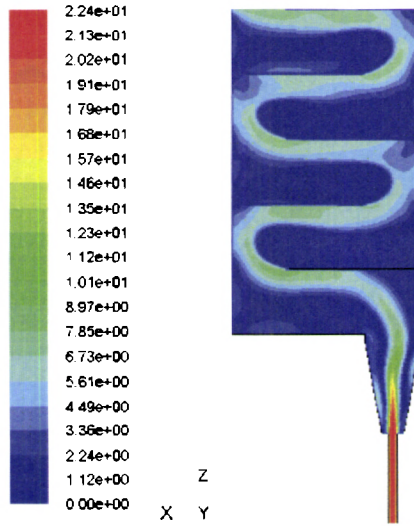
Fig. 7.3 Simulation with four baffles (mass flow rate - $45\text{kg/m}^2\text{h}$)



Contours of Static Temperature (K)



Contours of Total Pressure (pascal)



Contours of Velocity Magnitude (m/s)

Fig. 7.4 Simulation with four baffles (mass flow rate – 130 kg/m²h)

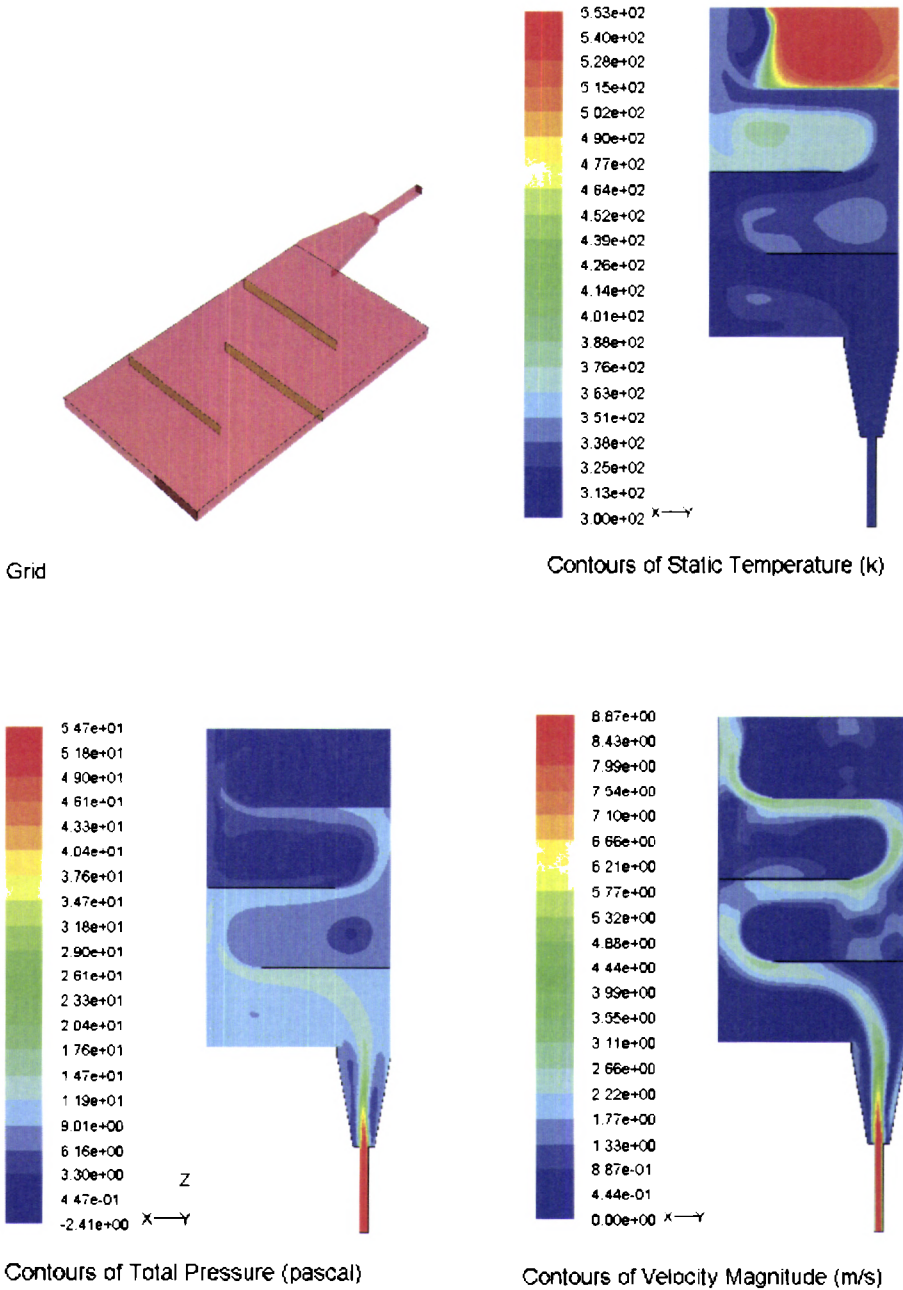


Fig. 7.5 Simulation with three baffles (mass flow rate – $45 \text{ kg/m}^2\text{h}$)

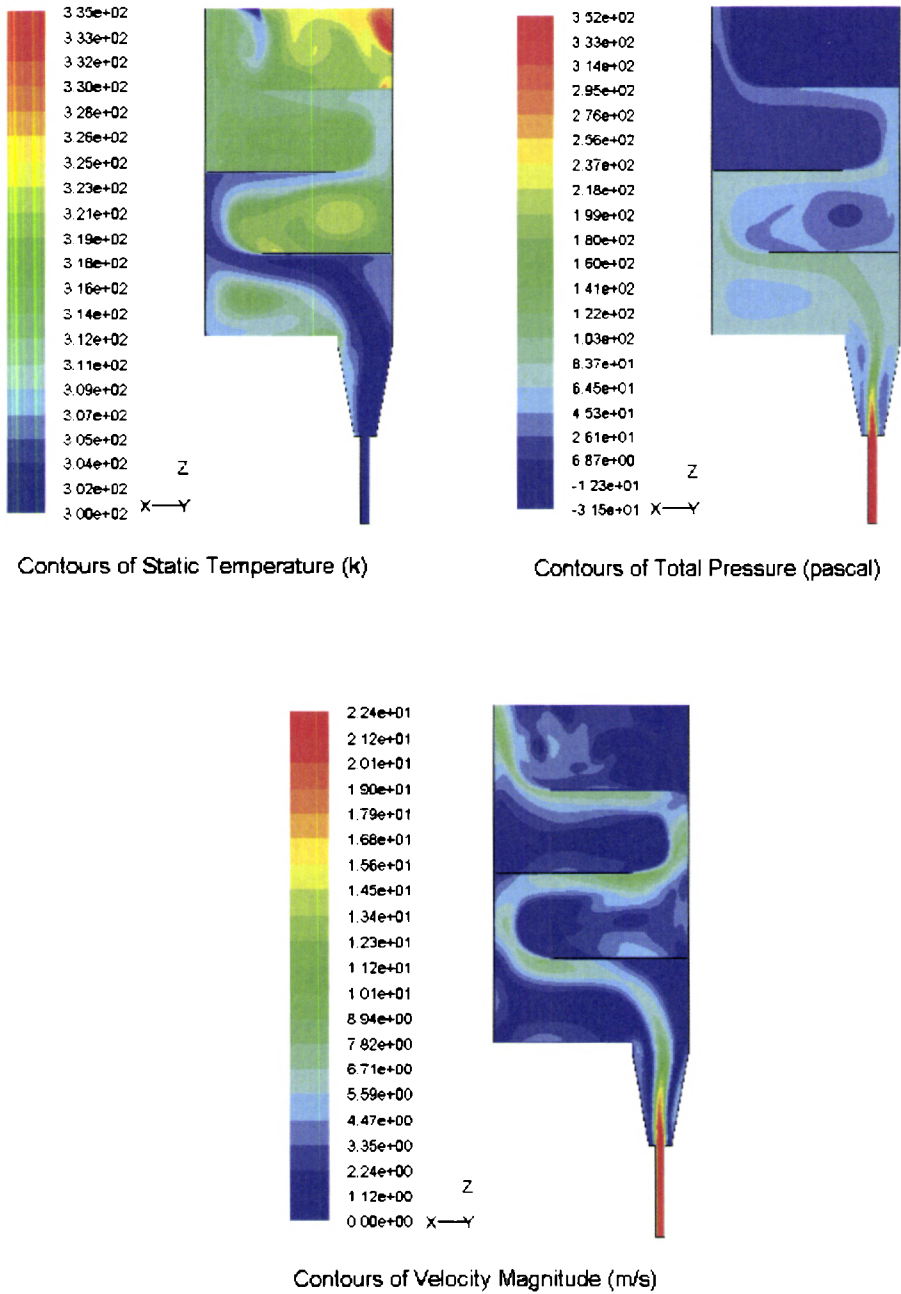


Fig. 7.6 Simulation with three baffles (mass flow rate – $130 \text{ kg/m}^2\text{h}$)

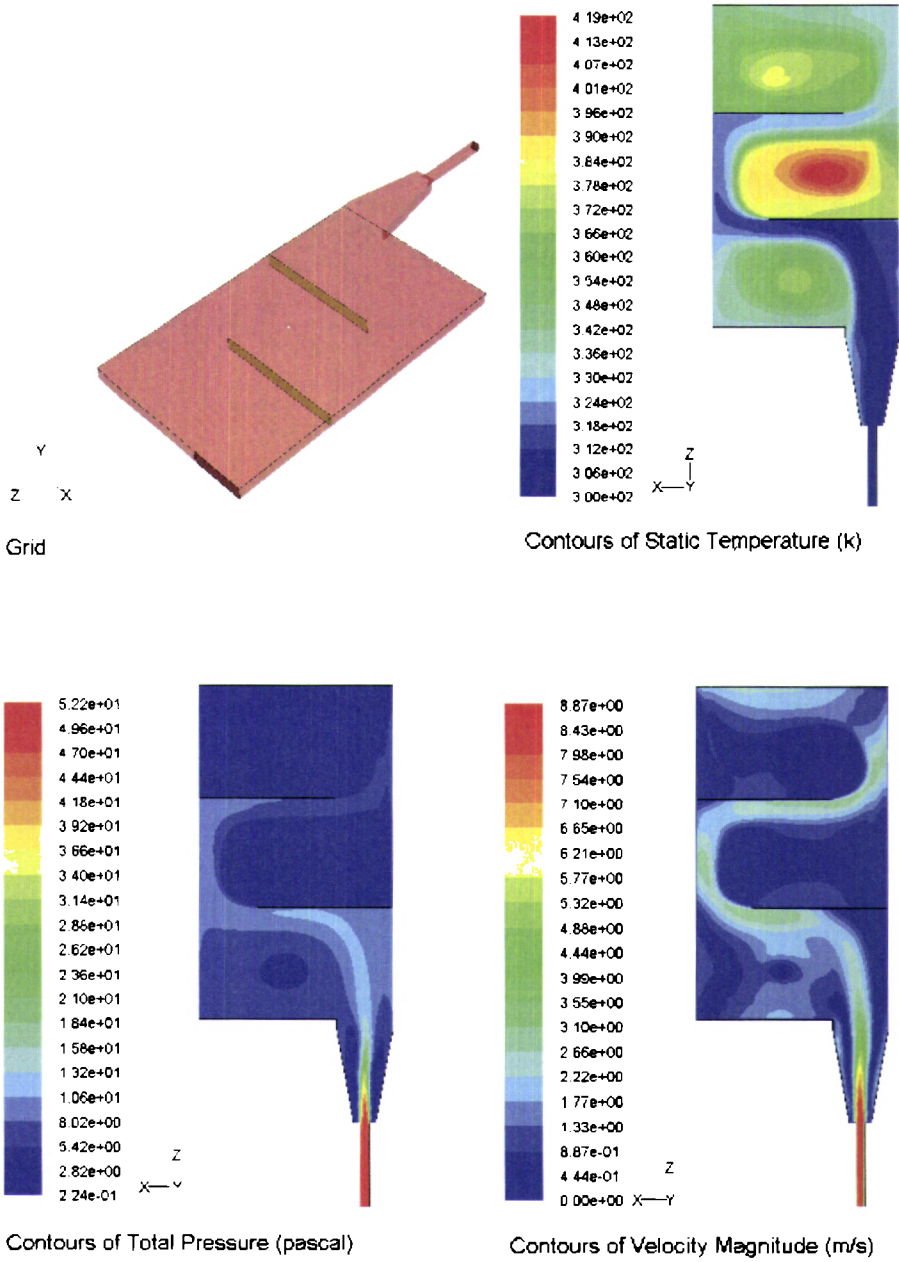


Fig. 7.7 Simulation with two baffles (mass flow rate – 45 kg/m²h)

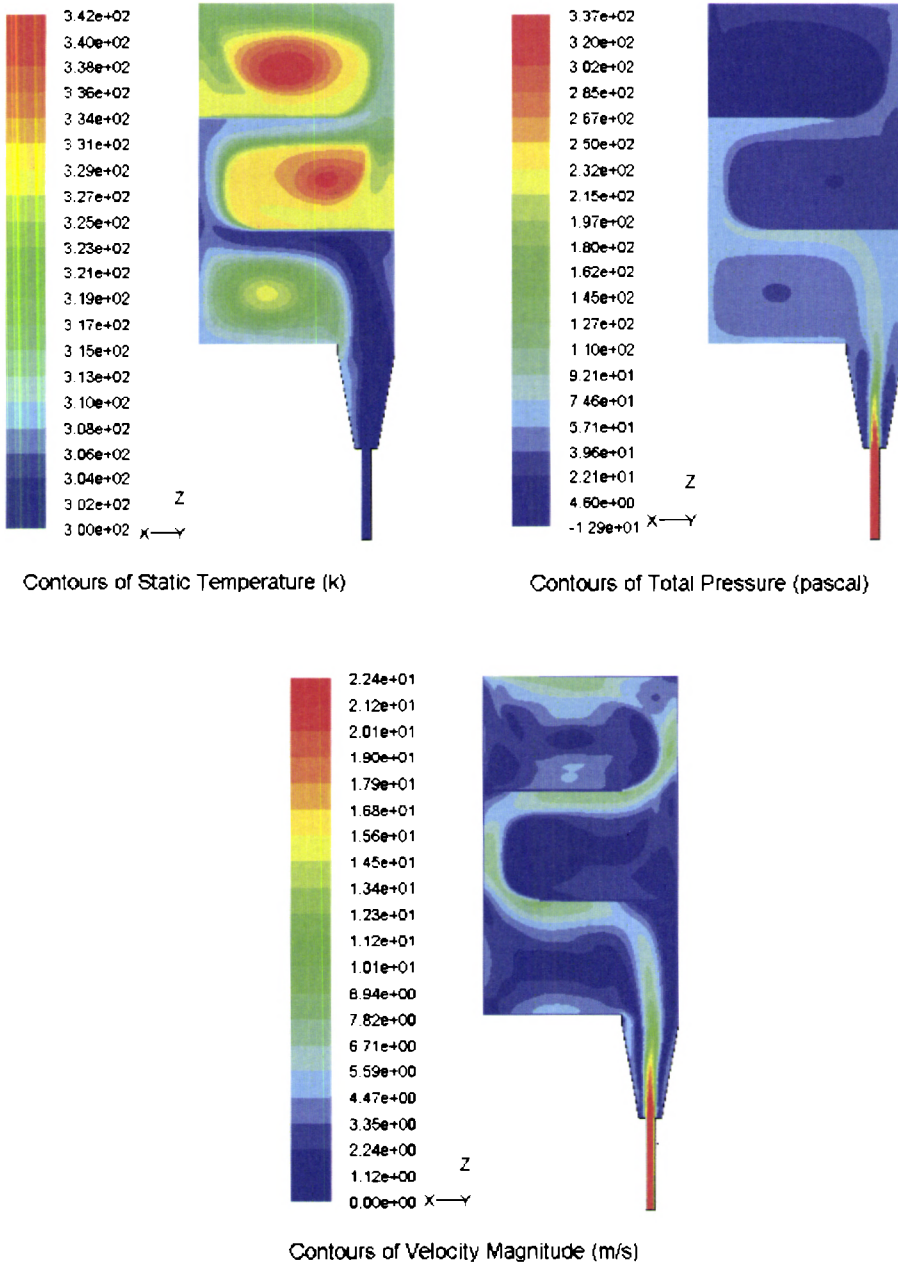


Fig. 7.8 Simulation with two baffles (mass flow rate – $130 \text{ kg/m}^2\text{h}$)

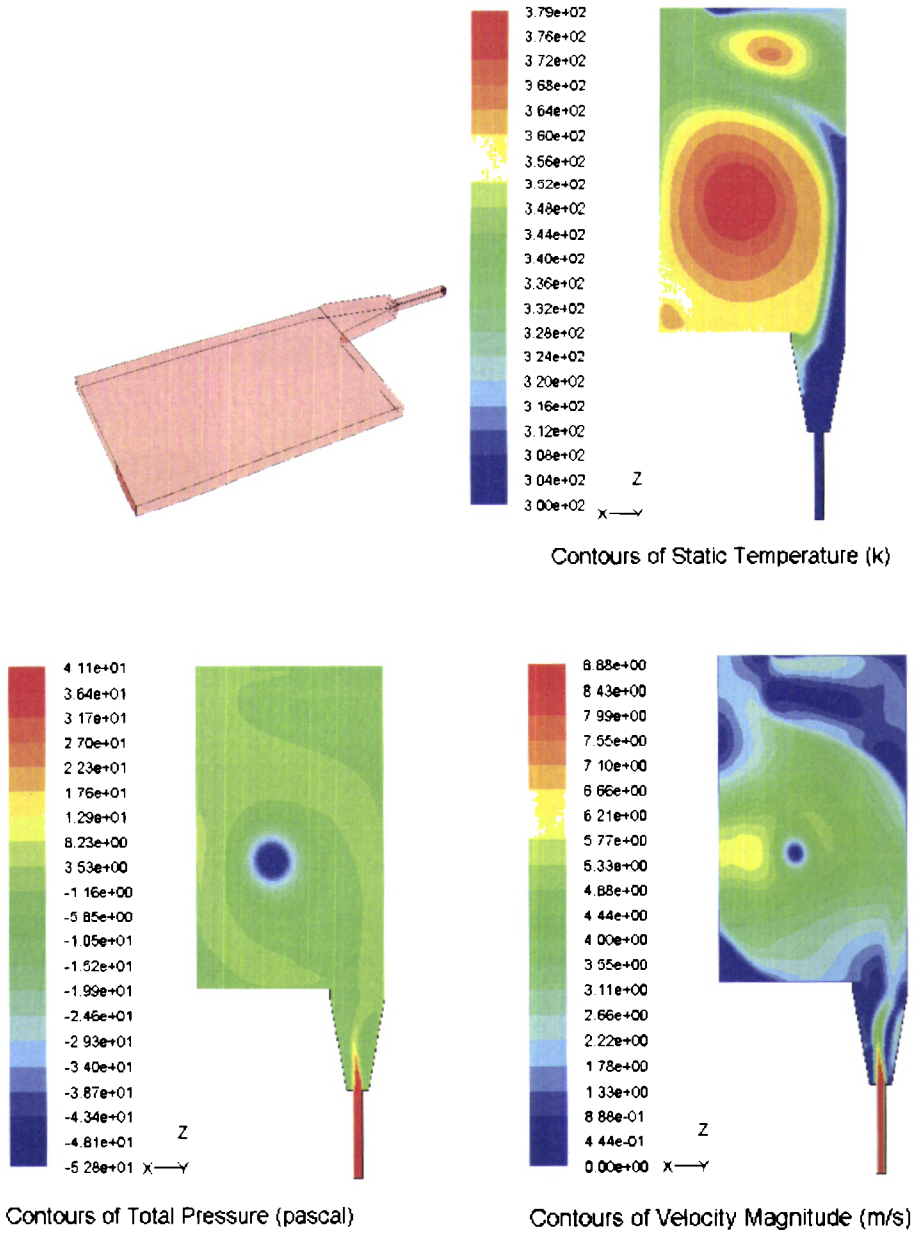


Fig. 7.9 Simulation without baffle (mass flow rate – $45 \text{ kg/m}^2\text{h}$)

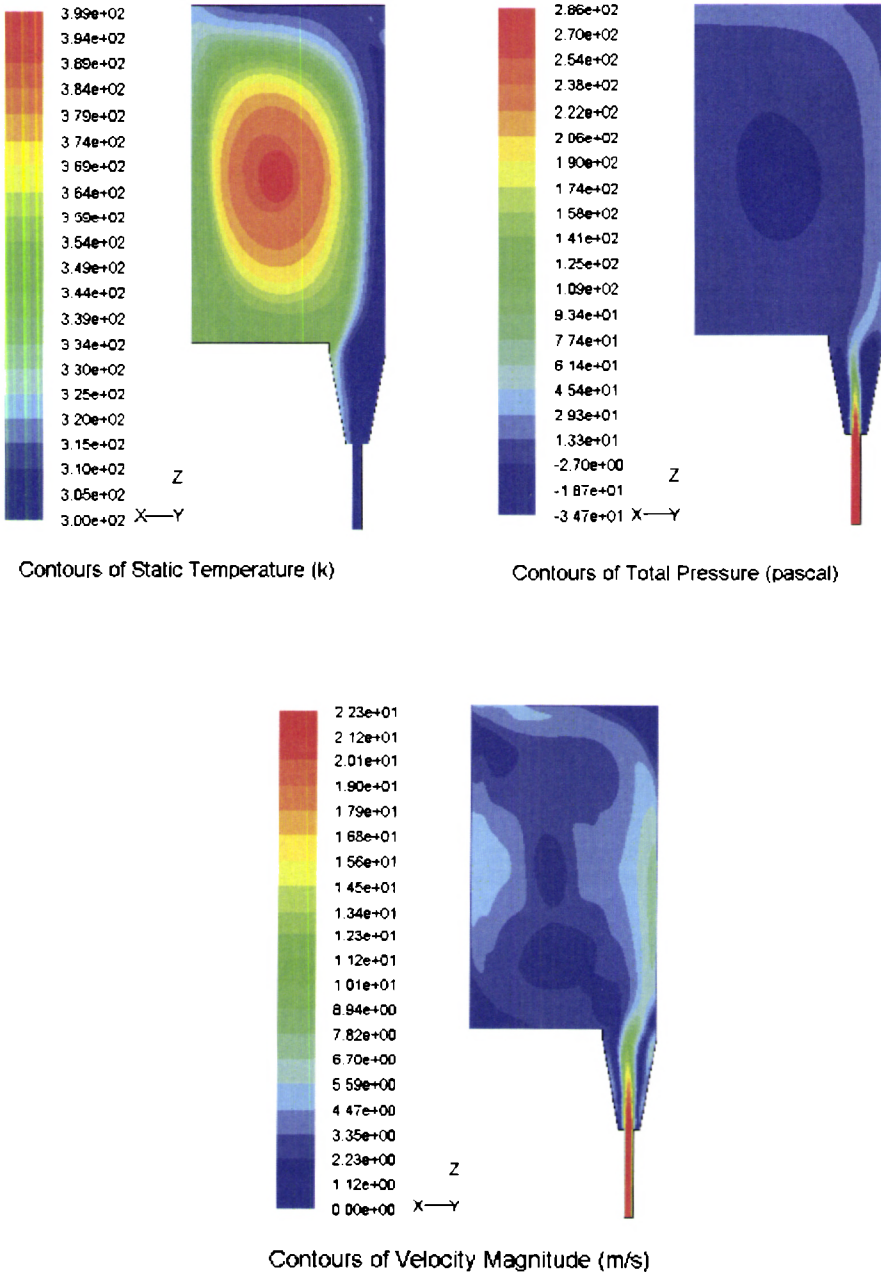


Fig. 7.10 Simulation without baffle (mass flow rate – $130 \text{ kg/m}^2\text{h}$)

7.5.2 Temperature Output with and without Baffles

The comparison results of temperature output for both simulation and experimental study on solar air heater for five mass flow rates is given in Fig. 7.11. The analysis was done for copper collector provided with two baffles and the collector specifications are exactly identical as described in Table 3.1 of chapter 3. It was evident from the analysis that the difference between both CFD and experimental data was nominal. The maximum temperature was attained for a flow rate of 45 kg/m²h for both experimental and CFD analysis. At low mass flow rate, the difference in temperature was 6.4°C and at high mass flow rates the difference was negligible.

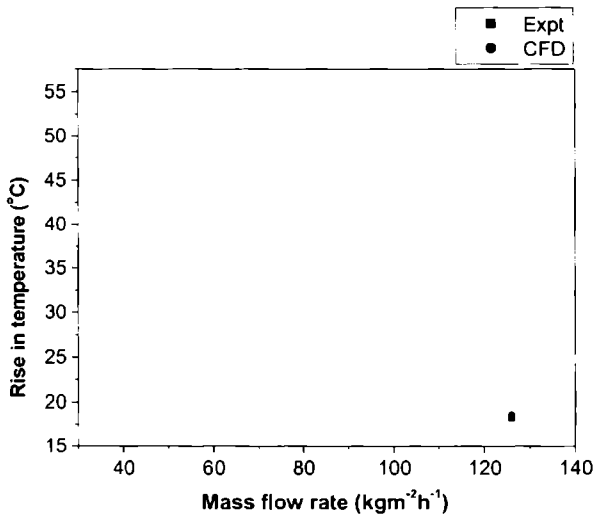


Fig. 7.11 Temperature difference for collector with two baffles under different mass flow rates for both experimental and CFD analysis

Similarly a study was done to compare both the analysis of the collector without baffles (Fig. 7.12). As compared to earlier analysis, disparity was more in this case. The difference in temperature for the simulation results was always on the higher side.

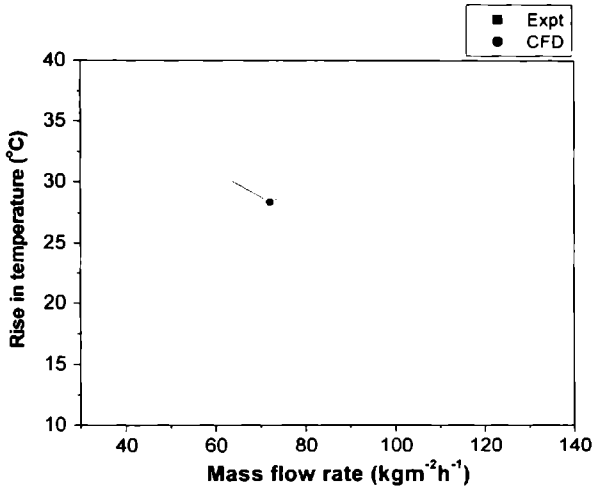


Fig. 7.12 Temperature difference for collector without baffles under different mass flow rates for both experimental and CFD analysis

7.5.3 Pressure Drop with and without Baffles

Pressure drop of collector with and without baffles for different mass flow rates are shown in Fig. 7.13 and Fig. 7.14. The analysis showed that the simulation result was much higher than experimental results, particularly in the higher mass flow rates. As seen in the experimental study, the pressure drop increased with mass flow rate in numerical analysis also.

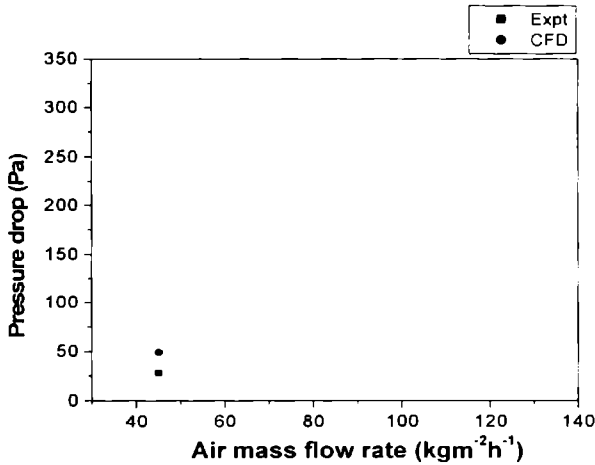


Fig. 7.13 Pressure drop of collector with baffles

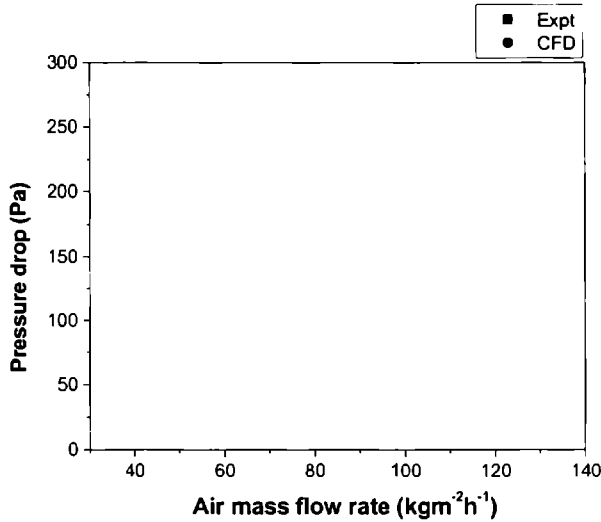


Fig. 7.14 Pressure drop of collector without baffles

7.5.4 Effect of Number Baffles for Temperature Output

Another simulation study was performed for finding out the variation in temperature output with the number of baffles in the air flow path of the collector. The collector was subjected to different mass flow rates and the output of the collector was analyzed for two, three and four equidistant baffles. A maximum rise in temperature of 47.67°C was recorded for collector with two baffles. The temperature output recorded for collector with three baffles for all the mass flow rate was less than that of collector with two baffles. Theoretically increase in number of baffles should increase the temperature output, but this also depends on how baffles are arranged inside the air heater box. Here the position of three and four baffles was not optimized (assumed that baffles are located equidistant).

As seen in the simulation plot that there is many flow separation in case for three baffles which led to less contact with hot plate and eventually it caused low temperature output. Similarly in the case of four baffles

although flow separation is less but still the non optimization of baffle position resulted low output. It was evident from the study that as the mass flow rate increased, temperature output decreased. The variation of temperature with the provision of two, three and four baffles are given in Fig. 7.15. Maximum temperature was attained for a mass flow rate of 45 kg/m²h for all the cases investigated.

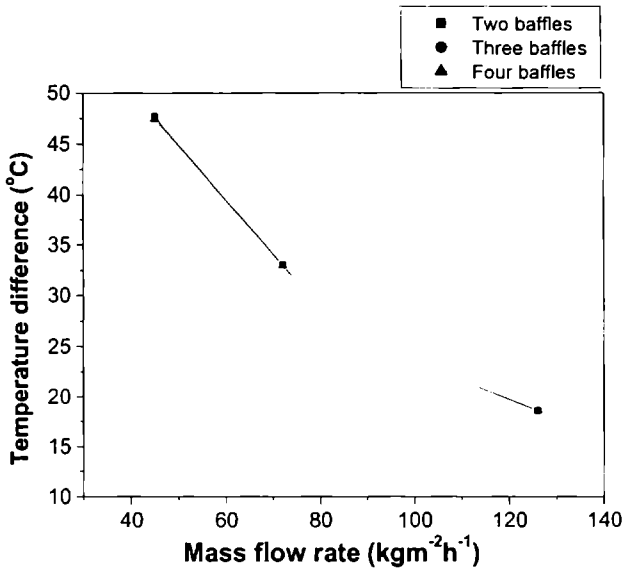


Fig. 7.15 Comparison of temperature difference of collector with two, three and four baffles (CFD) analysis

7.5.5 Variation of Pressure Drop with Number of Baffles

The pressure drop across the collector fitted with two, three and four baffles was also studied. This revealed that, as mass flow rate increased pressure drop also increased. As expected, collector with more number of baffles created a higher pressure drop. Even though the difference in pressure drop was least in the low mass flow region, it was apparent for high mass flow rates. The pressure drop with the provision of two, three and four baffles for different mass flow rates are given in Fig. 7.16.

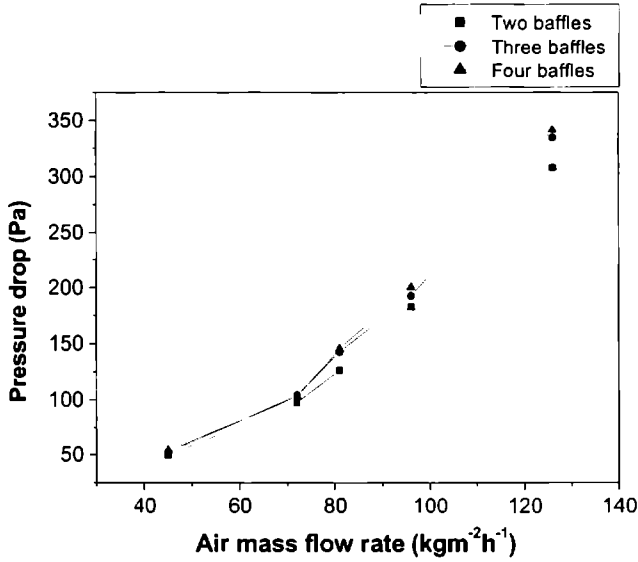


Fig. 7.16 Comparison of pressure drop of collector with two, three and four baffles (CFD) analysis

7.6 Conclusion

A comparative analysis of underflow solar air heater with numerical simulation tools was carried out. The results illustrated that CFD tool has its own advantages in the field of solar air heater research.

Flow modeling to optimize flow distribution and prediction of the heat transfer performance were done for-

- 1) Solar air heater without baffles
- 2) Solar air heater with two baffles
- 3) Solar air heater with three baffles
- 4) Solar air heater with four baffles

The models could simulate the overall flow properties in the solar air heater. Following conclusions were drawn from the results:

- 1) CFD results were validated qualitatively against the experimental data with and without baffles.
- 2) It was found that simulation on air heater with two baffles provided good agreement with experimental data for temperature output, while the cases of three baffles and four baffles were not able to predict the expected behavior. The temperature output of the collector with two baffles for both simulation and experimental results were almost matching. The pressure drop observed for simulation results were higher than experimental data, particularly for high flow rates.
- 3) As mass flow rate increased, temperature output decreased while pressure drop increased.
- 4) High velocity zones were the region where heat transfer coefficient was high and were mainly responsible for the heat transfer. Recirculation zones (dead zones) have impact on the temperature output.
- 5) Mathematical model could predict the performance of solar air heater to a reasonable accuracy.
- 6) However, for the air heater with three and four baffles, temperature output predicted was lower than the expected value. Simulation study revealed that collector with two baffles given high temperature output compared to three and four baffles.

References

- [1] S. V. Patankar, Numerical Heat Transfer and Fluid Flow, McGraw-Hill, New York, 1980.
- [2] D.A. Anderson, J.C. Tannehill and R. H. Pletcher, Computational Fluid Mechanics and Heat Transfer, Hemisphere Publishing Corporation, 1984.
- [3] Fluent manuals for preprocessing, solver and post-processing.
- [4] <http://www.fluent.com/solutions/articles/ja087.pdf>
- [5] M. Biona, A. Culaba, E. Serafica and R. Del Mundo, Performance Curve Generation of An Unglazed Transpired Collector For Solar Drying Applications.<http://www.retsasia.ait.ac.th/Publications/WRERC%202005/UPD-paper1-WRERC05-final.pdf>
- [6] C. Wang, Z. Guan, X. Zhao and D. Wang, Numerical simulation study on transpired solar air collector, Renewable Energy Resources and a Greener Future VIII-3-4, ICEBO 2006, Shenzhen, China, 2006.
- [7] XinshiGe, HongYe, Solar air heating system, Solar Energy 1, 13-14, 2003.

SUMMARY AND CONCLUSIONS

In the present study, various types of solar air heaters were designed, developed and performance analysis was carried out. Performance evaluation of solar air heaters with provision of baffles to the air passage area was the main focus of the work. It was proven beyond doubt that solar air heaters with the baffles can efficiently promote air turbulence, thereby increasing the heat transfer coefficient and efficiency. Amongst different collectors tested, 'underflow collector' with black chrome copper as absorber plate and the baffles proved to be the ideal type. The maximum temperature difference recorded at the outlet of this collector was 54.1°C for a flow rate of 45 kg/m²h and this is an important factor. The average efficiency of the collector with baffles was more than twofold higher than that of without baffles for the same mass flow rate. The additional pumping power due to baffles was ostensible, proving that the collector with baffles scores on every count.

A glimpse to the performance of other collectors tested revealed that the matrix collector with wire mesh absorber was the second in the rating of maximum temperature output. The maximum rise of temperature above ambient was 43.3°C, when the system was subjected a flow rate of 45 kg/m²h and the temperature recorded was appreciably high. The matrix collector exhibited an improved thermal performance with higher heat transfer rate to the air flow and lower friction losses compared to flat plate air collectors of conventional design. Because of these unique features these two collectors are well recommended for industrial applications to gain reasonable temperature output for both low and high mass flow rates without much drop in efficiency. But the problem with wire mesh absorber plate is its susceptibility to corrosion and hence copper collector proved to be the

ideal choice. Thermal performance of all other collectors with baffles was found to be satisfactory. The study revealed that for overflow collectors, rise in temperature and efficiency was least for all the mass flow rates.

A 46 m² roof integrated solar air heating system was designed, installed and commissioned at a Food Processing Centre in Kerala. The development was based on the experience gained by the experimental study carried out on pilot model solar air heaters. The system had a capacity to dry 200-250 kg fresh vegetables/fruits per batch. The maximum temperature recorded at the output of the solar collector was 76.6°C. During the study, the dryer was loaded with 200 kg of fresh pineapple slices of 5 mm thick. The initial moisture content of 82 % was reduced to the desired level (<10 %) within 8 hours. A detailed performance analysis was done by 3 methods namely 'annualized cost method', 'present worth of annual savings' and 'present worth of cumulative savings'. The drying cost for 1 kg pineapple was calculated as Rs. 11, when it was dried using solar drier. But it was Rs. 19.73 in the case of electric dryer. Economic analysis showed that the cumulative present worth of annual savings for drying pineapple over the life of the solar dryer turned out to be approximately 17 million rupees. The capital investment of the dryer was Rs. 550,000 and the payback period of the dryer was found to be 0.54 year. The life span of the solar dryer was assumed to be 20 years. The payback period was calculated to be just 0.54 year, which was also very less considering the life of the system (20 years). Performance of the dryer was quite satisfactory from the date of installation.

A latent heat thermal energy storage system based on Phase Change Material (PCM) was developed and its performance was analyzed. Acetamide (CH₃CONH₂) was used as PCM and it was filled in a specially fabricated stainless steel container having adequate heat transfer facility. A novel efficient solar cabinet dryer, particularly meant for drying vegetables and fruits, was also developed. The PCM container was integrated with the

solar cabinet dryer to study the feasibility of energy storage for drying applications. The dryer was an indirect type with an aperture area of 1.27 m². Two axial fans provided in the dryer accelerated the drying processes. The absorber plate of the dryer achieved a maximum temperature of 97.2°C, when it was studied under no load condition. The maximum air temperature in the dryer was 78.1°C, which was 45°C higher than corresponding ambient temperature. A detailed economic analysis was done using 3 methods namely 'annualized cost method', 'present worth of annual savings' and 'present worth of cumulative savings'. Drying cost for 1 kg bitter gourd was calculated as Rs. 17.52 and it was Rs. 41.35, in the case of electric dryer. The life span of the solar dryer was assumed to be 20 years. The cumulative present worth of annual savings over the life of the solar dryer was calculated for bitter gourd drying as Rs. 31,659, which was much higher than the capital cost of the dryer (Rs. 6500). The payback period was calculated as 3.26 years, which was very less considering the life of the system (20 years). So the dryer would dry products free of cost during almost entire life span. The quality of the product dried in the solar dryer was competent with the branded products available in the market. A detailed study was undertaken with PCM integrated into the dryer. The drying performance was evaluated and compared with open sun drying. The dryer was loaded with 4 kg ripe banana having an initial moisture content of 78%. The final desired moisture content of 15% was achieved within 12.5 hours, but the sample kept in the open sun drying could not reach its final desired moisture content in the same duration. It was found that the product loaded in the dryer during night time had a reduction in moisture content of 2.41% and the reduction in moisture due to evening drying was 3.21%. The PCM integrated dryer, designed and fabricated in the present work, could reduce the drying duration and maintained a warm atmosphere inside the dryer during night

hours. This prevented the deterioration of the product even if there was no sunshine.

A cost effective and simple solar greenhouse was designed and fabricated for evaluating its suitability for industrial drying application. Temperature of different regions of solar greenhouse was continuously monitored, along with solar radiation and ambient temperature, from 9.00 a.m to 5.00 p.m solar time. The greenhouse was loaded with copper cake, which was an effluent generated by a zinc manufacturing industry. Two courses of studies were mainly undertaken with the present experimental set-up. Maximum temperature recorded in the greenhouse when it was loaded with 60 kg and 550 kg of copper cake were 46.8°C and 50.6°C respectively. The objective of the study was to reduce the drying duration of copper cake, which is a valuable effluent, generated by the industry. The initial moisture content at the time of loading was 40% and the final desired moisture content for the separation of copper was 10%. The normal drying duration of this effluent, without any arrangement, was forty five to sixty days, while it was only ten days when the system was loaded with 550 kg sample. With the present experimental set-up, the drying duration of the sample was reduced considerably along with the reduction of storage space required for the effluent material in the factory premises.

Comparative analyses of solar air heater with numerical simulation tools have several important results. Simulation studies included analysis of variation of the temperature output for different mass flow rates, effect of number of baffles in collector output temperature, and pressure drop across the collector. The results showed that CFD tools have its own advantages in the field of solar air heater research. It is a powerful assistant tool for researching and is worth to apply in this area.

SUGGESTIONS AND RECOMMENDATIONS

The experimental study conducted on pilot model solar air heaters helped us to design and install a 46 m² roof integrated solar air heater with a batch type solar dryer, particularly meant for drying fruits and vegetables. Research work on experimental model enabled us to optimize the mass flow rate and to decide the model best for a particular requirement. The solar drying system was installed in a Food Processing Centre and a group of women are operating ~~the system~~ **it**. **This proved as a model to use solar energy for income generation and poverty alleviation among poor rural women.** The success of the project suggests to go for more such systems and the potential is vast.

The proliferation of this type technology is an urgent need of the hour, particularly in the context of fast depleting of conventional fuels. Food processing industries consume lot of conventional fuel and the introduction of this technology will cause a considerable reduction of precious fossil fuel consumption. It is felt that very poor dissemination of the solar air heating technology for hot air generation/drying is mainly due to the complexity of the system. But the proper design of the system, accounting heat and mass transfer phenomenon during drying process alleviates this stumbling block and this in turn, causes the spreading of this technology into a new orbit.

A policy should be evolved for mandatory use of solar air heaters in food industries, which utilizes conventional fuel for drying and similar processes. In this case the solar air heater may be used as full energy delivery (FED) unit or partial energy delivery (PED) unit, depending on the quantity of energy requirements. Another potential area where the use of solar air heater is to be made mandatory is industrial heating. Solar air heaters are well suited to generate temperature in the range of 90°C and the industries which require high temperature can utilize solar air heating system as a preheating unit.

The simple greenhouse technique is found to be much suitable for low temperature drying applications in industry. Moreover, it resulted in faster drying of the toxic effluent enabling the extraction of valuable material out of it.

The incorporation of PCM based thermal energy storage in drying is suitable in small solar dryers. It can help to create a warm atmosphere inside the dryer during night hours, protecting the product from spoilage. The integration of PCM storage in large solar air heaters will result in sudden discharge of heat from the storage medium to the flowing air due to the high mass flow rate supplied by the blower. Hence PCM storage is recommended in small scale solar dryers. PCM based storage can be used for a large number of charging/discharging cycle.

In order to achieve better CFD simulations and to validate these, some recommendations for simulations are given on the basis of the present study.

- 1) Simulation should be performed with entire geometry of solar air heater with wall roughness.
- 2) More refined predictions can be achieved by using more advanced turbulence models and wall treatments [such as Reynolds Stress Model (RSM)] considering the anisotropic nature of turbulence.
- 3) More simulations should be performed in order to investigate effect of grid-refinement on the solution that is to check grid independence.
- 4) The predictions of the radiative heat transfer can be improved by using a buoyancy model to model natural convection effects correctly.
- 5) Effects of number of baffles on heat transfer output needs to be validated against experimental data, which is currently not available.
- 6) It is recommended to optimize the baffle position for three and four baffle model in order to investigate the impact on heat transfer.
